Vegetable oils as a platform for the design of novel Hyperbranched Polyesters

Blandine Testud

université de BORDEAUX

R

THÈSE PRÉSENTÉE

POUR OBTENIR LE GRADE DE

DOCTEUR DE

L'UNIVERSITÉ DE BORDEAUX

ÉCOLE DOCTORALE DES SCIENCES CHIMIQUES

SPÉCIALITÉ : Polymères

Par Blandine TESTUD

VEGETABLE OILS AS A PLATFORM FOR THE DESIGN OF NOVEL HYPERBRANCHED POLYESTERS

Les huiles végétales comme plateforme pour la conception de nouveaux polyesters hyper-ramifiés

Sous la direction de : Pr. Henri CRAMAIL
Co-directeur : Pr. Daniel TATON / Co-encadrant : Dr. Etienne GRAU

Soutenance le 8 décembre 2015

Devant la commission d'examen formée de :

M. CAILLOL, Sylvain	Ingénieur de recherche, ENSCM-CNRS	Rapporteur
M. FREY, Holger	Professeur, Université de Mayence	Rapporteur
M. GRAU, Etienne	Maitre de conférence, Université de Bordeaux	Examinateur
Mme. HILLAIRET, Caroline	Chef de projets, SAS PIVERT	Examinateur
M. PINTORI, Didier	Chef de projets Lipochimie, ITERG	Examinateur
M. TOURNILHAC, François	Directeur de recherche, ESPCI ParisTech	Examinateur
M. CRAMAIL, Henri	Professeur, Université de Bordeaux	Directeur de thèse
M. TATON, Daniel	Professeur, Université de Bordeaux	Directeur de thèse

« Le chemin ne finit pas. Plus on avance, plus la route s'ouvre à nous. »

Henri Miller

Remerciements

Il n'y a pas de recette miracle : la thèse est faite d'une bonne dose de labeur, de persévérance, de découvertes et surtout de rencontres marquantes. La réalisation de ses travaux n'aurait en effet pas pu être possible sans la contribution, de près comme de loin, d'un grand nombre de personnes que je tiens à remercier à travers ces quelques lignes.

Tout d'abord, je voudrais exprimer ma reconnaissance à M. Holger Frey, Professeur à l'Université de Mayence, et M. Sylvain Caillol, Ingénieur de recherche à l'Université de Montpellier, qui m'ont fait l'honneur d'être les rapporteurs de ce manuscrit, ainsi qu'à M. François Tournilhac, Directeur de recherche à l'ESPCI, pour avoir accepté de présider mon jury de thèse. Je les remercie de l'intérêt qu'ils ont pu porter à mes travaux, pour la discussion scientifique qui s'en est suivie, ainsi que pour leurs remarques pertinentes.

Je souhaiterais exprimer ma gratitude à la SAS PIVERT (*Picardie Innovations Végétales Enseignements et Recherches Technologiques*), organisme financeur de ce projet, pour m'avoir donné l'opportunité de réaliser cette thèse et à nos partenaires de l'ITERG (*Centre technique et industriel des huiles et des corps gras*) pour cette enrichissante collaboration. Je remercie plus particulièrement les Drs Caroline Hillairet, Chef de projets à la SAS PIVERT, et Didier Pintori, Chef de projet à l'ITERG pour leur aide précieuse et leur enthousiasme. Ce fut un plaisir de travailler avec eux tant professionnellement que personnellement.

Je tiens à vivement remercier le trio infernal de directeurs et encadrant de thèse qui m' a suivi durant ces trois années, en commençant par le Pr. Henri Cramail pour la confiance qu'il m'a accordé, ses conseils avisés et sa présence réconfortante malgré un emploi du temps bien chargé. Je lui suis reconnaissante de m'avoir encadré tout en me laissant une grande autonomie de travail et la possibilité de marquer ce projet de mon empreinte. Je pense aujourd'hui pouvoir dire que j'ai bien grandi après ces 3 années passées au sein de son équipe (*Fatty team* un jour, *fatty team* toujours). Je voudrais également remercier le Pr. Daniel Taton de s'être mêlé, au début peut-être malgré lui, de cette thèse. Ce fut un honneur de travailler à ses côtés et d'avoir pu partager son amour pour la science. Sa rigueur et son goût pour l'excellence sont de véritables qualités qui m'auront marquées. J'espère avoir été à la hauteur de ses exigences.

Enfin, un grand merci au Dr. Etienne Grau qui n'a jamais été officiellement mon co-directeur mais ce fut tout comme. Même s'il m'a rendu la vie infernale pendant trois ans, je n'en serais pas arrivée là sans lui. Je le remercie pour son aide précieuse, toutes ses idées aussi farfelues soit-elles, nos discussions scientifiques (et le fameux « j'ai une question ? »), son implication (quand bien même je baissais les bras, il y avait toujours quelqu'un pour y croire en ce projet et c'était lui), et enfin pour avoir veillé sur moi comme un père de substitution.

J'ai une pensée toute particulière pour mes stagiaires, mes young padawans, Arnaud Jaud et Lionel Longe qui m'ont beaucoup appris sur la patience et la diplomatie. Je tiens à saluer leur engagement et leur contribution au développement de la seconde plateforme de monomères (et oui, ils en ont manipulé des thiols, parfois très odorants et à foison). Par ailleurs, merci d'avoir égayé ma paillasse et le poulailler (N1-37) durant votre passage.

Mes remerciements vont également auprès de Christelle Absalon et Patricia Castel de la plateforme analytique *CESAMO* pour la réalisation des analyses par spectrométrie de masse MALDI-TOF, vers Ahmed Bentaleb du *Centre de Recherche Paul Pascal* (CRPP) pour son implication dans les essais de diffraction des rayons X, et enfin auprès de Noel Pinaud et Jean-Michel Lasnier pour la réalisation des analyses par spectroscopie RMN HR MAS.

Je voudrais également remercier tous les membres passés et présents, permanents comme non permanents, du LCPO qui font qu'il fait si bon travailler dans ce laboratoire (que j'ai d'ailleurs beaucoup de mal à quitter aujourd'hui), et plus particulièrement toutes les personnes responsables de la maintenance et du bon fonctionnement des appareils de mesure : Anne-Laure pour la spectroscopie RMN, Nicolas, Amélie et Yannick pour les chromatographies d'exclusion stérique, la dream team constituée de Gérard (et sa bonne humeur quotidienne) et Cédric pour les analyses thermo-mécaniques et enfin Eric, et la patience infinie dont il fait preuve face à une chromatographie Flash très capricieuse.

Je tiens à exprimer ma sympathie à tous ceux sans qui ce laboratoire ne tournerait pas rond, je pense notamment aux différentes mamans du LCPO : Michèle, Nicole, Catherine et maintenant Dominique, Corinne et Bernadette, mais également à Loic, l'homme à tout faire (merci de m'avoir fourni les litres de DCM quotidien que je te réclamais) et Claude.

Un grand merci à tous les doctorants, post-doctorants et stagiaires, dont j'ai pu croiser le chemin durant cette thèse et notamment, à l'ensemble des membres de la Fatty team (*le gras, c'est la vie* ☺): Thomas pour m'avoir lancé sur ce sujet, Lise, Audrey, Estelle pour son soutien au quotidien, Prakash pour les coups de main au laboratoire (*Come on Thibaud*), Océane et Geoffrey (attention, c'est bientôt à votre tour), Léa, Pierre-Luc, Dounia, Etienne, Enrique, Matthieu pour ta bonne humeur communicative (*t'es hyperbranché comme mec, tu le sais ça* !), Coraline (*c'est la manip' de ta vie !*) et Mathilde, et les nouveaux venus Hélène, Martin et Quentin (les polymères hyper-ramifiés sont entre de bonnes mains, la relève est assurée). Je n'oublie pas mes demi-frères et demi-sœurs de la DT team, et plus particulièrement Paul la fraise, Winnie (alias Zwinnie), Camille et Romain.

Mais également aux anciens qui étaient là à mes débuts : Antoine, Maréva, Jun, Vincent, Maud, Carine, Romain, Jules, Sylvia, Charlotte, Loic, Hélène, à tous ceux qui ont terminé leur odyssée en 2015 (*We did it* et ça en valait la peine. A présent, une page se tourne. Je vous souhaite très sincèrement et à tous une bonne continuation. Qui sait le monde de la chimie est petit, nos chemins se recroiseront sûrement.) : Déborah, Olivia, Kévin, Edgar, et enfin à tous ceux pour qui l'aventure LCPO continue : Marie, Mehdi, Jérémie, Benjamin, Zhen, Mickael, Alex, Guillaume, Laurie, Jérémy, Pierre, Ariane, Laura, Gauvin, Margot, Cony, Khalid, Ségolène… j'en oublie sûrement certains mais le cœur y est.

J’ai gardé le meilleur pour la fin. Comment aurais-je traversée cette aventure sans mes triplettes, Elise et Estelle ainsi que Julie et Amélie ? Nous avons tout partagé, de nos plus belles découvertes à nos pires désillusions. Merci de m’avoir supporté pendant ces trois ans (*oh, j’ai beaucoup râlé je le sais*), d’avoir tenté de m’initier au sport et à la couleur (*ce n’est pas en vain*), pour nos soirées, nos fous-rire, nos voyages aux quatre coins de la France et d’ailleurs (je vous le promets, on ira à Bilbao ensemble un jour). Quelques lignes ne suffiront pas pour vous remercier de cette amitié qui m’a tant apporté.

Merci enfin à tous les extérieurs au LCPO, anciens de CBP, amis de l’ADOC, mon *Spacey* pour m’avoir sorti la tête de mes cahiers le week-end, et à ma famille qui par son soutien inconditionnel, a également œuvré à l’accomplissement de ce travail malgré la distance.

General Table of Contents

Résumé en français

Les huiles végétales comme plateforme pour la conception de nouveaux polyesters hyper-ramifiés

Un intérêt particulier se porte depuis maintenant une trentaine d'années sur les polymères à architecture dendritique.[1–3] Dotés d'une densité de ramification élevée, ces matériaux sont caractérisés par une topologie compacte et globulaire. Du fait de cette conformation sphérique, ils ont un comportement très différent de leurs homologues linéaires : ils présentent par exemple en solution une viscosité bien plus faible même pour des masses molaires élevées, une solubilité plus importante, ainsi qu'une fonctionnalité plus élevée. Les polymères hyper-ramifiés[4–6,7] appartiennent au même titre que les dendrimères[8] à la famille des polymères dendritiques. Ces matériaux sont néanmoins très différents sur le plan moléculaire. Les polymères hyper-ramifiés sont en effet dotés d'une structure beaucoup plus irrégulière que les dendrimères du fait de leur mode de préparation en 'one-pot'. La simplicité de synthèse de ces polymères a néanmoins favorisé leur développement à grande échelle. Ils sont aujourd'hui très largement utilisés comme additifs pour des formulations variées (peintures, adhésifs) ou matériaux d'encapsulation (cosmétiques, médecine), etc.[9,10]

La grande majorité des polymères hyper-ramifiés actuellement commercialisés est issue de ressources fossiles.[11–13] Bien que les plastiques, avec une production globale annuelle d'environ 300 millions de tonnes,[14] ne contribuent qu'à hauteur de 7% de la consommation mondiale de pétrole,[15] l'industrie de la plasturgie doit faire face à la raréfaction de cette ressource, et par conséquent, à la montée des prix que cela engendre. A cela, viennent s'ajouter des préoccupations environnementales (réchauffement climatique, émission croissante de gaz à effet de serre, gestion des déchets, etc.) et de santé publique qui incitent à la recherche de solutions plus durables, plus respectueuses de l'Homme et de son environnement. En ce début de 21ème siècle, l'utilisation de ressources renouvelables non fossiles est donc apparue comme une véritable nécessité. Une attention toute particulière a été portée à la biomasse (lignine, cellulose, sucre, huiles végétales) comme seule source abondante de structures carbonées.[16] En effet, le temps de régénération du carbone issu de la biomasse se chiffre tout au plus en dizaine d'années, alors que celui des ressources fossiles est évalué en millions d'années.

Durant cette dernière décennie, de nombreuses initiatives pour valoriser la biomasse se sont développées. Le concept de bio-raffinerie est né afin de produire à partir de ces ressources renouvelables de l'énergie, du carburant ainsi qu'une bio-plateforme de molécules permettant le développement de substituts bio-sourcés aux produits pétro-sourcés. Les biopolymères et polymères bio-sourcés issus de ses bio-raffineries intègrent aujourd'hui progressivement notre paysage économique avec une production mondiale estimée en 2014 à 1,7 millions de tonnes.[17]

Parmi les ressources renouvelables disponibles, les huiles végétales se sont avérées présenter un large potentiel pour le développement de polymères biosourcés. Cette matière première, avec une production globale annuelle évaluée à 176 millions de tonnes en 2014/2015,[18] est abondante, variée, peu onéreuse et ne présente aucun danger pour l'Homme ou son environnement. L'utilisation d'huiles végétales comme précurseurs de synthèse en chimie des polymères a déjà fait l'objet de nombreuses études.[19–21] L'accès à une large gamme de polymères thermoplastiques comme thermodurcissables a été démontré. La synthèse de polymères d'architecture hyper-ramifiée à partir de ces dérivés oléagineux a, en revanche, été très peu décrite.

Dans ce contexte, ce sujet de thèse s'est attaché à développer une gamme de nouveaux polymères hyper-ramifiés bio-sourcés issus d'huiles végétales. Cette étude a été financée par la SAS PIVERT (*Picardie Innovations Végétales, Enseignements et Recherches Technologiques*). A l'interface de la recherche académique et du monde industriel, l'Institut pour la Transition Energétique P.I.V.E.R.T. a pour finalité le développement d'une filière française compétitive dans le secteur de la chimie du végétal à partir de la biomasse d'origine oléagineuse. Ces travaux de thèse s'inscrivent dans le cadre du projet HYPERBIOPOL réalisé au *Laboratoire de Chimie des Polymères Organiques* (LCPO) sous la direction des Prs. Henri Cramail et Daniel Taton, et en partenariat avec le *Centre Technique Industriel des Huiles et des Corps Gras* (ITERG, Pessac).

Les huiles végétales sont constituées de triglycérides qui après transestérification dans le méthanol, génèrent des esters méthyliques d'acide gras. Ces dérivés oléagineux présentent de nombreux sites réactifs, notamment des fonctions esters et des doubles liaisons, se prêtant à des modifications chimiques et donc à la conception de nouveaux précurseurs de topologie contrôlée. Lors de ce projet de thèse, nous avons tout naturellement orienté nos recherches vers le développement de polyesters d'architecture hyper-ramifiée, afin de tirer profit des groupements fonctionnels dors-et-déjà existants sur ces dérivés d'acide gras.

Dans un premier temps, un état de l'art a été réalisé concernant la synthèse de polyesters hyper-ramifiés. L'utilisation d'huiles végétales ayant été très peu décrite, cette étude bibliographique s'est tout d'abord portée sur des systèmes issus de ressources fossiles. Les principales voies de synthèse permettant l'accès à des polyesters hyper-ramifiés y sont passées en revue. Compte tenue de l'importante activité scientifique dans ce domaine,[6,22–26] l'objectif n'était pas de fournir un examen exhaustif mais plutôt d'identifier les principaux avantages, inconvénients et limites de chacune des méthodologies de synthèse développées jusqu'à ce jour, à travers des exemples clés afin d'orienter notre stratégie.

La deuxième partie de ce chapitre bibliographique couvre les récents développements concernant la modification chimique des huiles végétales visant la conception de précurseurs plurifonctionnels, et le cas échéant, la synthèse des polyesters hyper-ramifiés correspondants est décrite en détails. La plupart des études recensées implique la polycondensation de monomères de type AB_n présentant des fonctions ester et alcool. Pour ce faire, plusieurs voies de fonctionnalisation des dérivés oléagineux ont été étudiées afin d'introduire les fonctions hydroxyles manquantes par (i) addition de thiol-ène,[27,28] hydrogénation d'huiles végétales époxydées[29] et hydroformylation.[30,31] Enfin, seuls deux exemples traitent de la préparation de polyesters hyper-ramifiés *via* l'approche $A_2 + B_3$, c'est-à-dire par copolymérisation de diacides comme l'acide azélaïque[32] ou un dimère d'acide oléique[33] avec le glycérol, sous-produit de la transestérification des triglycérides par le méthanol. Dans l'ensemble, ces polyesters hyper-ramifiés n'ont été caractérisés que très sommairement. Les degrés de ramifications de ces structures n'ont par exemple été déterminés que dans de rares cas.

Fort de cet état de l'art, voici donc la stratégie que nous avons adopté. Nous avons également choisi de privilégier une approche par polycondensation de monomères de type AB_n ($n \geq 2$). Cette voie de synthèse est apparue plus viable d'un point de vue industriel, puisque selon la théorie de Flory elle s'accompagne d'un risque de réticulation nul.[34] Le projet HYPERBIOPOL s'est alors organisé autour de trois grands axes : (i) la synthèse de précurseurs plurifonctionnels de type AB_2, A_2B ou AB_3 portant des fonctions ester et alcool par modification chimique d'esters méthyliques d'acide gras, (ii) le développement de procédés de polymérisation simple et efficace pour la construction de polyesters hyper-ramifiés et (iii) la caractérisation de la structure fine ainsi que des propriétés thermiques des matériaux obtenus. Tout au long de cette démarche, nous avons veillé dans la mesure du possible, à respecter les principes de la chimie verte, et notamment à limiter le nombre d'étapes réactionnelles, l'utilisation de solvants trop toxiques et à opter le cas échant pour des procédés catalytiques par opposition aux méthodes stœchiométriques.

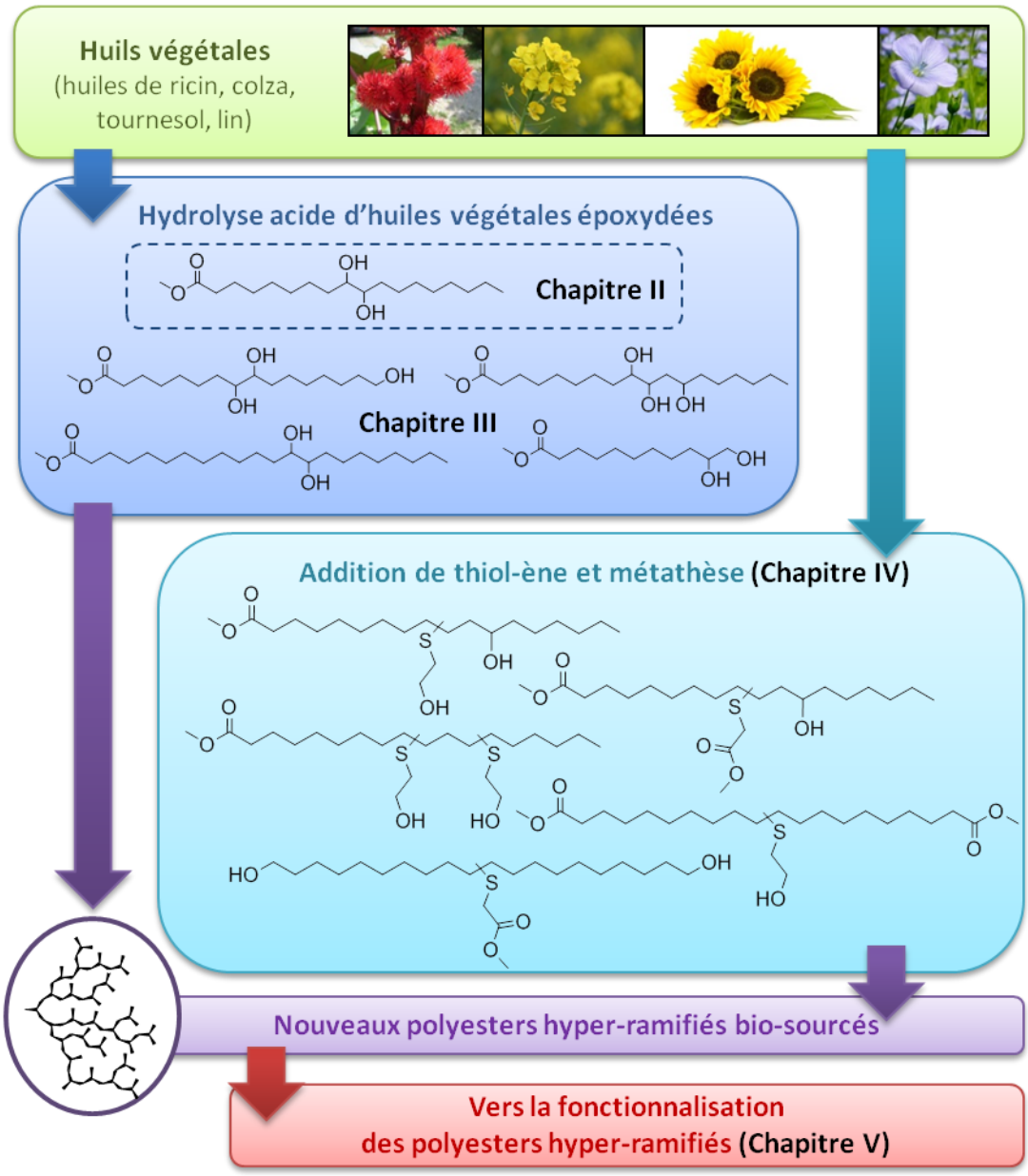

Figure 1. Plan du manuscrit de thèse

Les chapitres II, III et IV exposent les résultats expérimentaux concernant la synthèse de polyesters hyper-ramifiés à partir de dérivés oléagineux. Pour ce faire, deux voies de fonctionnalisation ont été envisagées afin d'accéder à des précurseurs plurifonctionnels de type $AB_{n,\ n\geq 2}$. Dans chacun des cas, la chimie mise en œuvre implique des réactions sur les doubles liaisons internes ou terminales de ces acides gras.

Une première plateforme comprenant 5 monomères de type AB_2/AB_3 a été obtenue par *époxydation* suivie d'une *hydrolyse acide* des oxiranes formés. Ce procédé permet d'introduire en deux étapes des alcools secondaires en position vicinale. Appliqué à l'oléate de méthyle, cette méthode a permis l'accès à un monomère singulier de type AB_2 : le 9,10-dihydroxystéarate de méthyle, abrégé M2HS. Ce synthon a été utilisé comme modèle afin d'appréhender la réactivité de tels précurseurs en polymérisation. Une étude fine de

l'influence des conditions opératoires (temps, température, nature et concentration en catalyseurs, etc.) a abouti à la construction de polyesters hyper-ramifiés présentant des masses molaires comprises entre 3000 et 10000 $g.mol^{-1}$, ainsi que de larges dispersités allant jusqu'à 15. Les meilleurs résultats ont été obtenus en présence de trois catalyseurs aux mécanismes d'activation très différents: la base organique 1,5,7-triazabicyclo[4.4.0]déc-5-ène (TBD), le méthanolate de sodium et l'acétate de zinc anhydre.

La caractérisation de la structure fine de ces polyesters hyper-ramifiés a été conduite par spectroscopie de résonance magnétique nucléaire (RMN) du proton. Cette technique nous a permis de distinguer des signaux caractéristiques de chacune des unités terminales (T), linéaires (L) et dendritiques (D) de nos matériaux et ainsi, de calculer leurs degrés de ramifications (DB) à l'aide de la formule établie par Frey.[35] Les valeurs obtenues sont comprises entre 0,07 et 0,45, ce qui reste inférieurs au 0,5 prédit par la théorie. Plusieurs facteurs se sont révélés influencés ce degré de ramifications, et notamment (i) le taux de conversion, (ii) les masses molaires et plus étonnant encore, (iii) le catalyseur de polymérisation utilisé. En effet, nous avons pu constater que l'acétate de zinc favorisait la formation d'architectures plutôt linéaires caractérisées par des degrés de ramifications inférieurs à 0,26, alors que les polymérisations catalysées par le TBD aboutissaient à des polyesters présentant des structures beaucoup plus ramifiées et caractérisées par des degrés de ramifications allant jusqu'à 0,45. Enfin comme attendu, ces polyesters hyper-ramifiés se sont révélés amorphes, la présence de ramifications empêchant l'enchevêtrement des chaines. Des températures de transition vitreuse comprises entre -33 et -20°C ont d'ailleurs été atteintes. Pour finir, des analyses thermogravimétriques ont montré que ces polyesters hyper-ramifiés présentaient de bonnes stabilités thermiques, caractérisées par des températures de dégradation à 5% comprises entre 254 et 332°C.

Fort des résultats prometteurs obtenus à partir de M2HS, nous avons par la suite cherché à diversifier cette plateforme de monomères tout en conservant une méthodologie de synthèse simple et efficace. Pour ce faire, le procédé d'époxydation/ ouverture d'époxyde a été appliqué à d'autres substrats comme les esters méthyliques d'acide ricinoléique, undécénoique et érucique issus des huiles de ricin et de colza. Des synthons aux architectures variées présentant une fonctionnalité plus élevée pour M3HS, un espacement plus important entre les points de ramifications (11 atomes de carbone contre 7) en ce qui concerne M2HB, ou marqué par l'absence de chaines pendantes pour M2HU ont ainsi été obtenus. L'aleuritate de méthyle (MA), un synthon naturel de type AB_3 issu de l'huile de musc, a également été inclus dans cette étude. Ce monomère a attiré notre attention car il présente un alcool primaire en position terminale non encombré stériquement.

L'ensemble de ces différences structurales ont eu un impact sur les propriétés thermiques des polyesters hyper-ramifiés correspondants. La fonctionnalité supérieure de M3HS/MA, a notamment permis de moduler leurs températures de transition vitreuse. En effet, à masses molaires égales, les polyesters hyper-ramifiés dérivés de M3HS/MA présentent des T_gs plus élevées que les matériaux obtenus à partir de M2HS, et comprises entre -20 et 9°C. Ceci s'explique par le fait que contrairement aux polymères linéaires, la température de transition vitreuse de polymères hyper-ramifiés est gouvernée par leurs extrémités de chaine. L'absence de chaines pendantes, tout comme la formation d'une structure plus linéaire du fait d'une réactivité plus importante de l'alcool primaire de MA vis-à-vis de ses deux alcools secondaires, ainsi qu'un espacement plus important entre les points ramifications, ont quand à eux conférer une certaine flexibilité aux chaines polymères dotant les matériaux issus de la polycondensation de M2HB, M2HU et MA d'un caractère semi-cristallin. Des températures de fusion comprises entre 20 et 60°C ont été atteintes.

Des suivis cinétiques réalisés avec M2HS ont néanmoins mis en évidence un effet de substitution négatif. La proximité des deux alcools secondaires portés par les monomères de cette première plateforme, s'est en effet révélée sensiblement limiter par gêne stérique les degrés de ramifications et probablement, les masses molaires atteignables. D'autres voies de fonctionnalisation ont alors été envisagées afin de synthétiser des monomères plus réactifs. Une seconde plateforme comprenant 5 synthons de type AB_2/A_2B a ainsi été développée en faisant appel à des réactions d'*addition de thiol-ène* et de *métathèse*. Considérée comme une réaction de chimie « click », l'addition de thiol-ène a donné accès à des précurseurs plurifonctionnels en une étape, au lieu de deux par la voie précédente, facile à mettre en œuvre et aux rendements élevés. Par ailleurs, elle a permis d'introduire des alcools primaires plus réactifs que les alcools secondaires portés par les monomères de la précédente plateforme ; ainsi que des fonctions ester aboutissant à la synthèse de monomères de type A_2B, par opposition aux structures de type AB_2 préparées jusqu'à présent. La fonctionnalisation par addition de thiol-ène a également été couplée à des réactions de métathèse de manière à espacer les fonctions réactives, et ainsi minimiser l'encombrement stérique durant la polymérisation.

Les premiers essais ont très vite démontrés que ces monomères soufrés présentaient une réactivité plus importante que leurs prédécesseurs en polymérisation. Des polyesters hyper-ramifiés de masses molaires équivalentes voire supérieures, comprises entre 3000 et 13000 $g.mol^{-1}$, ont été obtenus en des temps plus courts et/ou en travaillant à des températures de polymérisation bien inférieures. Ces matériaux se sont révélés présenter des propriétés amorphes comme semi-cristallines en fonction de la structure du monomère départ, ainsi que

de bonnes stabilités thermiques ($T_d^{5\%}$ = 266-313°C). Des températures de transition vitreuse plus faibles que les polymères hyper-ramifiés issus de la première plateforme, dans l'intervalle -56 à -35°C, ont été atteintes du fait de la présence de liens thio-éthers conférant une flexibilité plus importante aux chaines polymères.

En conclusion, nous pouvons affirmer sur la base de l'ensemble de ces résultats, que nous avons atteint nos objectifs initiaux à savoir le développement d'une gamme de polyesters hyper-ramifiés à partir d'une ressource renouvelable peu onéreuse : la biomasse oléagineuse. Pour ce faire, plusieurs méthodologies de synthèse simples et sure impliquant des réactions d'époxydation, d'addition de thiol-ène et de métathèse, ainsi que des polycondensations en masse (soit en l'absence de solvant) ont été privilégiées. La plateforme ainsi obtenue rassemble 10 monomères plurifonctionnels aux structures variées. L'ensemble des différences structurales ont permis de moduler la densité de ramifications des polyesters hyper-ramifiés correspondants, ainsi que leurs propriétés thermiques.

Il est important de préciser qu'un véritable savoir-faire a été développé quand à la polymérisation de ces systèmes, et notamment l'identification par spectrométrie de masse MALDI-TOF de réactions secondaires d'étherification intercaténaires à l'origine de la formation de matériaux gélifiés. Afin de palier ce phénomène de réticulation, une étude fine de l'influence des conditions opératoires a été menée au cas par cas. Plusieurs solutions se sont révélées concluantes: abaisser la température, le temps de réaction ainsi que la charge en catalyseur, travailler en milieu dispersé (en solution) ou encore opter pour une catalyse enzymatique. Toutes n'ont néanmoins pas été optimisées jusqu'à ce jour.

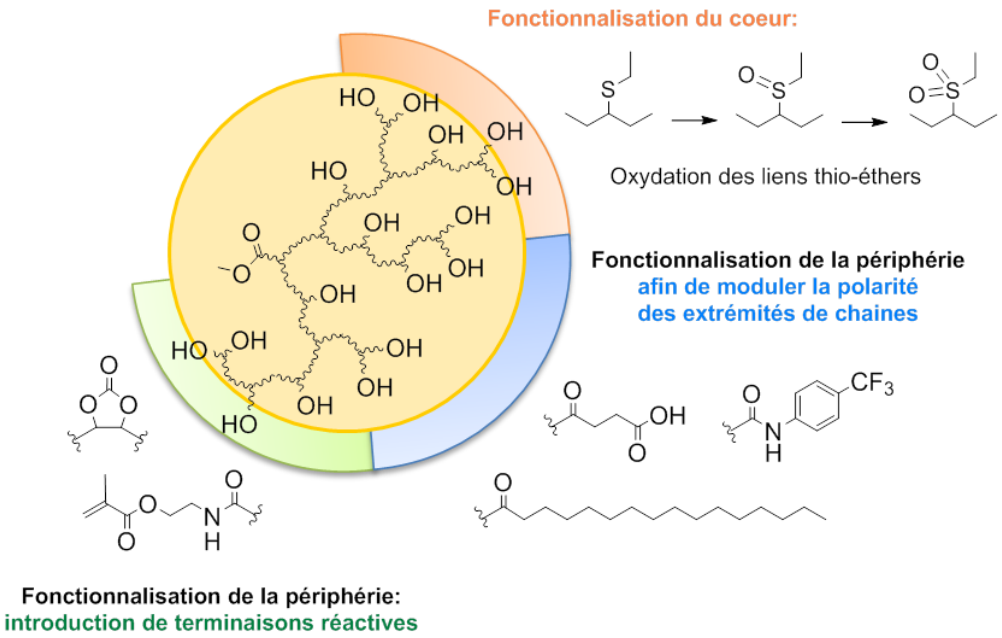

Figure 2. Fonctionnalisation du cœur et de la périphérie de polyesters hyper-ramifiés bio-sourcés

Pour finir, et ce afin de valoriser les polyesters hyper-ramifiés développés au cours de ce projet, nous avons envisagé de les fonctionnaliser. Le chapitre 5 rassemble les résultats préliminaires obtenus (Figure 2). Nous avons cherché à mettre à profit d'une part la présence de liens thio-éthers au cœur de polymères issus de la seconde plateforme dans des réactions d'oxydation, et d'autre part la multivalence de ses matériaux, c'est-à-dire leurs grands nombres de fonctions terminales dans diverses réactions de dérivatisation. En ce sens, plusieurs groupements d'intérêt ont été introduits en périphérie de polyesters hyper-ramifiés issus de la polycondensation de M2HS dont des fonctions acide, des chaines alkyles ainsi que des composés fluorés afin de moduler la polarité des extrémités de chaine, ou encore des unités réactives de type carbonate cyclique à 5 centres ou encore des entités méthacrylate. Pour ce faire, des réactions simples et sûres d'estérification des fonctions hydroxyles terminales de ces polymères hyper-ramifiés, ou d'addition d'isocyanates fonctionnels, ont été privilégiées. L'ensemble de ces modifications chimiques ont permi de moduler à la fois les propriétés thermiques, ainsi que la solubilité des

Le projet HYPERBIOPOL était un sujet exploratoire qui offre aujourd'hui de nombreuses perspectives, notamment industrielles marquées par le dépôt de deux brevets. D'un point de vue plus fondamental, des efforts doivent être menés pour réaliser une montée en échelle des productions. A ce titre, l'ITERG travaille actuellement sur le scale-up des polyesters hyper-ramifiés obtenus à partir de M2HS. Il est par ailleurs primordial d'approfondir la caractérisation des propriétés physico-chimiques de ces matériaux, et tout particulièrement leurs propriétés rhéologiques. Ces polyesters hyper-ramifiés sont en effet de bons candidats pour des applications de type modificateurs de rhéologie ou lubrifiants. Enfin, il serait intéressant d'une part d'envisager la synthèse de polyesters hyper-ramifiés *via* l'approche $A_2 + B_3$ du fait de la librairie importante des diesters et polyols dors-et-déjà disponibles à partir d'huiles végétales, et d'autre part de poursuivre les efforts engagés en fonctionnalisation du cœur comme de la périphérie de ces systèmes au regard d'applications ciblées bien évidemment.

References

(1) Voit, B. I. *Acta Polym.* **1995**, *46* (2), 87–99.
(2) Tomalia, D. A.; Fréchet, J. M. J. *J. Polym. Sci. Part A Polym. Chem.* **2002**, *40* (16), 2719–2728.
(3) Frey, H. *Macromol. Chem. Phys.* **2007**, *208* (15), 1613–1614.
(4) Hult, A.; Johansson, M.; Malmström, E. In *Branched Polymers II*; Roovers, J., Ed.; Advances in Polymer Science; Springer Berlin Heidelberg, 1999; Vol. 143, pp 1–34.
(5) Gao, C.; Yan, D. *Prog. Polym. Sci.* **2004**, *29* (3), 183–275.
(6) Voit, B. I.; Lederer, A. *Chem. Rev.* **2009**, *109* (11), 5924–5973.
(7) Yan, D.; Gao, C.; Frey, H. *Hyperbranched polymers: Synthesis, Properties, and Applications*; John Wiley & Sons, Inc., 2011.
(8) Tomalia, D. A.; Christensen, J. B.; Boas, U. *Dendrimers, Dendrons and Dendritic polymers: Discovery, Applications and the Future*; Cambridge University Press, 2012.
(9) Yates, C. R.; Hayes, W. *Eur. Polym. J.* **2004**, *40* (7), 1257–1281.
(10) Zheng, Y.; Li, S.; Weng, Z.; Gao, C. *Chem. Soc. Rev.* **2015**, *44*, 4091–4130.
(11) Perstorp. *Boltorn, advancing performance & confort*.
(12) BASF. Lupasol http://www.basf.ca/group/corporate/ca/en_GB/brand/LUPASOL.
(13) Froehling, P. *J. Polym. Sci. Part A Polym. Chem.* **2004**, *42* (13), 3110–3115.
(14) PlasticsEurope. *Plastics - the facts 2014/2015*; 2015.
(15) Mülhaupt, R. *Macromol. Chem. Phys.* **2013**, *214* (2), 159–174.
(16) Okkerse, C.; van Bekkum, H. *Green Chem.* **1999**, *1* (2), 107–114.
(17) European Bioplastics. European Bioplastics: market http://en.european-bioplastics.org/.
(18) Foreign Agricultural Service. *Oilseeds: World Markets and Trade*; 2015.
(19) Meier, M. A. R.; Metzger, J. O.; Schubert, U. S. *Chem. Soc. Rev.* **2007**, *36* (11), 1788–1802.
(20) Montero de Espinosa, L.; Meier, M. A. R. *Eur. Polym. J.* **2011**, *47* (5), 837–852.
(21) Maisonneuve, L.; Lebarbé, T.; Grau, E.; Cramail, H. *Polym. Chem.* **2013**, *4* (22), 5472–5517.
(22) McKee, M. G.; Unal, S.; Wilkes, G. L.; Long, T. E. *Prog. Polym. Sci.* **2005**, *30* (5), 507–539.
(23) Voit, B. I. *J. Polym. Sci. Part A Polym. Chem.* **2005**, *43* (13), 2679–2699.
(24) Zhang, X. *Prog. Org. Coatings* **2010**, *69* (4), 295–309.
(25) Žagar, E.; Žigon, M. *Prog. Polym. Sci.* **2011**, *36* (1), 53–88.
(26) Kricheldorf, H. In *Polycondensation: History and results*; Springer Berlin Heidelberg, 2014; pp 147–159.
(27) Türünç, O.; Meier, M. A. R. *Macromol. Rapid Commun.* **2010**, *31* (20), 1822–1826.
(28) Bao, Y.; He, J.; Li, Y. *Polym. Int.* **2013**, *62*, 1457–1464.
(29) Petrović, Z. S.; Cvetković, I. *Contemp. Mater.* **2012**, *III* (I), 63–71.
(30) Petrović, Z. S.; Cvetković, I.; Milić, J.; Hong, D.; Javni, I. *J. Appl. Polym. Sci.* **2012**, *125* (4), 2920–2928.
(31) Milic, J.; Teraoka, I.; Petrovic, Z. S. *J. Appl. Polym. Sci.* **2012**, *125* (S2), 586–594.
(32) Wagner, E.; Bruchmann, F.; Haering, D.; Keller, P.; Pouhe, T. Method for producing highly functional hyperbranched polyesters by means of enzymatic esterification. US 7081509, 2006.
(33) Zhang, Y.; Yang, Y.; Cai, J.; Lv, W.; Xie, W.; Wang, Y.; Gross, R. A. In *Biobased Monomers, Polymers, and Materials*; Smith, P. B., Gross, R. A., Eds.; ACS Symposium series: Washington, 2012; p 111.
(34) Flory, P. J. *J. Am. Chem. Soc.* **1952**, *74* (1932), 2718–2723.
(35) Hölter, D.; Burgath, A.; Frey, H. *Acta Polym.* **1997**, *48* (1-2), 30–35.

List of abbreviations

Monomers

2HSA = 9,10-dihydroxystearic acid
FA(s) = fatty acid(s)
FAME(s) = fatty acid methyl ester(s)
HOSO = high oleic sunflower oil
M2HB = methyl 13,14-dihydroxybehenate
M2HU = methyl 10,11-dihydroxyundecanoate
M2HS = methyl 9,10-dihydroxystearate
M3HS = methyl 9,10,12-trihydroxystearate
MA = methyl aleuritate

Chemicals (reactants, solvents)

4TFPI= 4-(trifluoromethyl)phenyl isocyanate
bis-MPA= 2,2-bis(methylol)proprionic acid
DABCO = 1,4-diazabicyclo[2.2.2]octane
DBU = 1,8-diazabicyclo[5.4.0]undec-7-ene
DBTO = dibutyltin oxide
DCM = dichloromethane
DMPA = 2,2-dimethoxy-2-phenylacetophenone
DMSO = dimethylsulfoxide
DMF = N, N-dimethylformamide
IEMA= 2-isocyanatoethyl methacrylate
m-CPBA = *meta*-chloroperbenzoic acid
m-TBD = 7-methyl-1,5,7-triazabicyclo[4.4.0]dec-5-ene
MeOH = methanol
*t*BuOH = *tert*-butanol
TBD = 1,5,7-triazabicyclo[4.4.0]dec-5-ene
TEA = triethylamine
THF = tetrahydrofuran
$Zn(OAc)_2$ = anhydrous zinc acetate

Polymers

HBP(s) = hyperbranched polymer(s)
HBPE(s) = hyperbranched polyester(s)
HPG(s) = hyperbranched polyglycerol(s)
LPE(s) = linear polyester(s)
PAMAM(s) = poly(amidoamine)(s)
PE = polyethylene
PEI = poly(ethyleneimine)
PLA = poly(lactide)
PS = polystyrene

Miscellaneous

1D/2D = one dimensional/ two dimensional
P.I.V.E.R.T. = Picardie innovation végétale enseignements et recherches technologiques

Techniques

COSY = homonuclear correlation spectrocopy
DSC = differential scanning calorimetry
DEPT-135 = distortionless enhanced polarization transfer
ESI MS = electrospray ionization mass spectrometry
FT-IR = fourier transformed infrared spectroscopy
GC = gas chromatography
HSQC = heteronuclear single quantum coherence
MALDI-TOF MS = matrix-assisted laser desorption ionization-time of flight mass spectrometry
NMR = nuclear magnetic resonance
SEC = size exclusion chromatography
TGA = thermogravimetric analysis
WAXS = X-ray diffraction patterns at wide angles

Characteristic parameters

$Đ$ = dispersity
DB = degree of branching
$\overline{DP}_n$ = degree of polymerization
$\overline{M}_n$ = number average molecular weight
$\overline{M}_w$ = weight average molecular weight
T = temperature
$T_d^{5\%}$ = temperature corresponding to 5wt% loss
T_c = crystallization temperature
T_g = glass transition temperature
T_m = melting temperature

Polymerization Techniques

ATRP = atom transfer radical polymerization
CMM = couple-monomer methodology
CWP = chain-walking polymerization
DMM = double-monomer methodology
GTP = group transfer polymerization
MCM = multi-component methodology
PTP = proton transfert polymerization
SCROP = self-condensing ring opening polymerization
SCVP = self-condensing vinyl polymerization
SMM = single-monomer methodology

General Introduction

During the 20th century, as a result of the extensive exploitation of fossil resources (oil and gas), a wide range of synthetic polymers became available on the industrial scale. Plastic key features, namely their low cost, facile processing, high versatility and performance have met the needs of highly diversified markets (textile, food, housing, transportation, communication, health, etc.). So much that polymers have become indispensable to our daily life. Plastics whose worldwide production increased from less than 2 million tons in 1950 to almost 300 million tons in 2013,[1] represent nowadays 7% of the annual oil consumption.[2]

Since the pioneering work of Hermann Staudinger on the fundamental principles of polymerization in 1920s, numerous polymers of various architectures have been successfully synthesized and commercialized. Among them, the family of *dendritic polymers*, which emerged in the 80s, is recognized as the fourth main class of macromolecules following the more traditional linear, branched and cross-linked polymers (Figure 3). Dendritic structures which mainly comprise the hyperbranched polymers (HBPs) and the dendrimers, have attracted major attention because of their highly branched three-dimensional compact and globular architecture. This unusual structure endows them with unique properties such as a high functionality, a lower viscosity and a higher solubility than that of their linear analogues of the same molar mass.[3,4]

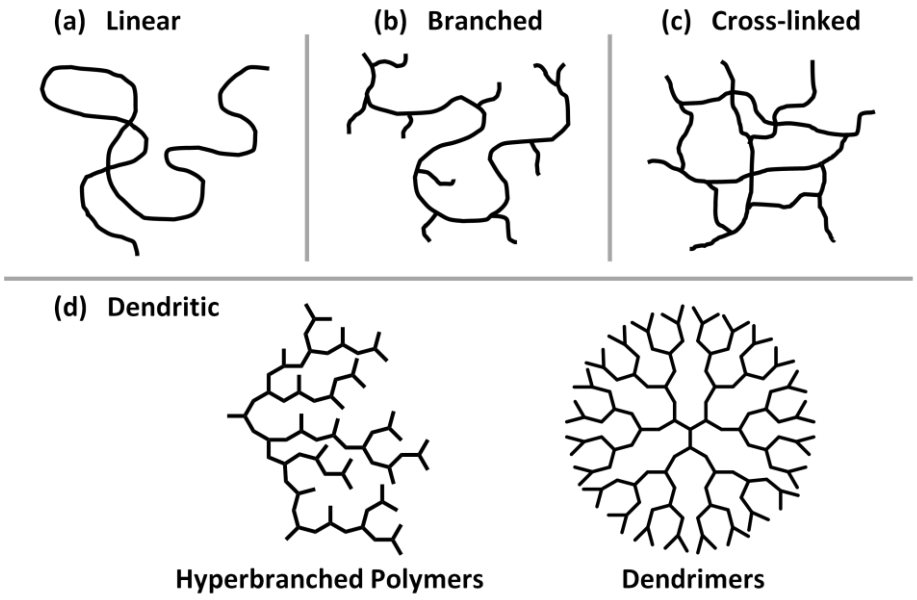

Figure 3. Major classes of polymer architectures

Dendrimers are usually prepared in demanding multi-step synthetic procedures. In contrast to their perfectly branched analogues, HBPs are of special interest because they are obtained in a one-pot polymerization. This process limits the control over molar masses and branching accuracy but affords a much more simple and economic route to highly branched materials. From the beginning, HBPs are considered as suitable products for large scale production and have been commercialized as additives or materials for encapsulation, for diverse applications, including paintings, coatings, adhesives, sensors, catalysts or in biomedicine, to only name a few.[5]

At the time of this writing, all the commercially available HBPs are petroleum-based. However, in a context of both price volatility of oil, and limited/uncertain supply of fossil resources, there is an urgent need to release the polymer industry from its dependence on pretroleum resources.[6] Global warming and additional environmental concerns (waste production, energy demand, etc.) push the search towards alternative *renewable resources*. This term relates to any vegetable or animal species, which is exploited in a sustainable way, without its depletion, and renewed in a reasonable time scale. Particular attention has been paid to biomass (carbohydrates, lignin, terpenes, plant oils, proteins and others) as the only sustainable source of carbon.[7] Indeed, biomass offers a regeneration time which is measured in years rather than hundreds of millions of years for fossil resources.

In this context, the concept of bio-refinery (Figure 4) has been developed as a facility that integrates biomass conversion processes and equipments to produce value-added bio-products (chemical building blocks and materials) and bio-energy (fuels, power and heat).[8,9] The use of renewable feedstocks is not enough to ensure a sustainable future. Green chemistry methods need to be applied in such product manufacturing.[10,11] Bio-refineries already give access to a wide range of chemicals and materials, including some bio-based and biodegradable polymers. Indeed, the global production capacity of bioplastics accounted for 1.7 million tons in 2014 and is expected to reach with further developments 7.8 million tons in 2019.[12] There are three different routes to produce 'bioplastics': (i) direct use or modification of natural polymers (lignin, cellulose, starch),[13] (ii) polymerization of bio-based building blocks extracted from biomass by fermentation/chemical modification, (iii) polymerization *via* micro-organism fermentation of sugars and lipids found in nature as it is the case for the poly(hydroxyalkanoate)s.[14] Nowadays, a large range of bio-based and biodegradable polymers are produced including either some mimic of petroleum-based plastics *e.g.* bio-PET, bio-PE, and new materials such as poly(lactide) (PLA), regenerated cellulose, starch blends, etc.[12]

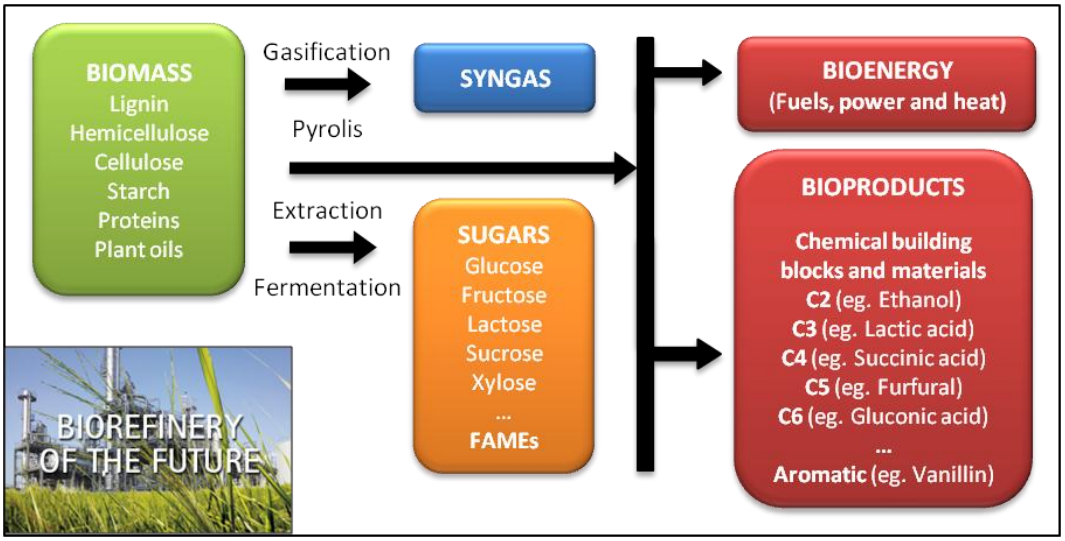

Figure 4. Schematic illustrated concept of an integrated biorefinery

This thesis takes place in the frame of the HYPERBIOPOL project (WP3P7) in collaboration with the *Laboratoire de Chimie des Polymères Organiques* (*LCPO*) and the *Centre Technique Industriel des Huiles et Corps Gras* (*ITERG*, Pessac, France), and has been financially supported by the SAS PIVERT.[15] At the interface of academic research and industry, this society in charge of the Institute for Energetic Transition (ITE) P.I.V.E.R.T. aims at developing a competitive plant-based chemistry using a renewable and promising raw material: the oilseed biomass. Plant oils and their derivatives actually offer many advantages apart from their renewable nature. Their abundant availability with a global production of 176 million tons in 2014/2015,[16] relative low cost and rich application possibilities make them industrially attractive as daily demonstrated in oleo-chemistry (paints, coatings, cosmetics, surfactants, lubricants, etc.). The use of plant oils in polymer chemistry has already been investigated and the synthesis of a large range of polymeric materials including some thermosets and thermoplastics has been demonstrated.[17–19]

The purpose of this thesis is to broaden the palette of accessible vegetable oil-based materials to HBPs. The main constituents of plant oils are triglycerides, which provide after transesterification with methanol some fatty acid methyl esters (FAMEs). By taking advantages of the naturally-occurring ester and alcohol functional groups present in FAMEs, this thesis aims at developing a range of novel hyperbranched polyesters (HBPEs) with tunable properties that can be valued in very different industries. The synthesis of vegetable oil-based linear polyesters has been extensively studied in recent years. Several relevant reviews have been devoted to that topic.[17,19–22] In contrast, the use of plant oils for the preparation of HBPEs remains scarce.[23–27] The scope of possibilities was thus virtually endless.

This manuscript is divided into five chapters (Figure 5) and structured as indicated hereafter. The first chapter is devoted to the state-of-the-art on HBPEs, from petroleum to vegetable oil-based systems. After a detailed introduction to the field of HBPs, this bibliographic study will outline the different synthetic approaches developed over the past decades to prepare HBPEs. In view of the important scientific activity in this area, the intention is not to provide a comprehensive review, but rather illustrates the major advantages, drawbacks and limitations of each synthetic methodology through representative examples. This section will thus give the reader the basics to understand the main challenges and achievements of this work. The second part of this chapter covers recent developments in the chemical modification of vegetable oils enabling the design of strategic multifunctional precursors of HBPEs and, when appropriate, the syntheses of the related HBPEs are described in details. This discussion will highlight the great, and yet untapped, potential of vegetable oils and define synthetic possibilities for the development of sustainable HBPEs.

The following chapters (Chapters II, III and IV) expose the experimental results regarding the synthesis of vegetable oil-based HBPEs. In this PhD work, the approach by polycondensation of AB_n-type monomers ($n \geq 2$) was favored. Plant oils and/or FAMEs were chemically modified to synthesize multifunctional precursors of AB_n-type featuring ester and alcohol moieties. For that purpose, several methods of functionalization involving the double bonds present in triglycerides were investigated, namely, *via* the acid hydrolysis of epoxidized vegetable oils (Chapters II and III) and thiol-ene/metathesis coupling reactions (Chapter IV). Simple and efficient processes of polymerization were then, developed yielding novel HBPEs by polycondensation of the oily-derived monomers. Throughout this study, a point to consider was to respect whenever possible some of the "Twelve Principles of Green Chemistry" such as, apart from the use of renewable resources, the use of less hazardous and safer chemicals, the reduction of intermediates and wastes, and the use of catalytic reagents instead of stoichiometric chemicals.[10]

In Chapter II, emphasis is placed on the synthesis, characterization and subsequent polycondensation of methyl 9,10-dihydroxystearate (M2HS). This peculiar AB_2-type monomer prepared by acid hydrolysis of epoxidized high oleic sunflower oil was used as model compound to study the reactivity of such precursors in polycondensation. Its polymerization behavior is discussed in detail. Special attention is then paid to the characterization of the fine structure as well as the specific properties of the related HBPEs, with a focus on the determination of the degree of branching by NMR spectroscopy.

Chapter III describes our efforts to extend the platform of multifunctional precursors prepared by acid hydrolysis of epoxidized vegetable oils, with the idea of obtaining HBPEs with tunable properties. The synthesis of a series of novel AB_2-type monomers of varied chain lengths between two branching points, but also AB_3-type precursors, derived from castor, rapeseed and musk oils, is presented. Therefore, the influence of the monomer structure on the branching density, thermal stability and thermo-mechanical properties of the corresponding HBPEs is discussed, in the light of the results previously obtained with M2HS. Lastly, the gelation phenomenon, by which the polycondensation of AB_n-type monomers was observed to result in cross-linked polymers instead of soluble materials, is examined.

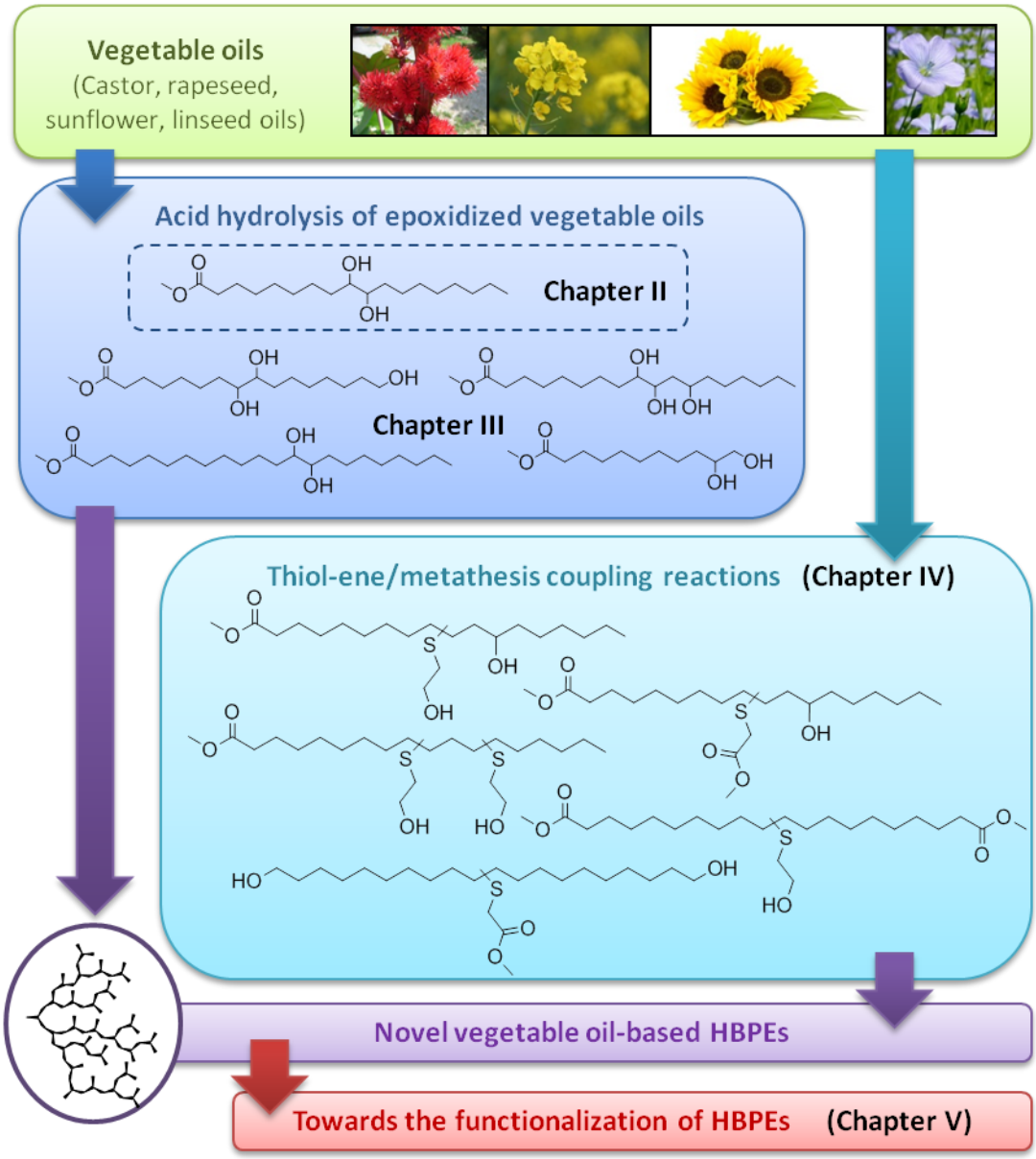

Figure 5. Organization of the manuscript

Chapter IV is dedicated to the development of a novel platform of AB_2-type monomers of higher reactivity, *via* thiol-ene/metathesis coupling reactions. The 1,2-diol structure generated by acid hydrolysis of epoxidized vegetable oils was indeed shown to limit somehow the molar masses and DB values achievable by the HBPEs, due to steric hindrance. Other routes were thus investigated to functionalize the FAMEs. The thiol-ene addition allowed the incorporation of primary alcohols, known to be more reactive than the secondary ones previously studied; while the metathesis coupling reaction enabled to drive apart the reactive functions thereby minimizing steric hindrance. This second platform of AB_2-type monomers broadened the scope of oily-derived HBPEs to thiolated materials. The impact of the introduction of sulfur atoms into the very core of the HBPs is discussed on their thermal stability and thermo-mechanical properties.

Lastly, Chapter V presents our preliminary investigations into the post-functionalization of either the core or the periphery of some of the HBPEs synthesized in the course of this thesis, with the idea of tuning their properties and thus opening the scope of their applications. Examples of post-modification include the oxidation of sulfur-containing HBPEs described in Chapter IV to their polysulfoxide and polysulfone analogues, as well as the derivatization of hydroxyl-ended HBPEs derived from M2HS. The introduction of several functional groups of various polarities such as carboxylic acids, alkyl tails, fluoro-containing compounds, methacrylate and even 5-membered cyclic carbonate moieties, is examined.

References

(1) PlasticsEurope. *Plastics - the facts 2014/2015*; 2015.
(2) Mülhaupt, R. *Macromol. Chem. Phys.* **2013**, *214* (2), 159–174.
(3) Yan, D.; Gao, C.; Frey, H. *Hyperbranched polymers Synthesis, Properties, and Applications*; John Wiley & Sons, Inc., 2011.
(4) Voit, B. I.; Lederer, A. *Chem. Rev.* **2009**, *109* (11), 5924–5973.
(5) Zheng, Y.; Li, S.; Weng, Z.; Gao, C. *Chem. Soc. Rev.* **2015**, *44*, 4091–4130.
(6) Sorrell, S.; Speirs, J.; Bentley, R.; Brandt, A.; Miller, R. *Energy Policy* **2010**, *38* (9), 5290–5295.
(7) Okkerse, C.; van Bekkum, H. *Green Chem.* **1999**, *1* (2), 107–114.
(8) Axelsson, L.; Franzén, M.; Ostwald, M.; Berndes, G.; Lakshmi, G.; Ravindranath, N. H. *Biofuels, Bioprod. Biorefining* **2012**, *6* (3), 246–256.
(9) National Research Energy Laboratory. Biorefinery http://www.nrel.gov/biomass/biorefinery.html.
(10) Anastas, P.; Eghbali, N. *Chem. Soc. Rev.* **2010**, *39* (1), 301–312.
(11) Sheldon, R. A. *Green Chem.* **2014**, *16*, 950–963.
(12) European Bioplastics. European Bioplastics: market http://en.european-bioplastics.org/.
(13) Laurichesse, S.; Avérous, L. *Prog. Polym. Sci.* **2014**, *39* (7), 1266–1290.
(14) Chen, G.-Q. *Chem. Soc. Rev.* **2009**, *38* (8), 2434–2446.
(15) Institut PIVERT. Institut PIVERT http://www.institut-pivert.com/.
(16) Foreign Agricultural Service. *Oilseeds: World Markets and Trade*; 2015.
(17) Meier, M. A. R.; Metzger, J. O.; Schubert, U. S. *Chem. Soc. Rev.* **2007**, *36* (11), 1788–1802.
(18) Montero de Espinosa, L.; Meier, M. A. R. *Eur. Polym. J.* **2011**, *47* (5), 837–852.
(19) Maisonneuve, L.; Lebarbé, T.; Grau, E.; Cramail, H. *Polym. Chem.* **2013**, *4* (22), 5472–5517.
(20) Okada, M. *Prog. Polym. Sci.* **2002**, *27* (1), 87–133.
(21) Türünç, O.; Meier, M. A. R. *Eur. J. Lipid Sci. Technol.* **2013**, *115* (1), 41–54.
(22) Vilela, C.; Sousa, A. F.; Fonseca, A. C.; Serra, A. C.; Coelho, J. F. J.; Freire, C. S. R.; Silvestre, A. J. D. *Polym. Chem.* **2014**, *5*, 3119–3141.
(23) Türünç, O.; Meier, M. A. R. *Macromol. Rapid Commun.* **2010**, *31* (20), 1822–1826.
(24) Bao, Y.; He, J.; Li, Y. *Polym. Int.* **2013**, *62*, 1457–1464.
(25) Petrović, Z. S.; Cvetković, I. *Contemp. Mater.* **2012**, *III* (I), 63–71.
(26) Petrović, Z. S.; Cvetković, I.; Milić, J.; Hong, D.; Javni, I. *J. Appl. Polym. Sci.* **2012**, *125* (4), 2920–2928.
(27) Zhang, Y.; Yang, Y.; Cai, J.; Lv, W.; Xie, W.; Wang, Y.; Gross, R. A. In *Biobased Monomers, Polymers, and Materials*; Smith, P. B., Gross, R. A., Eds.; ACS Symposium series: Washington, 2012; p 111.

Chapter I. From Petroleum to vegetable oil-based Hyperbranched Polyesters

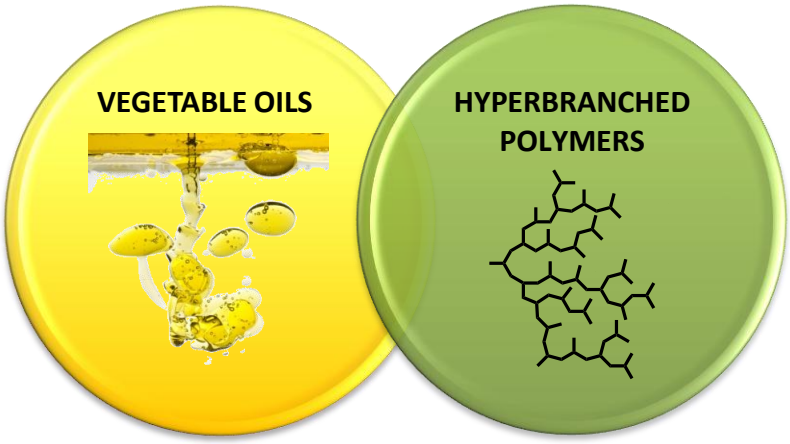

Table of contents

1. Hyperbranched Polymers: general concepts

"Life is branched" as claimed in the introduction of the monograph entitled *Hyperbranched Polymers, Synthesis, Properties and Applications*, by Deyue Yan, Chao Gao and Holger Frey.[1] Indeed, branching is of high importance in nature and universe. From non-living to living objects, it occurs anywhere and anytime at all scales from light-year to millimeter (Figure I-1).

Figure I-1. Selected branching patterns observed in universe and nature (from left to right: Crab nebula, forked lightening, tree, nervures, vascular network). All images were obtained from Internet.

In polymer science, branching has been known for a while. In 1950s, Flory dedicated several chapters in his *Principles of Polymer Chemistry* to non-linear polymers.[2] For many years, however, branched materials have been considered as undesired products of side reactions or intermediates to polymeric networks. In 1980s, branching finally emerged as an attractive phenomenon with the development of anionic living polymerization which opened the way to the synthesis of well-controlled branched architectures, such as stars, combs and graft copolymers.[3] Nowadays, branching reactions following either a random or a controlled manner, are viewed as an important topic in the design of functional macromolecules.

1.1. Introduction to dendritic polymers

Dendritic polymers refer to highly branched macromolecules with a three dimensional architecture. Recognized as the fourth major class of polymers, after the more traditional linear, branched and cross-linked macromolecules, the family of dendritic polymers is divided as follows: (a) dendrons and dendrimers, (b) linear-dendritic hybrids, (c) dendronized polymers, (d) dendrigrafts and dendrimer-like polymers, (e) hyperbranched polymers, (f) hyperbranched polymer brushes, (g) hyperbranched polymer-grafted linear macromolecules and (h) hypergrafts or hyperbranched polymer-like macromolecules as depicted in Figure I-2.

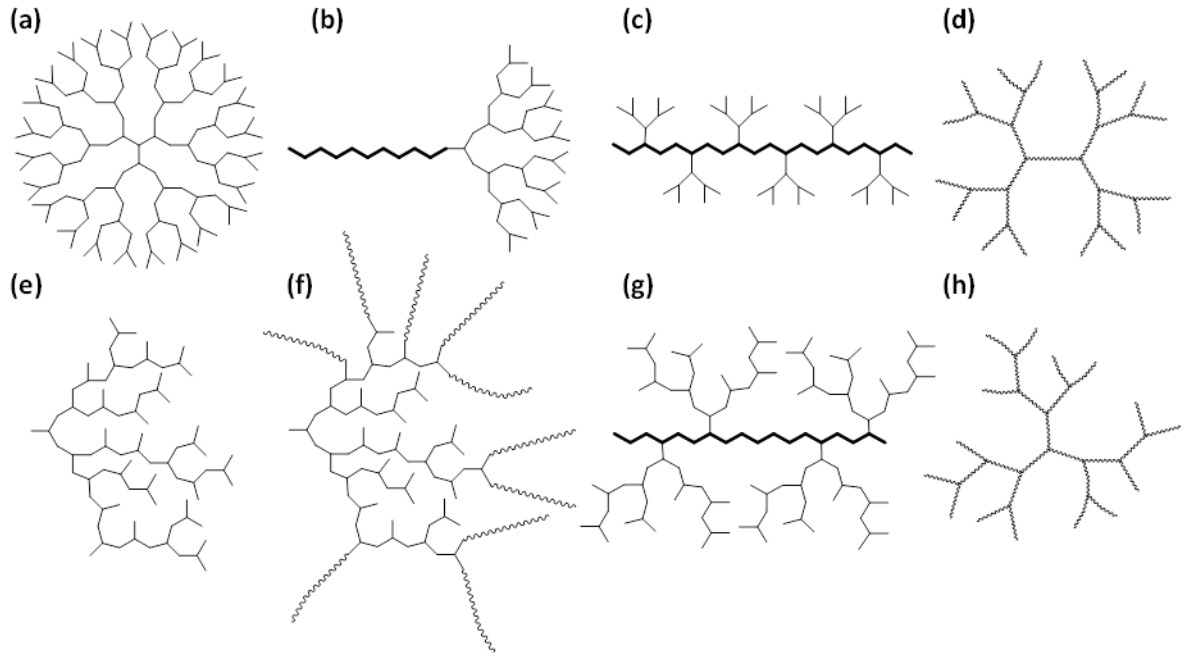

Figure I-2. Dendritic polymers with different structures (a) dendrimers, (b) linear-dendritic hybrids, (c) dendronized polymers, (d) dendrimer-like polymers, (e) hyperbranched polymers, (f) hyperbranched polymer brushes, (g) hyperbranched polymer-grafted linear macromolecules and (h) hypergrafts

Attention was first drawn to dendrimers by Vögtle and coworkers in 1978.[4] Also known as arborols, star-burst or cascade polymers, dendrons and dendrimers are well-defined macromolecules with a perfectly branched and highly symmetric structure. Two main methodologies were developed to access such regular architectures (Figure I-3).[5,6] The divergent approach was introduced by Tomalia and Newkome in 1980s.[7,8] This strategy consists in an iterative process where the dendritic structure is built, generation after generation, from a multifunctional core to the periphery. On the contrary, *via* the convergent approach reported by Hawker and Fréchet, the synthesis starts from the surface and proceeds inwards yielding dendron building blocks that are connected to a central core in a final step.[9,10] In either way, tedious stepwise synthetic procedures (protection, deprotection, purification) are often required to perfectly control the dendrimer structure, size and functionality.

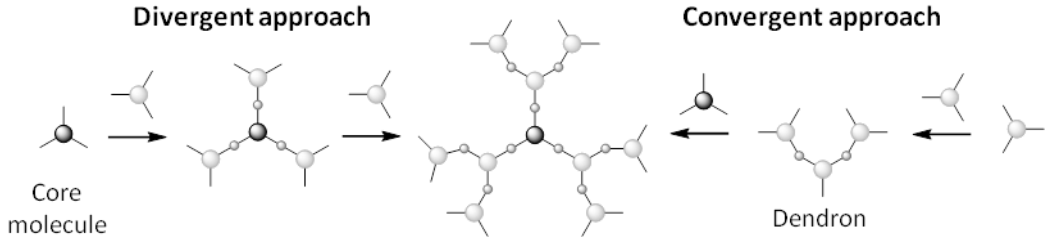

Figure I-3. Dendrimer growth by the divergent and convergent approaches

Other dendritic structures of higher complexity were further developed. For instance, dendronized polymers (c) consist of a linear polymer backbone carrying numerous side dendrons. They can be synthesized by several approaches including the direct polymerization of dendron-monomers (*macromonomer* route), the grafting of dendrons to a linear backbone (*grafting-onto* route) or the divergent growth of dendrons from a linear core (*divergent* route). Dendrimer-like polymers, dendrigrafts (d) and hypergrafts (h) are highly branched macromolecules, mimics of dendrimers and hyperbranched polymers of larger size (from ten to hundreds of nanometers) since they are built from linear polymeric building blocks *via* either controlled or random branching.

For more details, numerous reviews and books were published on dendrimers,[11,12] linear-dendritic hybrids,[13] dendronized polymers,[14,15] dendrimer-like polymers,[16,17] dendrigrafts[18] and hypergrafts.[19] This chapter will focus on the synthesis, modification and applications of hyperbranched polymers, with a special emphasis on the family of polyesters (HBPEs).

1.2. Hyperbranched polymers

1.2.1. History of Hyperbranched Polymers

The theoretical foundation of hyperbranched polymers is signed by Flory and coworkers. In 1940s, they introduced the concept of "highly branched species" and "degree of branching" when they applied statistical methods to investigate the molecular size distribution of three dimensional polymers in the state of gelation.[20–22] Systems considered as a part of this study were networks obtained by condensation of bifunctional (A_2) and tri- (B_3) or tetrafunctional (B_4) monomers above a critical conversion corresponding to the gelation point (Scheme I-1). In 1952, Flory demonstrated on the basis of theoretical developments, that soluble polymers with branching points in each repeating unit (*branch-on-branch* topology) could be synthesized without leading to cross-linking systems. The process described consisted in the polycondensation of monomers bearing antagonist functions: one functional group (A) and two or more (B) ones capable of reacting with A ($AB_{n,\ n\geq2}$-type monomers).[23]

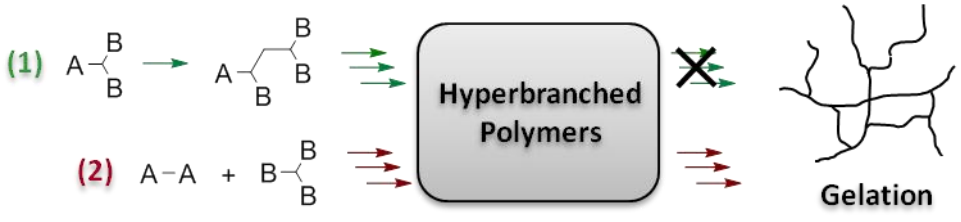

Scheme I-1. Synthetic strategy towards HBPs and networks according to Flory approach

The term "hyperbranched polymers" (HBPs) was coined more than 25 years later by Kim and Webster. These two researchers of DuPont company reported the first intentional synthesis of hyperbranched polyphenylenes warranted as a patent in 1987.[24,25] Since then, HBPs have attracted a growing interest regarding their synthesis, modification and wide range of potential applications as confirmed by the increasing number of publications as seen in Figure I-4.

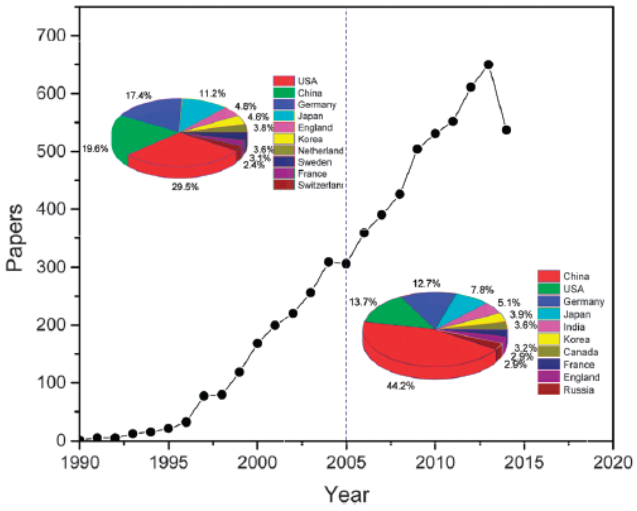

Figure I-4. Publication numbers during 1990 and 2014 with the topic "hyperbranched polymers" searched by ISI Web of Science[26]

A point to consider is that prior to Kim and Webster's definition, several 'non intentional' syntheses of branched macromolecules have been reported. In particular, the work of Berzelius at the end of the 19th century on the formation of a resin from tartaric acid (A_2B_2 monomer) and glycerol (B_3) must be mentioned. Later, Smith, Callahan, Arsem, Dawson and Howell studied the reaction between phtalic anhydride (A_2) and glycerol. Kienle showed, in 1939, that this system displayed lower viscosity than the synthetic linear polymers reported by Staudinger.[27,28] Finally, Kricheldorf described in 1982 the preparation of highly branched aromatic polyesters by polycondensation of AB_2 and AB-type monomers.[29]

1.2.2. Degree of branching

HBPs are usually presented as imperfect but affordable analogues of dendrimers and were at least considered as such in their early stages of development.[30] Dendrimers indeed attracted first the attention of a rather academic community, due to their challenging synthesis and the beauty of their perfectly branched structure. However, time-consuming multistep reactions with tedious isolation and purification procedures are required to prepare them. Even if efforts are currently made to reduce the number of steps and simplify procedures making use of click-chemistry techniques,[31] large scale applications of dendrimers remain limited.

In contrast to their perfectly branched analogues, HBPs emerged from industrial activity.[30] Their synthesis in 'one-pot' affords a much more simple and economic route to branched materials, in line with the current industrial processes. Yet, as a result of statistical growth, control is lost over molar masses and branching accuracy. HBPs show therefore a less regular architecture than dendrimers, broader molar mass distributions and, above all, a lower branching density (Figure I-5).

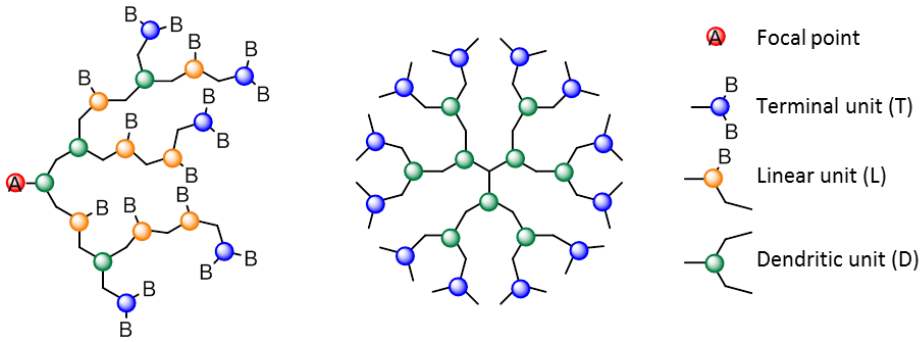

Figure I-5. Different subunits in HBPs obtained by polycondensation of AB_2-type monomer and dendrimers

One important parameter of dendritic polymers is their degree of branching (DB). This DB factor, comprise between 0 and 1, was introduced to quantify the branching density of this kind of architecture. As shown in Figure I-5, HBPs prepared by polycondensation of AB_2-type monomers are characterized by three different subunits: some terminal (T), linear (L) and dendritic (D) ones depending on the number of unreacted B groups, *i.e.* 2, 1 and 0, respectively. Based on these definitions, Fréchet and coworkers[32] defined in the 1990s the DB as being equal to the following ratio:

$$DB_{Fréchet} = \frac{D + T}{D + T + L} \qquad \textbf{(I-1)}$$

DB is equal to 1 for perfectly branched dendrimers, whereas randomly branched HBPs show values lower than 1. Assuming that this expression is only correct for high molar mass HBPs, Frey and coworkers[33] extended the equation (I-1) as followed:

$$DB_{Frey} = \frac{2D}{2D + L} \qquad \textbf{(I-2)}$$

Both definitions are commonly used nowadays and lead to similar results at high conversions. However, if some unreacted AB_2 monomers are included in the calculations, overestimation of the terminal units occurs and the DB coined by Frey tends to be smaller than the one defined by Fréchet. Besides, equation (I-2) does not require determination of terminal units T. Importantly, equations (I-1) and (I-2) are also applicable to products of A_2 + B_3 polymerizations. However, other models were developed to calculate the DB of HBPs prepared by polycondensation of $AB_{n,\, n>2}$ monomers.[33]

Direct and indirect methods have been developed to determine the DB of HBPs. Among them, NMR spectroscopy has been proven to be the most powerful tool. This technique indeed enables to distinguish characteristic signals of each repeating unit (T, L and D) in the HBPs. ^{1}H NMR spectroscopy is the most useful approach to access DB values. Quantitative ^{13}C and for heteroatom-containing HBPs, ^{15}N, ^{19}F, ^{29}Si and ^{31}P NMR spectroscopies have also been successfully applied. These nuclei generally provide spectra with less overlapping signals, easier to analyze. Two-dimensional NMR (2D NMR) techniques are usually required to solve the complex spectra obtained in one dimension. Sometimes even model compounds, mimics of linear and dendritic motifs, have to be synthesized to correctly assign the characteristic peaks of each subunit. Other techniques should be mentioned such as the *degradative approach*. This direct method consists in the degradation of HBPs into their dendritic, linear and terminal units, motifs that are quantified in a next step by chromatographic analyses.[34]

Finally, in cases where neither NMR techniques nor degradation are feasible, other approaches have been developed to indirectly estimate the DB of HBPs, such as viscometry. This method is based on the Mark-Houwink-Sakurada equation:

$$[\eta]=K\,M_v^{\alpha} \qquad \textbf{(I-3)}$$

where K and α are the Marc-Houwink-Sakurada constants. HBPs exhibit lower intrinsic viscosity ([η]) than their linear analogues of the same molar masses (M_v), which results in lower values of the α exponent, *i.e.* 0.5 to 1 for linear polymers, to less than 0.5 for HBPs.[35]

As pointed out by Frey and coworkers, the DB of HBPs prepared from AB_2-type monomers tends after completion to a plateau with a value of 0.5, assuming that the two B functions are of equal reactivity and no intramolecular cyclization or secondary reactions occur. Values commonly reported are yet in the range 0.4-0.8. Deviations from the theory can be ascribed to the "non-respect of Flory's theory requirements". In practice, the presence of cycles, products of intramolecular reactions, was detected by electrospray ionization (ESI) or matrix-assisted laser desorption ionization-time (MALDI-TOF) mass spectrometry to significant extent in some cases.

Moreover, the DB can be altered by: (i) modifying polymerization conditions (temperature, nature of catalyst, loading in catalyst, solvent, etc.), (ii) copolymerization of AB and AB_2-type monomers and (iii) host-guest inclusion of AB_2-type or multifunctional monomers.[36] Some methods have even been investigated to enhance the DB value by: (i)

addition of core molecules of $B_{f,\ f\geq 2}$ type, (ii) direct polymerization of dendrons with linear units, (iii) increasing the reactivity of the remaining B groups of linear units, (iv) post-functionalization of the so-formed HBPs to convert linear units to dendritic ones and (v) using specific catalysts.

The DB is a parameter of high importance since it impacts many physical and chemical properties of HBPs including glass transition, crystallization and melting behaviors, thermal stability, melting/solution viscosity, encapsulation capability, self-assembly behavior, optoelectronic properties, etc.[37]

1.2.3. General properties

HBPs and dendrimers are often discussed together as dendritic materials, both having as common features, a high branching density as well as a compact and globular architecture. This unusual structure endows them with unique properties compared to linear polymers. Of particular interest is their lower viscosity reported both in solution and in the molten state.[38]

The relationship between intrinsic viscosity ([η]) and molar mass (M) for different polymer topologies is shown in Figure I-6. As pointed out by Turner and coworkers, solution behavior of HBPs differs from dendrimers.[39] Indeed, while dendrimers show a "bell-shape behavior", the intrinsic viscosity of HBPs follows the Marc-Houwink-Sakurada equation (I-3), *i.e.* increases with increasing molar masses. Nevertheless viscosities of both dendrimers and HBPs remain smaller than that of their linear analogues of same molar masses. The relationship between intrinsic viscosity and molecular architecture has been investigated in more detail by Fréchet.[40]

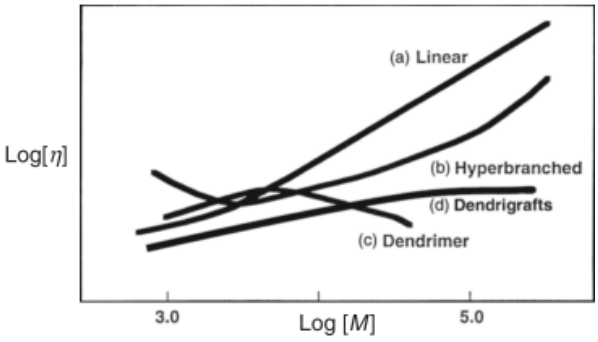

Figure I-6. Schematic plots for the relationship between intrinsic viscosity ([η]) and molar mass (M) for various polymer topologies[1]

Moreover, in solution, dendritic materials generally feature a higher solubility than their linear analogues. This property was proven to be tuned, to a large extent, by the nature of their end-groups.

Another distinct difference with linear polymers induced by the branched backbone is the lack of entanglements, making HBPs and dendrimers rather brittle materials. This has restricted the use of dendritic polymers as thermoplastics to applications where the mechanical strength is of minor importance. The presence of branching points preventing the polymeric chains from crystallization, HBPs are usually referred as amorphous materials. Some exceptions have however been reported, where crystallinity was provided by modification with long chains[41] or dilution of the branching pattern.[42] The formation of liquid crystalline structures was even observed.[43]

In addition, the high functionality of dendritic polymers, that is their large number of terminal functional groups, offers the possibility for further modification and opens the scope of potential applications.

Table I-1. Comparison of HBPs with linear polymers and dendrimers inspired from reference [1]

Polymer	Linear	Hyperbranched	Dendrimer
Structure		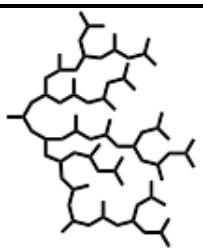	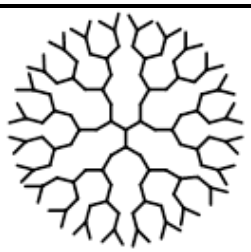
Topology	1D	3D, irregular	3D, regular
Synthesis	one-step	one-pot	multi-steps
Scaling-up	Easy, already done	Easy, already done	Difficult, limited
$Đ$	≥1	>2	1
DB	0	0.4-0.8	1
Viscosity	High	Low	Very low
Solubility	Low	High	Very high
Entanglement	Strong	Weak	Very weak or absence
Strength	High	Low	Very Low
Functionality	Chain-ends (2)	Dendritic and Linear units (>>2)	Dendritic units (>>2)

The main differences between HBPs, dendrimers and linear polymers are listed in Table I-1. As detailed above, the analogy between HBPs and dendrimers is limited to their physical and chemical properties, including low viscosity, high solubility, lack of entanglements and high functionality. Otherwise, HBPs exhibit irregular architecture characterized by DB value lower than 1, and broad molar mass distribution (usually $Đ > 2$), while dendrimers show perfectly branched structure (DB = 1) with extremely narrow dispersity ($Đ = 1$). Nevertheless, due to their cost-effective synthesis in one-pot, HBPs have attracted much industrial attention.

1.2.4. Methodologies of synthesis

Up to now, several methodologies have been developed to access HBPs. All these methods have in common the use of well-defined synthons bearing two reactive but antagonist functions commonly called A and B. A recent classification based on the number of monomers involved in polymerization includes 4 main categories: single-monomer methodology (SMM), double-monomer methodology (DMM), couple-monomer methodology (CMM) and multi-component methodology (MCM) as outlined in Scheme I-2.

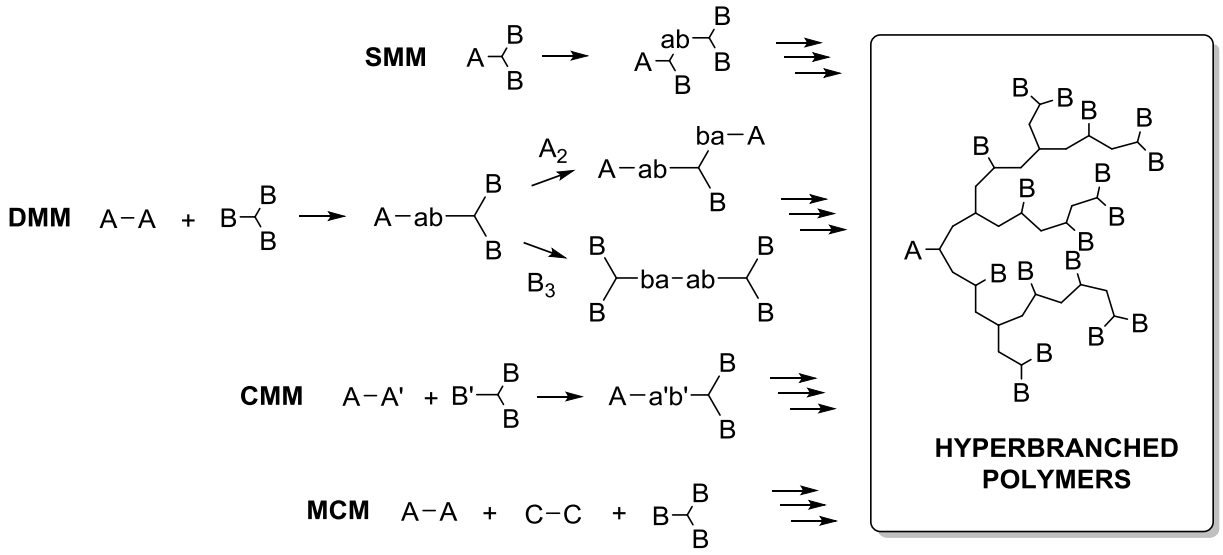

Scheme I-2. Methodologies of synthesis used to prepare HBPs. The A, B, A', B' and C functions represent unreacted groups, ab and a'b' reacted ones.

SMM consists in the homopolymerization of $AB_{n\geq 2}$-type monomers (or latent AB_n-type) following a step-growth mechanism. This strategy covers several techniques of polymerization: (i) the classic polycondensation of AB_n-type monomers, (ii) self-condensing vinyl polymerization (SCVP), (iii) ring-opening multibranching polymerization (ROMBP) sometimes called self-condensing ring-opening polymerization (SCROP), (iv) proton transfer polymerization (PTP), (v) chain-walking polymerization (CWP) and (vi) dialkyne polycyclotrimerization.

Polycondensation of AB_n-type monomers is certainly the most widely studied synthetic approach to HBPs. Generally, *n* equals 2 but the use of AB_3, AB_4 and AB_6 monomers has also been described to a much lower extent. As pointed out by Flory, this strategy yields HBPs without the risk of gelation provided that (i) A reacts with B exclusively without side reactions, (ii) all B groups are of equal reactivity during the whole polymerization process and (iii) reactions do not involve internal cyclization.[23]

However, gelation may occur experimentally due to some side reactions that can be evidenced, for instance, by ESI or MALDI-TOF MS analyses. A point to consider is that the formation of insoluble materials does not necessarily mean that cross-linking occurs. Gels can be observed when intermolecular interactions, such as hydrogen bonding, are strong enough to create a temporary 3D network.

Kinetics of AB_n-type polycondensation was investigated in detail giving access to the analytical expressions of several molecular parameters of HBPs. The number-, weight-average degrees of polymerization ($\overline{DP}_n$ and $\overline{DP}_w$) and the dispersity ($Đ$) of polymers obtained by polycondensation of AB_n-type monomers are summarized in Table I-2.[44]

Table I-2. Average degrees of polymerization ($\overline{DP}_n$, $\overline{DP}_w$) and dispersity ($Đ$) of polymers prepared by polycondensation of AB_n-type monomers ($n \geq 1$) as a function of the conversion of A group, x.

Monomer type	AB	AB_2	AB_n
$\overline{DP}_n$	$1 / (1-x)$	$1 / (1-x)$	$1 / (1-x)$
$\overline{DP}_w$	$(1+x) / (1-x)$	$(1-x^2/2) / (1-x)^2$	$(1-x^2/n) / (1-x)^2$
$Đ = \overline{DP}_w / \overline{DP}_n$	$1+x$	$(1-x^2/2) / (1-x)$	$(1-x^2/n) / (1-x)$

Dispersity of HBPs obviously increases with the increasing conversion in monomers and reaches, after completion (x tends to 1), higher values than for linear polymers ($Đ > 2$). Even if in practice $Đ$ usually remains smaller than the predicted values, this is considered as one of the major drawbacks of HBPs for certain applications. Various techniques have been developed to narrow this $Đ$ including (i) copolymerization with core molecules of B_f-type,[45] (ii) slow addition of monomers into the reaction mixture[46] and (iii) classification by dialysis of precipitation.

Frey, Müller, Yan and coworkers established expressions of DB for HBPs prepared by polycondensation of AB_2-type monomers as a function of conversion (x):

$$DB = \frac{2x}{5 - x} \qquad \textbf{(I-4)}$$

As discussed earlier, at full conversion, DB reaches 0.5 assuming that the two B functions are of equal reactivity during the whole polymerization process.[33]Intuitively, however, the formation of a linear unit may affect the reactivity of the remaining B group. This change was introduced as the "substitution effect" and expressed *via* the reactivity ratio r of the rate constants of the formation of linear (k_L) and dendritic units (k_D) (Scheme I-3).

By enhancing the reactivity of the remaining B function, the formation of dendritic units is favored over linear ones ($k_D > k_L$, that is $r > 1$). Hence, DB values higher than 0.5 are obtained (*positive substitution effect*). For instance, several groups including our team,[47] successfully achieved DB of 1 by using several strategies as reviewed by Ueda and coworkers.[48] Inversely, DB remains small when the reactivity of the second B group is reduced (*negative substitution effect*), due to steric hindrance for example.

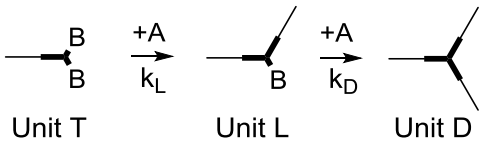

Scheme I-3. Definition of the rate constants of the formation of linear and dendritic units k_L and k_D

On the other hand, HBPs can also be prepared by *polyaddition of AB_n-type monomers*. This approach was developed by Hobson and coworkers in 1997 for the synthesis of hyperbranched analogues of Tomalia poly(amidoamine)(s) dendrimers (PAMAMs).[49]

In contrast to the step-growth techniques detailed so far, *SCVP*, *ROMBP* and *PTP* involve chain-growth mechanisms. These approaches consist in the homopolymerization of compounds featuring both an initiating and a polymerizable groups coined as inimers. This can be achieved following vinyl polymerization, ring-opening polymerization and proton-transfer polymerization techniques, respectively. Inimers are of general structure AB*, where B refers to an initiating site capable of reacting with A after activation (B*). In SCVP, approach introduced by Fréchet in 1995,[50] a vinyl group is used as the monomer part of the inimer. Once the polymerization is initiated, a dimer is formed containing one vinyl group and two active sites: A*(propagating) and B* (initiating). Inimers act thus as latent AB_2-type monomers as shown in Scheme I-4. As for the ROMBP, the A function refers to a heterocycle, *e.g.* epoxide, oxetane, lactone, etc. This technique particularly suited for the synthesis of hyperbranched polyglycerols (HPGs) via the anionic ring-opening polymerization of glycidol.[51]

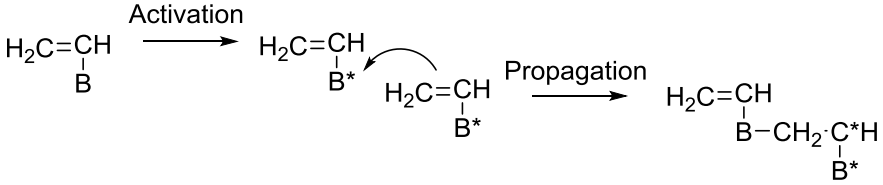

Scheme I-4. Initial steps in SCVP

SCVP, ROMBP and PTP broadened the scope of polymerizable monomers to styrene, acrylate, methacrylate derivatives and cycles, *e.g.* epoxides, lactones, carbamates, etc. Moreover, these techniques generally offer a better control over DB and molar mass

distributions, especially when coupled with controlled chain-growth processes, *e.g.* group-transfert polymerization (GTP) or atom transfer radical polymerization (ATRP).[52,53]

Chain-walking polymerization and *polycyclotrimerization of dialkynes* are two specific techniques. The former enabled to synthesize hyperbranched polyethylenes (PEs) by finely tuning the transition-metal polymerization catalyst. Guan and coworkers indeed demonstrated that PE topology varies from linear to highly branched at low ethylene pressure.[54] The cyclotrimerization of diynes is a century-old reaction recently applied to the preparation of hyperbranched polyphenylenes by Tang's group.[55]

DMM involves the copolymerization of symmetric monomer pairs with equal reactivity such as the classic $A_2 + B_3$ strategy. Obviously other combinations are possible, *e.g.* $A_2 + B_4$, $A_3 + B_4$, etc. This strategy offers the advantage of the commercial availability of A_x, B_y monomers (in contrast to the AB_n-type) but yields cross-linked polymers above a critical conversion corresponding to the gelation point. Key parameters to delay it are the A_2/B_3 molar ratio, the solution concentration, the polymerization conversion and the order of monomer addition.

To completely prevent gelation, a third approach has been developed, the so-called *couple-monomer methodology* (CMM). This strategy consists in the copolymerization of asymmetric monomer pairs with unequal reactivity such as the AA' + B'B_2 approach developed by Yan and Gao (Scheme I-2). If A' reacts faster with B' than A with B, AB_2 intermediates are predominantly formed *in situ* in the early stages of polymerization and thus reaction proceeds via SMM mechanisms. Various other approaches have been reported such as $A_2 + BB'_2$, $A_2 + CB_n$, $AB + CD_n$, $A^* + CB_2$, $A^* + B_n$, etc. CMM broadened the structure and diversity of the HBP family to macromolecules with alternating different units, *e.g.* poly(sulfoneamine)s, poly(ester amine)s, poly(amidoamine)s, poly(urea-urethane)s.[1,56]

When three or more monomers are involved in the synthesis of HBPs, the strategy is called *multi-component methodology* (MCM). This approach is the most recently reported methodology. It still proceeds in one-pot following a step-growth mechanism, but relies on a sequence-controlled pathway. For instance in Scheme I-2, the reaction between A and C leads to the formation of D function. This intermediate group is the only one capable of reacting with B affording HBPs with rather 'controlled' architecture. In this context, isocyanate-based multi-component routes such as Passerini[57] and Ugi reactions have been successfully applied to the preparation of HBPs.

The above-described synthetic strategies cover most general methods to prepare HBPs. For more details, numerous relevant books[1,38] and reviews[30,56,58–62] have been published in the past 15 years. The recent achievements from click chemistry to MCM,[26] tend to develop HBPs with tailorable structures and topologies (from compact to segmented architecture). An increase in the structural variety and complexity of the designed macromolecules has also been observed from the simple copolymerization with core molecules and/or chain extenders, to the functionalization of HBP core and/or periphery. Combinations of highly branched structures with linear building blocks give rise to linear-dendritic hybrids such as HBP brushes, hypergrafted polymers *via* some "grafting onto", "grafting from" and "grafting through" approaches,[63,64] hyper-macs and further complex architectures (Figure I-2). Even non-covalent bonding and self-assembly have been used to synthesize HBPs.

1.2.5. Applications

From the beginning, HBPs are considered as suitable materials for large-scale production. Up to now, many applications have been reported as additives or products of encapsulation in diverse fields including surface coatings, resins, lubricants, sensors, catalysis, nanotechnology, and so-on (Figure I-7).[26,65] Most of the uses of HBPs take advantage of their globular shape, low viscosity, absence of entanglements and large number of reactive end-groups. Besides, modification of these terminal functional groups enables to customize their thermal, rheological and solution properties. Functionalization of HBPs turns out to be a powerful tool to design dendritic polymers with tailor-made properties.

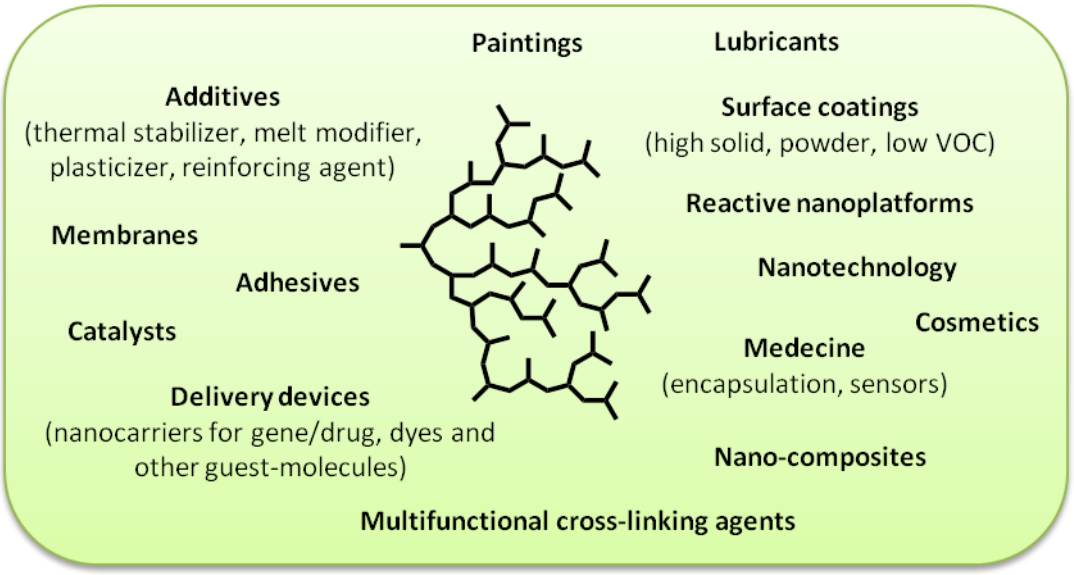

Figure I-7. Proposed applications for HBPs

A recent issue of *Chemical Society Reviews* (2015, volume 44) dedicated to dendrimers and HBPs has stressed that various new applications are being explored. For instance, advanced optical, electrical and magnetic properties of HBPs are increasingly studied for uses as light-emitting, non-linear optical or conductive materials. Supramolecular self-assembly of HBPs is also an emerging research area. Despite their irregular architecture, various morphologies (tubes, micelles, vesicles) have already been achieved with amphiphilic hyperbranched systems. Moreover, HBPs show great potential for bioapplications (drug delivery, gene transfection, bioimaging, antibacterial/antifouling materials, etc.). Dendritic polymers represent versatile carriers not only of gene/drugs but also dyes and multiple other guest-molecules. Encapsulation and controlled-released systems based on HBPs have attracted increasing attention.[66]

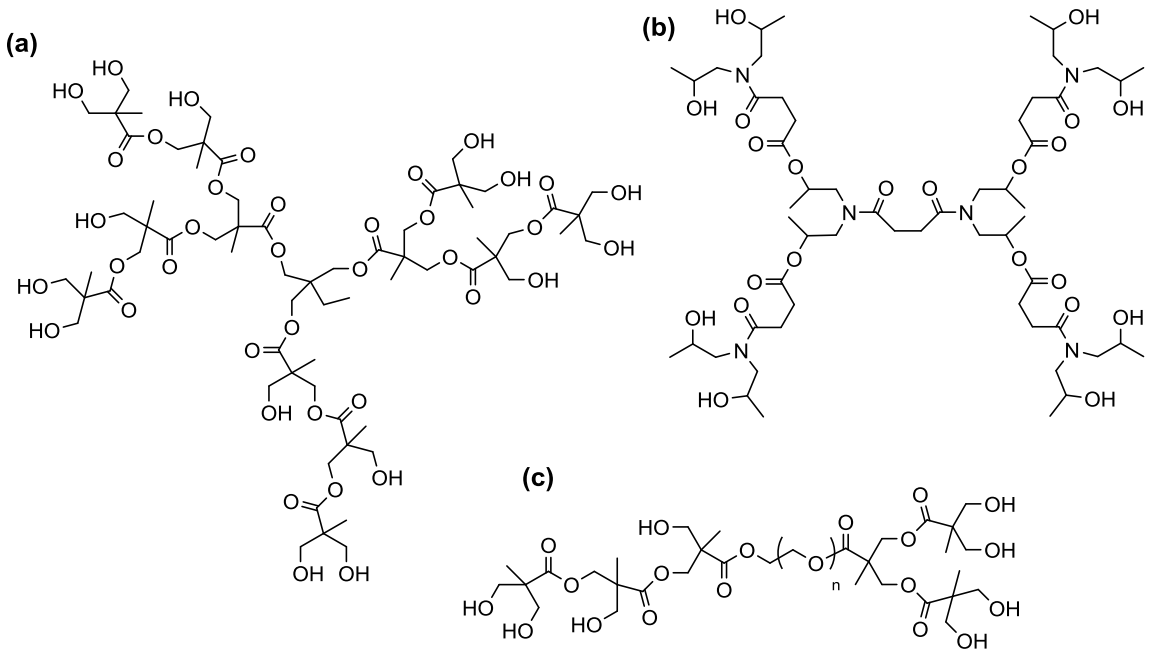

Scheme I-5. Idealized structures of (a) Boltorn™, (b) Hybrane S1200 and (c) PFLDHB-G2-PEG6k-OH

HBP market is dominated by the Boltorn™ line products commercialized by Perstorp.[67] These dendritic polyesters are obtained by polycondensation of 2,2-bis(methylol)propionic acid using various core molecules. Hydroxyl-terminated HBPEs are used as additives for flexible polyurethane foams in automotive seating applications or precursors of UV curing formulations. Once modified with unsaturated fatty acids or other non-ionic groups, these derivatives represent interesting additives for solvent or water-borne paintings. HB poly(esteramide)s are also commercialized by DSM under the trade name of Hybrane,[68] as well as poly(ethyleneimine)s produced by BASF and known as Lupasol®[69], mainly for resin and coating applications. HyperPolymers[70] offers HPGs for sale. More recently Polymer Factory[71], a major provider of advanced dendritic polymers, commercializes some linear-dendritic hybrids of Boltorn and PEG, as depicted in Scheme I-5 (c).

The next section is devoted to the literature on HBPEs and more specifically on the different synthetic approaches developed to access them. Over the past decade, several comprehensive reviews were published on HBPs covering various aspects of this topic including *e.g.* the appraisals on branched polyesters with special focus on branching dilution by Long and coworkers,[72] the work of Voit and coworkers on hyperbranched and highly branched polymers[62] and, more recently, the monograph edited by Yan, Gao and Frey[1]. In addition, recent developments in the synthesis, modifications and applications of aromatic HBPEs were addressed apart by Zhang,[73] and Ghosh and coworkers.[74]

2. Hyperbranched polyesters

Polyesters are an important class of hyperbranched polymers. Their relative ease of synthesis and the availability of suitable raw materials have indeed prompted the research in this field. Early works were related to the synthesis of hyperbranched copolyesters[29] while considerable research in the 1990s addressed aliphatic, aliphatic-aromatic and aromatic hyperbranched polyesters (HBPEs). The field of aliphatic HBPEs is mainly focused on the use of 2,2-bis(methylol)propionic acid (bis-MPA) as AB_2-type building block, the base monomer of the Boltorn® range that has been commercialized by Perstorp. Low molar mass aliphatic HBPEs have found applications in coatings and resins, fields where the combination of their high functionality, low viscosity and improved miscibility was of high interest. Aromatic HBPEs have also been extensively studied in the literature, but in contrast to their aliphatic analogues, their high melting points and glass transition temperatures have restricted their uses to blends, sensors or non-linear optics.

The following discussion aims at providing an overview of the different synthetic techniques developed up to date to prepare HBPEs including (1) polycondensation of AB_n-type monomers, (2) ring-opening multibranching polymerization of AB* inimers, and copolymerization of both (3) symmetric, *i.e.* $A_2 + B_3$, and (4) asymmetric, *i.e.* $A^* + B_3$, $AA^*/A_2 + B_2$, monomer pairs. Special emphasis is placed on the aliphatic HBPEs prepared by polycondensation of bis-MPA. Major contributions to the characterization of the fine structure of these hyperbranched systems are detailed. Note however that functionalization of the as-generated HBPs is out of the scope of this literature survey.

2.1. Polycondensation of AB_n-type monomers

Polycondensation of AB_n-type monomers was the main approach used to prepare HBPEs. The majority of the monomers involved were of AB_2-type. In rare cases, the use of AB_3 and AB_4 monomers was also reported. Most of the reactions involved the condensation between hydroxyl and carboxyl groups associated with appropriate activation processes. Even though, according to Flory's theory, there is no risk of gelation in such a method, it was recommended that the monomers be freshly synthesized. The occurrence of several side reactions, including cyclization, was indeed reported making the control over molar masses quite complex. The presence of side reactions was found to highly depend on the monomer architecture. Indeed, aliphatic HBPEs were noted to be more prone to gelation than aromatic ones. Polycondensations were often carried out in bulk, due to the easy one-step process in the presence of appropriate catalysts, but solution polymerizations were also applied providing milder reaction conditions and thus minimizing side reactions. As required for all polycondensations, the low molar mass products need to be removed to drive the reactions towards completion by applying vacuum in the melt or under nitrogen blowing in solution. The synthesis of a large variety of branched polyester structures has been successfully reported in this way, including some aromatic, aromatic-aliphatic and aliphatic HBPEs.

2.1.1. Aromatic HBPEs

The two AB_2-type monomers, namely, 3,5-dihydroxybenzoic acid (21-1) and 5-hydroxyisophthalic acid (21-2) given in Scheme I-6, were frequently used as building blocks to prepare aromatic HBPEs. Various modifications of these compounds were reported since their thermal stabilities are not sufficient to enable their direct esterification in the melt. Hydroxyl and carboxyl groups were often activated by acetylation or trimethylsilylation.

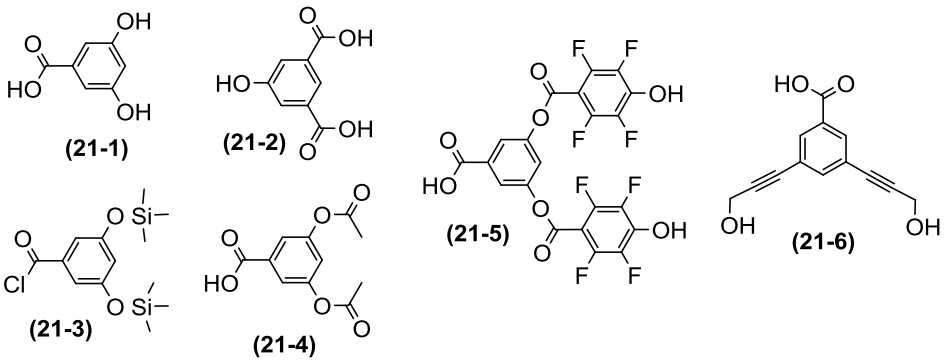

Scheme I-6. Examples of AB_2-type monomers for the synthesis of aromatic HBPEs

For instance, Kricheldorf and coworkers described as early as 1982 the synthesis of hyperbranched copolyesters starting from 3,5-bis(trimethylsiloxy)benzoyl chloride (21-3).[29] The homopolymerization of this highly activated AB_2 monomer was further investigated by Fréchet and coworkers. Polycondensations were attempted in bulk at high temperatures in between 190-275°C in the absence[32] and presence[75] of catalysts such as DMF or trimethylamine hydrochloride (Scheme I-7, pathway A). Hydroxyl-terminated HBPEs were isolated after pouring the solution of the crude product in methanol to hydrolyze the trimethylsiloxy groups. The highest molar masses ($\bar{M}_w$) of 100 000 g.mol^{-1} according to SEC-MALLS analyses were achieved at the temperature of 200°C, using 10 mol% of Me_3NHCl as polymerization catalyst. Higher reaction temperatures led to a decrease in the macromolecular characteristics assigned to the occurrence of side reactions.

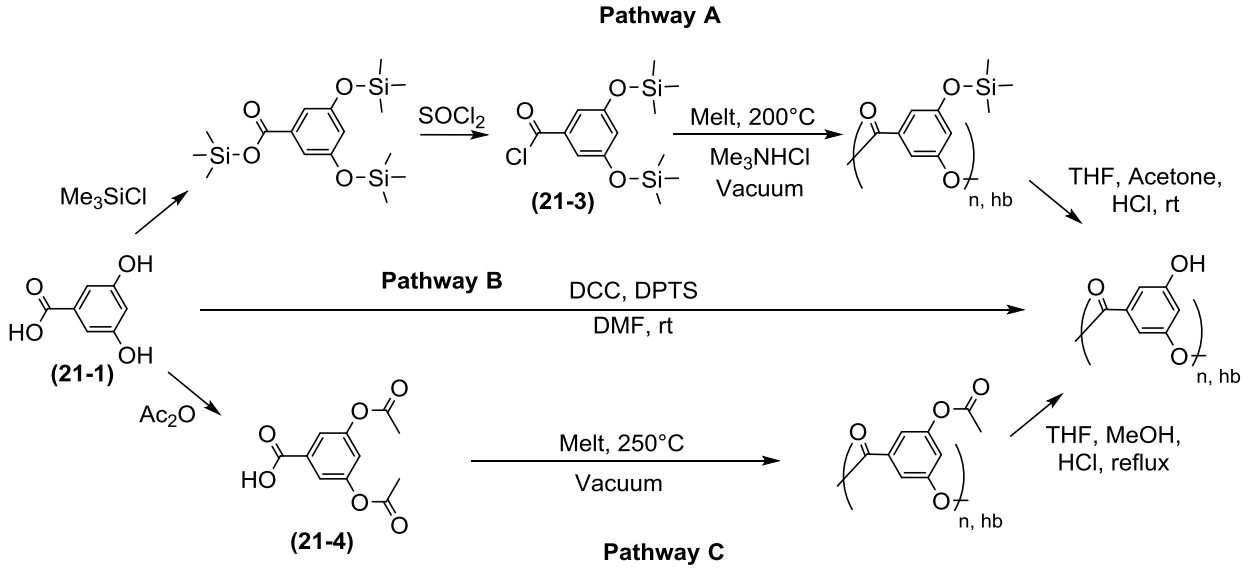

Scheme I-7. Different pathways to all-aromatic HBPEs in bulk and in solution: polycondensation (A) in bulk of 3,5-bis(trimethylsiloxy)benzoyl chloride, (B) in solution of 3,5-dihydroxybenzoic acid and (C) in bulk of 3,5-diacetoxybenzoic acid. hb: hyperbranched polymers.

Likewise, Turner and coworkers reported the preparation of another precursor of aromatic HBPEs, the 3,5-diacetoxybenzoic acid (21-4).[76] By comparison with (21-3), its melt polycondensation required higher reaction temperatures (Scheme I-7, pathway C). At 250°C, soluble aromatic HBPEs with $\bar{M}_w$ > 1 000 000 g.mol^{-1} and significantly broad dispersities, *i.e.* not measured since the polymer eluted at SEC column exclusion limit, were obtained as determined by universal calibration using differential viscometry detector. In both cases, relatively high DB values of 0.55-0.60 were achieved as measured by spectroscopic techniques (^{1}H or ^{13}C). In addition, hydroxyl-terminated HBPEs displayed, as expected, amorphous properties, high glass transition temperatures (T_g) in the range 190-226°C and thermal stabilities up to 411°C.

Synthetic routes to activated monomers are however time-consuming and overall yields are usually low with the need to further release the phenolic terminal groups. Although numerous other aromatic HBPEs were prepared by melt polycondensation of acetylated or trimethylsilylated AB_2[39,77] and AB_3[78] monomers, alternative procedures were investigated in order to limit the occurrence of side reactions yielding insoluble materials. For instance, Voit and coworkers performed the polycondensation of the unmodified 3,5-dihydroxybenzoic acid (21-1) at room temperature in DMF using dicyclohexylcarbodiimide (DCC) as coupling agent.[79] 4-(dimethylamino)pyridinium-4-tosylate (DPTS) was added as catalyst to suppress the formation of *N*-acylurea (Scheme I-7, pathway B). In contrast to previous results obtained in the melt-phase, colorless hydroxyl-terminated HBPEs with lower molar masses ($\overline{M}_w$ = 27 800 g.mol^{-1}) and dispersity ($Đ$ = 3.2), as determined by SEC-MALLS analyses, were achieved. Products showed however similar DB values of 0.60.

Similarly, Jen and coworkers reported the one-step synthesis of hyperbranched aromatic fluoropolyesters starting from the AB_2 monomer (21-5) using DCC/DPTS as condensing agents.[80] These substrates were post-functionalized with thermally cross-linkable aromatic trifluorovinyl ethers for optical waveguide applications.

Another interesting AB_2-type monomer was synthesized by Blencowe and coworkers.[81] 3,5-Bis(3-hydroxylprop-1-ynyl)benzoic acid was prepared using a Sonogoshira cross-coupling with a palladium catalyst system (21-6). As a result of the thermal instability of the monomer, its polymerization was conducted in rather mild conditions using in this case 1,3-diisopropylcarbodiimide (DIC)/4-dimethylamino-pyridine (DMAP) as condensing agents in solution of THF. Due to the high rigidity of (21-6), low molar masses of 2 500-11 000 g.mol^{-1} and DB values in between 0.22 and 0.33 were achieved.

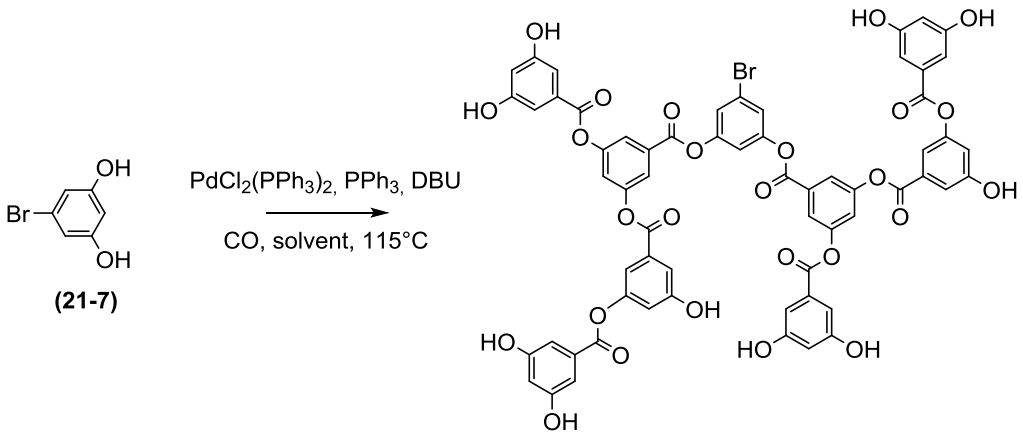

Scheme I-8. Polymerization of 5-bromoresorcinol *via* the palladium-catalyzed carbon monoxide insertion reaction[82]

Another worthy synthetic route to aromatic HBPEs is the palladium-catalyzed carbon monoxide (CO) insertion reaction (Scheme I-8). Polymerizations of AB_2 (3,5-dibromophenol) and A_2B (5-bromoresorcinol, 21-7) monomers were investigated in presence of CO, DBU as a base and $PdCl_2(PPh_3)_2$,PPh_3 in solution at 115°C.[82] While the hydroxyl-terminated HBPEs derived from (21-7) showed good solubility in organic solvents such as methanol, DMF or DMSO, end-capping of the HBPEs prepared from the AB_2-type monomers with phenol or *m*-cresol was required to allow their solubilization. Polymerization of the A_2B monomers yielded HBPEs with lower molar masses than the AB_2 precursors (900-1 400 g.mol^{-1} *vs.* 3 700-3 900 g.mol^{-1}) highlighting the occurrence of aryl-aryl side reactions involving the bromide moieties.

2.1.2. Aromatic-aliphatic HBPEs

The introduction of alkyl chains in the backbone of precursors of aromatic HBPEs leads to a decrease in the glass transition temperature (T_g) of the resulting polymers enabling to perform their melt polycondensations at lower temperatures. For instance, Turner and coworkers described the synthesis of 5-(2-hydroxyethoxy)isophthalic acid (Scheme I-9, 21-8) by ethoxylating the phenolic alcohol of (21-2) with ethylene oxide.[39] Polymerization of this AB_2-type monomer was then conducted at 190°C in the melt-phase using dibutyltin diacetate (Bu_2SnAc_2) as catalyst. In these conditions, the formation of anhydrides usually observed during the polycondensation of 5-acetoxyisophthalic acid at 250°C and assigned to the occurrence of intermolecular dehydration side reactions, could be avoided. The so-formed aromatic-aliphatic HBPEs displayed equivalent branching density than their all-aromatic analogues (DB = 0.50), and reduced T_g to 150°C. The use of these carboxylic acid-ended HBPEs for the preparation of self-assembly films by an electrostatic layer-by-layer technique was incidentaly investigated.[83]

Other interesting aromatic-aliphatic HBPEs were prepared by Hawker and coworkers starting from different 4,4-bis(4'-hydroxyphenyl)pentadecanoic acid esters (21-9).[34,84] These AB_2-type monomers were found to undergo quasi-ideal statistical polycondensations with a very low tendency toward cyclization, less than 5%. The highest molar masses ($\bar{M}_w$) of 128 000 g.mol^{-1} and dispersity of 3.7, according to SEC-MALLS analyses, were achieved by heating the phenyl derivative under vacuum in the presence of cobalt acetate at 190°C during one hour and then 225°C during 2 hours. The DB determined by hydrolysis of the resulting HBPEs, was essentially the same (DB = 0.49), irrespective of the starting AB_2 monomers.

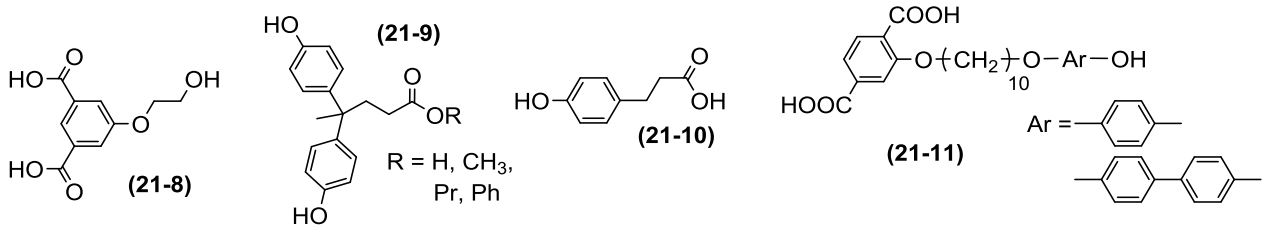

Scheme I-9. Examples of AB_2 and AB monomers for the synthesis of aromatic-aliphatic HBPEs

Schallausky and coworkers described an elegant route to tune the branching density as well as the thermal properties of aromatic-aliphatic HBPEs derived from (21-9) by copolycondensation with 3-(4-hydroxyphenyl)propionic acid (21-10).[42,85] The AB monomer was introduced in different proportions, up to 78 mol%. Copolymerizations of the AB_2 and AB monomers were carried out at room temperature in DMF in the presence of DCC/DPTS as condensing agents. The DB of the resulting copolyesters was shown to decrease with an increase in the content of AB monomers (Figure I-8). The thermal behavior of the HBPEs was influenced as well by the incorporation of AB units. While the glass transition temperature T_g was expected to decrease with increasing DB values, the opposite behavior was observed. Indeed, T_g values were found to decrease from 150 to 81°C with an increase in comonomer content (AB). This phenomenon was explained by the higher flexibility of the polymer structures following the incorporation of AB units. Very recently, Khalyavina and coworkers reported that the influence of the DB of hydroxyl-ended HBPEs on their glass transition temperature (T_g) can be completely overlapped by the hydrogen bonding effect.[86] Taking as examples two samples with identical amount of phenolic end-groups per unit, comparable T_g values of 155 and 152°C were obtained while these polyesters displayed completely different branching density, *i.e.* DB = 0.08 *vs.* 0.50.

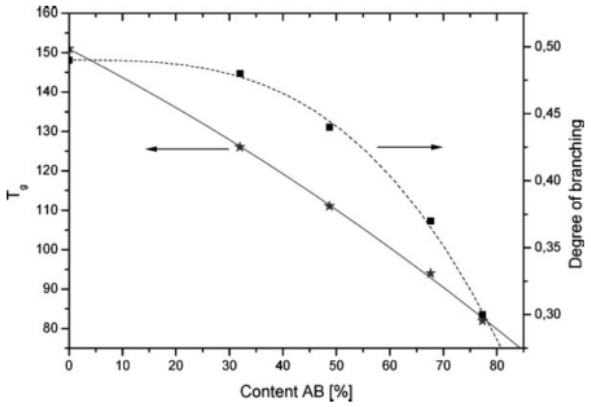

Figure I-8. Influence of the content in AB units on the DB and T_g of HBPEs prepared by polycondensation of 4,4-bis(4'-hydroxyphenyl)pentadecanoic acid and 3-(4-hydroxyphenyl)propionic acid[42]

The presence of rigid and flexible segments was even shown to endow aromatic-aliphatic HBPEs with liquid crystal (LC) properties.[87,88] For instance, Hahn and coworkers described the preparation and subsequent polycondensation of two AB_2-type monomers derived from terephthalic acid (Scheme I-9, 21-11). The so-formed HBPEs displayed molar masses of 7 000-15 000 $g.mol^{-1}$ but relatively low degree of branching (DB = 0.37-0.43) compared to previous literature. This was partly explained by the steric hindrance created by the alkoxy spacer substituent attached in *ortho* position of one of the carboxylic acid groups. The LC properties were investigated by DSC and optical microscopy. HBPEs with carboxylic acid end-groups were reported to form nematic phases above their glass transition temperatures, whereas their methyl ester counterparts did not show LC properties. This was likely due to the formation of hydrogen bonds between terminal moieties playing an important role in the mesophase formation.

2.1.3. Aliphatic HBPEs

As already mentioned, the field of aliphatic HBPEs is focused around 2,2-bis(methylol)propionic acid (bis-MPA), one easily available AB_2-type monomer bearing one carboxylic acid and two hydroxyl functional groups (Scheme I-10, 21-12). The first preparation of HBPEs derived from bis-MPA dated back to the 1990s. Since then, this system and its derivatives have been the subject of numerous investigations regarding their synthesis, properties, characterization, theory, modifications and applications. All the progress in this area has been well documented in recent reviews published by Žagar and Žigon,[89] and Malkoch and coworkers.[90]

2.1.3.1. Synthesis of HBPEs by polycondensation of bis-MPA

The synthesis of HBPEs derived from bis-MPA, *i.e.* poly(bis-MPA), was reported in absence or in the presence of core molecules.[38,91] In both cases, polymerizations were preferably performed in bulk, but solution polycondensations were also suitable. Malmström and Hult reported the self-polycondensation of bis-MPA, *i.e.* without any core molecule, in bulk using sulfuric acid as catalyst (Scheme I-10).[92] The low molar mass condensation product, here water, was first removed with argon flow at low conversions, and then under reduced pressure at higher conversions. Reaction temperatures were maintained in the range 140-170°C to avoid undesired reactions such as etherifications or transesterifications. The formation of insoluble materials was however observed for conversions in the carboxylic acid moieties higher than 90-92%.

Prior to gelation, HBPEs displayed low molar masses ($\bar{M}_n$) in between 1 000-2 500 g.mol^{-1} and very broad dispersities (up to 10). It was also shown that the self-polycondensation of bis-MPA followed second-order kinetics with respect to the carboxyl groups.

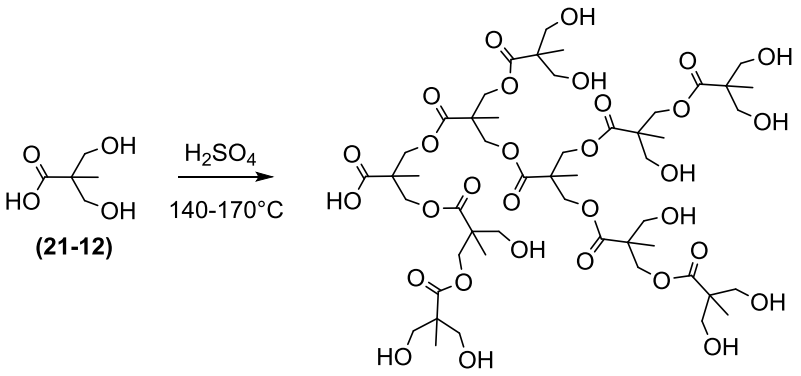

Scheme I-10. Self-polycondensation of bis-MPA using sulfuric acid as catalyst

The use of core moieties of B_f-type in the preparation of poly(bis-MPA) was shown to greatly reduce the risk of gelation. Hult and coworkers indeed described the polymerization of bis-MPA in the presence of tri(methylol)propane (Scheme I-11, TMP, 21-13) as B_3 core molecule.[93] Polycondensations were conducted in bulk using *p*-toluenesulfonic acid as catalyst at 140°C, which is below the melting point of bis-MPA, *i.e.* 190°C. The two-phase system obtained where bis-MPA slowly dissolved in a low-viscosity core melt instead of melting itself, was believed to improve the selectivity towards esterification polymerization. A pseudo-one step procedure was followed. Indeed, in order to keep the ratio of free bis-MPA to dendritic hydroxyl groups as low as possible, the AB_2 monomer was added in successive portions. The introduction of core resulted in HBPEs of higher molar masses in the range 3 000-6 000 g.mol^{-1} according to PS calibration, while dispersities were lower than 2 ($Đ$ = 1.36-1.92). Likewise, numerous other polyols were investigated as core molecules (Scheme I-11), PP50 being a mixture of molecules with various arm lengths.[92,94–96]

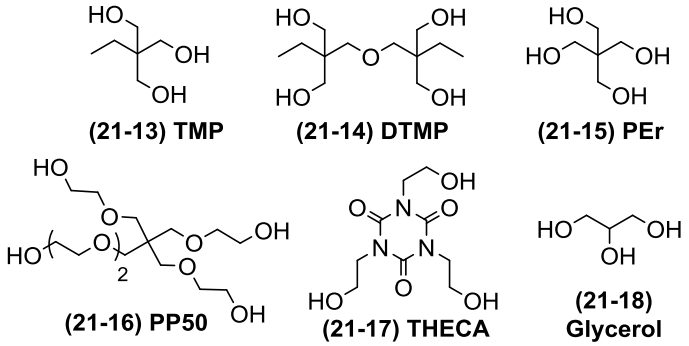

Scheme I-11. Polyol core molecules used in the synthesis of poly(bis-MPA): (21-13) tri(methylol)propane - TMP, (21-14) di(trimethylolpropane) - DTMP, (21-15) pentaerythritol - PEr, (21-16) PP50, (21-17) 1,3,5-tri(2-hydroxyethyl)cyanuric acid – THECA and (21-18) glycerol

The degree of branching of poly(bis-MPA) HBPEs was determined by ^{13}C NMR spectroscopy from the quaternary carbon signals, as shown in Scheme I-12.[93] HBPEs prepared by self-polycondensation of bis-MPA were found to display DB values of 0.35 and 0.32 according to Fréchet and Frey definitions, respectively, which is lower than the 0.5 predicted by the theory. Even if the occurrence of side reactions may contribute to the limitation of the DB, a negative substitution effect was highlighted by kinetics studies.[97] The formation of linear units was indeed found to be favored over dendritic ones. This phenomenon was explained by the lower reactivity of the hydroxyl groups in linear units due to steric hindrance.

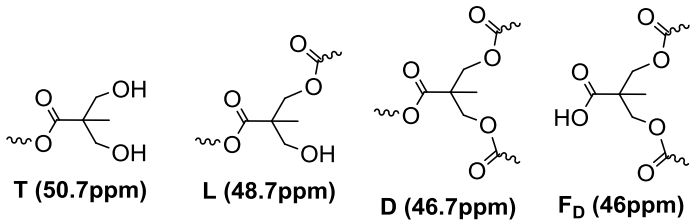

Scheme I-12. Structural units in poly(bis-MPA) HBPEs: (T) terminal, (L) linear, (D) dendritic and (F_D) focal units. In brackets are the quaternary carbon chemical shifts in ppm in the ^{13}C NMR spectra.

However, the DB of poly(bis-MPA) HBPEs was enhanced to 0.76 and 0.70, by polymerization of AB_4 preformed trimers of bis-MPA.[94] Unfortunately, the kinetics of polycondensation of the trimer moieties turned out to be very slow, which was justified by the lower accessibility of the carboxylic acid groups. Similarly, an increase in DB values up to 0.47 and 0.44 was noted for the polycondensation of bis-MPA with TMP core molecules and assigned to the pseudo-one-step procedure followed.

More recently, Fradet and coworkers demonstrated the high efficiency of imidazolium-based Brønsted acid ionic liquids (BAILs) as solvent and catalyst for the polycondensation of bis-MPA.[98] In less than 2 hours, in 3-butyl-1-(butyl-4'-sulfonic acid)imidazolium hydrogen sulfate ([BBSIm]HSO_4), aliphatic HBPEs with higher molar masses of 9 800-10 900 g.mol^{-1} ($\bar{M}_w$) and branching density (DB = 0.36-0.49) were achieved.

2.1.3.2. Synthesis of HBPEs by copolymerization of bis-MPA and AB monomers

Variations in the structure of poly(bis-MPA) HBPEs were brought by copolymerization with various AB monomers. As early as 1998, Hedrick and coworkers described the preparation of α-carboxylic-ω-dihydroxy functional AB_2-type macromonomers using oligomers of ε-caprolactone as linear segments and bis-MPA as branching points (Scheme I-13, 21-19, 21-20). Well-defined AB_2-type macromonomers were synthesized through the 'living' ring-opening polymerization (ROP) of ε-caprolactone using aluminium benzyloxide or tin octoate as intiators.[99,100]

Their subsequent polycondensations were reported, either at room temperature in the presence of DCC/DPTS as condensing agents, or at 110°C using *p*-TSA.[101] The so-formed HB poly(ε-caprolactone)s displayed higher molar masses than the homopolymers of bis-MPA (35 000 to 93 000 g.mol^{-1}), but a lower degree of branching (DB = 0.37). In addition, the introduction of linear segments was found to impact the thermal behavior of the materials. While poly(bis-MPA) HBPEs were amorphous with T_g values around 40°C, HB poly(ε-caprolactone)s displayed semi-crystalline properties with melting points (T_m) in the range 39 to 57°C. The same team further described the synthesis of one bis(hydroxymethyl)-substituted-ε-caprolactone (21-21).[102] Unlike previous literature, the self-polymerization of this 'AB*-B_2'-type monomer performed at 110°C in presence of catalytic amounts of $Sn(Oct)_2$, involved the ROP of the lactone ring. This route is discussed in more detail in the next section (see Chapter III.2.2).

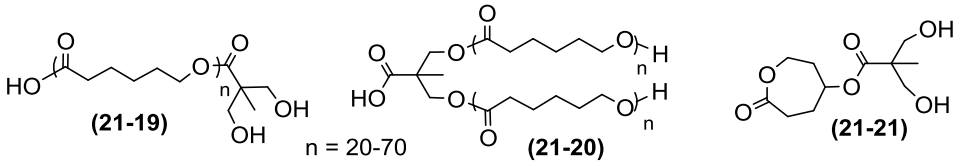

Scheme I-13. Macromonomers derived from bis-MPA and ε-caprolactone

Other long-chain branched copolyesters were prepared *via* the concurrent ROP/AB_2 polycondensation of ε-caprolactone and 2,2-bis(hydroxylmethyl)-butyric acid, using either enzymes, *i.e.* immobilized Lipase B[103] or $HfCl_4(THF)_2$ and diphenyl ammonium triflate as catalysts.[104] The same strategy was even implemented to synthesize HB poly(lactide)s.[105]

2.1.3.3. Side reactions in polycondensation of bis-MPA

In the 1990s, the use of aliphatic monomers for the preparation of HBPEs was somewhat debated due to their general tendency to undergo degradation side reactions upon thermal treatment, *i.e.* decarboxylation, cyclization or dehydration.[38] Indeed, the synthesis of poly(bis-MPA) HBPEs, with and without core molecules, was shown to be subjected to numerous side reactions. Most of them give rise to the formation of cyclic structures (Scheme I-14).

Cyclization can take place intramolecularly *via* the esterification reaction of the carbonyl group in the focal point with a hydroxyl function of the same HBPE molecule (**A**), but also *via* the etherification reaction between two hydroxyl groups (**B**). In addition, cyclic structures can be formed by intramolecular hydroxyl-ester interchange reactions. When this reaction occurs between groups of the same branch, it results in the formation of two species of lower molar masses, one of them containing a cyclic branch (**C**).

In contrast, this interchange reaction just leads to a rearrangement of the HBPE macromolecule and molar masses remain unchanged, when it takes place between two groups of different branches as shown in Scheme I-15 (D). Cyclization can reduce the molar masses and DB values achievable but does not explain the formation of cross-linked materials. Gelation is due to etherification reaction that takes place intermolecularly leading to more than one focal group per molecule (Scheme I-15, E).

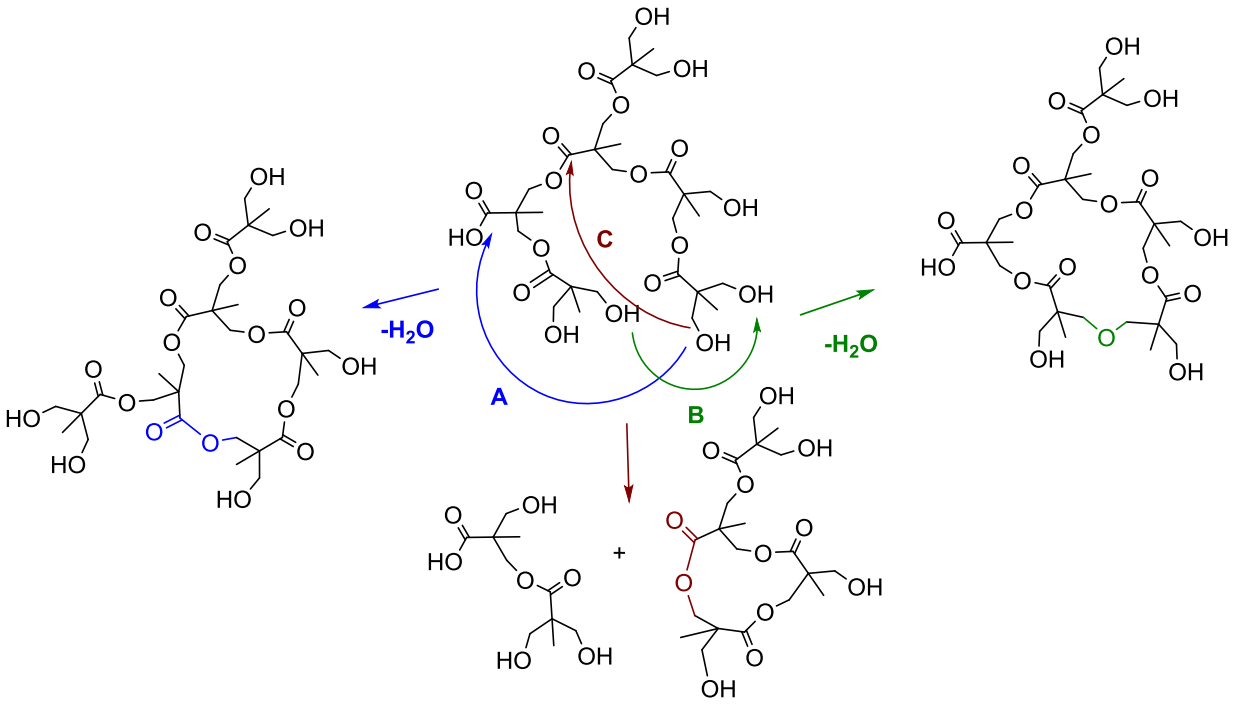

Scheme I-14. Possible side reactions in poly(bis-MPA) HBPEs leading to cyclization: (A) intramolecular esterification reaction, (B) intramolecular etherification reaction and (C) intramolecular hydroxyl-ester interchange between groups of the same branch

The role of cyclization in poly(bis-MA) HBPEs has been extensively studied, theoretically and experimentally. In 1999, Dušek and coworkers developed a kinetic model describing the polycondensation of bis-MPA without core molecules and demonstrated that: (1) at a given conversion, the fraction of HBPEs containing a cyclic branch increased with increasing degrees of polymerization and overall, (2) the molar ratio of the cyclic structures increased with the increasing conversion to converge to unity.[106] The occurrence of cyclization was then evidenced experimentally by ESI[107] and MALDI-TOF[108,109] mass spectrometry (MS). In both cases, some side populations were detected at *m/*z-18g.mol^{-1}, *i.e.* value indicating the elimination of water with respect to the set of peaks originating from the regular poly(bis-MPA) structure. However, MS alone did not allow identifying by which mechanism the cyclic structures were formed, pathways A, B and C, all leading to the same molar-mass decrease.

Burgath and coworkers used NMR spectroscopy and vapor pressure osmometry (VPO), in combination to MALDI-TOF MS, to investigate cyclization during the polycondensation of bis-MPA, in the presence of TMP and PEr as core molecules.[108] Molar masses calculated from ^{1}H NMR were systematically higher than the absolute values measured from VPO, suggesting the occurrence of cyclization reactions involving the focal point, *i.e.* through ester bonds. Žagar and coworkers implemented the same strategy building on absolute molar masses measured by SEC-MALLS.[107]

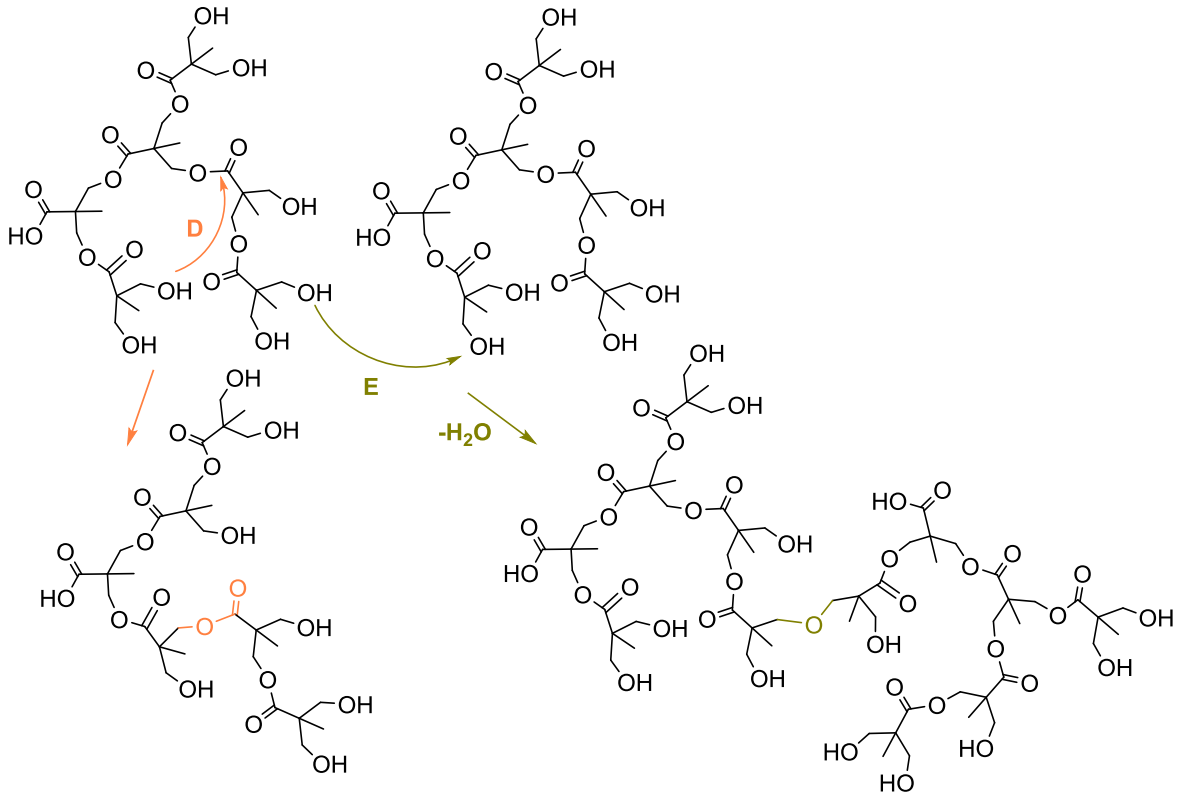

Scheme I-15. Possible side reactions in poly(bis-MPA) HBPEs: (D) intramolecular hydroxyl-ester interchange between groups of different branches and (E) intermolecular etherification reaction

The occurrence of intra/intermolecular etherification side reactions was revealed by ^{13}C NMR through the presence of characteristics signals of ether methylene carbons (-CH_2-O-CH_2-) at 72-73 ppm, and of the corresponding quaternary carbons at 49.3 and 47.3 ppm.[109,110]

Komber and coworkers determined the amount of ether side products by ^{1}H NMR after alkaline hydrolysis of some poly(bis-MPA) HBPEs.[110] In these conditions, all ester bonds were cleaved while the ether units remained stable. The molar content in ether bonds evaluated in between 1 to 12% was shown to depend on the catalyst and temperature of polymerization. Fradet and coworkers could differentiate the intermolecular from the intramolecular etherification process by MALDI-TOF MS analysis of HBPEs prepared by polycondensation of bis-MPA, in the presence of PEr as core molecule.[109]

Although the occurrence of all these side reactions was stated regardless the presence or not of a core molecule, these same core moieties have a role to play. For instance, while the extent of cyclization in poly(bis-MPA) HBPEs was lower with PP50 as core molecule compared to TMP, the risk of gelation proved higher with PEr in comparison to the self-polycondensation. Overall, side reactions were found to greatly reduce both molar masses and branching density achievable. One exception is the intermolecular etherification that particularly increased the weight average molar masses. Nowadays, there is a weak understanding of the gelation phenomenon. Apart from the fact that these etherification reactions were shown to rather occur at high reaction temperatures, long reaction times and high conversions in carboxylic acid groups, the formation of cross-linked materials remains an open issue.

2.2. Ring-opening multibranching polymerization

An alternative route to aliphatic HBPEs refers to as the ring-opening multibranching polymerization (ROMBP). This approach is based on the use of AB* monomers, also called as inimers, combining hydroxyl groups as initiating moieties (B) with lactones as polymerizable moieties (A). After catalytic activation of B groups, polymerization proceeds *via* a pseudo-chain growth mechanism involving the ring-opening polymerization of the cyclic moieties. Inimers thus represent latent AB_2-type monomers, the branching points being generated upon ring-opening.

One major advantage of the ROMBP approach compared to conventional polycondensation is the absence of condensation products facilitating the access to high molar mass HBPs with moderate dispersities. However, due to the low commercial-availability of heterocycles eligible for this pathway, only a few examples of HBPEs prepared by the ROMBP approach have been reported up to date. In every case, stannous octoate, $Sn(Oct)_2$, was used to catalyze the polymerization of lactone-based inimers.

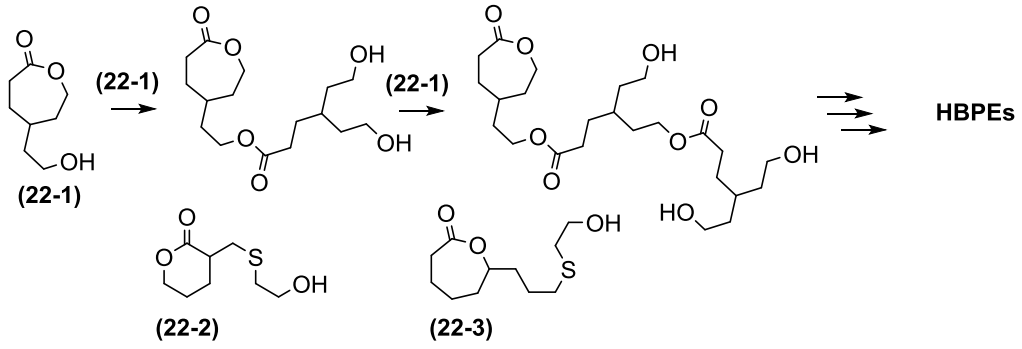

Scheme I-16. Examples of lactone-based inimers used in ROMBP

The first example dates back to 1999 when Fréchet and coworkers reported the synthesis of one monomer containing an *ε*-caprolactone ring as well as a primary alcohol group, *i.e.* the 4-(2-hydroxyethyl)-*ε*-caprolactone (Scheme I-16, 22-1).[111] Its subsequent polymerization carried out in bulk at 110°C in the presence of catalytic amounts of $Sn(Oct)_2$ (1 mol%) afforded HBPEs with molar masses ($\bar{M}_w$) of 65 000–85 000 g.mol^{-1} and a dispersity of 3.2. Lower loadings in stannous octoate gave higher molar masses, but for that purpose, prolonged reaction times were required. The chemical structure of the as-formed HBPEs was confirmed by MALDI-TOF MS, ^{1}H and ^{13}C NMR spectroscopies. This latter technique was successfully applied to determine the degree of branching. Calculated based on the definition established by Fréchet and coworkers (I-1), the DB was reported to equal the maximum theoretical value of 0.5.

Far more recently, Ritter and coworkers described the preparation of two hydroxyl-functionalized monomers by thiol-ene modification of six- and seven-membered unsaturated lactones (Scheme I-16, 22-2 and 22-3).[112] Both inimers were polymerized in similar conditions than 4-(2-hydroxyethyl)-*ε*-caprolactone to form the corresponding HBPEs. Only moderate molar masses ($\bar{M}_n$) in between 4 100-5 000 g.mol^{-1} ($Đ$ = 1.5-1.6), were achieved. DB values determined by ^{13}C NMR spectroscopy reached 0.66 and 0.64 with the valerolactone and caprolactone derivatives, respectively.

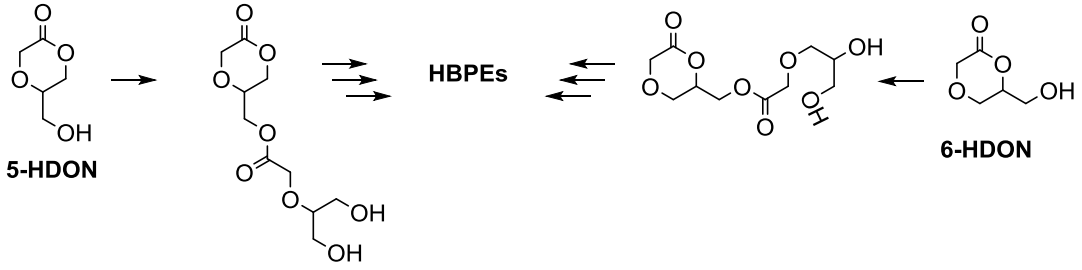

Scheme I-17. ROMBP of 5-HDON and 6-HDON for the preparation of HBPEs

Another interesting monomer was obtained by Zhuo and coworkers starting from glycerol *via* a four-step strategy (Scheme I-17).[113] The ROP of 6-hydroxy-methyl-1,4-dioxan-2-one (6-HDON) was conducted at 110°C in solution of toluene over longer reaction period, from 1 to 8 days. The related HBPEs displayed molar masses from 7 800 to 25 600 g.mol^{-1} with dispersities of 2-3 depending on the loading in catalyst. The best results were obtained for a concentration in $Sn(Oct)_2$ of 0.25 mol%. The lower DB values achieved of 0.4 according to ^{13}C inverse-gated NMR analysis were explained by the difference in reactivity between the primary alcohols of 6-HDON and the secondary ones formed upon ring-opening.

Likewise, Rokicki and coworkers reported the synthesis of 5-HDON and its application for the preparation of HBPEs by ROMBP (Scheme I-17).[114] This monomer was designed to ensure the exclusive presence of primary hydroxyl groups in the corresponding HBPEs. Primary alcohols endowed 5-HDON with a higher reactivity than 6-HDON, as confirmed in polymerization. Higher molar masses, in between 25 160-42 400 g.mol^{-1}, were reached in shorter reaction times from 1 to 3 days, by working at lower polymerization temperatures of 75-110°C. Lower dispersities of 1.74-2.01 were found as well. The branching density of the HBPEs could be tuned by the polymerization catalyst and/or reaction conditions. For instance, at 75°C, the organic base DBU appeared to favor the formation of highly branched architectures while $Sn(Oct)_2$-catalyzed ROMBP of 5-HDON yielded rather linear structures. An increase in the reaction time and/or temperature, however, promoted the branched structures with this metallic catalyst. HBPEs prepared by ROMBP of 5-HDON and 6-HDON were composed of glycerol and glycolic acid units, which make them potentially biodegradable and/ or biocompatible.

Similarly to the polycondensation of AB_n-type monomers route, variations into the structure of aliphatic HBPEs prepared by ROMBP were achieved by copolymerization with AB monomers. For instance, very recently, Fischer and coworkers reported the synthesis of HB poly(glycolide)s *via* the combined ROMBP of 5-HDON and glycolide, using $Sn(Oct)_2$ as catalyst.[115] The monomer to inimer ratio, *i.e.* 5-HDON/glycolide, allowed adjusting the chain length between every branching point, leading to a limitation of the solubility of the HBPEs at glycolide ratios above 70%. The relatively low DB values reached in between 0.23-0.36 implied the formation of long chain-branched copolyesters.

2.3. Copolymerization of symmetric monomer pairs: $A_2 + B_3$ approach

Due to the higher commercial availability of A_x and B_y ($x \geq 2$ and $y \geq 3$) monomers, the polymerization of *symmetric* monomer pairs has emerged as an interesting alternative to the conventional polycondensation of AB_n-type monomers to synthesize HBPEs. Among the various possible combinations, *e.g.* A_2 and B_4, A_3 and B_3, etc., the polycondensation of A_2 and B_3 monomers, also coined as the $A_2 + B_3$ approach, received significant attention in the last decade. The wide range of commercially available difunctional and trifunctional monomers bearing hydroxyl or carboxyl functions indeed allowed synthesizing a large variety of HBPEs, including all-aromatic, aromatic-aliphatic and aliphatic structures.

As highlighted previously, the A_2 + B_3 approach owns however one main drawback. According to Flory's theory, the formation of insoluble materials inevitably occurs above a critical conversion corresponding to the gelation point. Various methods were thus developed to avoid cross-linking and form soluble macromolecules of hyperbranched architecture. Key parameters to delay gelation include the A_2:B_3 ratio, the solution concentration, polymerization conversion and order of monomer addition.

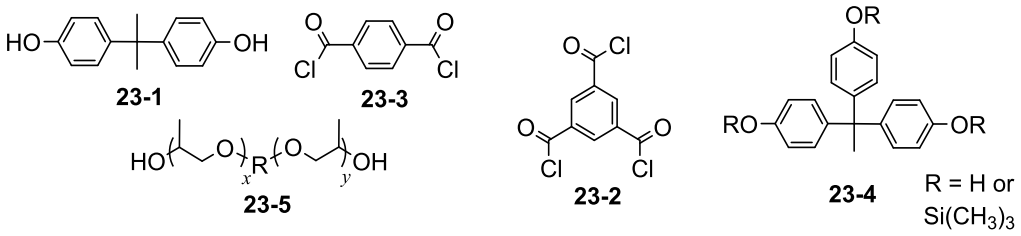

Scheme I-18. Examples of A_2 and B_3 monomers used for the synthesis of aromatic HBPEs

While a vast majority of HBPEs was synthesized in the melt phase due to the easy one-step process, the polycondensation of A_2 and B_3 monomers was preferably conducted in solution, the slow addition of monomers in dilute conditions allowing a better control over gelation. Long and coworkers reported the preparation of all-aromatic HBPEs by slow addition of a dilute solution of bisphenol-A (Scheme I-18, 23-1) as A_2 monomer to a dilute solution of 1,3,5-benzenetricarbonyl chloride (23-2) as B_3 counterpart.[116] The order of addition of the monomers was of high importance since the reverse yielded only cross-linked materials. Polycondensations were conducted at 25°C due to high reactivity of acyl chlorides, in chloroform using TEA as catalyst and maintaining the molar ratio A_2:B_3 at 1:1. Solution concentrations were hold around 0.08 mol.L^{-1} to avoid gelation. In these conditions, gel-free HBPEs with moderate molar masses of 3 300-9 300 g.mol^{-1} and branching densities of 0.47-0.55 were achieved.

Likewise, Voit and coworkers reported the synthesis of HBPEs with phenolic end-groups by polycondensation of terephthaloyl chloride (A_2, 23-3) with 1,1,1-tri(4-hydroxyphenyl)-ethane (B_3, 23-4) in solution of THF.[117] For comparison, the same HBPEs were synthesized in the melt-phase by polymerization of (23-3) and the silylated derivative of (23-4) at 145°C under dynamic vacuum. In both cases, various molar ratios A_2:B_3 of 3:2, 1:1, 3:4 and 1:2 were tested. This parameter was found to have a crucial influence on the properties of the resulting HBPEs. As the functionality ratio shifted towards the stoichiometric situation, *i.e.* A_2:B_3 of 3:2, polymers of higher molar masses ($\overline{M}_w$ = 11 000-28 000 g.mol^{-1}) and DB values in between 0.41-0.52 were achieved in good yields (> 80%). However, the risk of gelation increased as well to become unavoidable at the stoichiometric functionality ratio.

In this scenario, reactions were stopped before reaching the critical conversions corresponding to the gel points, that according to Flory's theory should occur at 70.7 and 86.6% conversion of A functionalities, respectively, for the 3:2 and 1:1 ratios of A_2:B_3. A close agreement was noted between gel points obtained experimentally and theoretically.[118] Overall, HBPEs prepared from solution polymerization tended to display at equivalent A_2:B_3 molar ratio, higher molar masses and branching density than samples synthesized in the melt-phase. By contrast, both products exhibited comparable T_g values of 210-220°C, no matter the synthetic route followed provided that their molar masses exceed 10 000 g.mol^{-1}.

A few studies still reported the successfull synthesis of HBPEs *via* the A_2 + B_3 approach in the absence of solvent. For instance, Unal and Long described the preparation of hyperbranched poly(ether ester)s by polycondensation of propylene glycol oligomers ($\bar{M}_n \approx 1060$ g.mol^{-1}, 23-5) as A_2 macromonomer, with trimethyl 1,3,5-benzenetricarboxylate, the methyl ester derivative of (23-2).[119] Transesterification polymerizations were carried out in bulk with a 1:1 molar ratio, using $Ti(OiPr)_4$ as catalyst at 150-180°C. Significantly high molar masses of 450 000 g.mol^{-1} ($\bar{M}_w$) and broad dispersity of 13.7, as determined by SEC-MALLS, were obtained by quenching the reaction immediately prior to gelation. Besides, the introduction of monofunctional end-capping agents such as poly(propylene glycol)monobutyl ether and dodecanol, either at the onset of polymerization or during the reaction allowed avoiding gelation up to 98% conversion.

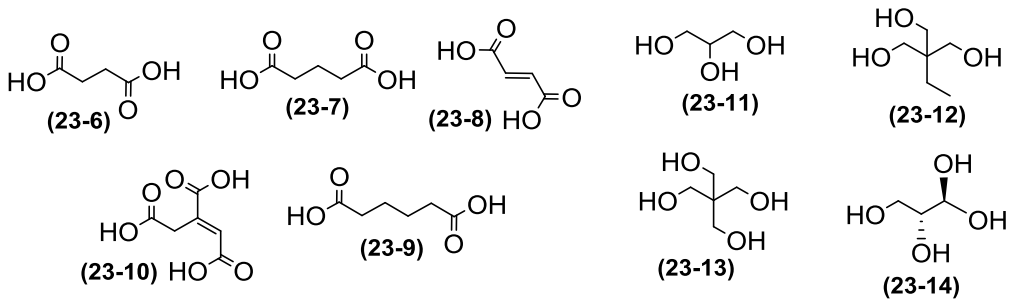

Scheme I-19. Examples of A_x and B_y monomers used for the synthesis of aliphatic HBPEs

Numerous aliphatic HBPEs were successfully prepared by polymerization of various A_x and B_y monomers in the melt. Some examples of diacids and polyacids, *i.e.* succinic (23-6), glutaric (23-7), fumaric (23-8), adipic (23-9) and aconitic acid (23-10), and polyols, *i.e.* glycerol, tri(methylol)propane, pentaerythritol, erythritol, are shown in Scheme I-19. A system that was particularly studied, involves adipic acid as A_2 monomer and glycerol as B_3 counterpart (Scheme I-20). Due to the unequal reactivity of its primary and secondary alcohols, glycerol rather acts as a B_2B^*-type monomer.

Stumbé and Bruchmann investigated the polycondensation of adipic acid with glycerol, in bulk at 150°C in the presence of catalytic amounts of dibutyltin oxide (DBTO) under reduced pressure.[120] Various molar ratios A_2:B_3, from 1:1, 1.2:1, 1.5:1 to 2:1, were tested. In any case, reactions were stopped after 6 to 8 hours as soon as the reaction mixture viscosities exceeded 5 000 mPa.s as measured at 100°C. The soluble HBPEs were obtained as clear and colorless viscous liquids. Molar masses ($\overline{M}_n$) and dispersities were found to increase with the A_2:B_3 ratio, from 1 750 to 3 050 g.mol^{-1} and 1.75 to 7.7, respectively. ^{13}C NMR spectroscopy gave DB values close to 0.48. Sebastian and Srinivas managed to reach significantly higher degree of branching up to 0.90 without gelation, by employing a series of Fe-Zn double-metal cyanide complexes (DMCs) as catalysts.[121,122] The micro-mesoporous architecture of DMCs was shown to act as a nano-reactor of the primary condensation of A_2 and B_3 molecules, forming AB_2 intermediates. Due to steric constraints, further polymerization continued outside the pores.

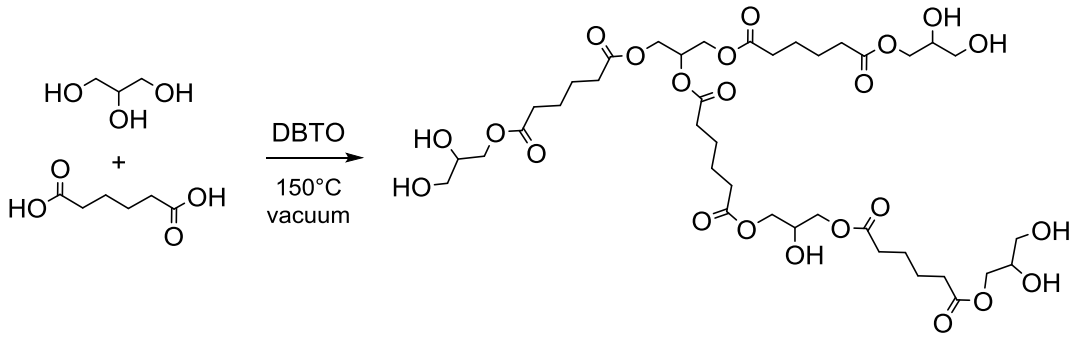

Scheme I-20. Synthesis of HBPEs *via* polycondensation of adipic acid and glycerol

More recently, Wyatt reported an efficient process of polymerization of glycerol with various diacids including glutaric, succinic and azelaic acid in solution of toluene.[123] Depending on the reaction conditions, soluble HBPEs with molar masses ($\overline{M}_n$) up to 445 000 g.mol^{-1} were achieved. The best results were obtained with glutaric acid with a molar ratio A_2:B_3 of 2:1 after 24 hours at 155°C.

Although only a few examples have been detailed in this study, the strength of the $A_x + B_y$ approach lies in the wide range of commercially available monomers, that allowed the synthesis of numerous HBPE structures, as recently reviewed by Kricheldorf.[124] The possibility to implement this same strategy with oligomeric precursors even enabled to tune in one-pot the distance between two branching points. Even though the risk of gelation is high, various efficient methods were developed to avoid the formation of 3D networks.

2.4. Copolymerization of asymmetric monomer pairs

In 2000, Yan and Gao set up another strategy to access HBPs, called the couple-monomer methodology (CMM). This approach consists in the copolymerization of *asymmetric* monomer pairs. Based on the unequal reactivity of its reagents, the formation of AB_n intermediates would predominantly occur *in situ*, in the early stage of polymerization, thereby suppressing any risk of gelation in comparison with the $A_2 + B_3$ approach. Two distinct strategies were investigated for the synthesis of HBPEs: the A* + B_n and AA*/A_2* + B_n approaches.

2.4.1. A* + B_n approach

The A* + B_n approach was first introduced by Kienle and coworkers as early as 1929.[27] However, at that time, only low molar mass products or insoluble materials were obtained. This strategy involves the copolymerization of dicarboxylic anhydrides (A*) with polyols (B_n) as shown in Scheme I-21. The A* monomer contains two latent functional groups, the second carboxylic acid function being formed after the reaction of A with B, giving rise to an AB_{n-1} intermediate.

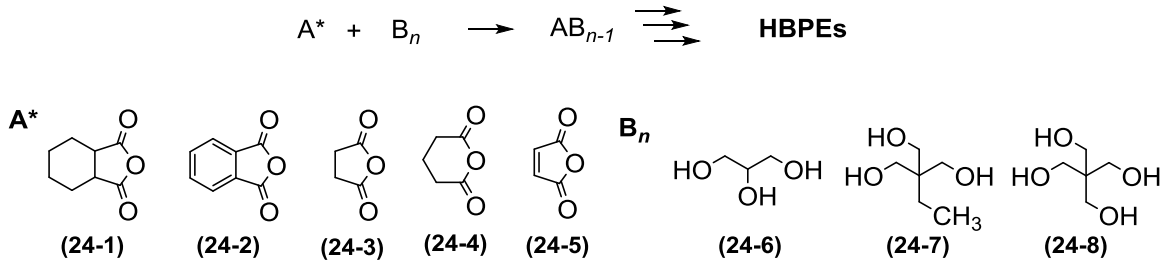

Scheme I-21. Examples of A* and B_n monomers used for the preparation of HBPEs

Various A* monomers were successfully used for the synthesis of HBPEs, including 1,2-cyclohexane dicarboxylic anhydride (24-1), phthalic anhydride (24-2), succinic anhydride (24-3), diglycolic anhydride (24-4) and maleic anhydride (24-5). In order to avoid network formation, it appeared crucial to remove water from the reaction mixture especially during the initial stage of polymerization. The presence of water, even as traces, indeed induced the ring-opening of the anhydrides, giving A_2 monomers and thus leading to insoluble materials within a couple of hours.

As a typical example, Gao, Yan and coworkers reported the preparation of HBPEs by polycondensation of succinic anhydride (24-3) with tri(methylol)proprane (24-7), as shown in Scheme I-22.[125] Only moderate molar masses ($\bar{M}_n$), *i.e.* in between 5 000-20 000 g.mol^{-1}, were achieved even after prolonged reaction times up to 10-20 hours at 140-150°C.

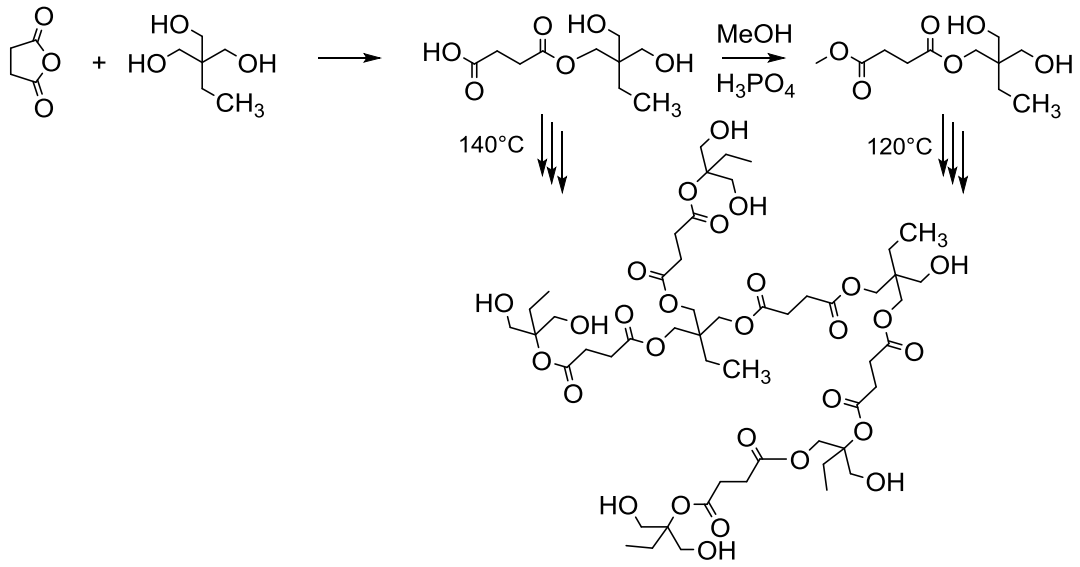

Scheme I-22. Synthesis of HBPEs by polycondensation of succinic acid and tri(methylol)propane

Polymerization of the A* and B_3 monomers was also attempted in the presence of methanol. In this case, AB_2-type intermediates predominantly formed *in situ* feature one methyl ester and two hydroxyl groups. In comparison, HBPEs prepared by the 'transesterification' route in milder reaction conditions, *i.e.* 120°C, displayed higher molar masses (30 000-120 000 g.mol^{-1}).

2.4.2. AA*/A_2* + B_2 approach

In the same vein, AA*-type monomers bearing one carboxylic acid and one anhydride functional group, such as benzene-1,2,4-tricarboxylic acid-1,2-anhydride (Scheme I-23, 24-9), were successfully copolymerized with various α,ω-diols (B_2) including 1,4-butanediol (24-13), 1,8-octanediol (24-14) and triethylene glycol (24-15).[126] Due to the higher reactivity of the anhydride over the carboxylic acid function in condensation, polymerization proceeds *via* the formation of A_2B-type intermediates featuring two carboxylic acid and one hydroxyl groups.

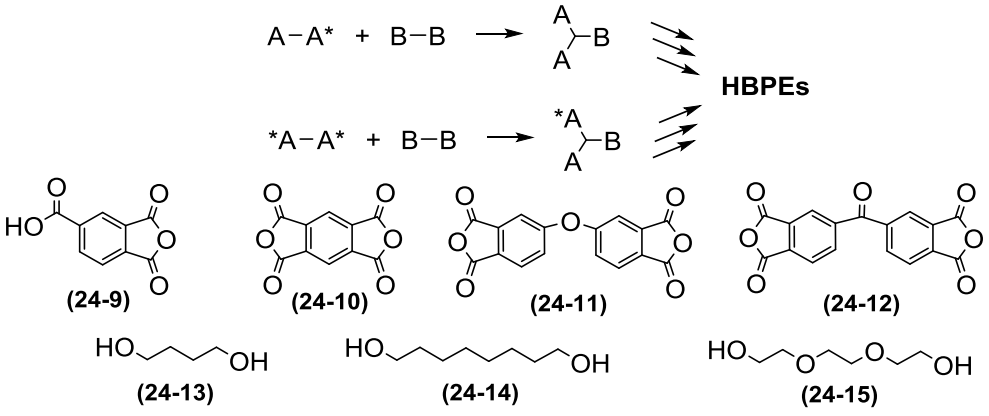

Scheme I-23. Examples of AA*, A_2* and B_2 monomers used for the preparation of HBPEs

Likewise the same strategy was implemented with A_2* monomers bearing two anhydride groups as reactive functions, such as pyromellitic dianhydride (24-10), 4,4'-oxydiphthalic anhydride (24-11) and benzophenone-3,3',4,4'-tetracarboxylic anhydride (24-12).

2.5. Conclusion

The purpose of this discussion was to provide an overview of the principle synthetic approaches developed over the past decades to prepare HBPEs. This review is certainly not exhaustive, but the intention was to illustrate the main advantages, drawbacks and limitations of each synthetic methodology, through representative examples.

Initially discussed was the conventional polycondensation of multifunctional AB_n-type monomers bearing carboxyl and hydroxyl units, as reactive functions. Theoretical as well as application aspects of this approach were extensively studied over the past 25 years. Polymerization kinetics was theorized and used to accurately calculate molecular parameters (DB, $\bar{M}_n$, $Đ$) at any point of conversion. Deviations from the theory were usually noticed and assigned to the occurrence of numerous unavoidable side reactions limiting the molar masses and degrees of branching achievable as exemplified with poly(bis-MPA) HBPEs. The synthesis of a large variety of HBPEs has been reported by polycondensation of mostly AB_2-type monomers. Variations into the structure were achieved by introduction of core molecules or copolymerization with various AB-type monomers.

HBPEs were prepared as well by copolymerization of symmetric monomer pairs. The higher commercial availability of A_2 and B_n-type precursors, compared to AB_n-type monomers, made this approach very attractive despite the high risk of gelation. More recently, new synthetic strategies including the ROMBP and copolymerization of asymmetric monomer pairs, *i.e.* A* + B_3, AA*/A_2* + B_2, broadened the structural variety of HBPEs. The overall trend is nowadays turned towards the dilution of the branching pattern by combination with linear segments yielding increasingly complex "linear-branched hybrid structures".

The present discussion was limited to the four main synthetic approaches giving access to HBPEs, but other more anecdotal pathways have been reported, including some specific combinations of CMM, *i.e.* A_2 + B'B_2 and A_2 + B_2 + B'B_2 approaches, and even click chemistry.

3. Towards vegetable oil-based HBPEs

Growing attention has been focused in recent years on polymers from renewable resources, but this concept has no merit of being new. The first examples of bio-based polymers date back to the 19th century with the synthesis of celluloid and vulcanized natural rubber. At that time, the demand in basic chemicals was largely satisfied by renewable feedstocks. However, with the petrochemical revolution of the 20th century, the production of polymers from fossil resources experienced an exponential growth. Nowadays, the trend is the opposite. In both a context of price fluctuations and uncertain supply of oil and gas, combined with environmental concerns (global warming, waste production, etc.), a renewed interest is driven to bio-based polymers. The use of renewable resources contributes to a sustainable development, understanding as "*acting responsibly to meet the needs of the present without compromising the ability of future generations to meet their own needs"*.[127] Biomass covers all plant renewable resources including carbohydrates (cellulose, hemicelluloses and starch), lignin, terpenes, proteins and vegetable oils. Each of these components can be chemically modified into a large range of precursors of bio-based polymers. Biomass also covers animal resources, but these latter are out of the scope of this thesis.

Overall, the use of renewable resources for the synthesis of HBPs has rarely been described in sharp contrast to their linear analogues. The oldest examples refer to hyperbranched *polypeptides* derived from naturally occurring AB_2-type amino-acids such as L-aspartic acid, L-glutamic acid and L-lysine (Scheme I-24, 30-2, 30-1, 30-3). The thermal polymerization of this latter monomer was described in detail.[128,129] Due to the asymmetric reactivity of its two amine groups, the branching density of hyperbranched polylysines was shown to be modulated by the reaction conditions, and notably the introduction of temporary protecting groups. Hypergrafts and other branched polyamides have also been prepared following iterative strategies based on the ROP of α-amino acid *N*-carboxy anhydrides (Scheme I-24, NACs, 30-4).[130]

The interest in hyperbranched *glycopolymers* steadily increased as well. Due to their biocompatible character, these materials showed high potential in biotechnology, medicine and food industry. Some highly branched glycopolymers were prepared by the incorporation of carbohydrates units in preformed HBPs as reviewed by Voit and coworkers.[131] The synthesis of hyperbranched polysaccharides from natural[132] or chemically modified saccharides (oxazoline[133] and anhydrosugars[134], Scheme I-24, 30-5) has also been reported.

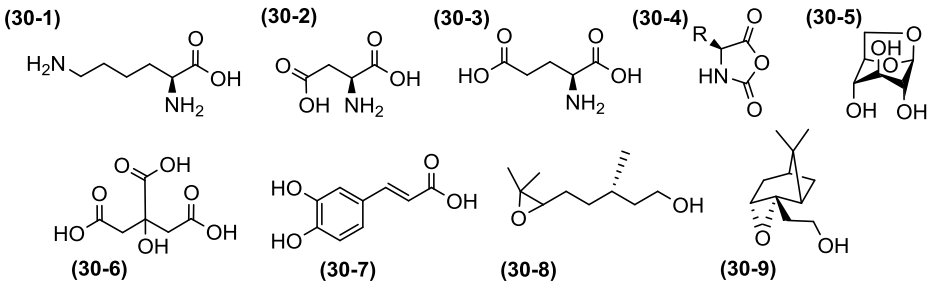

Scheme I-24. Multifunctional precursors of bio-based HBPs: (30-1) L-lysine, (30-2) L-aspartic acid, (30-3) L-glutamic acid, (30-4) NAC, (30-5) anhydrosugar, (30-6) citric acid, (30-7) caffeic acid, (30-8) citronellol oxide and (30-9) nopol epoxide

Only one example of cellulose-based HBPs was recently published. This was achieved by the polycondensation of AB_n-type monomers prepared from the reaction of acetylated oligomeric cellulose bromide with tyrosine.[135] Other bio-based HBPs worth pointing out include those obtained from citric acid (Scheme I-24, 30-6), caffeic acid (30-7) and terpenes. Citric acid is a tricarboxylic acid with a sterically hindered hydroxyl group. Since it decomposes slightly above its melting point (175°C), this AB_3-type monomer was rather involved in the preparation of copolyesters with various polyols, including glycerol.[136] Caffeic acid is a naturally occurring AB_2-type monomer, key intermediate in the biosynthesis of lignin. Some interesting recent studies deal with its copolymerization with various bio-based AB synthons including p-coumaric,[137] lithocholic[138] and 10-hydroxycapric[139] acids yielding photocrosslinkable polyesters of high thermal stability. Kaneko and coworkers even described the preparation of thermotropic liquid crystalline polymers by the acid-catalyzed polycondensation of caffeic and ferulic acids.[140] Lastly, hyperbranched *polyterpene alcohols* were successfully prepared by the cationic ROP of citronellol oxide and nopol epoxide (30-8 and 30-9).[141]

The next section discusses examples of vegetable oil-based HBPEs. Among renewable resources, plant oils represent one of the most promising raw materials owing to their abundant availability, relative low cost and inherent biodegradability. The use of vegetable oils in polymer chemistry has been extensively investigated and the synthesis of a plethora of polymeric materials (thermoplastics, thermosets) demonstrated.[142–144] Fatty acid derivatives already provide ester functions and unsaturations that are prone to functionalization. The following discussion covers the recent developments in the chemical modification of vegetable oils aiming at designing strategic multifunctional precursors of HBPEs, *i.e.* diesters, diols (even polyols) and hydroxyesters; and when appropriate the synthesis of the related HBPEs are described.

3.1. Vegetable oils: composition and production

Vegetable oils are composed of different triglycerides resulting from the esterification of glycerol with three fatty acids (FAs, Figure I-9). The fatty acids account for 95% of the total weight of triglycerides and their content is characteristic of each plant oil. Common FAs present chain lengths from 14 to 22 carbon atoms with 0 to 3 unsaturations and are termed by the shorthand notation "*number of carbon atoms*: *number of double bonds*". For instance, oleic acid which is a monounsaturated FA bearing 18 carbon atoms is abbreviated as C18:1. Some FAs like ricinoleic and vernolic acids bear other types of functionalities, respectively hydroxyl and epoxy groups. Table I-3 summarizes the FA composition of some industrial vegetable oils with the chemical structure of the main unsaturated FAs.

Table I-3. FA composition of the main industrial vegetable oils

	16:0	16:1	18:0	18:1	18:1 OH	18:2	18:3	20:0	20:1	22:1
Canola	4.1	0.3	1.8	60.9	-	21.0	8.8	0.7	1.0	-
Corn	10.9	0.2	2.0	25.4	-	59.6	1.2	0.4	-	-
Linseed	5.5	-	3.5	19.1	-	15.3	56.6	-	-	-
Olive	13.7	1.2	2.5	71.1	-	10.0	0.6	0.9	-	-
Palm	44.4	0.2	4.1	39.3	-	10.0	0.4	0.3	-	-
Soybean	11.0	0.1	4.0	23.4	-	53.2	7.8	0.3	-	-
Sunflower	6.1	-	3.9	42.6	-	46.4	1.0	-	-	-
Sunflower high oleic	6.4	0.1	3.1	82.6	-	2.3	3.7	0.2	0.4	-
Rapeseed high erucic	3.0	-	1.0	16.0	-	14.0	10.0	-	6.0	50.0
Castor	0.5-1	-	0.5-1	2-6	85-95	1-5	0.5-1	-	-	-

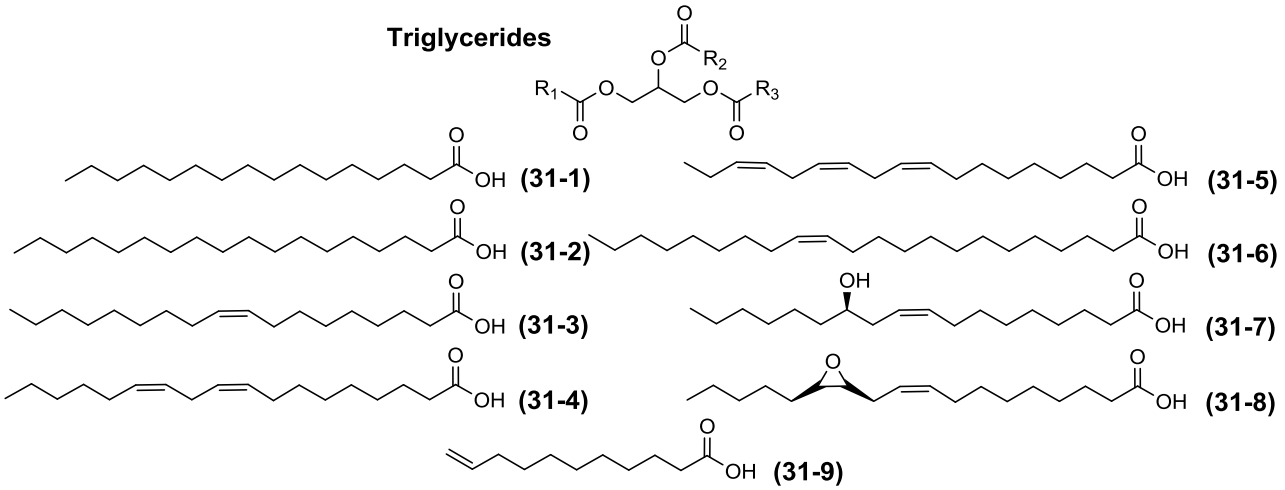

Figure I-9. Chemical structure of triglycerides and common FAs found in vegetable oils: (31-1) palmitic acid, (31-2) stearic acid, (31-3) oleic acid, (31-4) linoleic acid, (31-5) linolenic acid, (31-6) erucic acid, (31-7) ricinoleic acid, (31-8) vernolic acid and (31-9) undecenoic acid.

Apart from the plant, the FA composition of vegetable oils depends on numerous external factors including the crop and its location, the growing conditions, the season and the year.[145] Fatty acids (FAs) and fatty acid methyl esters (FAMEs) can be recovered and purified from vegetable oils respectively by saponification and transesterification with methanol in such purity that they can be used as polymer precursors by chemical conversions. Among commercially available FA derivatives, undecenoic acid should be mentioned (Figure I-9, 31-9). This useful shorter FA (C11:1) is obtained by steam cracking of ricinoleic acid.

Vegetable oils, which are annually renewable, are one of the most important sustainable raw materials for the chemical industry. Their abundant availability with an annual world supply and distribution of 176 million tons in 2014/2015, 20 million tons more than in 2012/2013,[146] and relative low cost make them industrially attractive. Besides, their inherent biodegradability is an asset to this sustainable development approach. About 20% of the global production is devoted to industrial applications, mainly as source of energy (fuels) but also as raw materials for the manufacture of surfactants, lubricants, paint formulations, cosmetic products, coatings and resins; compared with around 75% and 5% for food and feed uses, respectively.[147] The production of biodiesel experienced an exponential growth in recent years, and thus the production of glycerol as co-product has surpassed 2 million metric tons. Glycerol was already widely used in the cosmetic, pharmaceutical and food industries. Nevertheless, in the past few years, growing interest has been focused on the research of new uses to deal with the high volume availability of this product.[148,149]

Three main approaches have been considered to synthesize polymers from vegetable oils.[150] The first two routes consist in the use of triglycerides taking advantages of either the natural occurring functions, *i.e.* double bonds and hydroxyl groups; or after chemical modifications introducing targeted functional groups. Both approaches generally end-up with cross-linked polymers which constitute materials of interest for coating and resin applications. The main drawback of these routes is the lack of control on the network properties due to the heterogeneity and variability of the triglyceride substrates. The third approach relies on the chemical modification of purified FAs or FAMEs to design well-defined precursors of thermoplastic polymers. From these three approaches, a large range of thermoplastics and thermosets including polyesters, polyethers, polyurethanes, polycarbonates, etc. were developed.[142,143]

3.2. Derivatization of vegetable oils to HBPEs

As mentioned above, the synthesis of vegetable oil-based HBPEs remained scarce. This topic has been besides partly addressed in recent reviews focusing on sustainable[151] and oily-derived[144] polyesters. Two main routes have been developed to access oily-derived HBPEs, *via* either the homopolymerization of hydroxyester monomers of AB_n-type or the copolymerization of α,ω-diacids (diesters) with glycerol. The following discussion summarizes recent advances in the field of HBPEs based on vegetable oils, and outlines the literature on the derivatization of triglycerides and FA derivatives with ester and hydroxyl functions. The examples focus on the synthesis of diesters and hydroxyesters as multifunctional precursors of HBPEs. The reactive sites in triglycerides and FA derivatives available for chemical modifications include the carbon-carbon double bonds, the allylic carbons, the ester groups, the carbons in α-position of the ester groups and in some cases, the hydroxyl and epoxide moieties.

3.2.1. $A_2 + B_3$ approach

As highlighted previously (Chapter I, section 2.3), recent research reported the synthesis of a series of glycerol-based polyesters of hyperbranched architecture with various diacids, mainly short ones, *e.g.* succinic, adipic or phthalic acids, and even anhydrides. In this section, attention is focused on the α,ω-dicarboxylic acids of medium to long chains derived from vegetable oils. Note that this literature study is restricted to examples actually giving rise to soluble HBPEs, and not to gelled products.

In 2006, BASF patented a process for producing HBPEs by means of enzymatic esterification.[152] Among the examples of the invention, the copolymerization of glycerol with azelaic acid, one nine-carbon diacid obtained by ozonolysis of oleic acid, was described in detail with a stoichiometry of 1:1.2 using 10-15 wt% of Novozym®435 (*Candida Antartica* Lipase B) as catalyst. After 5 days at 70°C under atmospheric pressure in solution of dioxane, a colorless oil was obtained with molar masses ($\overline{M}_n$) of 4 800 g.mol^{-1} and fine dispersity ($Đ$ = 1.8). Not to be confused, only low molar mass prepolymers were prepared by polycondensation of glycerol with sebacic acid for cross-linking in a second step. This ten-carbon diacid is produced by alkali pyrolysis of ricinoleic acid. Polyglycerol sebacate is indeed a biocompatible and bioresorbable material, showing potential applications in the biomedical field.[153]

Another interesting diacid was obtained by Gross and coworkers *via* the biochemical conversion of oleic acid with *Candida tropicalis* (Scheme I-25).[154] While DBTO showed poor activity to catalyze the polycondensation of 1,18-cis-9-octadecenedioic acid and glycerol ($\bar{M}_n$ < 1 750 g.mol^{-1}), the synthesis of poly(oleic diacid-co-glycerol) was reported to be highly efficient with Novozyme®435 and produced high molar mass HBPEs ($\bar{M}_n$ = 6 000-10 000 g.mol^{-1}). This result was somewhat surprising owing to the well-known regioselectivity of the Lipase B for primary alcohols. However, Gross and coworkers demonstrated just a few years earlier, that polyesters of hyperbranched architecture can be obtained by the Novozyme 435-catalyzed polycondensation of glycerol and adipic acid simply after prolonged reaction times up to 42 hours.[155] But actually, in the early stages of polymerization, *i.e.* the first 18 hours, only linear copolyesters were formed.

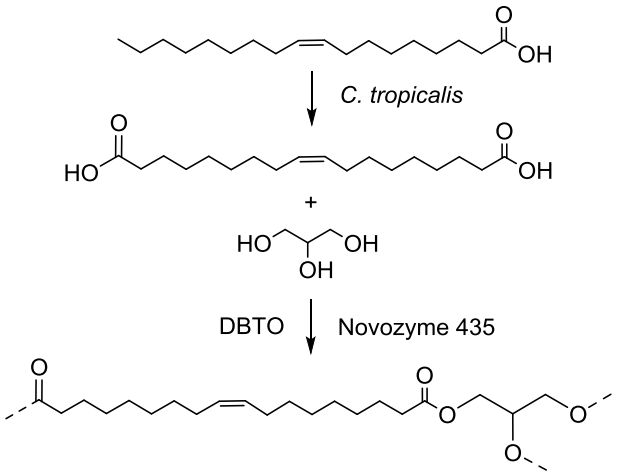

Scheme I-25. Biochemical conversion of oleic acid into 1,18-cis-9-octadecenedioic acid and subsequent polycondensation with glycerol

Further diversification of the poly(oleic diacid-co-glycerol) structure was achieved by altering the stoichiometry of oleic acid to glycerol from 1:1 to 1.5:1. The as-formed HBPEs exhibited DB values in the range 0.13-0.31, good thermal stabilities with $T_d^{5\%}$ above 384°C and interestingly, a semi-crystalline character with multiple melting peaks in between -32.6 and -6.9°C. These studies constitute the only examples of the preparation of vegetable oil-based HBPEs through the $A_2 + B_3$ approach.

3.2.2. Polycondensation of AB_n monomers

The synthesis of vegetable oil-based HBPEs by polycondensation of AB_n-type monomers requires the preparation of precursors bearing both hydroxyl and ester functions in their structures. For that purpose, three different methods were investigated. Meier and Li's groups, both used the *thiol-ene addition* of 1-thioglycerol on methyl 10-undecenoate to prepare the following AB_2 monomer (Scheme I-26).[156,157] The most efficient route with a 95% yield achieved in less than one hour, was developed by Bao and Li. The reaction was carried out at room temperature under UV irradiations (λ = 365nm), in the presence of a catalytic amount of photoinitator, the 2,2-dimethoxy-2-phenylacetophenone (DMPA).

Türünç and Meier performed the subsequent polycondensation of this AB_2-type monomer, with and without glycerol as core molecule, using TBD as catalyst at 120°C resulting in HBPEs with moderate molar masses ($\bar{M}_n$ = 3 500-4 400 g.mol^{-1}, $Đ$ = 1.87-2.85). Li and coworkers achieved significantly higher molar masses ($\bar{M}_n$ = 11 400-60 400 g.mol^{-1}) and broader dispersities ($Đ$ = 5.2-25.3) using a metallic catalysis based on $Ti(OBu)_4$, Sb_2O_3 or $Zn(OAc)_2$ working at 160-170°C. DB values determined by quantitative ^{13}C NMR were in between 0.38-0.54, which is in agreement with the 0.5 predicted by the theory. Generally, branching completely prevents crystallization but these HBPEs exhibited in both cases a semi-crystalline character with melting points in between 40 and 51°C. This interesting behavior was assigned to the long aliphatic chain between two branching points.

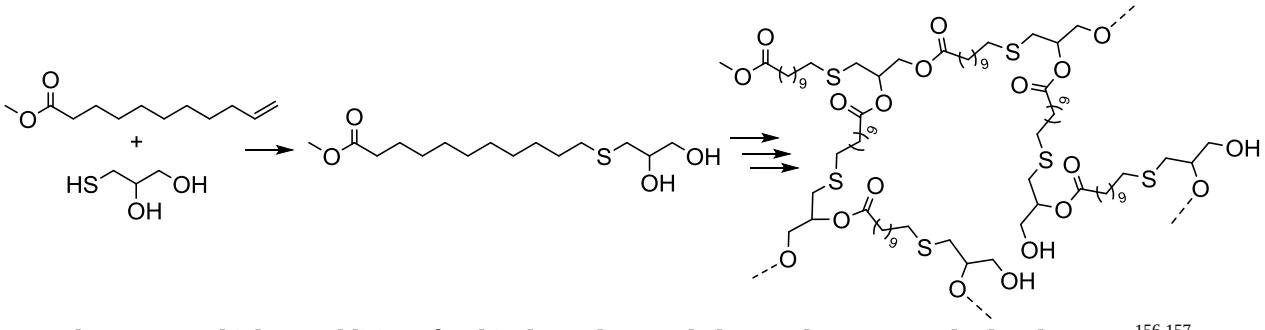

Scheme I-26. Thiol-ene addition of 1-thioglycerol on methyl 10-undecenoate and related HBPEs[156,157]

Parzuchowski and coworkers described the 4-step synthesis of another interesting AB_2-type monomer (Scheme I-27), the latter stage consisting in the thiol-ene addition of ethyl mercaptoacetate on an allylic derivative of glycerol. Its polycondensation was investigated under various conditions. While tin-based catalysts such as $Sn(Oct)_2$ or Bu_2SnO yielded rubber-like gels above 120°C, HBPEs with molar masses ($\bar{M}_n$) of 2 600-3 900 g.mol^{-1} and DB values in the range 0.44-0.52 were achieved with the Chirazyme L1 at 90°C.[158]

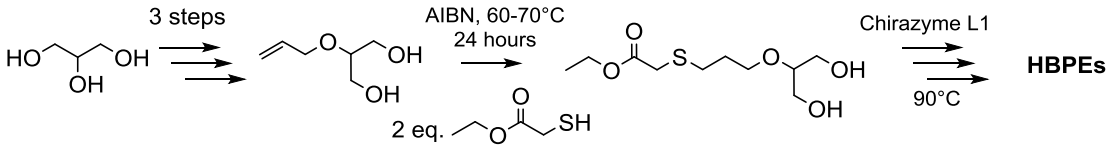

Scheme I-27. Ethyl{3-[2-hydroxy-(1-hydroxymethyl)ethoxy]propyl}thioacetate synthesis and related HBPEs

To target industrial applications, Petrović and coworkers reported an elegant route to hydroxylated fatty-acid methyl esters by hydrogenation and subsequent methylation of commercial epoxidized soybean oil (SBO, Figure I-10).[159] This process ended-up with a mixture of saturated (A, 14%), monohydroxylated (AB, 28%), dihydroxylated (AB_2, 54%) and trihydroxylated (AB_3, 3%) derivatives. The same mixture was copolymerized with methyl esters of castor oil (MECO), whose main component is methyl ricinoleate (AB, 90%) with a weight ratio of 60:40. Polyesters with moderated molar masses ($\bar{M}_n$ = 3 000g.mol^{-1}) and a rather linear structure were obtained within 9.5 hours at 200°C with $Ti(OiPr)_4$ as catalyst. These polyols were used in polyurethane flexible foams.

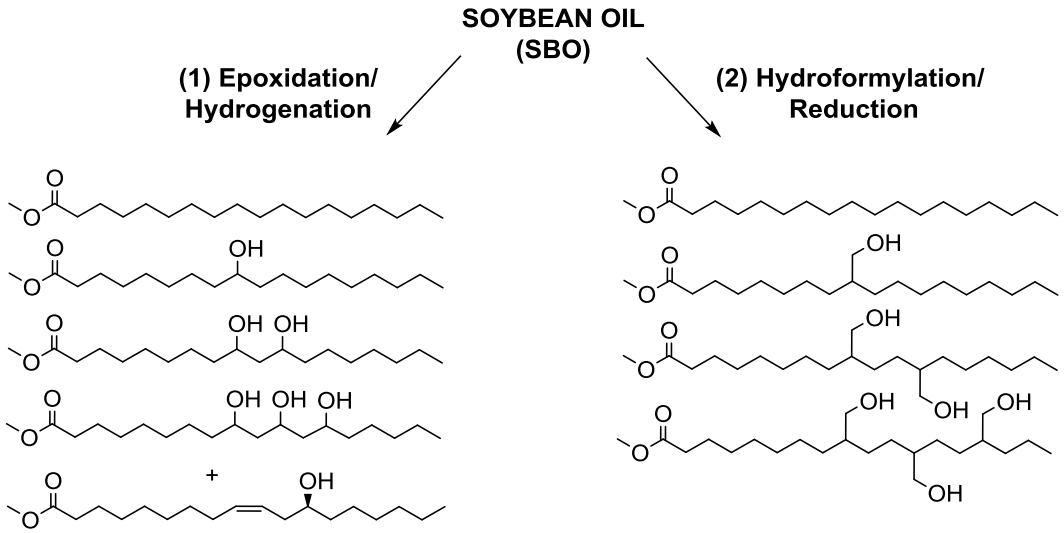

Figure I-10. Synthesis of branched polyesters by (1) epoxidation/ hydrogenation and (2) hydroformylation/ reduction of soybean oil (SBO)

The same group described the preparation of HBPEs with significantly higher molar masses up to 42 000 g.mol^{-1}, by transesterification of FAMEs, prepared by *hydroformylation* and subsequent methylation of SBO.[160] This route brings primary alcohols to FA derivatives that are more reactive than secondary ones (Figure I-10). High values of weight average functionality (f_w) were thus achieved, up to 23.2, despite the considerable amount of unsaturated and monohydroxylated components in the initial mixture (≈ 43%). In addition, the solution properties of these HBPEs were investigated by multiple-detection SEC in THF (light scattering, differential refractometer and viscosimetry detectors).[161] As expected, the

HBPEs exhibited a more compact and globular architecture than their linear analogues of the same molar masses, as well as a lower viscosity. Batch mode LS experiments were carried out to estimate the polymer-solvent interactions. Values achieved for the second viriel coefficient (A_2) were slightly positive, in the range 10^{-4} mol.mL.g^{-2}.

3.2.3. Other methodologies

Other remarkable routes have been investigated such as the Acyclic Triene Metathesis (ATMET) polymerization. This technique developed by Metzger and coworkers, was applied to high oleic sunflower oil (HOSO) to produce highly branched polyesters in solvent free conditions (Scheme I-28).[162] When the Hoveyda-Grubbs 2nd generation catalyst was used, triglycerides were copolymerized with methyl acrylate (MA) to prevent gelation. The initial ratio between triglycerides and MA was used to tune the molar masses of the prepared HBPEs. Maximum values of 5 000 g.mol^{-1} ($Đ$ > 20) were reached in nearly equimolar amounts (1:1.1). The homopolymerization of HOSO was achieved without the addition of chain stopper, using the 1st generation Grubbs catalyst.

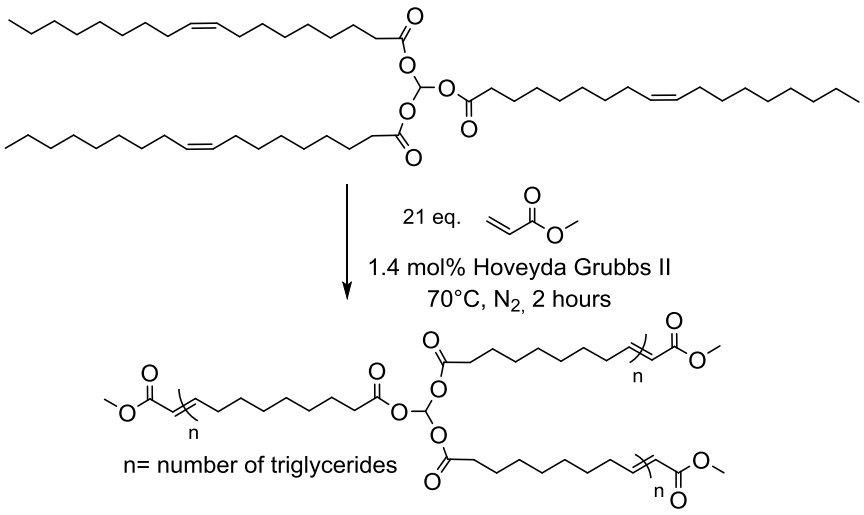

Scheme I-28. Acyclic triene metathesis polymerization of HOSO with MA as chain stopper

More recently, Araújo and coworkers performed the acyclic triene metathesis (ATMET) polymerization of linseed oil, *i.e.* whose main components are linoleic (18:2) and linolenic (18:3) acids, in miniemulsion evaluating the activity of different types of ruthenium-based catalysts.[163] Miniemulsion polymerizations with nonionic surfactants, *i.e.* Tween 80, Lutensol AT80, resulted in polymer nanoparticles with an average size around 200 nm. Molar masses, up to 5 800 g.mol^{-1} ($Đ$ = 1.6-3.1), were achieved with Umicore M2 and Hoveyda-Grubbs 2nd generation catalysts. Interestingly, gelation was not observed. The presence of oleic acid moieties and saturated fatty acids in linseed oil, acting as chain-stoppers, was indeed found to limit cross-linking.

Vilela and coworkers reported an innovative approach to thermo-reversible HBPs containing ester and imide linkages (Scheme I-29).[164] To this end, various multifunctional precursors were synthesized based on castor oil, *i.e.* methyl 10-undecenoate, and furan-derivatives including some bisfurans (A_2) and trismaleimides (B_3), as well as monomers incorporating both furan and maleimide moieties (AB_2, A_2B). While the Diels-Alder (DA) polymerization of $A_2 + B_3$ systems at 65°C yielded within a few days cross-linked materials, the polycondensation of AB_2 or A_2B monomers resulted in soluble HBPs with molar masses in between 35 200-67 200 g.mol^{-1} and relatively narrow dispersities ($Đ$ = 2.0-3.2). The application of the retro-DA depolymerization to the soluble or gelled polymers at 110°C ensured the regeneration of the starting materials.

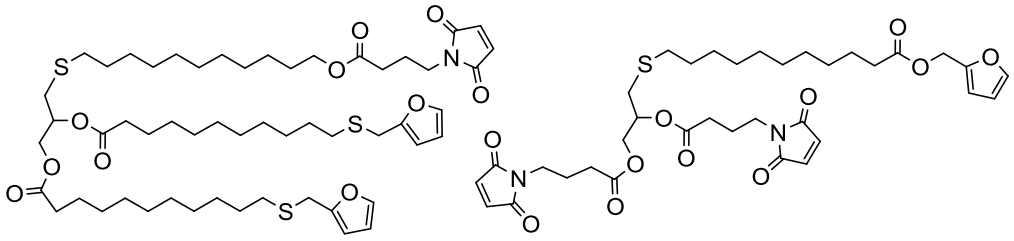

Scheme I-29. AB_2 and A_2B furan/maleimide monomers for the synthesis of HBPs

The synthesis of HBPs starting from plant oils has a short course, but it is worth pointing out that other types of polymers than polyesters, have been studied including some polyethers and polyurethanes. For instance, Rokicki and coworkers reported the efficient preparation of one latent AB_2 monomer from glycerol and dimethyl carbonate.[165] The anionic ring-opening polymerization of the obtained glycerol carbonate, which proceeds with CO_2 liberation, resulted in aliphatic HB polyethers whose structure is very similar to polyglycerols (Scheme I-30). The group of Karak extensively investigated in recent years the synthesis of bio-based hyperbranched polyurethanes from monoglycerides of various oils, *e.g.* castor, sunflower and *Mesua ferra* linseed oils, and their nanocomposites incorporating clay, graphene oxide, silver and magnetite particles for biomedical applications.[166–170]

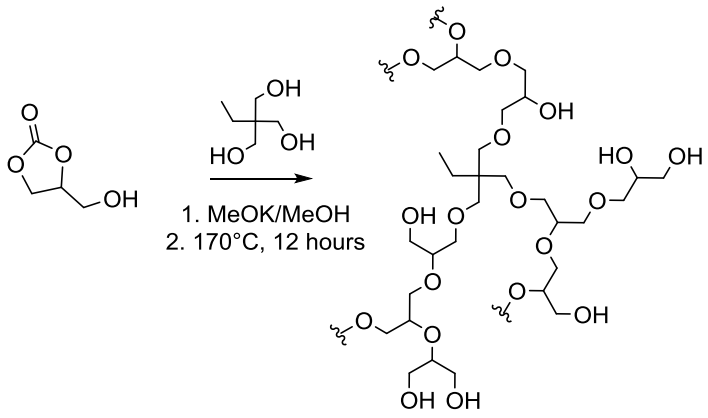

Scheme I-30. Anionic ring-opening polymerization of glycerol carbonate: synthesis of hyperbranched aliphatic polyethers

Conclusion and perspectives

The last 25 years have witnessed the rapid development of hyperbranched polymers. This field is no longer viewed as an emerging research area after an earlier starting point in the middle of the 20th century, but cannot be yet described as mature, since the related activities are still strongly expanding with more than 500 publications per year. Tremendous research efforts were made over the past decades to develop diverse synthetic approaches to HBPs, from the classical polycondensation of AB_n-type monomers described by Flory in 1940s to less conventional methods. As a result, not only AB_n and latent AB_n-type monomers but also commercially available multifunctional monomer pairs were successfully employed to prepare HBPs. Up to date, the synthesis of a large variety of HBPs with different chemical compositions and architectures has been demonstrated.

Among them, polyesters are likely one of the most versatile and important family of HBPs synthesized up to date. The wide availability of suitable monomers and their relative ease of synthesis have made this class of HBPs very attractive. In addition, the success of the commercially available Boltorn-type aliphatic HBPEs has prompted the research in this field. The synthesis of a wide range of HBPEs has been successfully reported, nearly exclusively starting from petroleum resources. However, in both a context of price volatility and uncertain supply of oil and gas, combined with environmental concerns (global warming, waste production), a lot of efforts have been made in recent years to replace fossil resources with renewable ones to improve the polyester sustainability.

In contrast to their linear analogues, the use of renewable resources, and more specifically vegetable oils, for the preparation of HBPEs is still in its infancy. Indeed, the synthesis of HBPEs starting from fatty acid derivatives has been scarcely described and yet, vegetable oils represent a promising class of raw materials. Despite the important currently available library of oily-derived diesters and polyols, the most studied approach to prepare HBPEs was the polycondensation of AB_n-type monomers bearing both ester and hydroxyl moieties. The double-monomer methodology, *i.e.* copolymerization of A_2 and B_n monomers, indeed owns one main drawback: gelation inevitably occurs above a critical conversion that can at least be determined by calculations. The results obtained by polycondensation of AB_n-type monomers are besides very encouraging since molar masses and DB values achieved, when they were characterized, are comparable with those previously reported in the literature on petroleum-based HBPEs. In addition, the use of vegetable oils was shown to confer to the

as-formed HBPEs hydrophobicity, low thermal transitions and against expectations, crystallinity due to the long aliphatic segments. This property is of high interest in a field nowadays dominated by the poly(bis-MPA) HBPEs.

In this context, this thesis aimed at developing a range of novel oily-derived HBPEs with tunable properties. In this regard, the approach consisting in the polycondensation of hydroxyester AB_n-type monomers was preferred, since this route is accompanied by a minimal risk of gelation. This process thus appeared more viable from an industrial standpoint, in the perspective of production scaling-up. Were used as raw materials some unsaturated FAMEs, as the presence of the double bonds implies plurifunctionnality. Several selective modifications of the unsaturations were implemented including the direct dihydroxylation by acid hydrolysis of epoxidized vegetable oils (Chapters II and III) and the thiol-ene/metathesis coupling reactions (Chapter IV). The AB_2/AB_3-type monomers were then successfully employed as building blocks for the synthesis of a set of renewable HBPEs with tunable properties. The structure-property relationships of the so-formed HBPEs were further investigated. As highlighted in this chapter, aliphatic HBPEs are prone, under thermal treatment, to several degradation reactions. Particular attention was thus paid to the occurrence of undesired side reactions, possibly limiting the molar masses and DB values achievable and, in some cases, leading to cross-linked polymeric materials.

References

(1) Yan, D.; Gao, C.; Frey, H. *Hyperbranched polymers: Synthesis, Properties, and Applications*; John Wiley & Sons, Inc., 2011.
(2) Flory, P. J. *Principles of Polymer Chemistry*; Cornell University Press: Ithaca, NY, 1953.
(3) Hadjichristidis, N.; Pitsikalis, M.; Pispas, S.; Iatrou, H. *Chem. Rev.* **2001**, *101* (12), 3747–3792.
(4) Buhleier, E.; Wehner, W.; Vögtle, F. *Synthesis (Stuttg).* **1978**, No. 2, 155–158.
(5) Voit, B. I. *Acta Polym.* **1995**, *46* (2), 87–99.
(6) Tomalia, D. A.; Fréchet, J. M. J. *J. Polym. Sci. Part A Polym. Chem.* **2002**, *40* (16), 2719–2728.
(7) Tomalia, D. A.; Baker, H.; Dewald, J.; Hall, M.; Kallos, G.; Martin, S.; Roeck, J.; Ryder, J.; Smith, P. *Polym. J.* **1985**, *17* (1), 117–132.
(8) Newkome, G. R.; Yao, Z.; Baker, G. R.; Gupta, V. K. *J. Org. Chem.* **1985**, *50* (3), 2003–2004.
(9) Hawker, C.; Fréchet, J. M. J. *J. Chem. Soc. Chem. Commun.* **1990**, *15*, 1010–1013.
(10) Hawker, C.; Fréchet, J. M. J. *J. Am. Chem. Soc.* **1990**, *112* (21), 7638–7647.
(11) Newkome, G. R.; Moorefield, C. N.; Vögtle, F. *Dendrimers and dendrons: Concepts, synthesis, Applications*; WILEY-VCH Verlag GmbH, 2004.
(12) Tomalia, D. A.; Christensen, J. B.; Boas, U. *Dendrimers, Dendrons and Dendritic polymers: Discovery, Applications and the Future*; Cambridge University Press, 2012.
(13) Gitsov, I. *J. Polym. Sci. Part A Polym. Chem.* **2008**, *46* (16), 5295–5314.
(14) Schlüter, A. D.; Rabe, J. P. *Angew. Chemie Int. Ed.* **2000**, *39*, 864–883.
(15) Frauenrath, H. *Prog. Polym. Sci.* **2005**, *30* (3–4), 325–384.
(16) Taton, D.; Feng, X.; Gnanou, Y. *New J. Chem.* **2007**, *31* (7), 1097.
(17) Konkolewicz, D.; Monteiro, M. J.; Perrier, S. *Macromolecules* **2011**, *44*, 7067–7087.
(18) Teertstra, S. J.; Gauthier, M. *Prog. Polym. Sci.* **2004**, *29* (4), 277–327.
(19) Hutchings, L. R. *Soft Matter* **2008**, *4* (11), 2150–2159.
(20) Flory, P. J. *J. Am. Chem. Soc.* **1941**, *63* (11), 3083–3090.
(21) Flory, P. J. *J. Am. Chem. Soc.* **1941**, *63* (11), 3091–3096.
(22) Flory, P. J. *J. Am. Chem. Soc.* **1941**, *63* (11), 3096–3100.
(23) Flory, P. J. *J. Am. Chem. Soc.* **1952**, *74* (1932), 2718–2723.
(24) Kim, Y. H. Hyperbranched Polyarylenes. US4857630, 1987.
(25) Kim, Y. H.; Webster, O. W. *Macromolecules* **1992**, *25* (21), 5561–5572.
(26) Zheng, Y.; Li, S.; Weng, Z.; Gao, C. *Chem. Soc. Rev.* **2015**, *44*, 4091–4130.
(27) Kienle, R. H.; Hovey, A. G. *J. Am. Chem. Soc.* **1929**, *51* (2), 509–519.
(28) Kienle, R. H.; Van Der Meulen, P. A.; Petke, F. E. *J. Am. Chem. Soc.* **1939**, *61* (9), 2258–2268.
(29) Kricheldorf, H. R.; Zang, Q.-Z.; Schwarz, G. *Polymer* **1982**, *23* (12), 1821–1829.
(30) Voit, B. I. *J. Polym. Sci. Part A Polym. Chem.* **2000**, *38* (14), 2505–2525.
(31) Arseneault, M.; Wafer, C.; Morin, J.-F. *Molecules* **2015**, *20* (5), 9263–9294.
(32) Hawker, C.; Lee, R.; Fréchet, J. M. J. *J. Am. Chem. Soc.* **1991**, *4588* (113), 4583–4588.
(33) Hölter, D.; Burgath, A.; Frey, H. *Acta Polym.* **1997**, *48* (1-2), 30–35.
(34) Kambouris, P.; Hawker, C. J. *J. Chem. Soc. Perkin Trans. 1* **1993**, No. 22, 2717–2721.
(35) Simon, P. F. W.; Müller, A. H. E.; Pakula, T. *Macromolecules* **2001**, *34* (6), 1677–1684.
(36) Chen, L.; Zhu, X.; Yan, D.; Chen, Y.; Chen, Q.; Yao, Y. *Angew. Chemie Int. Ed.* **2006**, *45* (1), 87–90.
(37) Zhu, X.; Zhou, Y.; Yan, D. *J. Polym. Sci. Part B Polym. Phys.* **2011**, *49* (18), 1277–1286.
(38) Hult, A.; Johansson, M.; Malmström, E. In *Branched Polymers II*; Roovers, J., Ed.; Advances in Polymer Science; Springer Berlin Heidelberg, 1999; Vol. 143, pp 1–34.
(39) Turner, S. R.; Walter, F.; Voit, B. I.; Mourey, T. H. *Macromolecules* **1994**, *27* (6), 1611–1616.
(40) Fréchet, J. M. J. *Science* **1994**, *263* (5154), 1710–1715.
(41) Schmaljohann, D.; Häußler, L.; Pötschke, P.; Voit, B. I.; Loontjens, T. J. A. *Macromol. Chem. Phys.* **2000**, *201* (1), 49–57.
(42) Schallausky, F.; Erber, M.; Komber, H.; Lederer, A. *Macromol. Chem. Phys.* **2008**, *209* (22), 2331–2338.
(43) Marcos, M.; Martín-Rapún, R.; Omenat, A.; Serrano, J. L. *Chem. Soc. Rev.* **2007**, *36* (12), 1889–

1901.
(44) Yan, D.; Zhou, Z. *Macromolecules* **1999**, *32*, 819–824.
(45) Zhou, Z.; Yan, D. *Polymer* **2000**, *41*, 4549–4558.
(46) Hanselmann, R.; Hölter, D.; Frey, H. *Macromolecules* **1998**, *31* (12), 3790–3801.
(47) Liu, N.; Vignolle, J.; Vincent, J. M.; Robert, F.; Landais, Y.; Cramail, H.; Taton, D. *Macromolecules* **2014**, *47* (5), 1532–1542.
(48) Segawa, Y.; Higashihara, T.; Ueda, M. *Polym. Chem.* **2013**, *4*, 1746–1759.
(49) Hobson, L. J.; M. Kenwright, A. *Chem. Commun.* **1997**, *19*, 1877–1879.
(50) Fréchet, J. M. J.; Henmi, H.; Gitsov, I.; Aoshima, S.; Leduc, M. R.; Grubbs, R. B. *Science* **1995**, *269*, 1080.
(51) Sunder, A.; Hanselmann, R.; Frey, H.; Mülhaupt, R. *Macromolecules* **1999**, *32* (13), 4240–4246.
(52) Simon, P. F. W.; Radke, W.; Müller, A. H. E. *Macromol. Rapid Commun.* **1997**, *18* (9), 865–873.
(53) Matyjaszewski, K.; Gaynor, S. G.; Kulfan, A.; Podwika, M. *Macromolecules* **1997**, *30* (17), 5192–5194.
(54) Guan, Z.; Cotts, P. M.; McCord, E. F.; McLain, S. J. *Science* **1999**, *283* (5410), 2059–2062.
(55) Xu, K.; Peng, H.; Sun, Q.; Dong, Y.; Salhi, F.; Luo, J.; Chen, J.; Huang, Y.; Zhang, D.; Xu, Z.; Tang, B. Z. *Macromolecules* **2002**, *35* (15), 5821–5834.
(56) Gao, C.; Yan, D. *Prog. Polym. Sci.* **2004**, *29* (3), 183–275.
(57) Deng, X.-X.; Cui, Y.; Du, F.-S.; Li, Z. *Polym. Chem.* **2014**, *5*, 3316–3320.
(58) Kim, Y. H. *J. Polym. Sci. Part A Polym. Chem.* **1998**, *36* (11), 1685–1698.
(59) Jikei, M.; Kakimoto, M. *Prog. Polym. Sci.* **2001**, *26* (8), 1233–1285.
(60) Yates, C. R.; Hayes, W. *Eur. Polym. J.* **2004**, *40* (7), 1257–1281.
(61) Voit, B. I. *J. Polym. Sci. Part A Polym. Chem.* **2005**, *43* (13), 2679–2699.
(62) Voit, B. I.; Lederer, A. *Chem. Rev.* **2009**, *109* (11), 5924–5973.
(63) Peleshanko, S.; Tsukruk, V. V. *Prog. Polym. Sci.* **2008**, *33* (5), 523–580.
(64) Schüll, C.; Frey, H. *Polymer* **2013**, *54* (21), 5443–5455.
(65) Inoue, K. *Prog. Polym. Sci.* **2000**, *25* (4), 453–571.
(66) Irfan, M.; Seiler, M. *Ind. Eng. Chem. Res.* **2010**, *49* (3), 1169–1196.
(67) Perstorp. *Boltorn, advancing performance & confort*.
(68) Froehling, P. *J. Polym. Sci. Part A Polym. Chem.* **2004**, *42* (13), 3110–3115.
(69) BASF. Lupasol http://www.basf.ca/group/corporate/ca/en_GB/brand/LUPASOL.
(70) HyperPolymers. Hyperbranched Polyglycerols www.hyperpolymers.com/orderinf.html.
(71) Factory, P. Dendritic Materials http://www.polymerfactory.com/.
(72) McKee, M. G.; Unal, S.; Wilkes, G. L.; Long, T. E. *Prog. Polym. Sci.* **2005**, *30* (5), 507–539.
(73) Zhang, X. *Prog. Org. Coatings* **2010**, *69* (4), 295–309.
(74) Ghosh, A.; Banerjee, S.; Voit, B. I. *Adv. Polym. Sci.* **2015**, *266*, 27–124.
(75) Wooley, K. L.; Hawker, C. J.; Lee, R.; Fréchet, J. M. J. *Polymer Journal*. 1994, pp 187–197.
(76) Turner, S. R.; Voit, B. I.; Mourey, T. H. *Macromolecules* **1993**, *26* (17), 4617–4623.
(77) Kricheldorf, H. R.; Staber, O. *Macromol. Rapid Commun.* **1994**, *15*, 87–93.
(78) Kricheldorf, H. R.; Stukenbrock, T. *J. Polym. Sci. Part A Polym. Chem.* **1998**, *36*, 2347–2357.
(79) Erber, M.; Boye, S.; Hartmann, T.; Voit, B. I.; Lederer, A. *J. Polym. Sci. Part A Polym. Chem. Chem.* **2009**, *47* (3), 5158–5168.
(80) Kang, S. H.; Luo, J.; Ma, H.; Barto, R. R.; Frank, C. W.; Dalton, L. R.; Jen, A. K. Y. *Macromolecules* **2003**, *36* (12), 4355–4359.
(81) Blencowe, A.; Davidson, L.; Hayes, W. *Eur. Polym. J.* **2003**, *39* (10), 1955–1963.
(82) Ishida, Y.; Jikei, M.; Kakimoto, M. A. *Polym. Adv. Technol.* **2000**, *11* (8-12), 698–704.
(83) Qiu, T.; Tang, L.; Tuo, X.; Zhang, X.; Liu, D. *Polym. Bull.* **2001**, *47* (3-4), 337–342.
(84) Chu, F.; Chu, F.; Hawker, C. J.; Hawker, C. J.; Pomery, P. J.; Pomery, P. J.; Hill, D. J. T.; Hill, D. J. T. *J. Polym. Sci. Part A Polym. Chem.* **1997**, *35* (9), 1627–1633.
(85) Khalyavina, A.; Schallausky, F.; Kombeiy, H.; Samman, M. Al; Radke, W.; Lederer, A. *Macromolecules* **2010**, *43* (7), 3268–3276.
(86) Khalyavina, A.; Häußler, L.; Lederer, A. *Polymer* **2012**, *53* (5), 1049–1053.
(87) Hahn, S.; Yun, Y.; Jin, J. *Macromolecules* **1998**, *31*, 6417–6425.
(88) Choi, S. H.; Lee, N. H.; Cha, S. W.; Jin, J. Il. *Macromolecules* **2001**, *34* (7), 2138–2147.

(89) Žagar, E.; Žigon, M. *Prog. Polym. Sci.* **2011**, *36* (1), 53–88.
(90) García-Gallego, S.; Nyström, A. M.; Malkoch, M. *Prog. Polym. Sci.* **2015**, *48*, 85–110.
(91) Johansson, M.; Malmström, E.; Hult, A. *Trends Polym. Sci.* **1996**, *4*, 398–403.
(92) Malmström, E.; Hult, A. *Macromolecules* **1996**, *29* (4), 1222–1228.
(93) Malmström, E.; Johansson, M.; Hult, A. *Macromolecules* **1995**, *28* (5), 1698–1703.
(94) Magnusson, H.; Malmström, E.; Hult, A. *Macromolecules* **2000**, *33*, 3099–3104.
(95) Jena, K. K.; Raju, K. V. S. N.; Prathab, B.; Aminabhavi, T. M. *J. Phys. Chem. B* **2007**, *111* (30), 8801–8811.
(96) Ikladious, N. E.; Mansour, S. R.; Rozik, N. N.; Dirnberger, K.; Eisenbach, C. D. *J. Polym. Sci. Part A Polym. Chem.* **2008**, *46*, 5568–5579.
(97) Chikh, L.; Tessier, M.; Fradet, A. *Macromolecules* **2008**, *41* (23), 9044–9050.
(98) Zhang, S.; Lemaire, V.; Feret, A.; Lefebvre, H.; Tessier, M.; Fradet, A. *Polym. Chem.* **2013**, *3*, 1538–1545.
(99) Trollsas, M.; Claesson, H.; Hedrick, J. L. *Macromolecules* **1998**, *31*, 3439–3445.
(100) Trollsas, M.; Hedrick, J. L. *Macromolecules* **1998**, *9297* (98), 4390–4395.
(101) Choi, J.; Kwak, S. *Macromolecules* **2003**, *36*, 8630–8637.
(102) Trollsas, M.; Lowenhielm, P.; Lee, V. Y.; Moller, M.; Miller, R. D.; Hedrick, J. L. *Macromolecules* **1999**, *32* (26), 9062–9066.
(103) Skaria, S.; Smet, M.; Frey, H. *Macromol. Rapid Commun.* **2002**, *23* (4), 292–296.
(104) Smet, M.; Gottschalk, C.; Skaria, S.; Frey, H. *Macromol. Chem. Phys.* **2005**, *206* (24), 2421–2428.
(105) Fischer, A. M.; Wolf, F. K.; Frey, H. *Macromol. Chem. Phys.* **2012**, *213* (13), 1349–1358.
(106) Dusek, K.; Somvarsky, J.; Smrckova, M.; Simonsick Jr., W. J.; Wilczek, L. *Polym. Bull.* **1999**, *42* (4), 489–496.
(107) Žagar, E.; Žigon, M. *Macromolecules* **2002**, *35* (27), 9913–9925.
(108) Burgath, A.; Sunder, A.; Frey, H. *Macromol. Chem. Phys.* **2000**, *201* (7), 782–791.
(109) Chikh, L.; Tessier, M.; Fradet, A. *Polymer* **2007**, *48* (7), 1884–1892.
(110) Komber, H.; Ziemer, A.; Voit, B. I. *Macromolecules* **2002**, *35* (9), 3514–3519.
(111) Liu, M.; Vladimirov, N.; Fréchet, J. M. J. *Macromolecules* **1999**, *32* (20), 6881–6884.
(112) Stöhr, O.; Ritter, H. *Polym. Int.* **2015**, *64* (1), 37–41.
(113) Yu, X. H.; Feng, J.; Zhuo, R. X. *Macromolecules* **2005**, *38* (15), 6244–6247.
(114) Parzuchowski, P. G.; Grabowska, M.; Tryznowski, M.; Rokicki, G. *Macromolecules* **2006**, *39* (21), 7181–7186.
(115) Fischer, A. M.; Schüll, C.; Frey, H. *Polymer* **2015**, *72*, 436–446.
(116) Lin, Q.; Long, T. E. *Macromolecules* **2003**, *36* (26), 9809–9816.
(117) Fan, Z.; Lederer, A.; Voit, B. I. *Polymer* **2009**, *50* (15), 3431–3439.
(118) Reisch, A.; Komber, H.; Voit, B. I. *Macromolecules* **2007**, *40* (19), 6846–6858.
(119) Unal, S.; Long, T. E. *Macromolecules* **2006**, *39* (8), 2788–2793.
(120) Stumbé, J.-F.; Bruchmann, B. *Macromol. Rapid Commun.* **2004**, *25* (9), 921–924.
(121) Srinivas, D.; Sebastian, J. Method for production of Hyperbranched Polyesters. WO 2012114357, 2012.
(122) Sebastian, J.; Srinivas, D. *Appl. Catal. A Gen.* **2013**, *464–465*, 51–60.
(123) Wyatt, V. T. *J. Am. Oil Chem. Soc.* **2012**, *89* (2), 313–319.
(124) Kricheldorf, H. In *Polycondensation: History and results*; Springer Berlin Heidelberg, 2014; pp 147–159.
(125) Wang, K.; Gao, C.; Huang, W.; Yan, D. *Polym. Prepr. (Am. Chem. Soc., Div. Polym. Chem.)* **2003**, *44* (1), 583–584.
(126) Wang, K.; Gao, C.; Haung, W.; Yan, D. *Polym. Prepr. (Am. Chem. Soc., Div. Polym. Chem.)* **2003**, *44* (1), 888–889.
(127) Report of the World Commission on Environment and Development: Our Common Future. *Towards Sustainable Development*; Rio de Janeiro, 1992.
(128) Scholl, M.; Nguyen, T. Q.; Bruchmann, B.; Klok, H. A. *Macromolecules* **2007**, *40* (16), 5726–5734.
(129) Scholl, M.; Nguyen, T. Q.; Bruchmann, B.; Klok, H. A. *J. Polym. Sci. Part A Polym. Chem.* **2007**, *45* (23), 5494–5508.

(130) Scholl, M.; Kadlecova, Z.; Klok, H. A. *Prog. Polym. Sci.* **2009**, *34* (1), 24–61.
(131) Voit, B. I.; Appelhans, D. *Macromol. Chem. Phys.* **2010**, *211* (7), 727–735.
(132) Kanazawa, A.; Okumura, S.; Suzuki, M. *Org. Biomol. Chem.* **2005**, *3* (9), 1746–1750.
(133) Kadokawa, J.; Sato, M.; Karasu, M.; Tagaya, H.; Chiba, K. *Angew. Chemie Int. Ed.* **1998**, *37* (17), 2373–2376.
(134) Satoh, T.; Kakuchi, T. *Macromol. Biosci.* **2007**, *7* (8), 999–1009.
(135) Guo, M.; Fei, M.; Liu, H.; Wu, X.; Yang, P. *Polym. Chem.* **2015**, *6*, 2822–2826.
(136) Adeli, M.; Rasoulian, B.; Saadatmehr, F.; Zabihi, F. *J. Appl. Polym. Sci.* **2013**, *129* (6), 3665–3671.
(137) Wang, S.; Tateyama, S.; Kaneko, D.; Ohki, S.; Kaneko, T. *Polym. Degrad. Stab.* **2011**, *96* (12), 2048–2054.
(138) Dong, W.; Li, H.; Chen, M.; Ni, Z.; Zhao, J.; Yang, H.; Gijsman, P. *J. Polym. Res.* **2011**, *18* (6), 1239–1247.
(139) Dong, W.; Ren, J.; Lin, L.; Shi, D.; Ni, Z.; Chen, M. *Polym. Degrad. Stab.* **2012**, *97* (4), 578–583.
(140) Wang, S.; Kan, K.; Jin, X.; Kaneko, T.; Kaneko, D. *Pure Appl. Chem.* **2012**, *84* (12), 2559–2568.
(141) Satoh, T.; Kinugawa, Y.; Tamaki, M.; Kitajyo, Y.; Sakai, R.; Kakuchi, T. *Macromolecules* **2008**, *41* (14), 5265–5271.
(142) Meier, M. A. R.; Metzger, J. O.; Schubert, U. S. *Chem. Soc. Rev.* **2007**, *36* (11), 1788–1802.
(143) Montero de Espinosa, L.; Meier, M. A. R. *Eur. Polym. J.* **2011**, *47* (5), 837–852.
(144) Maisonneuve, L.; Lebarbé, T.; Grau, E.; Cramail, H. *Polym. Chem.* **2013**, *4* (22), 5472–5517.
(145) Biermann, U.; Bornscheuer, U.; Meier, M. A. R.; Metzger, J. O.; Schäfer, H. J. *Angew. Chemie Int. Ed.* **2011**, *50* (17), 3854–3871.
(146) Foreign Agricultural Service. *Oilseeds: World Markets and Trade*; 2015.
(147) Gandini, A. *Green Chem.* **2011**, *13* (5), 1061–1083.
(148) Garcia, J. I.; Garcia-Marin, H.; Pires, E. *Green Chem.* **2014**, *16*, 1007–1033.
(149) Sutter, M.; Silva, E. Da; Duguet, N.; Raoul, Y.; Métay, E.; Lemaire, M. *Chem. Rev.* **2015**, *115* (16), 8609–8651.
(150) Ronda, J. C.; Lligadas, G.; Galià, M.; Cádiz, V. *Eur. J. Lipid Sci. Technol.* **2011**, *113* (1), 46–58.
(151) Vilela, C.; Sousa, A. F.; Fonseca, A. C.; Serra, A. C.; Coelho, J. F. J.; Freire, C. S. R.; Silvestre, A. J. D. *Polym. Chem.* **2014**, *5*, 3119–3141.
(152) Wagner, E.; Bruchmann, F.; Haering, D.; Keller, P.; Pouhe, T. Method for producing highly functional hyperbranched polyesters by means of enzymatic esterification. US 7081509, 2006.
(153) Rai, R.; Tallawi, M.; Grigore, A.; Boccaccini, A. R. *Prog. Polym. Sci.* **2012**, *37* (8), 1051–1078.
(154) Zhang, Y.; Yang, Y.; Cai, J.; Lv, W.; Xie, W.; Wang, Y.; Gross, R. A. In *Biobased Monomers, Polymers, and Materials*; Smith, P. B., Gross, R. A., Eds.; ACS Symposium series: Washington, 2012; p 111.
(155) Kulshrestha, A. S.; Gao, W.; Gross, R. A. *Macromolecules* **2005**, *38* (8), 3193–3204.
(156) Bao, Y.; He, J.; Li, Y. *Polym. Int.* **2013**, *62*, 1457–1464.
(157) Türünç, O.; Meier, M. A. R. *Macromol. Rapid Commun.* **2010**, *31* (20), 1822–1826.
(158) Parzuchowski, A. G.; Grabowska, M.; Jaroch, M.; Kusznerczuk, M. *J. Polym. Sci. Part A Polym. Chem.* **2009**, *46* (15), 3860–3867.
(159) Petrović, Z. S.; Cvetković, I. *Contemp. Mater.* **2012**, *III* (I), 63–71.
(160) Petrović, Z. S.; Cvetković, I.; Milić, J.; Hong, D.; Javni, I. *J. Appl. Polym. Sci.* **2012**, *125* (4), 2920–2928.
(161) Milic, J.; Teraoka, I.; Petrovic, Z. S. *J. Appl. Polym. Sci.* **2012**, *125* (S2), 586–594.
(162) Biermann, U.; Metzger, J. O.; Meier, M. A. R. *Macromol. Chem. Phys.* **2010**, *211* (8), 854–862.
(163) de O. Romera, C.; Cardoso, P. B.; Meier, M. A. R.; Sayer, C.; Araújo, P. H. H. *Eur. J. Lipid Sci. Technol.* **2015**, *117* (2), 235–241.
(164) Vilela, C.; Silvestre, A. J. D.; Gandini, A. *J. Polym. Sci. Part A Polym. Chem.* **2013**, *51* (10), 2260–2270.
(165) Rokicki, G.; Rakoczy, P.; Parzuchowski, P.; Sobiecki, M. *Green Chem.* **2005**, *7* (7), 529–539.
(166) Deka, H.; Karak, N.; Kalita, R. D.; Buragohain, A. K. *Polym. Degrad. Stab.* **2010**, *95* (9), 1509–1517.
(167) Deka, H.; Karak, N. *Polym. Adv. Technol.* **2011**, *22* (6), 973–980.

(168) Kalita, H.; Karak, N. *Polym. Adv. Technol.* **2013**, *24* (9), 819–823.
(169) Thakur, S.; Karak, N. *ACS Sustain. Chem. Eng.* **2014**, *2* (5), 1195–1202.
(170) Kalita, H.; Karak, N. *J. Appl. Polym. Sci.* **2014**, *131* (1), 39579–39587.

Chapter II. From methyl 9,10-dihydroxystearate to vegetable oil-based Hyperbranched Polyesters

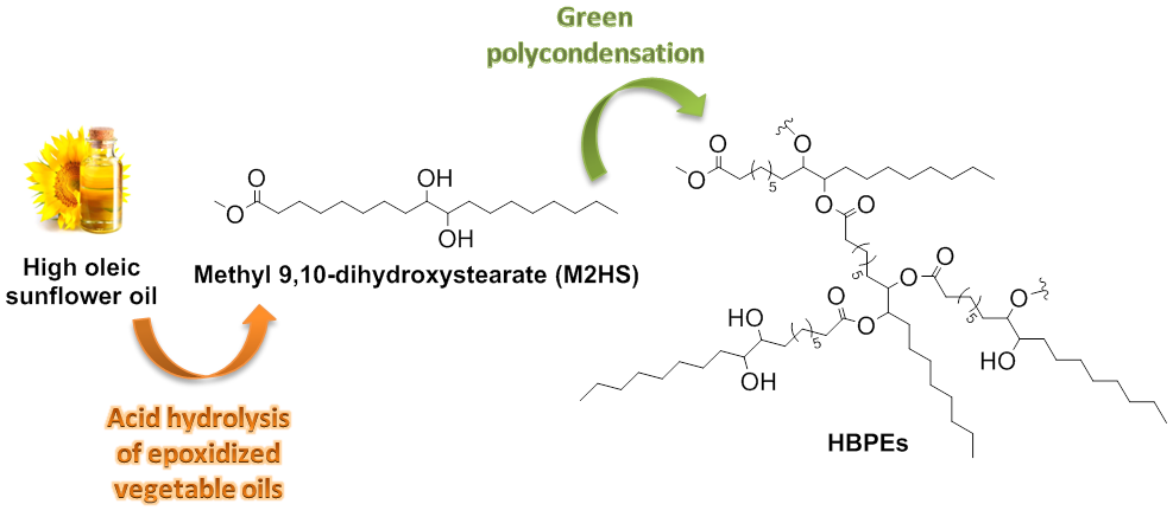

Part of this Chapter has been warranted as a European patent.[1]

Table of Contents

Introduction

As highlighted in the previous chapter, the literature of the past 30 years is highly rich with regards to the synthesis and characterization of petroleum-based hyperbranched polyesters (HBPEs).[2–7] Since the pioneering work of Kricheldorf and coworkers in 1982,[8] very strong synthetic activity has emerged in this field.[9] The term of HBPEs no longer only covers polyesters prepared by the classical polycondensation of AB_n-type monomers.[10] In the last 20 years, the family was extended to polymers obtained by ring-opening multibranching polymerization (ROMBP) of latent AB* monomers,[11–14] *i.e.* cyclic lactones bearing hydroxyl groups as initiating moieties; and to products prepared by copolymerization of both symmetric, *i.e.* $A_2 + B_n$,[6] and asymmetric monomer pairs, *i.e.* $A^* + B_3$, $AA^*/A_2^* + B_2$, $A_2 + B'B_2$, etc.[15]

In contrast, the use of plant oils for the preparation of branched polyesters has been rarely described. Till date, only a few examples have been published (Chapter I),[16–18] most of them involving the polycondensation of multifunctional hydroxyester precursors of AB_n-type.[19–22] Yet, HBPEs derived from renewable resources would be particularly attractive with the target of green and sustainable development. Vegetable oils represent a promising class of renewable feedstock for the polymer industry owing to their abundant availability, relative low cost, inherent biodegradability and low toxicity. Fatty acid methyl esters (FAMEs) are besides very interesting substrates, the presence of ester groups and double bonds enabling the design of a variety of multifunctional building blocks, suitable to the preparation of HBPEs.

With the aim at synthesizing novel oily-derived HBPEs, a set of renewable AB_n-type monomers featuring methyl ester and alcohol moieties was prepared by functionalization of FAMEs. For that purpose, several selective chemical modifications of the double bonds were implemented. The first route studied involves the acid hydrolysis of epoxidized vegetable oils. The epoxidation reaction is a conventional route for the derivatization of C-C double bonds with hydroxyl groups.[23] When applied to methyl oleate (C18:1), it leads to the formation of an AB_2-type monomer, namely, methyl 9,10-dihydroxystearate (M2HS). This chapter focuses on the synthesis and subsequent polymerization of this specific bio-based precursor of HBPEs.

In a first part, the preparation of M2HS, its isolation from the crude mixture and subsequent characterization were studied in detail. Once its purity was controlled, this AB_2-type monomer was subjected to polycondensation reaction under various conditions. A facile and efficient process of polymerization was set up yielding novel renewable HBPEs. In a second part, special attention was paid to the development of suitable tools to properly characterize the complex structure and the specific properties of these hyperbranched materials. Insights into their macromolecular characteristics and structural composition were obtained by Size Exclusion Chromatography (SEC) and ^{1}H-NMR spectroscopy. Determination of the degree of branching (DB) is besides discussed in detail. Investigations into the thermal stability and thermo-mechanical properties of these HBPEs are reported as well.

1. M2HS: Synthesis, Purification and Characterization

1.1. Monomer synthesis

The synthesis of M2HS has already been described in the literature.[24] Methyl 9,10-dihydroxystearate (CAS n°1115-01-1) is indeed currently commercialized by several suppliers of fine chemicals, *e.g.* Alfa Chemistry, 3B Scientific Corporation, DSK Biopharma, Aurora Fine Chemicals, Fluorochem, etc. However, the commercially available purity grade in between 90 and 95% is not satisfactory for the purpose of polycondensation reactions. Besides, as this thesis took place in partnership with the industrial technical center *ITERG*, there was from the start of the HYPERBIOPOL project a willingness to develop a platform of marketable chemicals (monomers/polymers). A method of synthesis was thus set up at the laboratory with the goal of obtaining this monomer in high purity.

Methyl oleate was converted into an AB_2-type synthon following a two-step strategy, as described in Scheme II-1. First, the internal double bonds of the FAME were epoxidized by reacting formic acid with a solution of hydrogen peroxide. The subsequent ring-opening of the as-formed epoxy rings was performed with water under acidic conditions, to produce the targeted monomer, methyl 9,10-dihydroxystearate (M2HS).

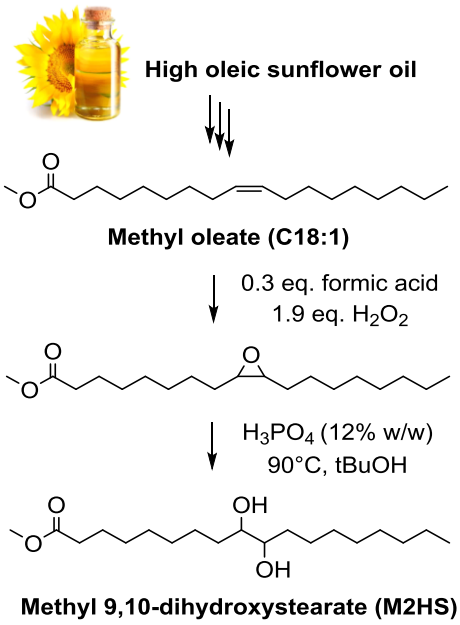

Scheme II-1. Synthetic pathway to M2HS

This synthetic route was performed and optimized at the research technical center *ITERG*. Some methyl esters of high oleic sunflower oil (HOSO) prepared on site by transesterification of refined HOSO with methanol, were used as raw materials. The fatty acid composition of the commercially available HOSO and its related methyl esters is given in Table II-1. In both cases, the content in methyl oleate (C18:1) reaches 84%.

Table II-1. Fatty acid composition of HOSO and related methyl esters

Unit	High oleic sunflower oil (HOSO)	Methyl esters of HOSO
C16:0	3.6	3.9
C16:1	0.1	0.2
C18:0	3.0	3.0
C18:1	**84.1**	**83.5**
C18:2	7.2	7.3
C18:3	0.1	0.1
C20:0	0.3	0.3
C20:1	0.3	0.3
C22:0	1.0	1.0
C22:1	0.4	0.3

The Prilezhaev reaction, *i.e.* the epoxidation of alkenes with peracids, is the conventional method used in industry for the epoxidation of fatty acids and their derivatives.[23] For safety issues, the peracid, here performic acid, was prepared *in situ* from hydrogen peroxide and its corresponding acid, formic acid.

As the reaction is exothermic, the solution of hydrogen peroxide was added drop-wise and the reaction temperature was maintained at 70-75°C with an ice bath. The epoxidized intermediates were isolated in the organic phase, neutralized with an aqueous solution of sodium hydroxide and dried under vacuum. The second step, *i.e.* the acid hydrolysis, was performed with an aqueous solution of phosphoric acid H_3PO_4 (12% w/w) under reflux at 90°C. *tert*-Butanol was added as a co-solvent. Once the reaction was completed, the organic phase was recovered, washed with water and *tert*-butanol was removed under vacuum distillation leading to a white solid. Each step was monitored by gas chromatography.

It is worth noting that in the course of this thesis a similar process was reported by Oleon company, and warranted as a patent in 2014.[24] Only the second step differs by the use of phosphorous acid H_3PO_3, instead of phosphoric acid H_3PO_4, in water media, *i.e.* no organic co-solvent is added.

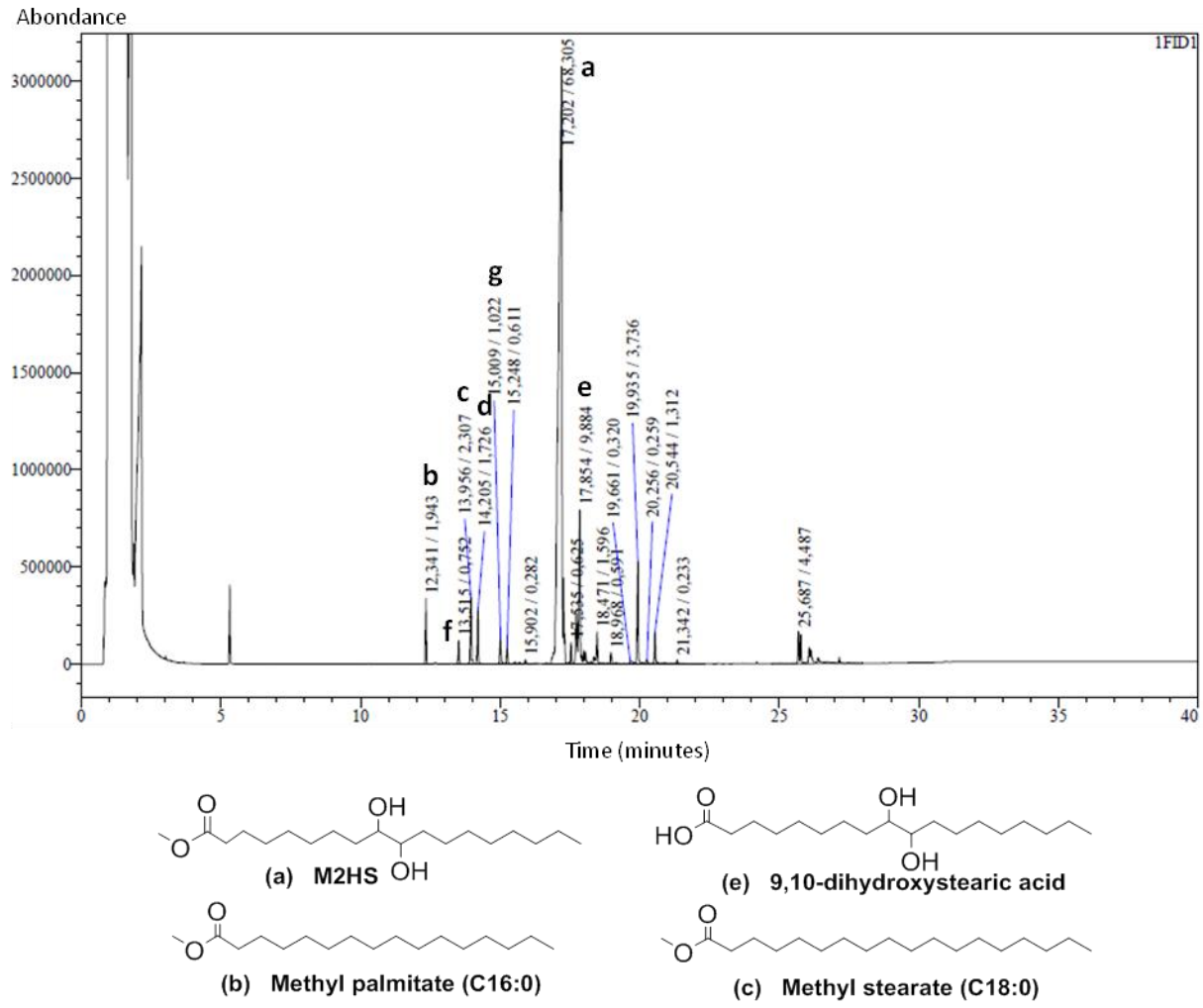

Figure II-1. GC-MS of crude M2HS

Before any purification, the crude product was analyzed by GC-MS and a complex mixture was detected, as observed in Figure II-1. Its composition was partly elucidated. M2HS eventually represents 68.3% (**a**) of the mixture. Some methyl esters of palmitic (1.9%, **b**), stearic (2.3%, **c**) and even oleic acid (1.7%, **d**) indicating that the epoxidation step was not complete, were identified. An acid fraction was also detected. Mainly composed of the acid form of M2HS, the 9,10-dihydroxystearic acid (9.9%, **e**), the mixture also included to a much lower extent some traces of palmitic (0.7%, **f**) and stearic acid (1%, **g**). The second step taking place under acidic conditions, a partial and uncontrolled hydrolysis of the FAMEs was inevitable. The remaining 10% refer to fatty acid derivatives of higher chain lengths (C20 to 22), compounds of higher molar masses like dimers and other non-identified impurities.

Petrović and coworkers managed to polymerize efficiently some mixtures of hydroxylated FAMEs of soybean oil with various functionalities (A, AB, AB_2 and AB_3), suggesting that it is not always necessary to isolate the multifunctional precursors of $AB_{n\geq 2}$-type to access HBPEs.[20,21] Accordingly, the reactivity of crude M2HS was thus tested in polymerization, without great conviction. Preliminary investigations were carried out in the melt-phase, in the presence of catalytic amounts of either anhydrous zinc acetate or TBD. This catalyst selection is further explained in section 2.1 of this chapter. The above mixture (Figure II-1) was subjected to polycondensation reaction following the procedure described by Li and coworkers[22], with one exception. The duration of the last stage of polymerization at 170°C was prolonged overnight instead of 4-5 hours, since our FA derivatives only bear secondary alcohols as reactive functions.

Table II-2. Influence of the purity grade of M2HS on the molar masses and dispersity of the HBPEs obtained in polymerization

M2HS purity grade (%)	**Crude mixture** (68.3%)		**Recrystallization** (88.9%)		**Recrys. and flash chrom.** (97.8%)	
Catalyst[1]	$Zn(OAc)_2$	TBD	$Zn(OAc)_2$	TBD	$Zn(OAc)_2$	TBD
x (%)[2]	58	33	83	45	94	100
$\bar{M}_n$[2] (g.mol^{-1})	1 300	1 300	1 700	1 200	4 700	4 200
$\bar{M}_w$[2] (g.mol^{-1})	1 500	1 500	2 300	1 400	75 400	14 100
$Đ$[2]	1.2	1.2	1.4	1.2	> 16	3.36

(1) Loading of 1.5wt%. (2) determined by SEC in THF - calibration PS standards. Procedure: 2 hours at 90°C under N_2, 2 hours at 120°C under N_2 and overnight at 170°C under dynamic vacuum.

As expected, only oligomers of low molar masses ($\bar{M}_n \leq$ 1 500 g.mol^{-1}) were obtained, with poor conversions ($x \leq 58\%$) irrespective of the catalyst employed (Table II-2). Special efforts were thus made to achieve chemically pure M2HS.

1.2. Isolation and characterization of M2HS

A two-step purification procedure was set up to isolate M2HS. First, a *recrystallization* was performed in apolar solvents such as pentane, heptane or cyclohexane, in order to remove the more apolar species, including the saturated FAMEs (see Figure SI II-1). The presence of these A-type derivatives is indeed problematic because they act as chain stoppers during the step-growth polymerization limiting the functionality of the obtained oligomers. However, after recrystallization, the results obtained in polymerization failed to show any real improvement, revealing the necessity to get rid of the acid fraction (Table II-2). FAs indeed feature a different reactivity than their methyl ester analogues and, in some cases, can poison the catalysts of transesterification employed.

To remove the FA derivatives, a *flash chromatography* was carried out in a second part on a silica column. Starting from a 98% dichloromethane/2% methanol solution and by gradually increasing the methanol concentration, two main peaks were distinguished, as can be seen in Figure II-2. These fractions were collected and analyzed by FT-IR spectroscopy.

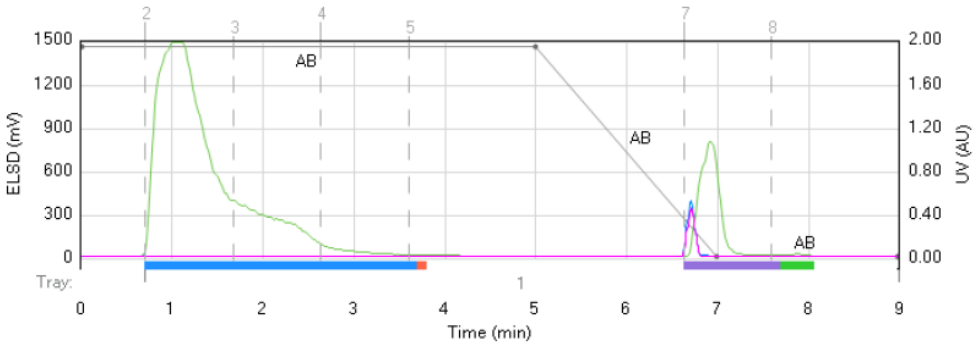

Figure II-2. Flash chromatography profile of crude mixture after hydrolysis of epoxidized HOSO, using a DCM/MeOH gradient and a silica column: ELSD detector (in green) and UV detector (in pink)

The FT-IR spectrum of crude M2HS is presented in Figure II-3 (1). The absorption band at 1 740 cm^{-1} was assigned to the stretching of the ester carbonyl group. The shoulder observed at lower wavenumbers (1 710 cm^{-1}) confirmed the presence of an acid fraction. After recrystallization in cyclohexane (Figure II-3 (2)), this shoulder was barely attenuated. By contrast, fraction 1 obtained after subsequent flash chromatography showed no more traces of acid (Figure II-3 (3)). Flash chromatography thus enabled to isolate the FA derivatives in the second fraction eluted at higher polarity, as shown in Figure II-3 (4).

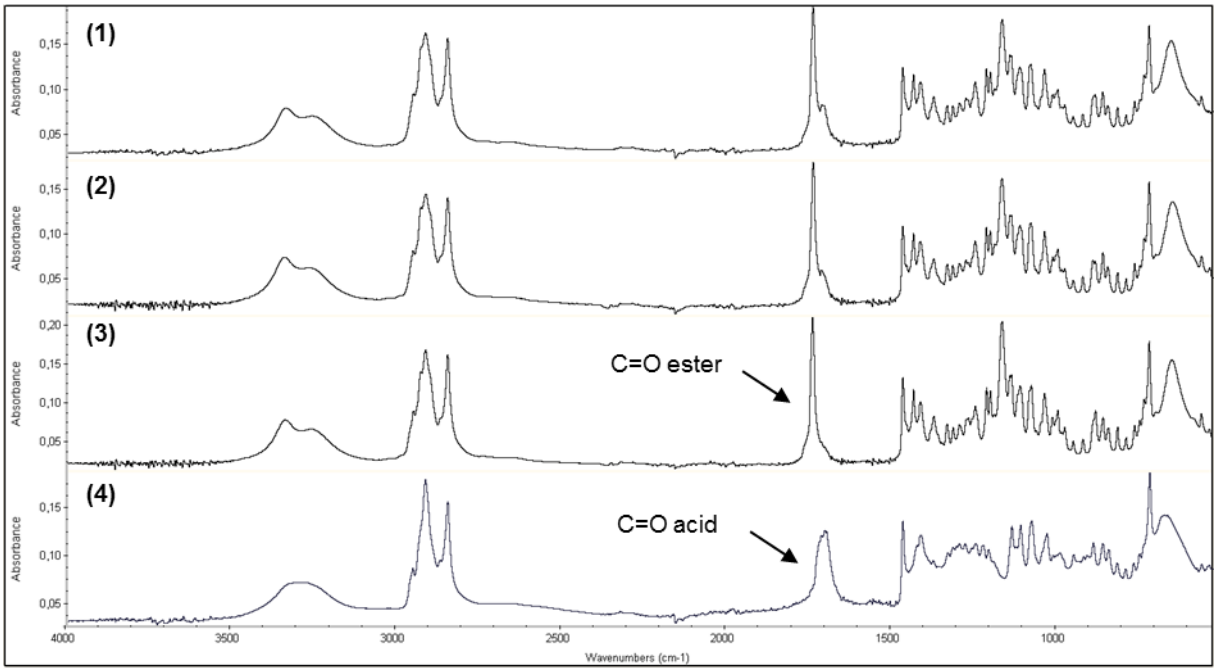

Figure II-3. Stacked FT-IR spectra of (1) crude mixture, (2) after recrystallization, (3) fraction 1 and (4) fraction 2 after flash chromatography

Gas chromatography was next performed to confirm the isolation of M2HS with a chemical purity over 97% (see supporting information, Figure SI II-2). In its pure form, M2HS was obtained as a white powder with a melting point of 70°C as determined by DSC. M2HS structure was fully characterized by ^{1}H NMR spectroscopy, as can be seen in Figure II-4.

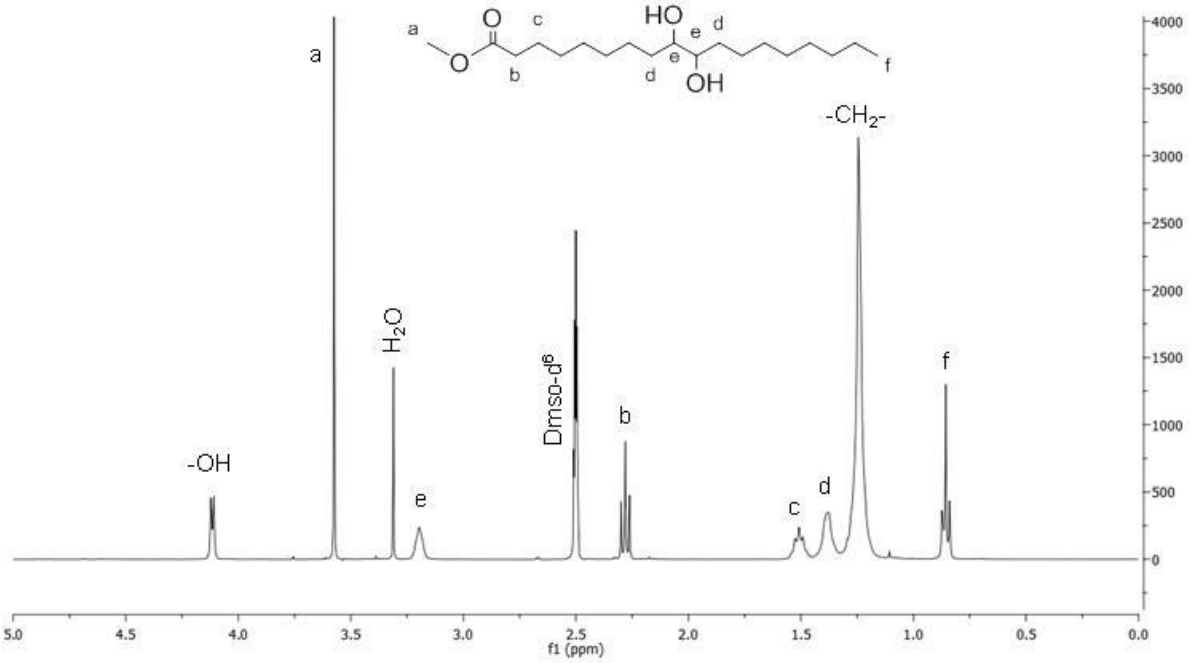

Figure II-4. ^{1}H NMR spectrum of M2HS in DMSO-d^{6}

The signal at 3.57 ppm (H_a) whose integral comes to 3, is characteristic of the methoxy group, while protons of the vicinal diol (-OH) and the adjacent ones on the α-carbons (H_e) are identified at 4.11 and 3.17 ppm, respectively. The high purity grade reached explained the good results obtained in polymerization (see further in Table II-2). Good conversions over 94% were indeed achieved. The so-formed materials even displayed slightly higher molar masses in between 4 200-4 700 $g.mol^{-1}$ than the results obtained by Petrović and coworkers with some methyl esters of hydroxylated castor and soybean oil.[20] For further information, polymerization of M2HS is presented and commented in the next section of this chapter (Chapter II.2).

Towards a production scaling-up

In the course of this thesis, the synthesis of M2HS was the purpose of scale-up. Nowadays, this monomer is being produced at the pilot scale, through batches of 50 kg on the "CEDOP" platform at *ITERG*. In contrast to the synthetic route, the purification procedure of M2HS was optimized at the LCPO on the gram scale. However, when transferring this protocol to the pre-industrial level, the removal of the acid fraction faced some scale-up issues. Indeed, flash chromatography is not a suitable technique for the purification of high volumes (< 20g).

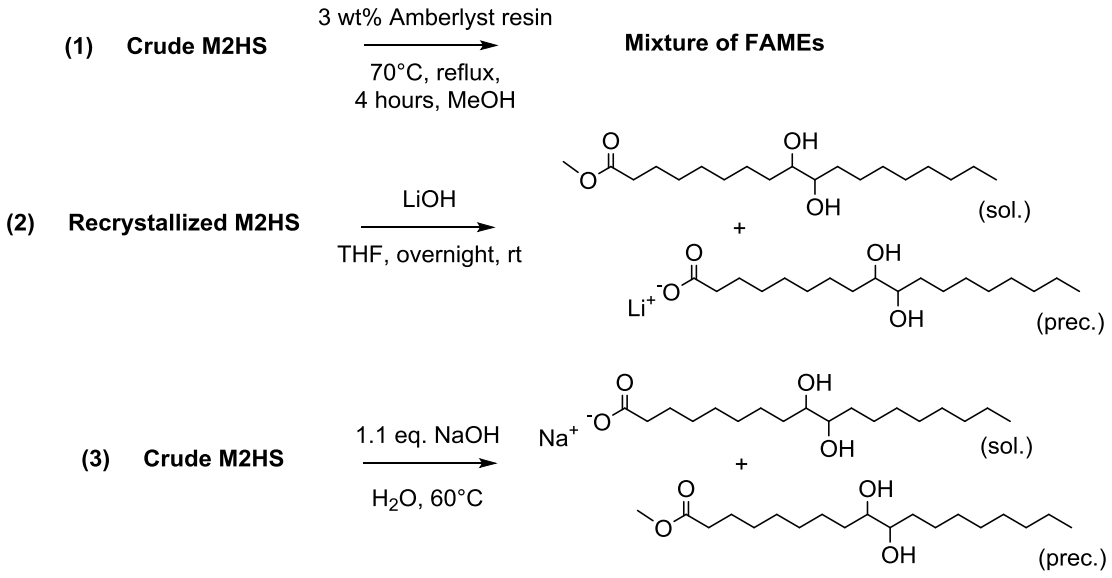

Scheme II-2. Pathways investigated for the removal of 9,10-dihydroxystearic acid

Additional attempts were thus implemented to find alternative solutions (Scheme II-2). Various methods have been investigated such as the post-esterification of the crude mixture prior to recrystallization. A few trials were performed in mild conditions using Amberlyst resin as acidic catalyst. However, the purity reached (93.5%) was not sufficient.

Another route consisted in the dissolution of the recrystallized mixture in THF, followed by the addition of lithium hydroxide. After overnight the precipitate formed, which corresponded to the lithium salt of 9,10-dihydroxystearic acid, could be removed from the solution. This technique yielded a purity of 97.6%, but lacked of selectivity. Indeed, M2HS partly precipitated with its acid form, thus decreasing the overall yield.

The option that was selected to be applied at the pre-industrial level consisted in the neutralization of the acid fraction with NaOH (aq.) in order to convert all the FAs into their water soluble sodium soaps. For that purpose, the acid value of crude M2HS was measured right after the acid hydrolysis of epoxidized HOSO. FAMEs were then extracted by simple filtration. In a final step, M2HS was recovered by recrystallization in cyclohexane in high yield (90%) and with a chemical purity over 98.6% as measured by GC.

To conclude, a novel AB_2-type monomer bearing one ester (A) and two alcohol (B) functions was successfully synthesized by acid hydrolysis of epoxidized HOSO. This approach includes the epoxidation of FAME unsaturations, followed by the ring-opening of the so-formed epoxides with water under acidic conditions. This simple route ensures the possibility of an easy industrialized production of this monomer. Due to the heterogeneity and variability of vegetable oils, the main challenge was to control the chemical purity of M2HS. Indeed, like every step-growth polymerization, polycondensation requires high monomer purity. The presence of some acid impurities was found to have dramatic impact on the molar masses of the polyesters prepared. Several techniques were thus studied to isolate M2HS at different scales including recrystallization, flash chromatography and neutralization. The next section focuses on the polymerization of M2HS. All results were obtained with monomer batches purified by recrystallization and flash chromatography.

2. Synthesis of M2HS-derived Hyperbranched Polyesters

Polycondensation of M2HS was therefore conducted in order to obtain renewable HBPEs. All transesterification polymerizations were performed in the melt following the two-step-one-pot methodology illustrated in Scheme II-3. First of all, the monomer was heated alone at 90°C above its melting point under dynamic vacuum, in order to remove any traces of solvent and especially water. This step was shown to be of high importance. After addition of the catalyst, oligomerization of the AB_2-type monomer took place at 120°C under nitrogen. Two hours later, the temperature was raised to 160°C and dynamic vacuum was applied during 13 hours, so as to reach high conversions by removing methanol as by-product from the reaction mixture.

2.1. Screening of catalysts

A screening of various transesterification catalysts was first performed with a loading of 1.5 wt% relative to monomer. The activity of different classes of commercially-available catalysts was examined including some metallic and organic systems.

Since the pioneering work of Carothers on polyester synthesis,[25] organometallic catalysts were found to play a very important role in condensation polymerizations, accelerating polymerization rates to produce high molar mass polymers with targeted physico-mechanical properties. Among the wide library of metal salts and complexes, *i.e.* most commonly alkoxides, developed up to date using Sb, Al, Ge, Zn, Sn, Fe, Bi, Ti, Zr and Y,[26] a selection of zinc, tin, antimony and titane-based catalysts was considered in this screening (Scheme II-3). Antimony-based catalysts currently dominate industrial condensation polymerization processes. However, the negative environmental impact of this element has prompted the research towards alternatives. In recent years, numerous studies attest to the relatively high activity of titanium alkoxide catalysts, *i.e.* $Ti(OBu)_4$ and $Ti(OiPr)_4$, for the synthesis of poly(ethylene terephtalate),[27] poly(butylene succinate)[28] but also linear oily-derived polyesters.[29,30]

The use of organic catalysts was also investigated in line with the development of environmentally friendly and high efficiency processes. Although organocatalysis, in its general sense, has been known for a while, the (re)emergence of the field of organocatalyzed polymerization dates back to 2001 with reports by Hedrick, Waymouth and coworkers who employed dialkylaminopyridines for the ROP of lactones and lactides.[31] Since then, numerous new families of organic catalysts have been investigated which rival metal-based alternatives for polyester synthesis, both in terms of activity and selectivity.[32,33] Relevant examples of efficient transesterification catalysts include *N*-heterocyclic carbenes[34] and guanidines. Among them, the commercially-available and easily handled base TBD (1,5,7-triazabicyclo[4.4.0]dec-5-ene), has attracted a growing interest. Its high efficiency in oily-derived polyester synthesis has been repeatedly highlighted in recent years.[19,35] Compared to organometallic catalysts, TBD was found to allow polymerization in milder conditions. In this study, two guanidines, TBD and its *N*-methyl derivative, *m*-TBD (7-methyl-1,5,7-triazabicyclo[4.4.0]dec-5-ene), the amidine base DBU (1,8-diazabicyclo [5.4.0]undec-7-ene) and the tertiary amine DABCO (1,4-diazabicyclo[2.2.2]octane) were investigated.

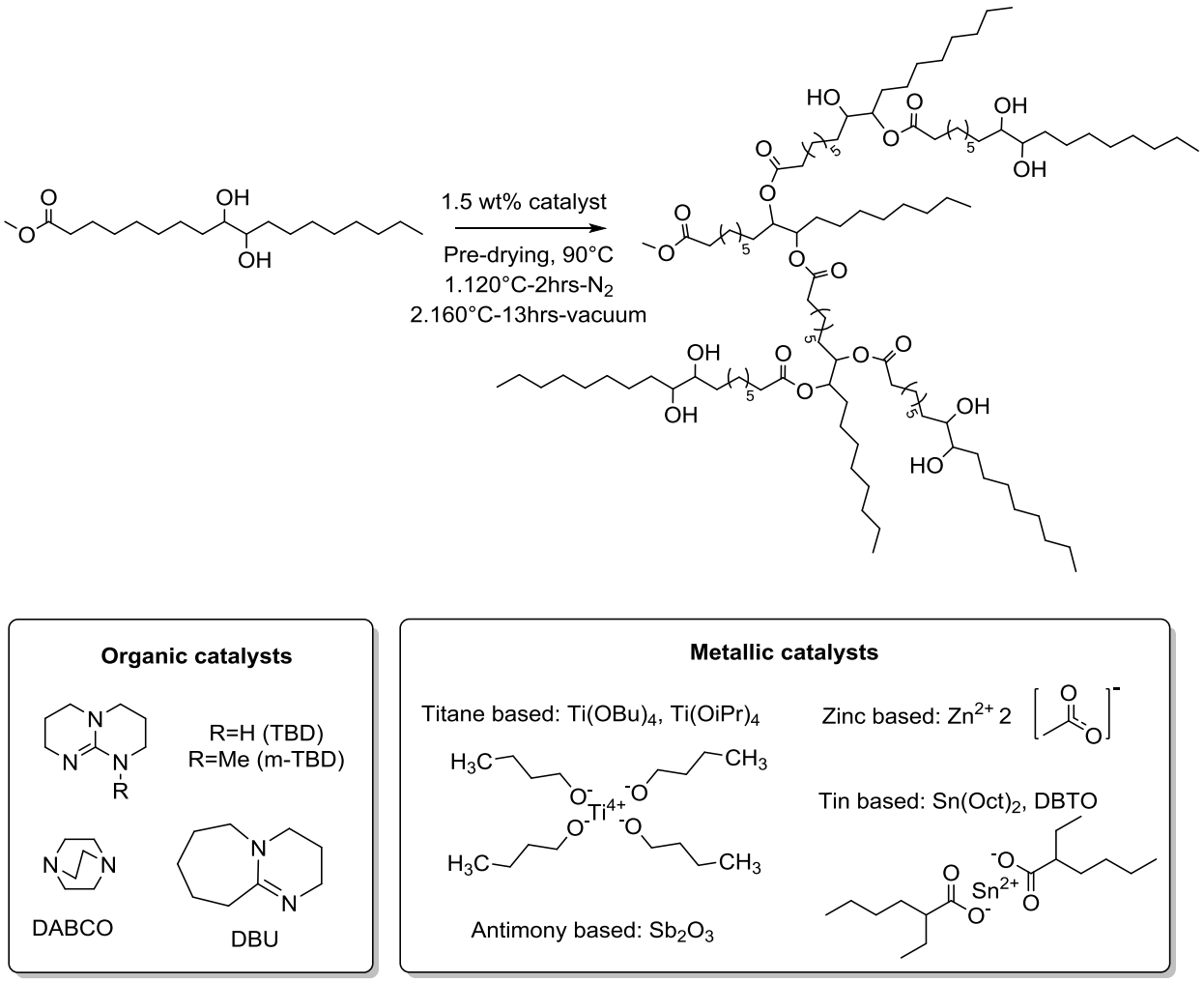

Scheme II-3. Transesterification catalysts tested in this work to polymerize M2HS

As polycondensations were performed in the melt, crude oligomers and polymers formed were analyzed by SEC without further purification. Results of this screening are summarized in Table II-3. Most of the metallic catalysts including titanium(IV) butoxide ($Ti(OBu)_4$) and isopropoxide ($Ti(OiPr)_4$), dibutyltin(IV) oxide (DBTO), antimony trioxide (Sb_2O_3), and the organic base, *m*-TBD, led to poor conversions and low molar mass oligomers. DABCO and DBU did not show any activity at all to catalyze the polycondensation of M2HS.

In contrast, anhydrous zinc acetate ($Zn(OAc)_2$), stannous octoate ($Sn(Oct)_2$), and TBD managed to polymerize M2HS efficiently. Colorless, highly viscous and sticky materials were obtained with conversions higher than 95%. P3, P7 and P8 showed molar masses ($\overline{M}_n$) in the range 3 000 to 4 000 $g.mol^{-1}$ relative to PS standards, *i.e.* corresponding to $\overline{DP}_n$ ranging from 10 to 12, and dispersities higher than 2, as expected for hyperbranched materials prepared by polycondensation of AB_n-type monomers.

Higher molar masses, *i.e.* in between 5 000 to 8 000 g.mol^{-1} could be achieved by increasing either the reaction time from 15 to 24 hours and/or the temperature up to 170°C, as demonstrated with zinc acetate and TBD (P3 *vs.* P4, P8 *vs.* P9/P10). The impact was even more important on the dispersities of these HBPEs. Indeed, significantly broader values were obtained (> 10) in agreement with the theory.[36] Overall, macromolecular characteristics of these HBPEs are consistent with the results obtained by Petrović and coworkers with hydrogenated methyl esters of epoxidized soybean oil ($\bar{M}_n$ = 3 000 g.mol^{-1}).[20]

Table II-3. Preliminary investigations of the step-growth polymerization of M2HS: catalyst screening

Entry	Catalyst	T(°C)[1]	x[2] (%)	$\bar{M}_n$[2] (g.mol^{-1})	$\bar{M}_w$[2] (g.mol^{-1})	$Đ$[2]
P1	$Ti(OBu)_4$	160	44	1 100	1 200	1.09
P2	$Ti(OiPr)_4$	160	48	1 200	1 300	1.08
P3	$Zn(OAc)_2$	160	98	3 500	9 500	2.71
P4	$Zn(OAc)_2$	170	94	6 300	96 500	>15
P5	DBTO	160	39	1 100	1 200	1.09
P6	Sb_2O_3	160	45	1 200	1 300	1.08
P7	$Sn(Oct)_2$	160	93	3 200	6 500	2.03
P8	TBD	160	100	4 100	10 100	2.46
P9	TBD	170	100	5 300	15 900	3
P10	TBD[3]	170	100	7 600	89 100	>12
P11	m-TBD	160	21	1 000	1 100	1.10
P12	DABCO	160	No polymerization			
P13	DBU	160				
P14	NaOMe	160	100	6 100	18 800	3.08

(1) Temperature of the last stage of polymerization. (2) determined by SEC in THF – calibration PS standards. (3) Duration of polymerization increased from 15 to 24 hours.

Temperatures lower than 160°C gave only oligomers of low molar masses ($\bar{M}_n$ < 1 500 g.mol^{-1}). Polycondensations performed at higher temperatures than 170°C yielded insoluble materials due to undesired side reactions. This phenomenon of gelation is investigated in detail in the next chapter. A point to consider with these side reactions is that their occurrence may explain why no full conversions were reached with zinc acetate as catalyst. Indeed, polycondensation only provides high molar mass polymers at full conversion. For instance, the polymer recovered with a $\bar{M}_n$ of 6 300 g.mol^{-1} left 6% of supposedly unreacted monomers (Table II-3, P4). We further realize that M2HS might form a monomeric lactone by cyclization (Scheme II-4) and it can be hypothesized that SEC did not allow the differentiation between the AB_2-type monomer and its cyclic form. Nonetheless, this hypothesis was not confirmed to date.

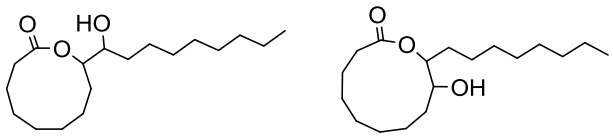

Scheme II-4. Possible monomeric lactones formed by cyclization

One should mention that sodium methoxide was a late entrant into this screening of catalyst, and yet this strong base afforded the highest molar masses of 6 100 $g.mol^{-1}$ ($Đ$ = 3.08) at full conversion. NaOMe is already widely used in oleochemistry as catalyst for the transesterification of crude vegetable oils.[37] Cheaper than other metallic or organic catalytic systems of this screening, it was tested for the needs of production scale-up at *ITERG*. Results obtained are really promising (Table II-3, P14).

2.2. Effect of the concentration in catalyst

$Zn(OAc)_2$ and TBD were selected to further investigate the influence of the loading in catalyst on the macromolecular characteristics of M2HS-based HBPEs. Zinc-based organometallic catalysts usually act as Lewis acids to initiate the condensation reaction as described in Scheme II-5. According to this electrophilic mechanism, the ester group is first activated by coordination to the metal species. This step lowers the electron density of the carbonyl atom, which facilitates the nucleophilic attack of the hydroxyl group from the alcohol.[27,38] Up to date, however, the mechanism of zinc alkoxide-catalyzed transesterification is not fully elucidated and still investigated by mechanistic and theoretical studies. Several pathways involving tetra[39] or hexacoordinated[40] intermediates have been suggested and discussed.

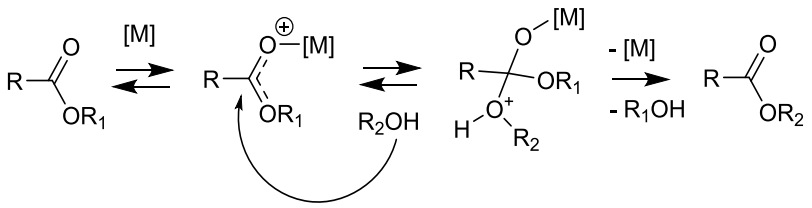

Scheme II-5. Proposed mechanism of zinc alkoxide-based catalysis of transesterification reactions. [M]: zinc alkoxide catalysts

The bicyclic guanidine TBD is a strong base (pKa = 26). This organic catalyst was shown to be effective for the ring-opening polymerization (ROP) of cyclic esters (lactides, lactones, etc.). This reaction was by the way the purpose of numerous mechanistic and kinetic investigations. Two possible catalytic mechanisms were proposed, as illustrated in Scheme II-6. In both cases, a cooperative dual activation is involved.

In pathway (a), TBD acts as a bifunctional nucleophilic catalyst of transesterification. An amide bond is intermediately formed by the attack of the amidine nitrogen on the ester carbonyl, before being cleaved by the subsequent nucleophilic attack of the H-bonded initiator or growing chain.[32,41] DFT calculations demonstrated that a nucleophilic mechanism was possible, but the fully H-bonding pathway (b) exhibited a lower energy barrier for transesterification.[42,43] In this case, two hydrogen bonds can establish: one between the amidine basic nitrogen and the alcohol enhancing its nucleophilicity, and the other between the ester carbonyl and the N-H group of TBD. It is difficult to state on which mechanism is involved in the polycondensation of M2HS. Since *m*-TBD was inefficient as catalyst, the presence of one proton on the TBD nitrogen seems crucial. The set up of an efficient purification procedure to remove any traces of acid from M2HS is even more relevant here.

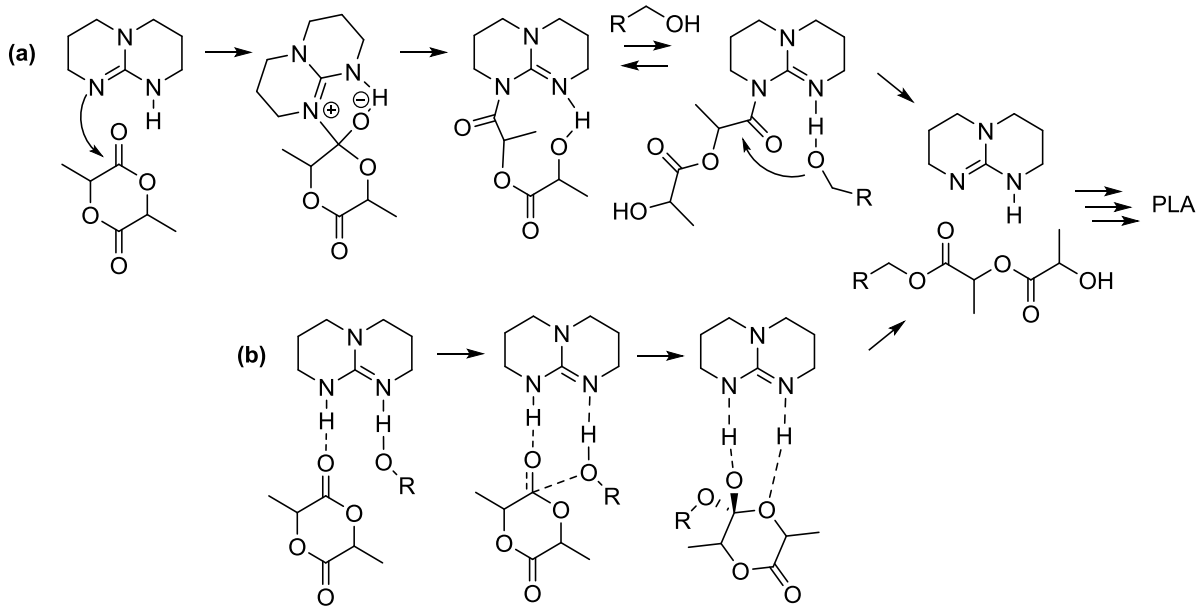

Scheme II-6. Proposed mechanisms for TBD-catalyzed ROP of LA *via* (a) nucleophilic mechanism and (b) H-bonding mechanism

Organic catalysts generally require higher concentrations in comparison with metallic ones. That is the reason why the effect of the concentration in TBD on the polycondensation of M2HS was studied on a larger range, from 0.5 to 10 wt%. Molar masses and dispersities of the as-formed HBPEs were determined by SEC in THF at conversions above 98%. As showed in Figure II-5, the volcano curve obtained reached a maximum of 10 000 $g.mol^{-1}$ for a loading in TBD of 5 wt%. By contrast, no such variation was noticed in the case of zinc acetate: similar molar masses were indeed achieved when the concentration in $Zn(OAc)_2$ was increased from 0.5 to 5 wt%. The observation of a maximum in plotting the catalyst concentration versus the molar masses has already been reported for other metal alkoxides used for polymerization, but at significantly lower loadings.[27]

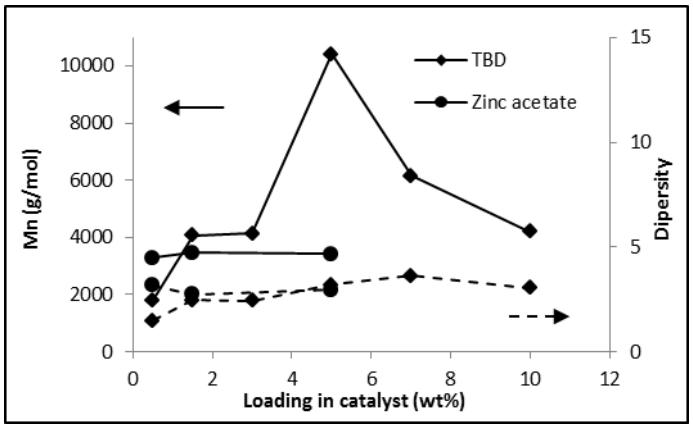

Figure II-5. Influence of the loading in zinc acetate and TBD on macromolecular characteristics of M2HS-based HBPEs. Conditions: pre-drying, first stage at 120°C under N_2 for 2 hours, second stage at 160°C under dynamic vacuum (solid lines: molar masses ($\bar{M}_n$), dashed lines: dispersity (*Đ*))

For instance, Gross and coworkers studied the melt polycondensation of ω-hydroxytetradecanoic acid, an AB-type fatty acid obtained by fermentation, using titanium tetraisopropoxide ($Ti(OiPr)_4$).[44] The optimum concentration for the titanium-based catalyst was described between 300 to 500 ppm. Further increase in the loading in $Ti(OiPr)_4$, up to 1 000 ppm, led to a decrease in the absolute molecular weights, as measured by SEC-MALLS, from 120 $kg.mol^{-1}$ to 77 $kg.mol^{-1}$. This phenomenon was explained by the competitive binding of the catalyst in both intrachain ester units and chain-end groups. As molar masses increase, the concentration in chain-ends decreases and thus metal ions preferably complex with intrachain ester oxygen atoms resulting in chain scission reactions. At high contents in $Ti(OiPr)_4$, molar masses appeared to reach a plateau, as observed in our case, justified as a consequence of the lower occurrence of ester groups along the chain (*vs.* end position).

In addition, it is noteworthy that while the macromolecular characteristics of M2HS-based HBPEs remained constant on the range 0.5-5 wt%, the apparent viscosity of the reaction mixtures increased with the loading in zinc acetate. The same phenomenon was reported by Cao and coworkers when they examined the synthesis of poly(tetramethylene succinate) catalyzed by titanium isopropoxide.[45] Based on indirect measurements, they suggested that the excess of $Ti(OiPr)_4$ was likely incorporated in the synthesized polyester chains as linkers of general structure $(RO)_nTi(OP)_m$, where RO and PO refer to alkoxide moieties and polymer chains, and the total of n and $m > 1$ was equal to 4. Similarly, zinc acetate may also act as multifunctional linker when introduced in excess.

To confirm this hypothesis, HBPE samples were analyzed both in solution and in bulk by NMR and FT-IR spectroscopies. The first technique yielded superimposed spectra irrespective of the initial content in $Zn(OAc)_2$. In contrast, FT-IR analyses revealed the appearance of a band at 1 580 cm^{-1} whose intensity increased with the loading in metal-based catalyst, as can be seen in Figure II-6. This might be interpreted with caution however, given that HBPEs were not further purified, as an indication of interactions between the zinc ion and the ester carbonyl moieties of HBPEs.

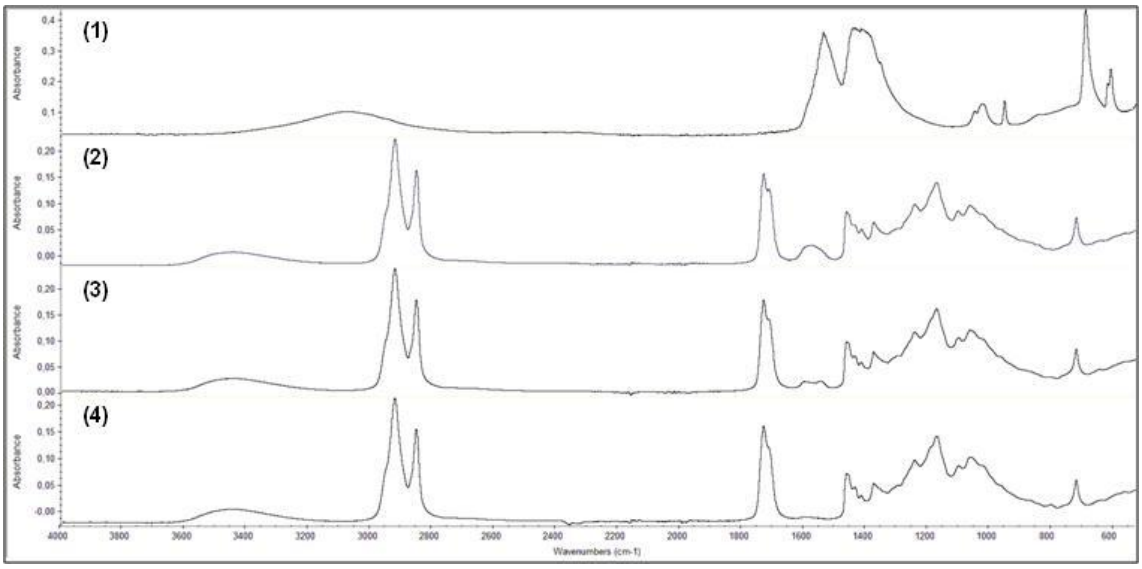

Figure II-6. Stacked FT-IR spectra of (1) zinc acetate, and HBPEs using zinc acetate as catalyst with a loading of (2) 5 wt%, (3) 1.5 wt% and (4) 0.5 wt%

To summary, novel bio-based polyesters were successfully synthesized by polycondensation of M2HS, one oily-derived AB_2-type monomer. For that purpose, a green and efficient synthetic process was purposely developed. Transesterification polymerizations were performed in the melt, namely in the absence of solvent, by using various catalysts. Zinc acetate, TBD and sodium methoxide, three systems with very different activation mechanisms, were shown to be the most effective catalysts for these syntheses achieving rather high molar masses, *i.e.*, in the range 3 000 to 10 000 $g.mol^{-1}$ and broad dispersities from 2 to > 15. The next section of this chapter is dedicated to the characterization of the fine structure of the so-formed polyesters, and the investigation of their thermal stability and thermo-mechanical properties.

3. Characterization of M2HS-based Hyperbranched Polyesters

3.1. Chemical structure and Degree of branching

Insights into the fine structure of the so-formed HBPEs were performed by ^{1}H NMR spectroscopy in $CDCl_3$ as shown in Figure II-7. Taking the ^{1}H NMR spectrum of P10 (Table II-3) as a typical example, the significant decrease in the intensity of the peak assigned to the methoxy group at 3.66 ppm provided evidence of polyester synthesis. The total disappearance of this signal must not be expected if polymerization of the AB_2-type monomer proceeds according to Flory's predictions,[10] namely without any inter or intramolecular side reactions involving the focal point A. Two-dimensional NMR techniques including ^{1}H-^{1}H COSY and ^{1}H-^{13}C HSQC were required to fully assign all peaks of this spectrum (see Figure SI II-3).

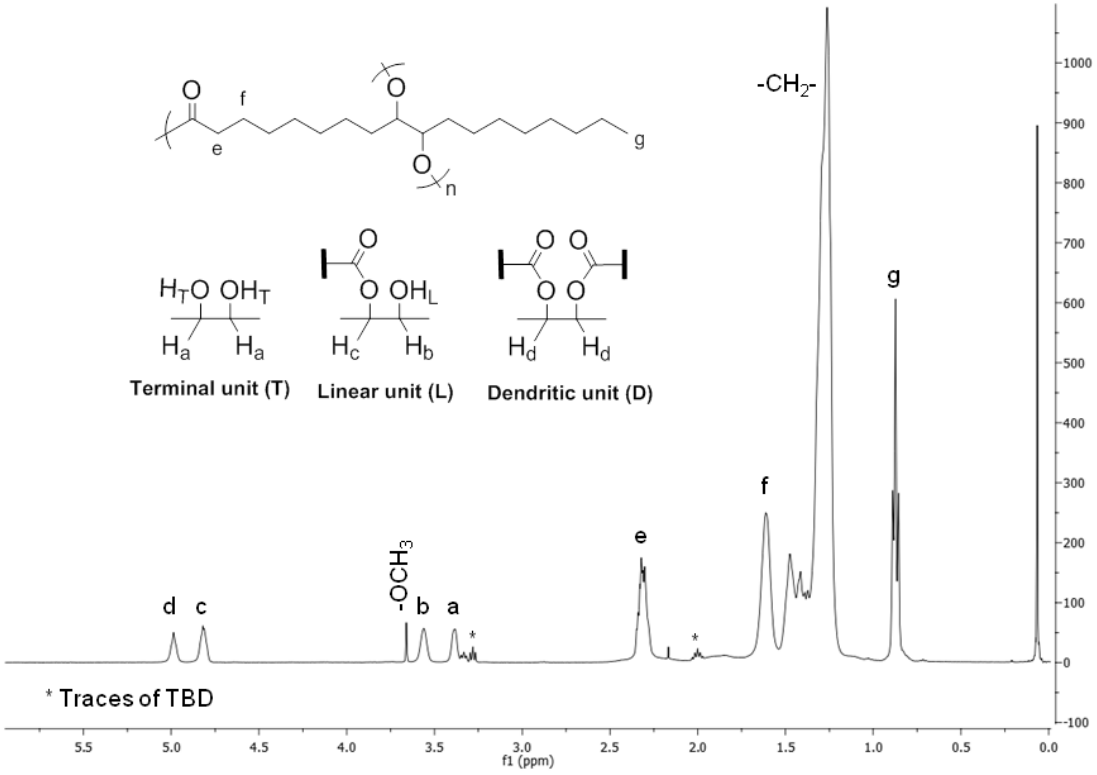

Figure II-7. ^{1}H NMR spectrum of P10 obtained by polycondensation of M2HS in $CDCl_3$

In agreement with the ^{1}H-NMR spectrum of M2HS, the peak at 3.38 ppm was attributed to the terminal unit (T) and identified as the protons adjacent to the vicinal diol on the α-carbons (H_a). After the first substitution, protons H_b and H_c, that are characteristic of the linear unit (L), are no longer chemically equivalent and display downfield signals at 3.56 and 4.81 ppm, respectively. One should note that the chemical shifts are equivalent after esterifying either the 9 or the 10-position. Finally, the peak at 4.99 ppm was assigned to the protons H_d of the dendritic unit (D).

Hence, ^{1}H NMR enabled to distinguish each of the three repeating units characteristic of HBPs obtained by polycondensation of AB_2-type monomers. This technique was thus used to determine the degree of branching of our bio-based HBPEs.

3.1.1. Determination of Degree of branching

The degree of branching (DB) is a key parameter of HBPs characterizing the difference in molecular structure of these materials in comparison to their linear analogues. This DB factor is comprised between 0 and 1. Two formulas have been established for the calculation of the DB of HBPs arising from the polycondensation of AB_2-type monomers. In 1990, Fréchet and coworkers,[46] first described the degree of branching as a function of the ratios of the three structural units of the polymer, namely terminal (T), linear (L) and dendritic (D):

$$DB_{Fréchet} = \frac{D + T}{D + T + L} \quad \textbf{(II-1)}$$

However, this definition was proved to be only valid for high polymerization degrees, otherwise even fully linear polymers would have a $DB_{Fréchet} > 0$. In the low molar mass region, another equation was thus suggested by Frey and coworkers[47]:

$$DB_{Frey} = \frac{2D}{2D + L} \quad \textbf{(II-2)}$$

Both definitions (I-1) and (I-2) were applied in the course of this study. As aforementioned, values for T, L and D were determined based on the respective integration of the protons H_a, H_c and H_d.

Interestingly, the DB of our oily-derived HBPEs was shown to be influenced by the solvent of analysis. Indeed, one single HBPE sample ($\bar{M}_n$ = 4 030 g.mol^{-1}, $Đ$ = 2.43) was characterized by ^{1}H NMR in several solvents of various polarity, including toluene-d_8, tetrahydrofuran-d_8, chloroform-d, dichloromethane-d_2, dimethylformamide-d_7, dimethylsulfoxide-d_6 as well as in a 1:1 (v/v) mixture of deuterated chloroform and DMSO. In each case, the calibration was performed against the known solvent residual peak, except for the mixture of $CDCl_3$:DMSO-d_6 where TMS was used as an external reference.

As can be seen in Figure II-8, ^{1}H NMR spectra obtained revealed similarities but also differences. Two additional peaks were identified in deuterated DMSO and DMF at 4.14-4.11 and 4.66-4.60 ppm, respectively and assigned to the hydroxyl groups of the terminal (-OH_T) and linear (-OH_L) units. In addition, chemical shifts characteristic of the three different subunits, appeared to be influenced by the polarity of the solvent even if no general trend could be drawn.

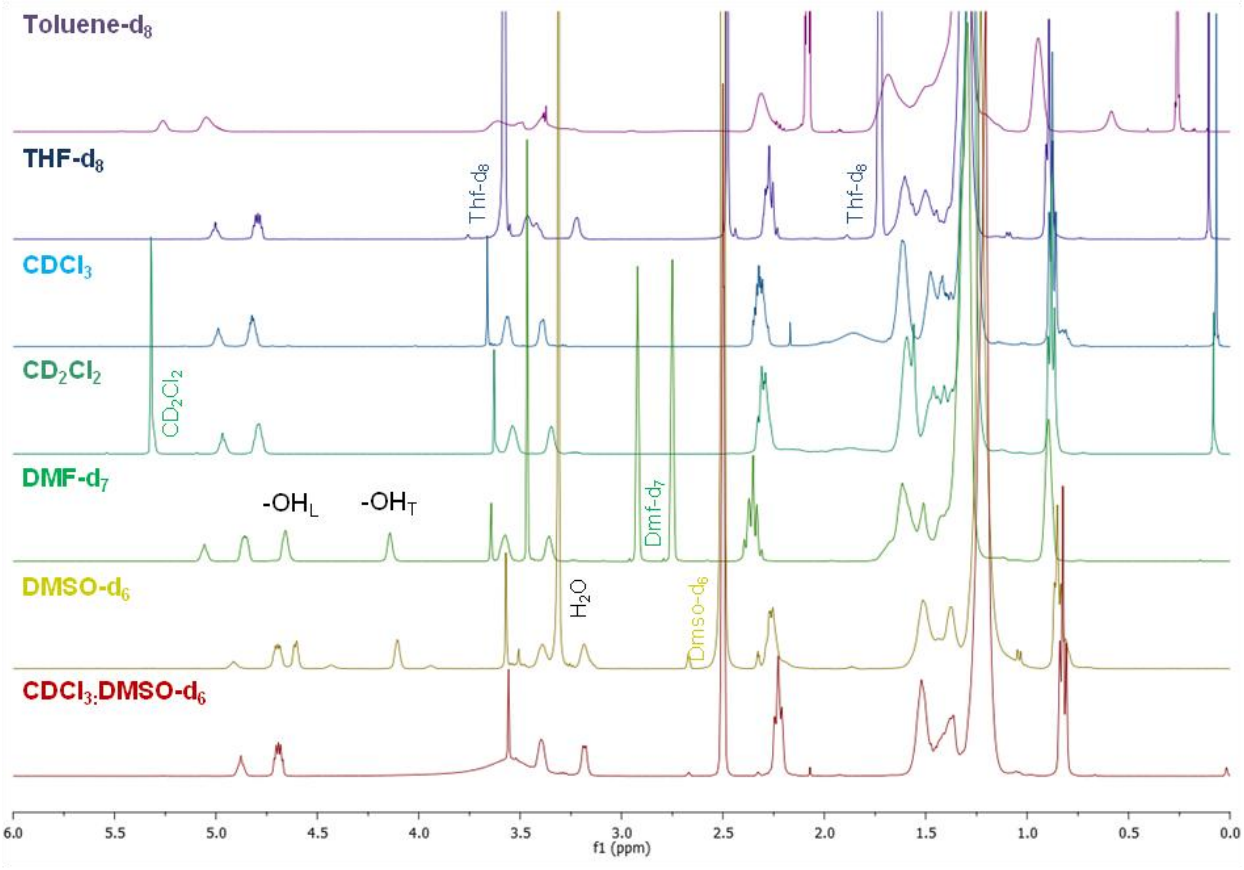

Figure II-8. Stacked ^{1}H NMR spectra of one single HBPE in various solvents (from up to down: toluene-d_8, THF-d_8, $CDCl_3$, CD_2Cl_2, DMF-d_7, DMSO-d_6 and 1:1 mixture of $CDCl_3$: DMSO-d_6)

Normalized values obtained for T, L and D, as well as DB_{Frey} and $DB_{Fréchet}$ are summarized in Table II-4. One can notice that whatever the solvent used for analysis, DBs calculated by using the Frey equation are smaller than those determined with the Fréchet expression. This can be explained by the presence of residual amounts of unreacted AB_2 monomers that were not detected by SEC analysis, and which led to an overestimation of the molar ratio of the terminal units (T). In the rest of this study, equation (I-2) was thus systematically preferred for the calculation of the degree of branching (DB).

Table II-4. Values for T, L, D, DB_{Frey} and $DB_{Fréchet}$ obtained by ^{1}H NMR

Solvent	Toluene-d_8	THF-d_8	$CDCl_3$	CD_2Cl_2	DMF-d_7	DMSO-d_6	$CDCl_3$/ DMSO-d_6
T[1]	nd	0.26	0.25	0.25	0.28	0.30	0.28
L[2]	0.58	0.58	0.59	0.60	0.59	0.59	0.59
D[3]	0.15	0.15	0.15	0.16	0.14	0.08	0.13
DB_{Frey}	0.34	0.34	0.34	0.34	0.32	0.21	0.31
$DB_{Fréchet}$	nd	0.41	0.40	0.41	0.43	0.39	0.41

T, L and D molar ratios determined based on the integration of (1) $H_a/2$ (2) H_c and (3) $H_d/2$.
nd. not determined

All DB_{Frey} values were found in the same range except in DMSO-d_6. The relatively strong underestimation observed (0.21 *vs.* 0.31) was correlated with the high polarity of this solvent. Indeed, the molar ratio, D, measured in DMSO-d_6 is significantly lower than in the other solvents. This is likely due to the fact that deuterated DMSO better solvates the hydrophilic linear and terminal units than the more hydrophobic dendritic ones. In rather apolar solvents, such as THF-d_8, $CDCl_3$ or CD_2Cl_2, the opposite effect is observed but to a much lower extent. The molar ratio in terminal unit, T, is indeed slightly underestimated (0.25 *vs.* 0.28). The most relevant solvents for the determination of the DB of these rather amphiphilic HBPEs turned out to be DMF-d_7 or a combination of $CDCl_3$/DMSO-d_6 (1:1 in vol.). Due to practical considerations, DB was measured in $CDCl_3$ for the rest of this study, assuming that values obtained would be slightly overestimated in this solvent (0.34 *vs.* 0.31).

One additional NMR experiment was run in order to check if the protons assigned to the dendritic units did not require longer time to relax in DMSO-d_6, compared to other solvents. This would have explained why the molar ratio D displayed such a low integral in DMSO-d_6. For that purpose, one HBPE sample was analyzed by ^{1}H NMR at different longitudinal relaxation times (T1), *i.e.* 5, 10 and 20 seconds (see supporting information Figure SI II-4). However, no impact was noted on the DB, values remaining constant and equal to 0.22.

Quantitative *^{13}C NMR* analyses were next carried out in $CDCl_3$ to confirm the DB values achieved. The pulse program was optimized with M2HS as model until the integral of the carbonyl carbon signal came to 1. The HBPE ^{13}C NMR spectrum given in Figure II-9, was analyzed as a mean to identify well-separated signals characteristic of the three different subunits (T, L and D). Two regions fulfill these requirements and allow the quantitative determination of the DB.

On the one hand, four signals were distinguished in the region of the alkoxy carbon atoms (70-80 ppm) at 76.33, 74.50, 73.59 and 72.50 ppm, and assigned to C_c, C_a, C_b and C_d carbon atoms, respectively. On the other hand, in the region of the carbonyl carbons (170-180 ppm), three distinct peaks were observed. The signal at 174.37 ppm was identified as the carbonyl carbon of the ester focal point. Its integral of 0.09 fits perfectly with the one of the methoxy carbon (-O**C**H$_3$) at 51.50 ppm. The two signals at 173.82 and 173.40 ppm were assigned to the carbonyl carbons of the linear (C_L) and dendritic units (C_D), respectively. Both sets of data led to a DB of 0.33, a value that was very close to that determined by ^{1}H NMR spectroscopy (0.34).

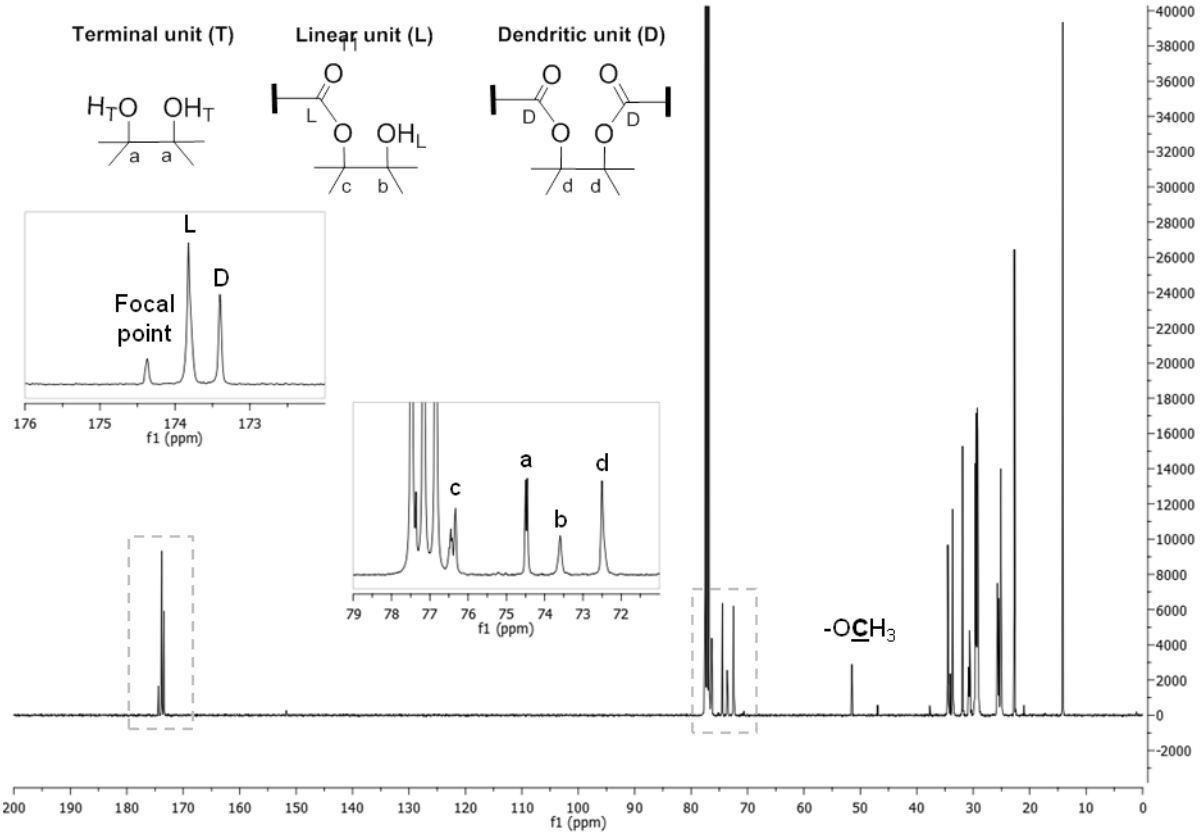

Figure II-9. ^{13}C NMR spectrum of M2HS-based HBPE in $CDCl_3$

To conclude, a simple and efficient method of measurement of the DB by ^{1}H NMR spectroscopy in $CDCl_3$ was set up. The study of the influence of the solvent of analysis revealed that DB values can be strongly underestimated when measured in rather polar media, such as DMSO-d_6. Quantitative ^{13}C NMR was also successfully applied for the determination of the DB of these oily-derived HBPEs. In the next section, investigations were carried out regarding the influence of key parameters (x, $\bar{M}_n$, catalyst of polymerization, etc.) on DB values.

3.1.2. Parameters affecting DB values

DB values obtained for these oily-derived HBPEs are in the range 0.07 to 0.45, which remains smaller than the 0.5 predicted by the theory.[47] In addition, the DB was shown to depend on numerous factors including the conversion rate (x), the molar masses of HBPEs and more interestingly, the catalyst of polycondensation employed as illustrated in Table II-5. Conversion dependence of DB values is discussed in the next section (Chapter II.3.1.3). Figure II-10 shows the evolution of the DB with the apparent molar masses measured by SEC (THF, calibration PS standards), for several HBPEs obtained by TBD-catalyzed polycondensation, all polymerizations having been carried out until completion (x = 100%). As expected, DB increases with molar masses of HBPEs until a plateau is reached at 0.43-0.45 above 6 000 g.mol^{-1}.

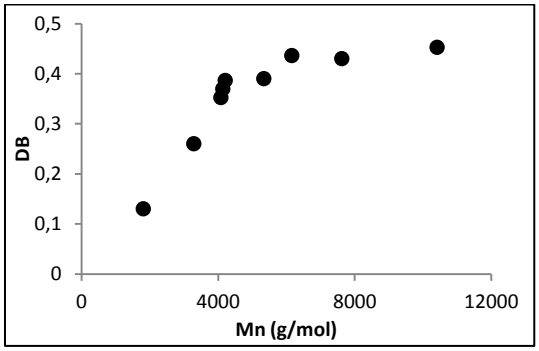

Figure II-10. Molar mass dependence of DB values for HBPEs obtained by TBD-catalyzed polycondensation

More importantly, the branching density of these HBPEs could be tuned as a function of the polymerization catalyst employed (Table II-5). Overall, TBD appeared to favor the formation of the most branched architectures, with DB values in the range 0.13 to 0.45. In contrast, zinc acetate-catalyzed polycondensations yielded HBPEs with a more linear structure and DBs lower than 0.26.

Table II-5. Catalyst dependence of DB values for M2HS-based HBPEs

Entry	Catalyst	x^1 (%)	$\bar{M}_n{}^1$ (g.mol^{-1})	$Đ^1$	$DB_{Frey}{}^2$
P2	$Ti(OiPr)_4$	48	1 200	1.08	0
P3	$Zn(OAc)_2$	98	3 480	2.74	0.07
P5	DBTO	39	1 100	1.09	0.05
P6	Sb_2O_3	45	1 200	1.08	0.11
P7	$Sn(Oct)_2$	93	3 200	2.03	0.21
P8	TBD	100	4 100	2.46	0.35
P14	NaOMe	100	6100	3.08	0.29

(1) SEC in THF – calibration PS standards. (2) ^{1}H NMR

Attempts to modify the branching architecture of these HBPEs were carried out and their impact on the DB was investigated. Polycondensation of M2HS was first performed in the presence of multifunctional core molecules of B_f-type (see Chapter I, section 2.1.3). Various polyols were tested as can be seen in Scheme II-7. Low-boiling point molecules such as 1,3-propranediol and glycerol did not give conclusive results. Incorporation of 1,12-dodecanediol into the polymer structure was confirmed by ^{1}H NMR but did not impact neither the molar masses nor the DB of the as-formed HBPEs.

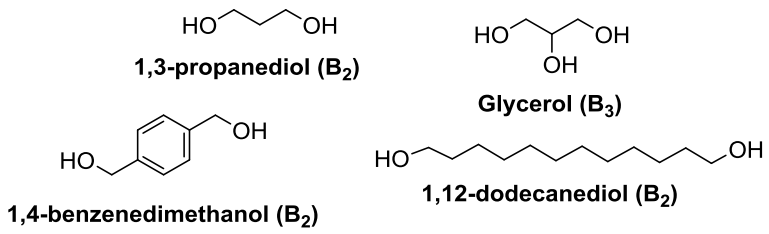

Scheme II-7. Multifunctional core molecules used in the synthesis of M2HS-based HBPEs

By contrast, copolymers of M2HS and 1,4-benzenedimethanol (BDM) with in-feed ratios of 2.5, 5 and 10 mol%, were successfully prepared under the same conditions to those used for the synthesis of the homopolymer with TBD as catalyst (see ^{1}H NMR spectrum in Figure SI II-5). All polymerizations were carried out until completion. As shown in Figure II-11, below 5 mol% of in-feed ratio in 1,4-benzenedimethanol, the DB roughly remained constant in the range 0.35 to 0.39, while the molar masses of the copolymers significantly increased from 4 000 to 6 300 g.mol^{-1} as expected. The addition of higher amounts of core molecule (10 mol%) led to a significant decrease both in molar masses and branching density, *i.e.* $\bar{M}_n$ = 2 800 g.mol^{-1} and DB = 0.27. The copolymer dispersity (*Đ*) was reported to follow the same trend than their molar masses while the introduction of core molecule is supposed to narrow the molecular size distribution.[48]

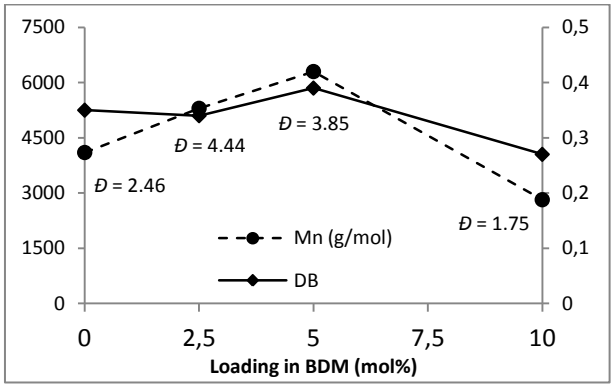

Figure II-11. Molar masses and DB of M2HS/1,4-benzenedimethanol hyperbranched copolymers

Besides, it is important to specify that in order to actually tune DB values, copolymerizations of M2HS with an AB-type monomer, namely methyl 12-hydroxystearate, were also carried out at different feed-ratios, using $Zn(OAc)_2$ as catalyst. However, all attempts resulted in oligomers of low molar masses (< 1 850 g.mol^{-1}). Hence, the syntheses of these copolymers were not continued.

3.1.3. Kinetics of polymerization

The conversion dependence of the degree of branching (DB) during the polycondensation of M2HS was investigated with two different catalysts, TBD and $Zn(OAc)_2$. Polymerization reactions were monitored by ^{1}H NMR spectroscopy in $CDCl_3$. Aliquots were directly taken out from the reaction mixture at different times and analyzed without further purification. Structure-dependent signals H_a, H_c and H_d were used for the quantitative determination of structural units T, L and D in HBPEs (see ^{1}H NMR assignment in p.94) and for the calculation of their degree of branching ($DB_{Fréchet}$, DB_{Frey}).

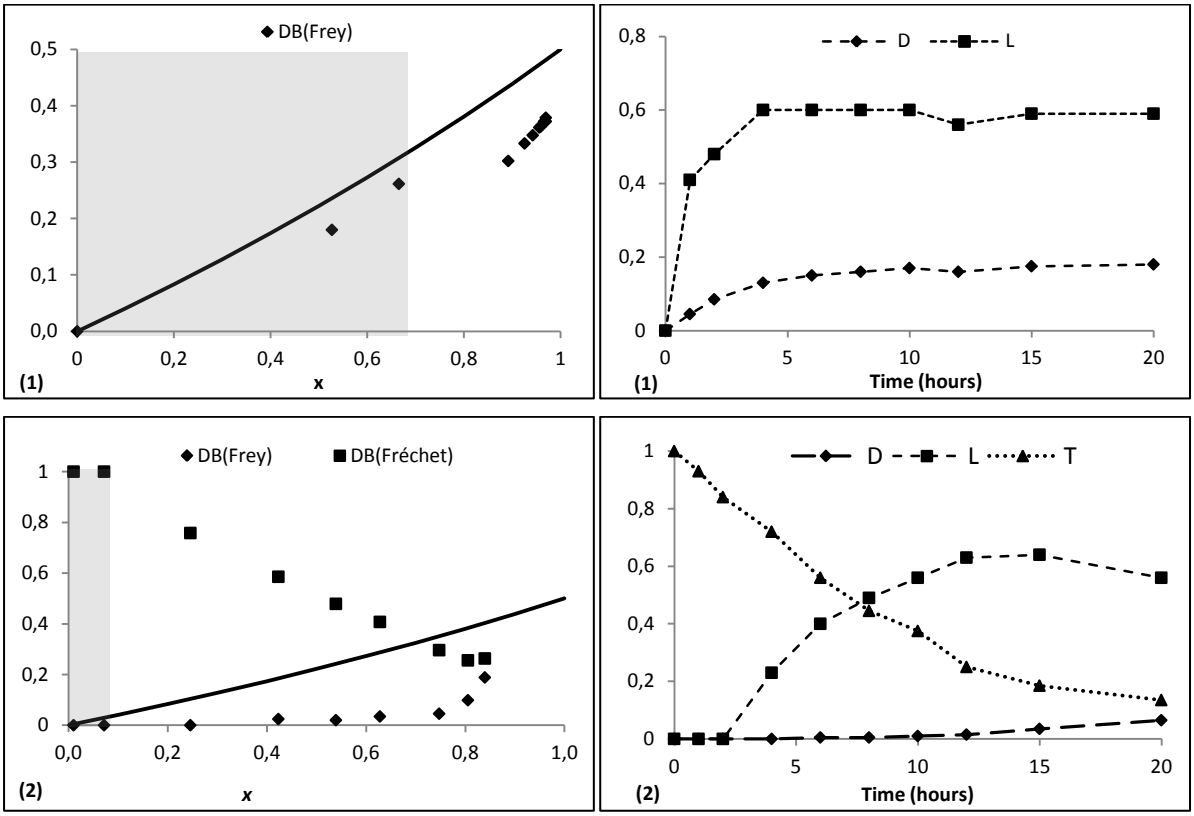

Figure II-12. Conversion dependence of the degree of branching (DB_{Frey}, $DB_{Fréchet}$) and time dependence of the structural units (D, L, T) for polycondensation of M2HS using as catalyst (1) TBD, (2) zinc acetate (solid lines: theoretical data, symbols: NMR data)

Due to the overlapping with TBD peaks, the ratio of the terminal units (T) could not be determined for HBPEs prepared with this organic catalyst. Therefore, $DB_{Fréchet}$ was only calculated for the zinc acetate-catalyzed polycondensation of M2HS. *x* corresponds to the conversion of the focal point A measured based on the intensity of the ester function peak at 3.66 ppm. The reproducibility of these kinetics was confirmed for the polymerization using TBD as catalyst.

Figure II-12 depicts the kinetic data obtained with (1) TBD and (2) zinc acetate. The discontinuity of the curves showing the evolution of DB with conversion (*x*) is explained by the fact that the first three points were recorded during the oligomerization stage (indicated by the grey zone), at 120°C, under nitrogen blowing; while the following data refer to the polymerization step that took place at 160°C under dynamic vacuum. As observed with zinc acetate, both definitions of DB (Fréchet and Frey) lead to similar result at high conversions. However, DB values achieved even with TBD never exceeded 0.4, which is lower than 0.5 predicted by the theory. Hölter and Frey,[47] as well as Yan, Müller and coworkers,[49] expressed the conversion dependence of the DB as follows:

$$DB = \frac{2x}{5 - x}\Big|_{k_L = k_D} \qquad \textbf{(II-3)}$$

This equation describes the ideal random polycondensation of AB_2-type monomers where the formation of linear (k_L) and dendritic (k_D) units takes place at equal reaction rates ($k_L = k_D$). In other words, the reactivity ratio *r* of the rate constants k_D/k_L is equal to 1.

Theoretical and measured data are compared in Figure II-12. Whatever the catalyst, experimental points remain below the theoretical line. This phenomenon has already been examined by Galina and coworkers as a *negative substitution effect*[50,9] indicating that the two hydroxyl functions of M2HS are not of equal reactivity during the whole polymerization. Once a linear unit is formed, the reactivity of the remaining alcohol ($-OH_L$) significantly decreases due to steric hindrance. The formation of linear units is thus favored over dendritic ones ($k_L >> k_D$, see Scheme II-8). According to previous literature,[50] a maximum DB value of 0.4 with TBD and 0.2 with zinc acetate implies a reactivity ratio *r* (k_D/k_L) of 0.5 and 0.1, respectively. This negative substitution effect is thus even more pronounced with zinc acetate, in agreement with the time dependence curves characteristic of each structural unit (Figure II-12).

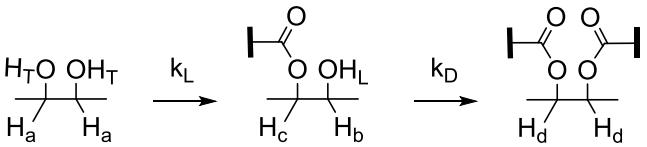

Scheme II-8. Rate constants of the formation of linear and dendritic units k_L and k_D

The close vicinity of the two reactive alcohols in M2HS certainly not only limits the DB values that can be reached by our HBPEs, but also their molar masses. This intrinsic limitation could indeed explain why the molar masses measured for M2HS-derived HBPEs did not exceed 10 000 g.mol^{-1}, while higher values were achieved by Petrović and coworkers with their hydroformylated methyl esters of soybean oil ($\bar{M}_n$ = 30 000-40 000 g.mol^{-1}),[21] as well as Li and coworkers ($\bar{M}_n$ = 11 400-60 400 g.mol^{-1}).[22]

3.2. Molar mass and molar mass distributions

SEC (THF, calibration PS standards) was also used to monitor the polymerization reactions previously described in section 3.1.3. Time dependence of (1) monomer conversion (*x*), and (2) molar masses ($\bar{M}_n$) and dispersity (*Đ*) are summarized in Figure II-13. The oligomerization stage, *i.e.* indicated by the grey zone, that took place at 120°C under nitrogen appeared less efficient with zinc acetate than TBD. Indeed, during the first two hours of polymerization, only dimers and trimers were formed with the organometallic catalyst in poor conversion ($x \leq 10\%$). Once the temperature was raised to 160°C and dynamic vacuum was

applied, an acceleration of the kinetics was observed. Molar masses therefore progressively increased with reaction duration, to reach 3 700 g.mol^{-1} at high conversion, above 96%. In contrast, faster kinetics of polymerization was observed when TBD was used as catalyst. Indeed, full conversion was achieved within 4 hours only. In the early stages of polymerization, molar masses were found to increase more rapidly with reaction duration to gradually leveled off at 7 500-8 000 g.mol^{-1} over 16 hours.

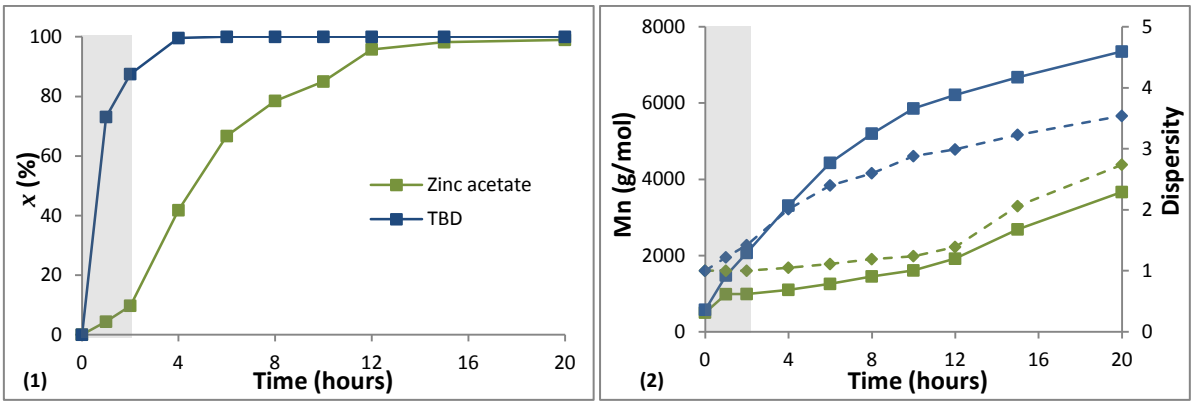

Figure II-13. Kinetics of zinc acetate and TBD-catalyzed polycondensation of M2HS: time dependence of (1) monomer conversion (*x*) and (2) molar masses and dispersity (solid lines: $\overline{M}_n$, dashed lines: *Đ*)

In addition, SEC provided valuable information about the formation mechanisms of the HBPE structure. Figure II-14 compares the SEC-RI traces of aliquots withdrawn during the TBD-catalyzed polycondensation of M2HS. In the early stages of reaction, chromatograms displayed conventional pattern of step-growth polymerization. These multimodal distributions stated the formation of intermediate oligomers of increasing degrees of polymerization ($\overline{DP}_n$).

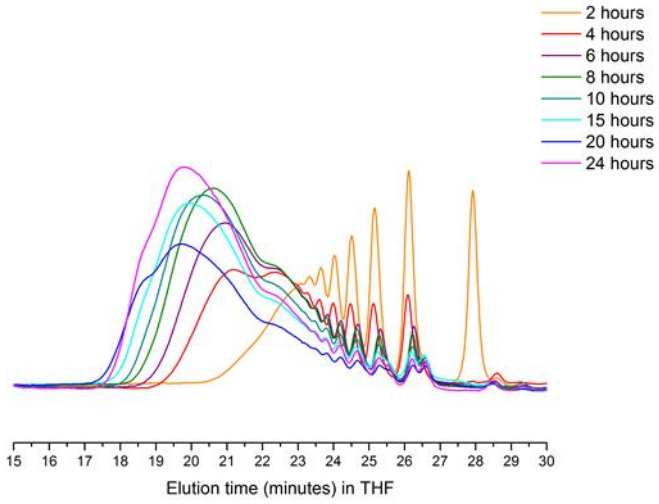

Figure II-14. SEC-RI traces of aliquots withdrawn at different reaction times, during the polycondensation of M2HS using TBD as catalyst (P16)

The disappearance of the peak at 27.9 minutes assigned to M2HS, evidenced a complete conversion within the first 4 hours of polymerization. After 15 hours of reaction, signals attributed to dimers and trimers at 26.4 and 25.3 minutes, respectively, were found to be split into two 'distinct' peaks. This was interpreted as being the result of the formation of oligomeric lactones by cyclization. The occurrence of this side reaction in AB_n as well as $A_2 + B_n$ polymerization processes, has been extensively studied in the past 20 years. In particular, Kricheldorf carried out extensive investigations on these cyclic structures and developed a cyclization theory in order to explain the deviations of the HBP structures from the cascade theory of Flory.[51] In the absence of focal point, *i.e.* methyl ester functions, these cyclic oligomers were no longer involved in the polymerization and remained even at the late stages of reaction, thereby contributing to the broadening of the molar mass distribution.

Beyond 20 hours, a shoulder was observed towards higher molar masses. Two hypotheses were put forward to explain this phenomenon, as a consequence of either (i) intermolecular rearrangements by transesterification or (ii) the occurrence of etherification side reactions. All the side reactions mentioned in this section are further examined by MALDI-TOF MS analysis in Chapter III of this manuscript.

In the course of this study, molar masses of our renewable HBPEs were determined by SEC in THF with a differential refractive index detector (RI), using calibration with linear PS standards. This technique is known to lead to apparent molar masses that can significantly deviate from their absolute values, given that HBPs display smaller hydrodynamic radii than their linear counterparts of the same molar mass.[4] In this specific case, overestimation of molar masses may also take place because of their large number of hydroxyl end-groups, developing their affinity to the solvent and/or the SEC column. Subsequent interactions can thus no longer be neglected.[52]

Another technique was thus investigated to accurately characterize the molar masses of the HBPEs coming from the previous kinetic experiments, using either zinc acetate or TBD, and referred to as P15 and P16, respectively. For that purpose, SEC was coupled with a multi-angle laser light scattering detector (MALLS). This combination is known to give the absolute weight average molar mass $\bar{M}_w$ of polymeric systems even of complex architecture, provided that the (*dn/dc*) value of the polymer in the solvent of analysis is known.

In addition, a linear reference (LPE) was synthesized for comparison purpose starting from methyl 12-hydroxystearate. This commercially available FAME is prepared by hydrogenation of methyl ricinoleate. Its polymerization was carried out under the same conditions described above for HBPE synthesis, using zinc acetate as catalyst (Scheme II-9). The as-formed linear polyesters were successfully characterized by ^{1}H NMR (see supporting information, Figure SI II-6).

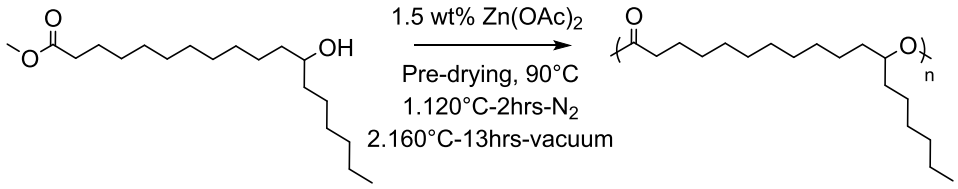

Scheme II-9. Polycondensation of methyl 12-hydroxystearate (linear reference, LPE)

Weight average molar masses ($\bar{M}_w$) determined with both RI and MALLS detectors, as well as specific refractive-index increments (*dn*/*dc*) of the three samples are summarized in Table II-6. *dn*/*dc* values, estimated with an assumption of 100% mass recovery, were found in the range 0.061-0.070 mL.g^{-1}. Typical errors were ±1 of the last digit. While the apparent molar masses of LPE, relative to PS calibration, appeared slightly overestimated compared to their absolute values provided by the MALLS detector; the opposite effect was observed with our HBPEs. The deviation was besides more pronounced with P16 than P15. This was interpreted as being the result of the higher branching density of P16, *i.e.* DB = 0.40 for P16 *vs.* 0.18 for P15.

Table II-6. Molar masses of HBPEs and LPE, measured by the use of relative (RI) and absolute (MALLS) determination methods

Entry	RI		MALLS		
	$\bar{M}_w$ (g.mol^{-1})	*Đ*	*dn/dc*[1] (mL.g^{-1})	$\bar{M}_w$ (g.mol^{-1})	*Đ*
P15	9 700	2.71	0.068	12 300 (±17%)	1.37 (±29%)
P16	40 100	3.68	0.070	68 700 (±5%)	1.49 (±12%)
LPE	19 100	2.59	0.061	17 400 (±13%)	1.19 (±22%)

(1) Typical errors are ± 1 of the last digit.

One point to consider is that the dispersities provided by MALLS were, irrespective of the polymerization catalyst employed, lower than 2. This was assigned to a lack of sensitivity of this detector in the low molar mass region. Indeed, taking as an example the SEC-RI and SEC-MALLS traces of P16, Figure II-15 clearly shows that while the concentration-sensitive RI detector displays a weak response in the high molar mass slice of the raw data, the molar mass-sensitive MALLS detector shows a poor response in the low molar mass region of the

chromatogram (elution time > 25 minutes). The determination by MALLS of the low mass region requires either a high contrast of the polymer solution to the solvent, *i.e.* high *dn*/*dc*, or a high concentration; conditions that were not fulfilled in such cases.

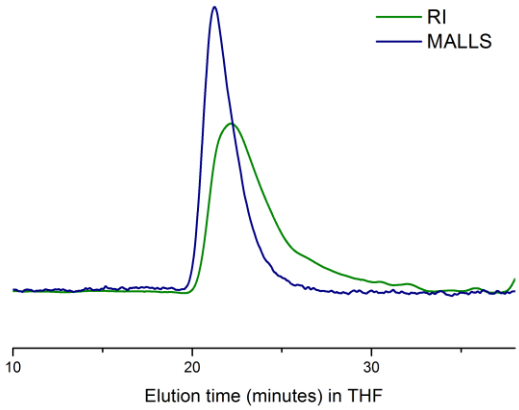

Figure II-15. SEC-RI and SEC-MALLS traces of P16

This discussion highlights how complex the characterization of the molar masses and molar mass distribution of HBPs can be. SEC-MALLS measurements lead to reliable information on the absolute weight average molar mass ($\overline{M}_w$) of our HBPEs, revealing a systematic underestimation of the values measured relative to PS standards. However, this single information is not enough with respect to the broad dispersities of our HBPEs. To achieve full characterization, the combination of SEC-RI-MALLS appears essential.

3.3. Thermal properties

Thermal properties of our renewable HBPEs were characterized by DSC analyses. As expected, our oily-derived highly branched polyesters displayed amorphous properties, their dendritic architecture preventing polymeric chains from crystallization (Figure II-16). In contrast, the linear reference prepared by polycondensation of methyl 12-hydroxystearate was semi-crystalline in nature and demonstrated melting and crystallization temperatures of -19 and -30 °C, respectively (Figure II-16). Glass transition temperatures of HBPEs (T_gs) were found in the range -32.5 to -20°C. Even if no general trend could be clearly drawn, the highest T_g values were achieved for DBs higher than 0.3. These observations highlight one distinctive feature of HBPs. In contrast to their linear counterparts, the end-group effect on T_g is very strong. In this case, the number of polar end-groups increasing with the branching density, this results in stronger interactions between molecules.

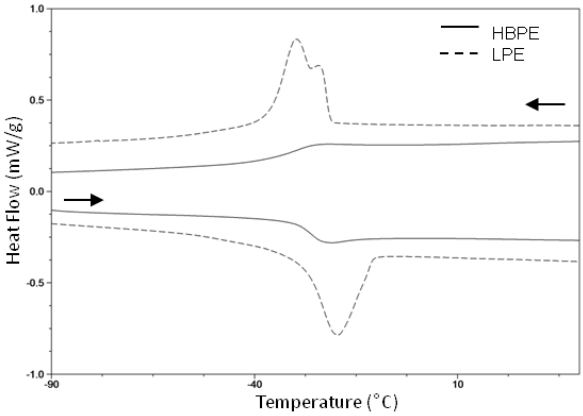

Figure II-16. DSC thermograms of M2HS-based HBPE and LPE (second cycle at 10°C/min)

Thermal stability of our HBPEs was also investigated by TGA analyses, under a nitrogen stream at a heating rate of 10°C.min^{-1}. DB did not seem to show any influence on the 5% degradation temperature ($T_d^{5\%}$). By contrast, the thermal stability of these HBPEs proved to depend on the catalyst of polymerization employed. Branched polymers synthesized using $Zn(OAc)_2$ indeed displayed lower $T_d^{5\%}$, in between 237 and 252°C, than materials obtained with TBD (306 to 338°C). Typical decomposition profiles of M2HS-derived HBPEs prepared using both catalysts are presented in Figure II-17. TGA derivatives of weight loss as a function of the temperature show one additional degradation step with the organometallic catalyst between 200 and 300°C.

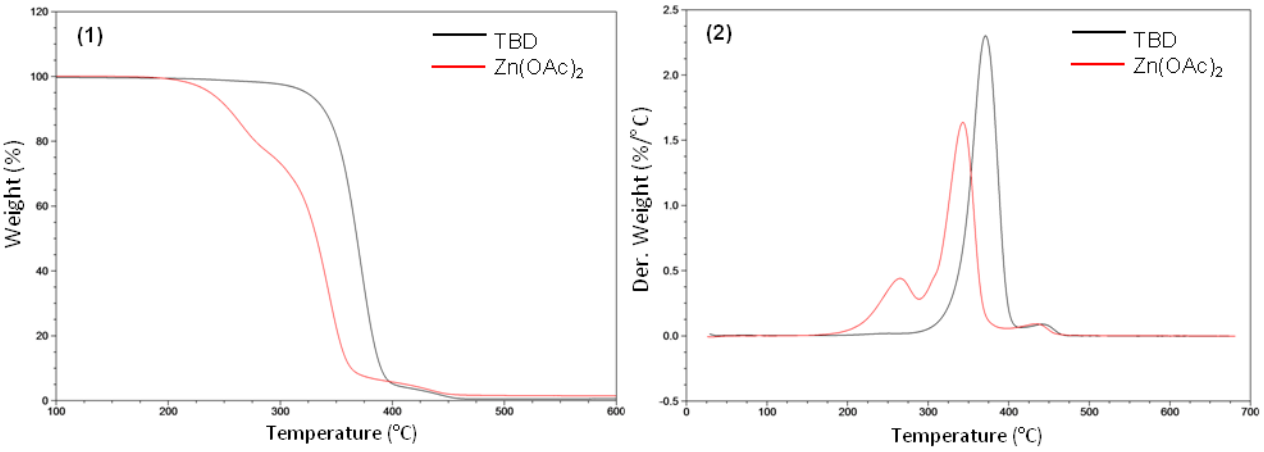

Figure II-17. (1) Weight loss as a function of temperature (2) Derivative of weight loss with temperature for M2HS-based HBPEs using zinc acetate and TBD as catalyst obtained from TGA experiments at 10°C/min under nitrogen atmosphere

This first weight loss was assigned to the thermal zinc acetate-catalyzed depolymerization of the HBPEs, knowing that all samples were characterized without further purification. This phenomenon has already been reported in the literature[27,45] and must be correlated to the conclusions reached regarding the effect of the loading in catalyst on the molar masses of the HBPEs in section 2.2 of this chapter.

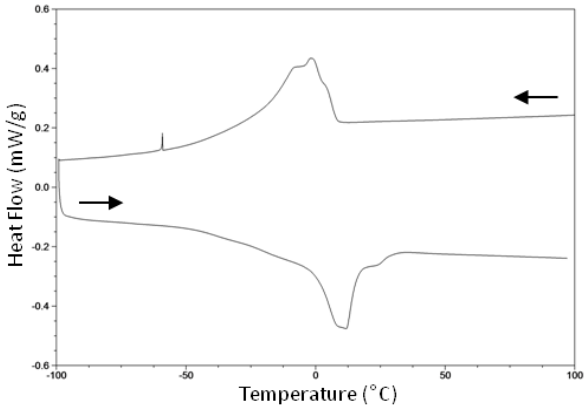

Figure II-18. DSC thermogram of HBPE prepared using zinc acetate after an isotherm of 15 minutes at 250°C

In this study, the depolymerization phenomenon was revealed by DSC. After an isotherm of 15 minutes at 250°C, the thermogram of HBPEs prepared using zinc acetate displayed an exothermic peak upon cooling at 10°C.min^{-1}, and one endothermic peak upon heating (Figure II-18). Since the HBPEs were amorphous, the crystallization observed could be due to the presence of either linear segments or monomer residues within the sample. It is important to notice that this phenomenon was not observed for HBPEs prepared with TBD.

Conclusion

The synthesis of an oily-derived AB_2-type monomer featuring one ester (A) and two alcohol (B) groups was successfully devised, following a two-step procedure. Methyl 9,10-dihydroxystearate (M2HS) was obtained by acid hydrolysis of epoxidized high oleic sunflower oil in high yield (90%) and with a chemical purity over 98%. A facile, green and efficient process of polymerization was then developed resulting in novel renewable HBPEs. Insight into their (macro)molecular characteristics was achieved by SEC in THF. Molar masses in between 3 000-10 000 $g.mol^{-1}$ and broad dispersities (> 2) were obtained. SEC-MALLS measurements, besides, revealed that these values determined relative to PS standards, were underestimated compared to their absolute molar masses. The DB calculated by ^1H NMR spectroscopy varied from 0.07 to 0.45, confirming the branching character of the as-devised polyesters. Their branching density was also found to dramatically depend on the catalyst of polymerization employed. While zinc acetate favored rather linear structures ($DB \leq 0.26$), TBD-catalyzed polycondensations tended to form more branched architectures ($0.13 \leq DB \leq 0.45$). M2HS-derived HBPEs displayed amorphous properties with glass transition temperatures in the range -32.5 to -20°C and expected thermal stabilities for oily-derived polyesters with $T_d^{5\%}$ varying from 306 to 338°C. Their degradation profile was found to be similar to their linear analogues prepared by transesterification polymerization of methyl 12-hydroxystearate.

A drawback has however been pointed out. Some kinetic investigations indeed highlighted the occurrence of a negative substitution effect. In other words, the proximity of the two secondary alcohols of the vicinal diols was demonstrated to limit somehow the molar masses and branching density achievable by steric hindrance. Nevertheless, results obtained with M2HS-based HBPEs are comparable to the existing data reported in the literature for poly(bis-MPA) HBPEs. Our oily-derived HBPEs thus proved to be good alternative of lower thermal transitions. The industrial perspectives of this work were thus covered by a European patent.[1]

The next chapter will discuss our efforts to extent the platform of AB_n-type monomers obtained by acid hydrolysis of epoxidized vegetable oils, in order to tune the structural, thermal and/or thermo-mechanical properties of related HBPEs. For that purpose, other substrates of various chain lengths such as the methyl esters of undecenoic (C11:1) or erucic (C22:1) acid, or of higher functionality using methyl ricinoleate (C18:1) were considered.

References

(1) Testud, B.; Grau, E.; Pintori, D.; Taton, D.; Cramail, H. New branched polymers, their preparation process and thereof. EU 14306642 A1, 2014.
(2) McKee, M. G.; Unal, S.; Wilkes, G. L.; Long, T. E. *Prog. Polym. Sci.* **2005**, *30* (5), 507–539.
(3) Voit, B. I. *J. Polym. Sci. Part A Polym. Chem.* **2005**, *43* (13), 2679–2699.
(4) Voit, B. I.; Lederer, A. *Chem. Rev.* **2009**, *109* (11), 5924–5973.
(5) Zhang, X. *Prog. Org. Coatings* **2010**, *69* (4), 295–309.
(6) Kricheldorf, H. In *Polycondensation: History and results*; Springer Berlin Heidelberg, 2014; pp 147–159.
(7) Ghosh, A.; Banerjee, S.; Voit, B. I. *Adv. Polym. Sci.* **2015**, *266*, 27–124.
(8) Kricheldorf, H. R.; Zang, Q.-Z.; Schwarz, G. *Polymer* **1982**, *23* (12), 1821–1829.
(9) Yan, D.; Gao, C.; Frey, H. *Hyperbranched polymers: Synthesis, Properties, and Applications*; John Wiley & Sons, Inc., 2011.
(10) Flory, P. J. *J. Am. Chem. Soc.* **1952**, *74* (1932), 2718–2723.
(11) Liu, M.; Vladimirov, N.; Fréchet, J. M. J. *Macromolecules* **1999**, *32* (20), 6881–6884.
(12) Yu, X. H.; Feng, J.; Zhuo, R. X. *Macromolecules* **2005**, *38* (15), 6244–6247.
(13) Parzuchowski, P. G.; Grabowska, M.; Tryznowski, M.; Rokicki, G. *Macromolecules* **2006**, *39* (21), 7181–7186.
(14) Fischer, A. M.; Schüll, C.; Frey, H. *Polymer* **2015**, *72*, 436–446.
(15) Gao, C.; Yan, D. *Prog. Polym. Sci.* **2004**, *29* (3), 183–275.
(16) Wagner, E.; Bruchmann, F.; Keller, S.-E. Method for producing highly functional, hyperbranched polyesters. US 0165177, 2005.
(17) Wagner, E.; Bruchmann, F.; Haering, D.; Keller, P.; Pouhe, T. Method for producing highly functional hyperbranched polyesters by means of enzymatic esterification. US 7081509, 2006.
(18) Zhang, Y.; Yang, Y.; Cai, J.; Lv, W.; Xie, W.; Wang, Y.; Gross, R. A. In *Biobased Monomers, Polymers, and Materials*; Smith, P. B., Gross, R. A., Eds.; ACS Symposium series: Washington, 2012; p 111.
(19) Türünç, O.; Meier, M. A. R. *Macromol. Rapid Commun.* **2010**, *31* (20), 1822–1826.
(20) Petrović, Z. S.; Cvetković, I. *Contemp. Mater.* **2012**, *III* (I), 63–71.
(21) Petrović, Z. S.; Cvetković, I.; Milić, J.; Hong, D.; Javni, I. *J. Appl. Polym. Sci.* **2012**, *125* (4), 2920–2928.
(22) Bao, Y.; He, J.; Li, Y. *Polym. Int.* **2013**, *62*, 1457–1464.
(23) Köckritz, A.; Martin, A. *Eur. J. Lipid Sci. Technol.* **2008**, *110* (9), 812–824.
(24) Blach, P.; Sambou M'Ban, S.; Allard, J.; Lemor, A. Procédé de préparation de diols vicinaux. FR 3003254, 2013.
(25) Carothers, W. H. *Chem. Rev.* **1931**, *8* (3), 353–426.
(26) Kricheldorf, H. R. *Chem. Rev.* **2009**, *109*, 5579–5594.
(27) Shah, T. ; Bhatty, J. ; Gamlen, G. ; Dollimore, D. *Polymer* **1984**, *25* (9), 1333–1336.
(28) Montaudo, G.; Rizzarelli, P. *Polym. Degrad. Stab.* **2000**, *70* (2), 305–314.
(29) Liu, C.; Liu, F.; Cai, J.; Xie, W.; Long, T. E.; Turner, S. R.; Lyons, A.; Gross, R. A. *Biomacromolecules* **2011**, *12* (9), 3291–3298.
(30) Lebarbé, T.; Grau, E.; Gadenne, B.; Alfos, C.; Cramail, H. *ACS Sustain. Chem. Eng.* **2015**, *3* (2), 283–292.
(31) Nederberg, F.; Connor, E. F.; Möller, M.; Glauser, T.; Hedrick, J. L. *Angew. Chemie Int. Ed.* **2001**, *40* (14), 2712–2715.
(32) Kiesewetter, M. K.; Shin, E. J.; Hedrick, J. L.; Waymouth, R. M. *Macromolecules* **2010**, *43* (5), 2093–2107.
(33) Fèvre, M.; Vignolle, J.; Gnanou, Y.; Taton, D. In *Polymer Science: A Comprehensive Reference*; Matyjaszewski, K., Möller, M., Eds.; Elsevier: Amsterdam, 2012; p 67.
(34) Fèvre, M.; Pinaud, J.; Gnanou, Y.; Vignolle, J.; Taton, D. *Chem. Soc. Rev.* **2013**, *42*, 2142–2172.

(35) Lebarbé, T.; Maisonneuve, L.; Nga Nguyen, T. H.; Gadenne, B.; Alfos, C.; Cramail, H. *Polym. Chem.* **2012**, *3* (10), 2842.
(36) Yan, D.; Zhou, Z. *Macromolecules* **1999**, *32* (3), 819–824.
(37) Demirbas, A. *Energy Convers. Manag.* **2008**, *49* (1), 125–130.
(38) Pang, K.; Kotek, R.; Tonelli, A. *Prog. Polym. Sci.* **2006**, *31* (11), 1009–1037.
(39) Coskun, N.; Er, M. *Turkish J. Chem.* **2005**, *29*, 455–461.
(40) MacDonald, W. *Polym. Int.* **2002**, *51* (10), 923–930.
(41) Kiesewetter, M. K.; Scholten, M. D.; Kirn, N.; Weber, R. L.; Hedrick, J. L.; Waymouth, R. M. *J. Org. Chem.* **2009**, *74* (24), 9490–9496.
(42) Simón, L.; Goodman, J. M. *J. Org. Chem.* **2007**, *4*, 1–19.
(43) Bibal, B.; Thomas, C. *Green Chem.* **2014**, *16*, 1687–1699.
(44) Liu, C.; Liu, F.; Cai, J.; Xie, W.; Long, T. E.; Turner, S. R.; Lyons, A.; Gross, R. A. In *Biobased Monomers, Polymers, and Materials*; ACS Symposium series: Washington, 2012; p 131.
(45) Yang, J.; Zhang, S.; Liu, X.; Cao, A. *Polym. Degrad. Stab.* **2003**, *81* (1), 1–7.
(46) Hawker, C.; Lee, R.; Fréchet, J. M. J. *J. Am. Chem. Soc.* **1991**, *4588* (113), 4583–4588.
(47) Hölter, D.; Burgath, A.; Frey, H. *Acta Polym.* **1997**, *48* (1-2), 30–35.
(48) Yan, D.; Zhou, Z. *Macromolecules* **1999**, *32*, 819–824.
(49) Yan, D.; Müller, A. H. E.; Matyjaszewski, K. *Macromolecules* **1997**, *30* (23), 7024–7033.
(50) Galina, H.; Lechowicz, J. B.; Walczak, M. *Macromolecules* **2002**, *35* (8), 3261–3265.
(51) Kricheldorf, H. R. *Macromol. Rapid Commun.* **2007**, *28* (18–19), 1839–1870.
(52) Sunder, A.; Bauer, T.; Mülhaupt, R.; Frey, H. *Macromolecules* **2000**, *33* (4), 1330–1337.

Experimental methods

Methyl 9,10-dihydroxystearate (M2HS) synthesis

Epoxidation step: Methyl esters of high oleic sunflower oil (40 kg, 133.3 mol) and formic acid (1.7 kg, 37.8 mol) were added in a reactor equipped with a mechanical stirrer, a dropping funnel and a condenser. The resulting mixture was heated at 40°C for 1 hour under stirring condition. At 40°C, hydrogen peroxide (35%, 24.4 kg, 251.6 mol) was added dropwise to the reactor using a dropping funnel to maintain the temperature in the reactor close to 70–75°C. As the reaction is exothermic, a cooling system was used to cool down the reactor. The reaction was monitored by gas chromatography and oxiran titration. The reaction mixture was then cooled down to room temperature and the aqueous phase was discarded. The organic layer was washed with an aqueous solution of sodium hydroxide (0.1 N) until the pH became neutral. The organic phase was then dried under vacuum at 60°C to afford a clear and slightly yellow liquid.

Hydroxylation step: Epoxydized methyl esters of high oleic sunflower oil (10 kg) were placed along with an aqueous solution of phosphoric acid (12 % w/w, 5 kg) and *tert*-butanol (3 kg) as solvent in a reactor equipped with a condenser and a mechanical stirrer. The resulting mixture was heated at 90°C under vigorous stirring. The reaction was monitored by gas chromatography. When the reaction was completed, the aqueous phase was discarded at 50°C. *tert*-Butanol was eliminated under vacuum distillation. The organic phase was then washed with hot water until the pH reached 6-7 and dried under vacuum to afford a white solid.

Methyl 9,10-dihydroxystearate (M2HS) isolation

Lab-scale procedure: M2HS was recrystallized in cyclohexane (3 times, 40-60 $g.L^{-1}$) and dried under vacuum to afford a white solid powder. The product was then dissolved in a minimum of dichloromethane (DCM) and injected in a Flash chromatography apparatus from Grace. The constituents were separated on a silica column, using a dichloromethane-methanol gradient and an Evaporating Light Scattering Detector (ELSD). Two fractions were collected corresponding to M2HS and its acid form. Its purity was determined by GC (97.8%).

Pilot-scale procedure: The acid value of the crude mixture was determined by titration with potassium hydroxide (KOH), right after the hydroxylation step. Crude M2HS was then melted at 70°C in a reactor equipped with a mechanical stirrer. An aqueous solution of sodium hydroxide (0.5 $mol.L^{-1}$) was added to the reaction vessel under vigorous stirring. The volume of this aqueous solution depends on the acid value previously measured (1.1eq. of NaOH/acid value). The neutralization reaction was kept at 70°C for about 30 minutes. The mixture was then cooled down to 50°C and both phases were separated. The organic phase was washed several times with warm water until the pH became neutral and then dried to afford the neutralized M2HS. In a final step, methyl 9,10-dihydroxystearate was recrystallized in cyclohexane to reach a purity of 98.6% as determined by GC analyses.

General procedure for HBPE synthesis

M2HS (0.5 g) was added to a Schlenk flask equipped with a magnetic stirrer, a nitrogen inlet tube and an oil-bath heating system. The monomer was firstly dried alone under dynamic vacuum, above its melting point at 90°C. This pre-drying step took one hour, after that the reaction mixture was placed under nitrogen blowing, the temperature was raised to 120°C and 7.5 mg (1.5 wt%) of catalyst was introduced in the reaction flask. The mixture was subsequently allowed to react under stirring at 120°C during 2 hours. Finally, the temperature was raised to 160°C and dynamic vacuum was applied for 13 hours in order to remove the released methanol. The crude product was obtained as a colorless and highly viscous material.

Copolymerizations with core molecules and AB-type monomers were performed following the same procedure. While low boiling point core molecules were added with the catalyst in the beginning of the oligomerization stage at 120°C under nitrogen blowing, methyl 12-hydroxystearate was introduced with a molar ratio of 10, 30, 50, 70 or 90% and dried with M2HS at 90°C under dynamic vacuum prior to polymerization.

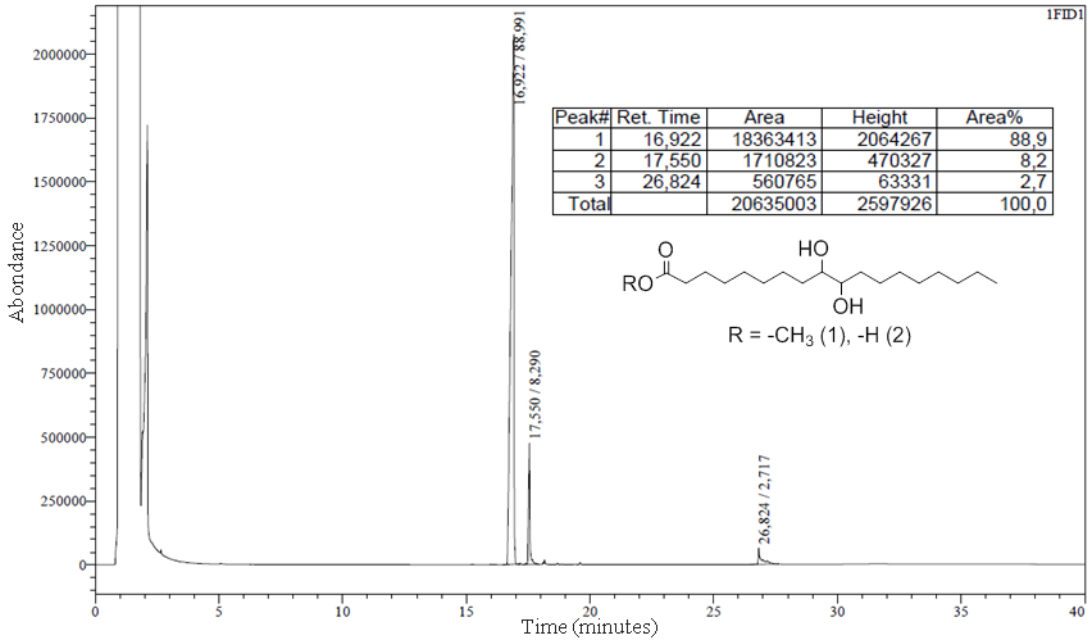

Figure SI II-1. Gas chromatogram of M2HS crude mixture after recrystallization in cyclohexane

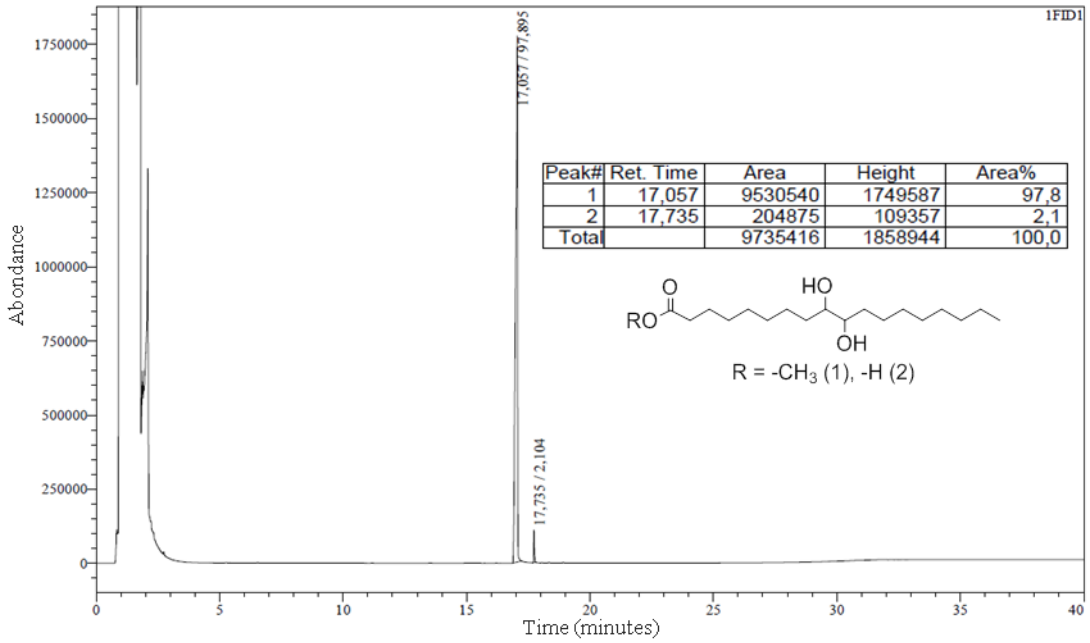

Figure SI II-2. Gas chromatogram of M2HS after recrystallization and flash chromatography

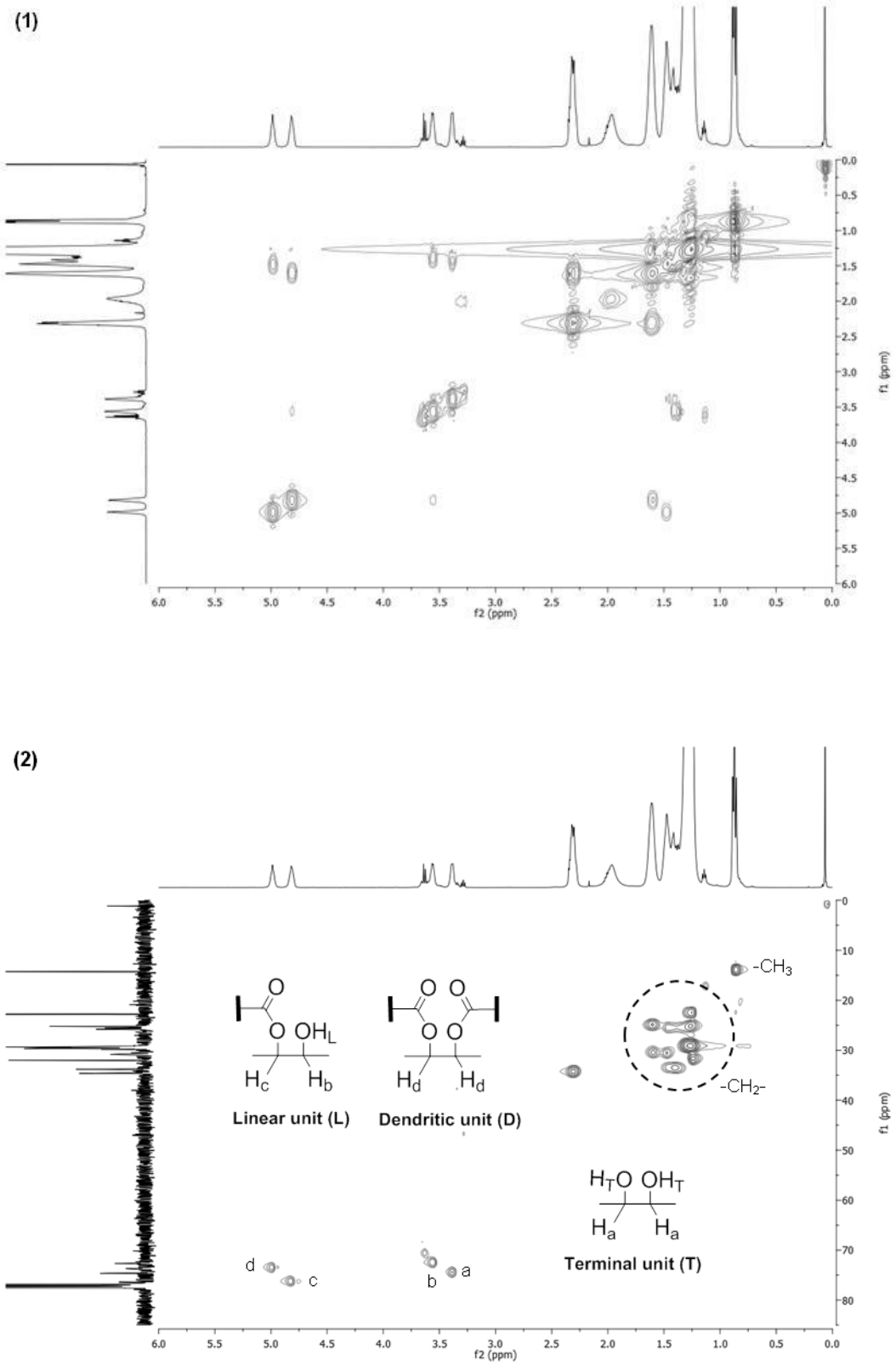

Figure SI II-3. (1) ^{1}H-^{1}H COSY and (2) ^{1}H-^{13}C HSQC of M2HS-based HBPE in $CDCl_3$

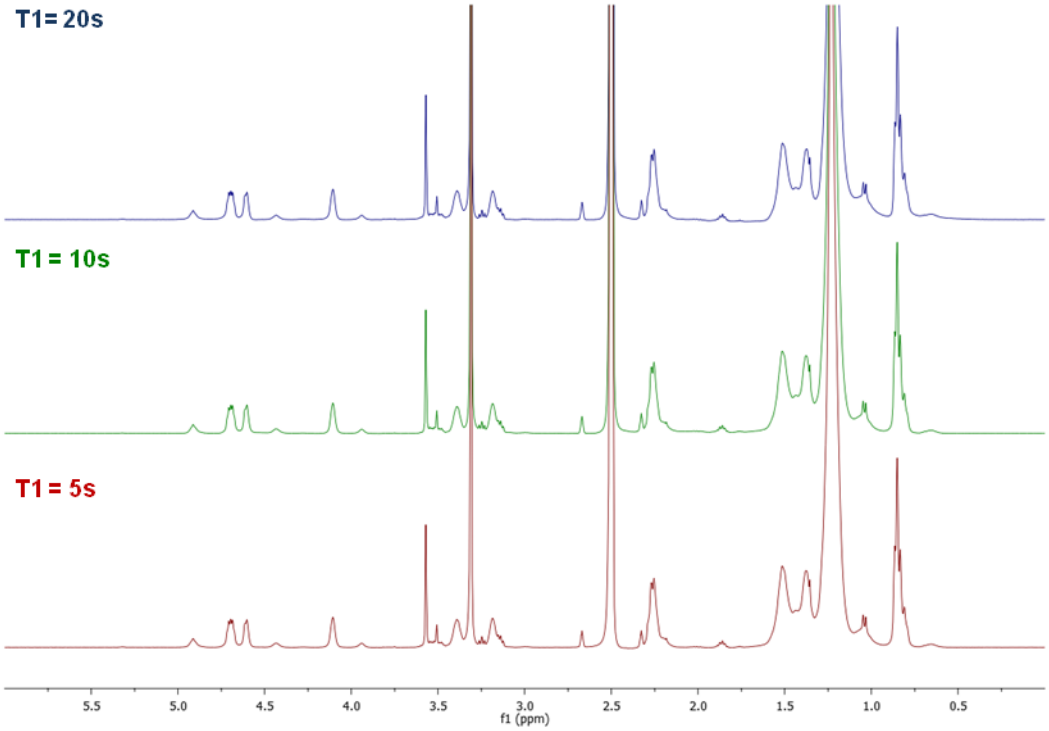

Figure SI II-4. Stacked ^{1}H NMR spectra of a HBPE in DMSO-d_6 at different longitudinal relaxation times of analysis (T1)

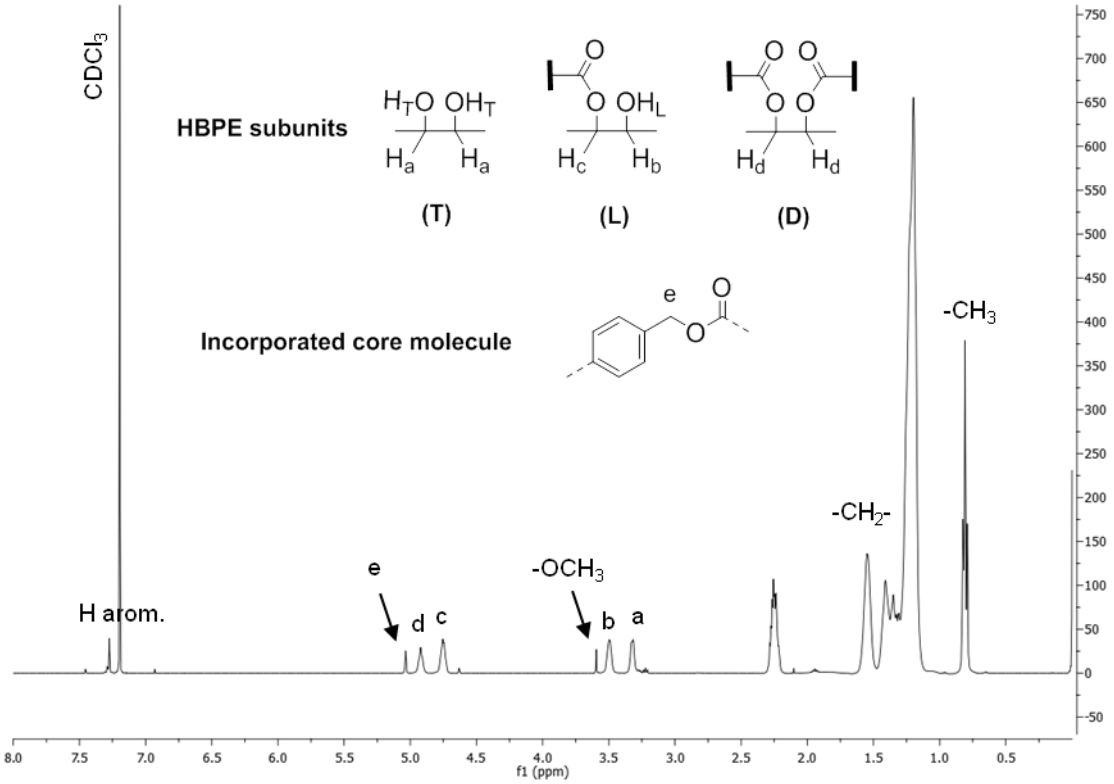

Figure SI II-5. ^{1}H NMR spectrum of a hyperbranched copolyester of M2HS/1,4-benzendimethanol in $CDCl_3$

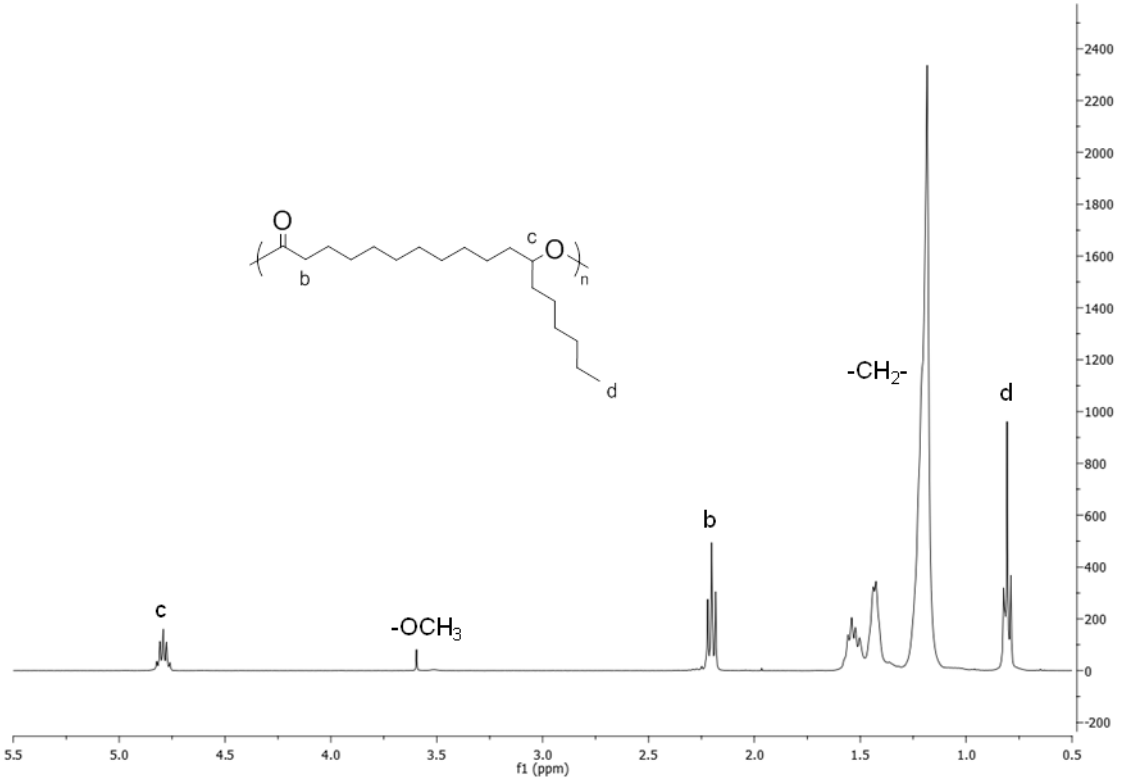

Figure SI II-6. ^{1}H NMR spectrum of LPE, linear reference prepared by polycondensation of methyl 12-hydroxystearate in $CDCl_3$

Chapter III. Towards a novel platform of AB_n-type monomers and related HBPEs *via* acid hydrolysis of epoxidized vegetable oils

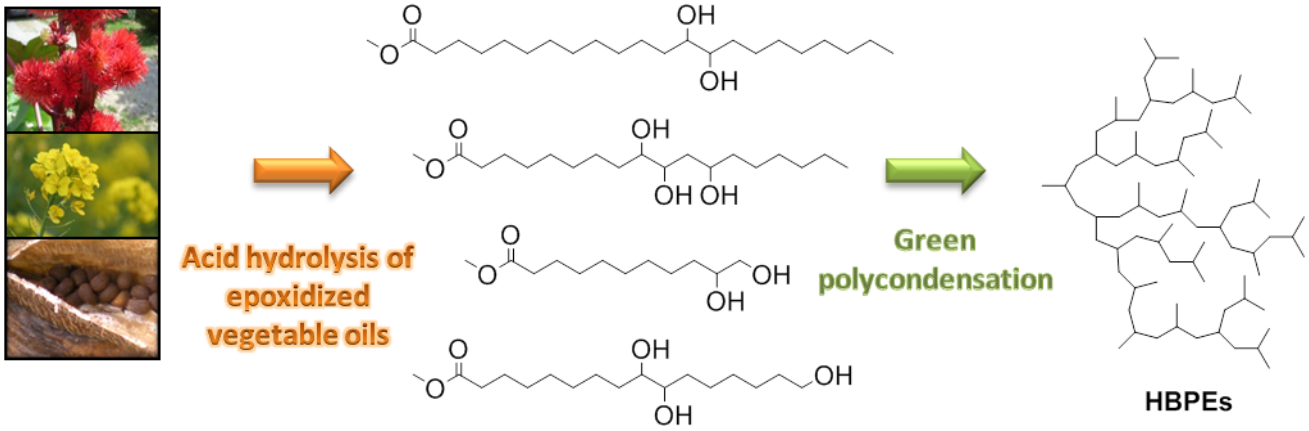

Part of this Chapter has been warranted as a European patent.[1]

Table of Contents

Introduction

In the previous chapter, vegetable oils were shown to be suitable renewable resources for the synthesis of a peculiar AB_2-type monomer and related HBPEs. M2HS was successfully prepared by acid hydrolysis of epoxidized high oleic sunflower oil (HOSO). The fine study of the influence of the polymerization conditions (time, temperature, nature and loading in catalysts, etc.) enabled to achieve HBPEs with molar masses ranging from 3 000 to 10 000 $g.mol^{-1}$ and branching density in the range 0.07 to 0.45.

In the present chapter, we wish to extend the platform of fatty acid-based multifunctional monomeric precursors prepared by acid hydrolysis of epoxidized vegetable oils, with the aim at obtaining HBPEs with tunable properties, while preserving a simple and efficient methodology of synthesis. For that purpose, methyl ester of erucic (C22:1), undecenoic (C11:1), ricinoleic (C18:1) and aleuritic acid (C16:0) were used as raw materials for the preparation of AB_n-type synthons (n = 2 or 3) bearing ester and alcohol moieties. The corresponding AB_2/AB_3 monomers of controlled purity were characterized by FT-IR, NMR and GC analyses. The influence of the precursor structure (functionality, length between two branching points, and presence of dangling chains or primary alcohols) in polycondensation reaction was next investigated, and the properties of the related bio-based HBPEs were evaluated. Characterizations by ^{1}H NMR, DSC, TGA and WAXS analyses were performed in order to determine their branching density, and analyze their crystallization ability as well as thermo-mechanical properties. Correlation between monomer structure and properties of tailor-made HBPEs will be discussed in the light of the results previously obtained with M2HS. In the course of this study, we noted that some polymers formed insoluble materials, presumably due to unexpected cross-linking. The gelation phenomenon by which polycondensation of AB_n-type monomers yielded cross-linked polymers, instead of soluble materials, was thus studied in more detail.

1. Synthesis of polyester precursors of AB_n-type from FA derivatives

In order to develop a range of HBPEs with tunable properties, the synthesis of four different monomers of AB_n-type bearing ester (A) and alcohol (B) moieties as reactive functions, was implemented (Scheme III-1). Three of these new monomers were prepared by acid hydrolysis of epoxidized vegetable oils, by analogy with the synthesis of M2HS described in the previous chapter, but starting from various substrates of interest.

Methyl ester of erucic acid is a monounsaturated FA derivative with a 22-carbon atom backbone (instead of 18 for methyl oleate) and a single double bond in the omega 9 position, *i.e.* occurring at the 9th position from the methyl end. This substrate was used as raw material for the synthesis of methyl 13,14-dihydroxybehenate (M2HB), with the idea of obtaining HBPEs of higher chain length between two branching points compared to M2HS-based materials (11 CH_2 *vs.* 7 CH_2). Similar modification of methyl ricinoleate, in which one hydroxyl group is already present, yielded methyl 9,10,12-trihydroxystearate (M3HS). This multifunctional precursor of higher functionality (n = 3) was prepared as a mean to tune the end-properties of the HBPEs. Lastly, methyl undecenoate (C11:1) was chosen to obtain methyl 10,11-dihydroxyundecanoate (M2HU) leading to HBPEs without dangling chains.

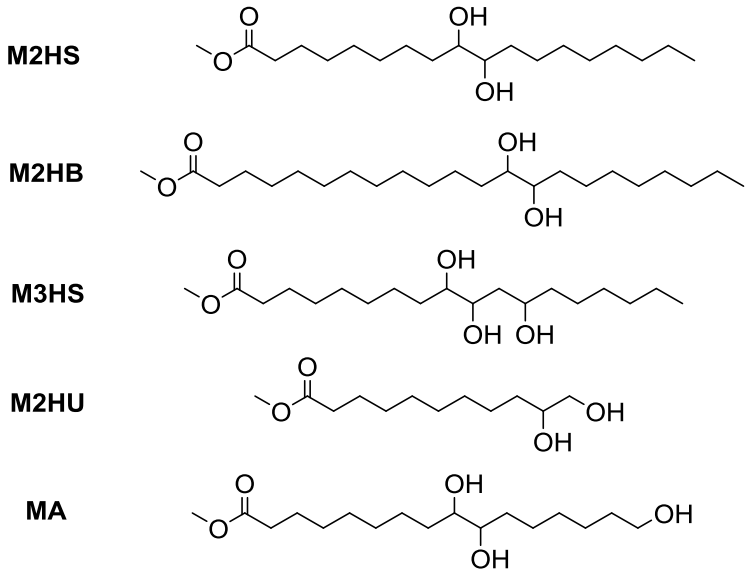

Scheme III-1. Plaftorm of AB_n-type monomers obtained by acid hydrolysis of epoxidized vegetable oils

Unlike other monomers of this platform, aleuritic acid is a naturally-occurring AB_3-type synthon derived from ambrettolide, a musk oil widely used in the perfume industry. Commercialized under its acid form, this monomer was esterified with methanol. Methyl aleuritate (MA) was also included in this study due the higher reactivity of its primary alcohol in ω-position, which was expected to favor the formation of less compact architectures. The chemical structure of the as-formed AB_n-type monomers was assessed by FT-IR and NMR spectroscopies. Their purity grade was determined by GC analysis.

1.1. Acid hydrolysis of epoxidized vegetable oils

Methyl esters of rapeseed oil and castor oil were used for the preparation of M2HB and M3HS, respectively, as illustrated in Scheme III-2. These syntheses were carried out at *ITERG* following the same procedure than that developed in Chapter II to obtain M2HS.

First, the internal double bonds of the FAMEs were epoxidized by reacting formic acid with a solution of hydrogen peroxide. The subsequent ring-opening of the so-formed epoxy-rings was performed with water under acidic conditions to produce the targeted monomers.

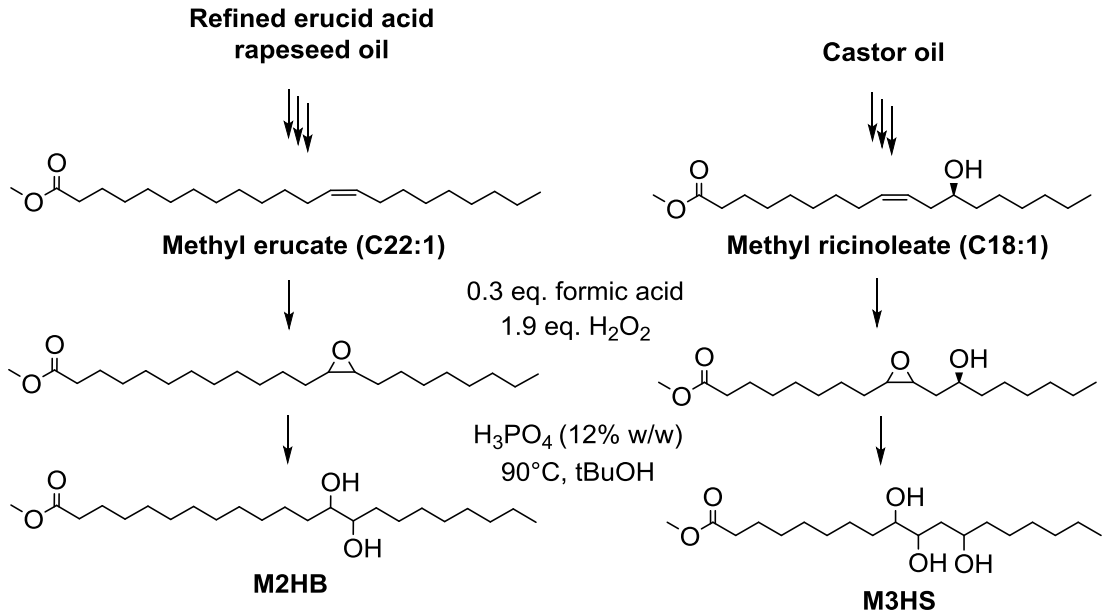

Scheme III-2. Synthetic pathways to M2HB and M3HS

To selectively isolate M3HS, a two-step purification procedure was carried out similarly to that implemented for M2HS, including a recrystallization in cyclohexane to get rid of the more apolar species, *e.g.* A-type monomers and traces of unreacted methyl ricinoleate. The resulting material was then purified by flash chromatography using a 95:5 (v/v) mixture of dichloromethane/methanol, to remove the acid fraction formed by hydrolysis during the ring-opening step. M3HS grade was confirmed by GC analyses showing purity over 98%. This AB_3-type monomer was however obtained in rather poor yield (≈ 25%) owing to the fact that the hydroxylation of methyl ricinoleate resulted in a mixture of four diastereoisomers and up to now, only one of them was shown to crystallize.[2–5] This purification procedure would thus need further optimization.

In contrast, M2HB was prepared in high yield (80%). This AB_2-type monomer was directly produced on the kilogram scale and benefited from the purification procedure optimized at the pre-industrial level for M2HS, *i.e.* neutralization of the acid fraction with NaOH (aq.) followed by recrystallization in heptane affording M2HB with a purity of 94%.

Both monomers were characterized by ^{1}H NMR spectroscopy (Figure III-1). The spectrum of M2HB was easily assigned in comparison with M2HS. As for M3HS, one can notice that due to the presence of a third alcohol group, the hydroxyl functions of the vicinal diol are no longer equivalent. Labile protons -OH_1, -OH_2 and -OH_3 indeed display distinct

signals at 4.15, 4.07 and 4.18 ppm, respectively, in deuterated DMSO. Their adjacent protons in α-position H_d, H_e and H_f are identified at 3.19, 3.51 and 3.59 ppm, respectively. 2D NMR techniques were required to fully assign the different peaks (see Figure SI III-2).

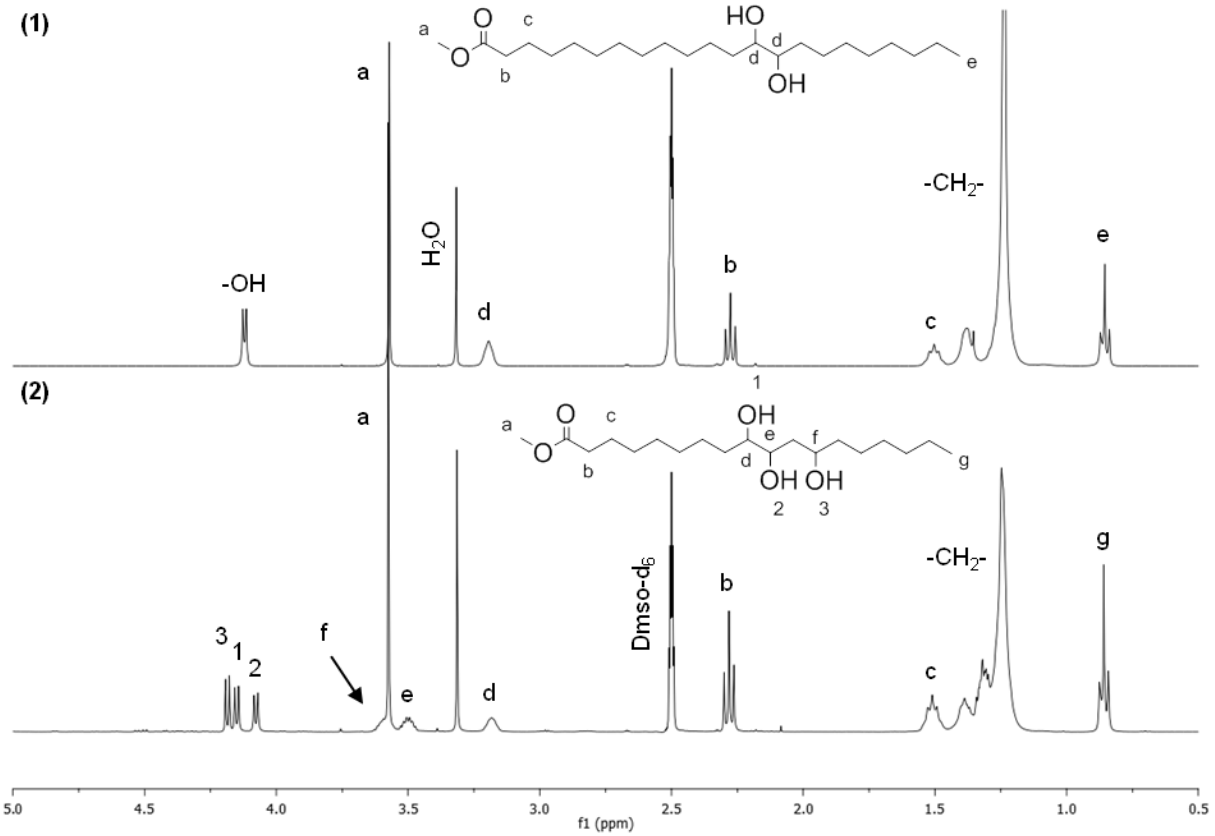

Figure III-1. Stacked ^{1}H NMR spectra of (1) M2HB and (2) M3HS in DMSO-d_6

The synthesis of M2HU has already been described in a patent by Solvay company in 1994.[6] The invention provides a process for the preparation of vicinal diols and/or epoxides by the oxidation of olefins, using hydrogen peroxide and an inorganic heptavalent rhenium catalyst as illustrated in Scheme III-3 (1). This route however was reported to lead to a complex product mixture where M2HU was obtained only in low yield (33%).

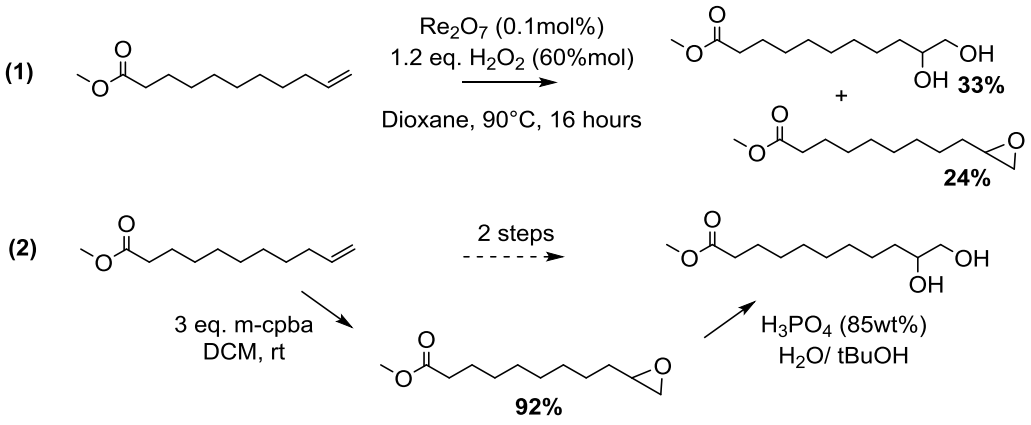

Scheme III-3. Synthetic pathways to methyl 10,11-dihydroxyundecanoate (1) patented by Solvay and (2) developed at the LCPO

M2HU was prepared at the LCPO following a two-step reaction scheme similar to the process developed by *ITERG* (Scheme III-3 (2)). Epoxidation of methyl undecenoate terminal double bonds was performed with 3-chloroperbenzoic acid (*m*-cpba) according to previous literature.[7] The reaction was carried out overnight at room temperature in solution of dichloromethane. The synthesis of the epoxides was monitored by the disappearance of the double bond protons at 5.78 ppm (H_d) and 4.91 (H_e, H_f), as can be seen in Figure III-2. The appearance of the characteristic multiplets of the epoxide moiety at 2.84, 2.64 and 2.38 ppm, confirmed the formation of methyl 10-epoxyundecenoate. After work-up (see Experimental and Supporting Information), methyl 10-epoxyundeceneoate was obtained as a viscous liquid in high yield (92%).

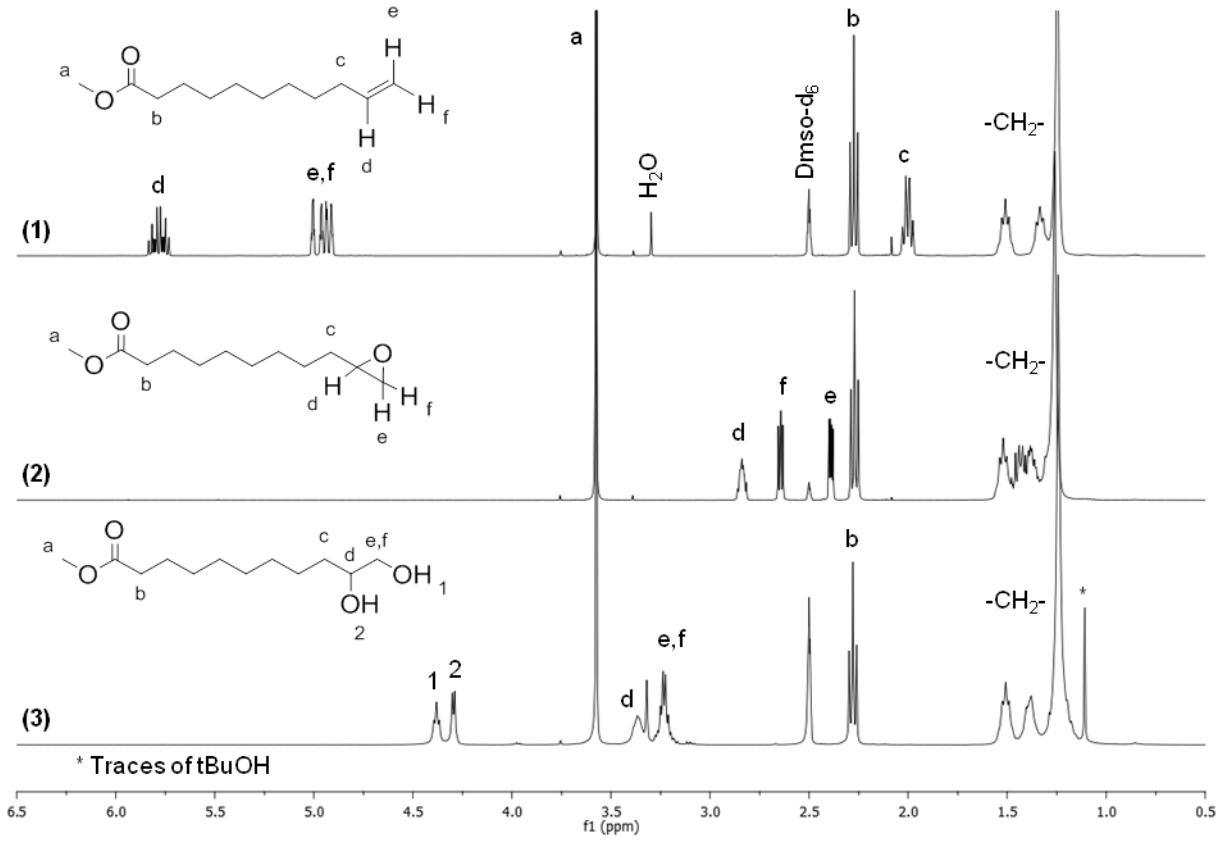

Figure III-2. Stacked ^{1}H NMR spectra of (1) methyl undecenoate, (2) methyl 10-epoxyundecenoate and (3) methyl 10,11-dihydroxyundecanoate in DMSO-d_6

The ring-opening of the epoxide function was then performed with water using catalytic amounts of phosphoric acid, H_3PO_4 (85 wt%), in *tert*-butanol as a co-solvent. After completion, the organic phase was isolated, washed with water and *tert*-butanol was removed under vacuum to afford M2HU. Various reaction conditions were tested as summarized in Table III-1 and yet, the yield of this step never reached higher values than 65%. The main side product of this reaction, which is besides water-soluble, was identified as being 10,11-dihydroxyundecanoic acid obtained by hydrolysis of the ester function.

Increasing the reaction time, temperature or loading in phosphoric acid appeared to favor the formation of this acid form, as it is reasonably logical to expect. A higher yield of 78% could be achieved by reducing the initial water intake (entry 6), though the conversion was incomplete in these conditions (83%).

Table III-1. Reaction condition screening of the hydroxylation of methyl 10-epoxyundecenoate

Entry	Time (hours)	T (°C)	H_2O:tBuOH[1]	H_3PO_4 (wt%)	Yield (%)[2]
1	4	90	1:1	5	47
2	2	90	1:1	5	53
3	4	70	1:1	5	58
4	4	90	1:1	3	65
5	4	70	1:1	3	59
6	2	90	1:2	3	78*
7	4	90	1:2	5	44

(1) volume ratio (2) yield in wt% (*) incomplete conversion (83%)

M2HU was obtained with a particularly high purity grade, over 99% (see supporting information, Figure SI III-3), and characterized by ^{1}H NMR spectroscopy (Figure III-2 (3)). Protons of the primary (-OH_1) and secondary (-OH_2) alcohols display signals at 4.38 and 4.30 ppm. Multiplets observed at 3.37 and 3.24 ppm correspond to the protons H_d and H_e, H_f in α-position, respectively.

The synthesis of M2HU was also monitored by FT-IR spectroscopy as shown in Figure III-3. The formation of the epoxidized intermediate was confirmed by the disappearance of the absorption band at 1 640 cm^{-1} characteristic of the C=C stretching and the appearance of a strong band at lower wavenumbers (734 cm^{-1}) assigned to the symmetric ring deformation of monosubstituted epoxides. The subsequent acid hydrolysis was assessed by the broad band centered at 3 500 cm^{-1} due to the -OH stretching.

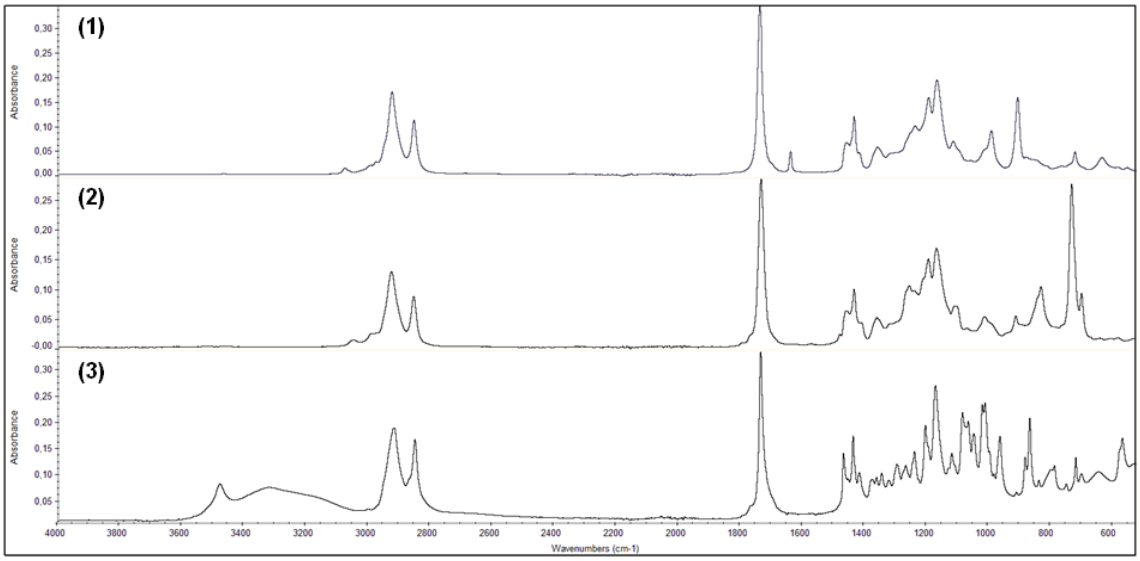

Figure III-3. Stacked FT-IR spectra of (1) methyl undecenoate, (2) methyl 10-epoxyundecenoate and (3) methyl 10,11-dihydroxyundecanoate

Other pathways have been investigated to obtain M2HU in higher yields, *i.e.* acid hydrolysis in milder conditions using Amberlyst resin as catalyst, direct dihydroxylation of methyl undecenoate with permanganate-based catalysts,[8] acid hydrolysis of epoxidized 10-undecenoic acid followed by its post-esterification,[9,10] without success.

1.2. Specific case of aleuritic acid

As mentioned above, aleuritic acid is a naturally-occurring AB_3-type synthon derived from musk ambrette seed oil. This compound was esterified under mild conditions to produce the targeted FAME, methyl aleuritate (MA). The reaction was carried out in methanol under reflux at 70°C using Amberlyst resin as catalyst with a loading of 20 wt% relative to monomer weight.

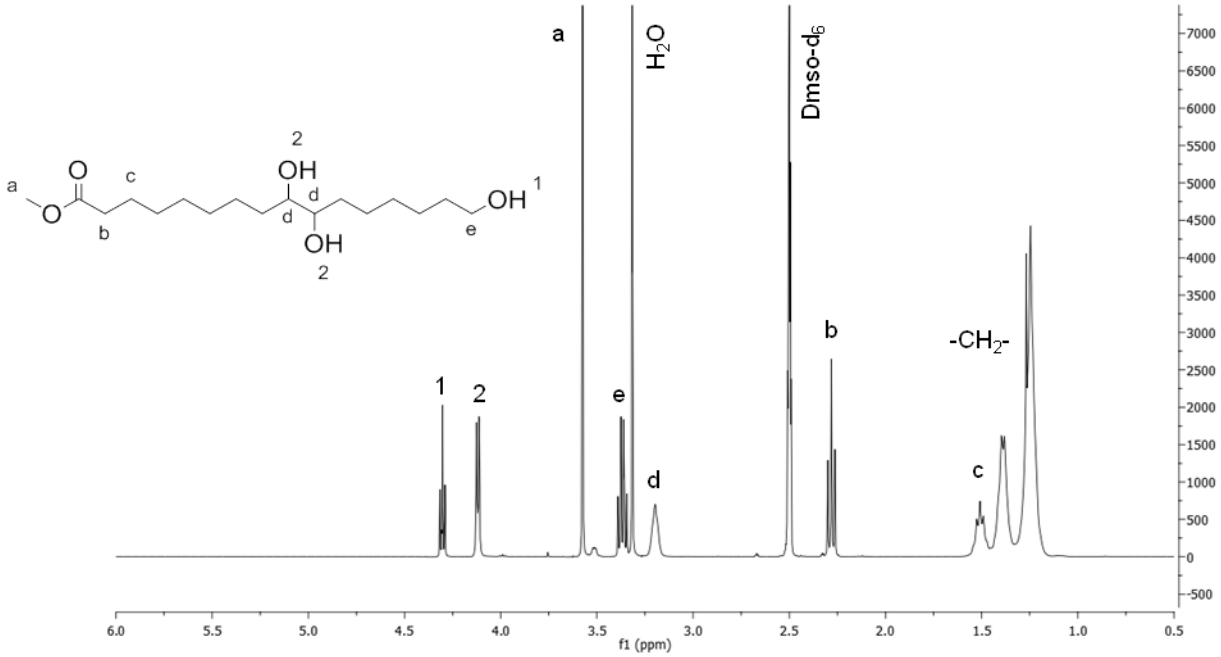

Figure III-4. ^{1}H NMR spectrum of methyl aleuritate in DMSO-d_6

MA was obtained in reasonable yield (75%). Figure III-4 shows its ^{1}H NMR spectrum in DMSO-d_6. The peak at 3.57 ppm whose integral comes to 3, confirms the success of the esterification. Primary and secondary alcohols -OH_1 and -OH_2 can be distinguished at 4.30 and 4.11 ppm, while their adjacent protons on the α-carbons are identified at 3.37 and 3.20 ppm, respectively.

Table III-2. Yield and purity grade of the AB_n-type monomers synthesized

Monomers	Yield (%)[1]	Purity (%)[2]
M2HB	80	94
M3HS	25	98.1
M2HU	60	99
MA	75	97.3

(1) yield in wt%. (2) determined by GC.

In summary, the platform of monomers synthesized by acid hydrolysis of epoxidized vegetable oils was extended to four other AB_n-type synthons bearing as reactive functions some ester and alcohol moieties. All monomers were obtained as white powders. Their chemical grade was confirmed by GC analyses as shown in Table III-2. The influence of the monomer structure on its reactivity in polycondensation is discussed in the next section.

2. Hyperbranched polyester synthesis

The four AB_n-type monomers described above were subjected to transesterification reaction. While M2HB and M3HS were shown to display similar reactivities than M2HS, polycondensation of M2HU and MA unexpectedly yielded insoluble materials. The gelation phenomenon by which cross-linked polymers are formed was studied in more detail in the following section. In addition, polymerization conditions were optimized considering the higher reactivity of the primary alcohols bearing by M2HU and MA.

2.1 Polycondensation of M2HB and M3HS

M2HB and M3HS were polymerized under the same conditions than M2HS, *i.e.* in the melt, following a two-step-one-pot procedure. After a one hour pre-drying where the monomer was heated alone at 90°C under dynamic vacuum, the catalyst was added at a loading of 1.5 wt%. The reaction mixture was allowed to oligomerize at 120°C during 2 hours under nitrogen blowing. In the last stage of polymerization, the temperature was increased to 160°C and dynamic vacuum was applied during 13 hours.

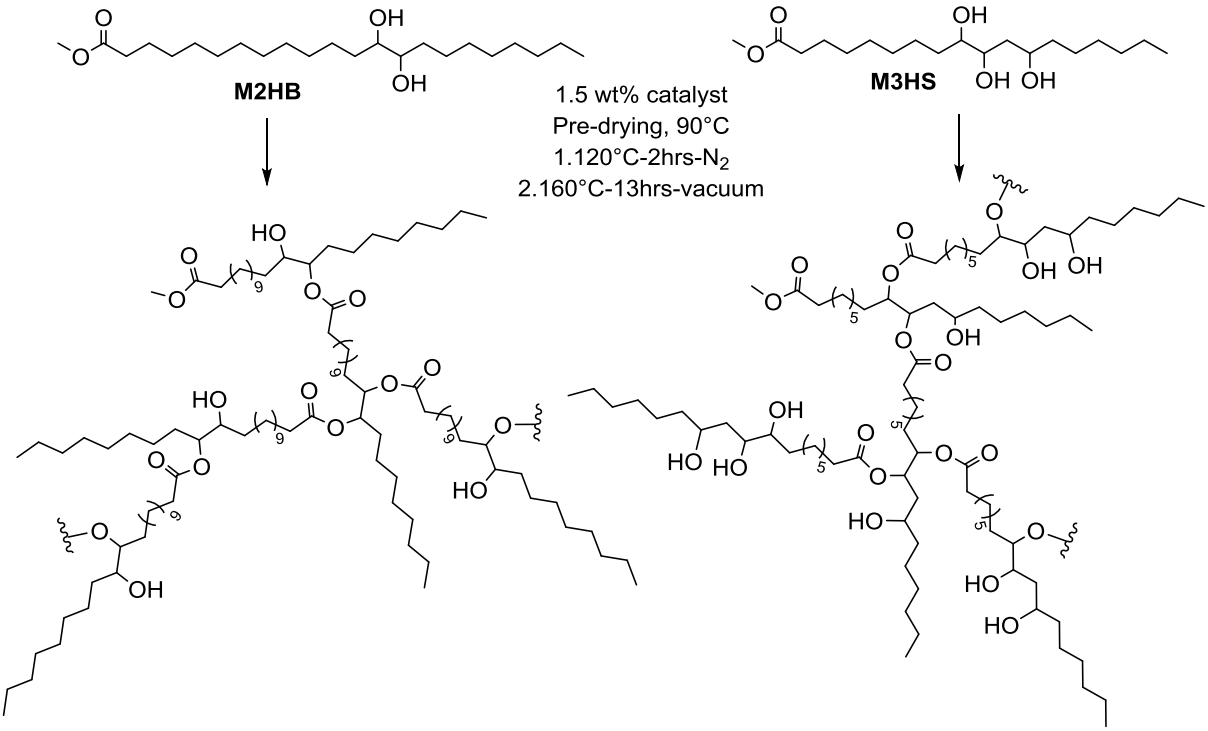

Scheme III-4. HBPE synthesis from M2HB and M3HS

Table III-3 gives the experimental details as well as the polymerization results. M2HB and M3HS featured similar reactivities than M2HS. Anhydrous zinc acetate, TBD and sodium methoxide yielded HBPEs with molar masses in the same range, from 3 000 to 9 200 g.mol^{-1}, and dispersities in between 1.93 and 4.05. Conversions above 95% were reached, except with stannous octoate, which demonstrated poor efficiency to catalyze the polycondensation of the AB_3-type monomer (P11). An increase in the reaction time, from 15 to 24 hours, resulted as well in higher molar masses and broader dispersities (P5 *vs.* P6).

Table III-3. Molar masses and dispersity of HBPEs obtained by self-condensation of M2HB and M3HS: comparison with M2HS

Entry	Monomer	Catalyst	x^1 (%)	$\bar{M}_n{}^1$ (g.mol^{-1})	$\bar{M}_w{}^1$ (g.mol^{-1})	$Đ^1$
P1	M2HS	$Zn(OAc)_2$	98	3 500	9 500	2.71
P2		TBD	100	4 100	10 100	2.46
P3		NaOMe	100	6 100	18 800	3.08
P4		$Sn(Oct)_2$	93	3 200	6 500	2.03
P5	M2HB	$Zn(OAc)_2$	95	3 000	5 800	1.93
P6		$Zn(OAc)_2{}^2$	98	5 600	61 500	>11
P7		TBD	100	5 600	17 100	3.05
P8		NaOMe	100	9 200	30 100	3.27
P9	M3HS	$Zn(OAc)_2$	97	3 800	9 800	2.58
P10		TBD	100	5 600	22 700	4.05
P11		$Sn(Oct)_2$	79	1 600	2 100	1.31
P12		NaOMe	98	4 600	13 000	2.83

(1) determined by SEC in THF – calibration PS standards. (2) Time of polymerization from 15 to 24 hours.

By contrast, under the same reaction conditions, polymerization of M2HU and MA led to the formation of insoluble gel-like materials within 8 and 3 hours, respectively. According to Flory's theory, the statistical polycondensation of AB_n-type monomers yields HBPs without the risk of gelation, provided that (i) A reacts with B exclusively and (ii) reactions do not involve internal cyclization.[11] However, side reactions were reported to usually accompany the synthesis of HBPs and that could be responsible for the cross-linking. These undesired side reactions were thus investigated by MALDI-TOF MS, as described below.

2.2 Gelation phenomenon

The gelation phenomenon turned out to be a difficult topic to address. Polycondensation of AB_n-type monomers does not result in cross-linked polymers in a predictable manner. The formation of insoluble materials however appeared to greatly depend on the initial reaction conditions applied. Comprehensive investigations were carried out with M3HS. Polycondensation of this AB_3-type monomer yielded cross-linked polymers as long as the reaction exceeded 24 hours, and this was observed whatever the catalyst employed (TBD or zinc acetate). Gelation occurred in earlier stage at higher loading in TBD, *i.e.* 5 wt% relative to monomer.

The temperature of polymerization was shown to play an important role as well. Polycondensation of M3HS was performed following the same two-step-one-pot procedure described above (Scheme III-4), but by varying the temperatures of oligomerization (T_1) and polymerization (T_2). Three different protocols were tested: (i) $T_1 = T_2 = 150°C$, (ii) $T_1 = 140$ °C and $T_2 = 180°C$, (iii) $T_1 = 200$ °C and $T_2 = 220°C$. In each case, zinc acetate was used as catalyst with a loading of 1.5 wt%. Polymerizations were monitored by SEC (THF, RI detector). For that purpose, aliquots were directly taken out from the reaction mixture at different reaction times and analyzed without further purification. Figure III-5 depicts the evolution of the monomer conversion (1), molar masses and molar distribution of the as-formed HBPEs ($\overline{M}_n$, $Đ$) (2) with time. At 150°C, only oligomers were achieved with molar masses lower than 1 500 $g.mol^{-1}$. As expected, increasing the temperature gave faster kinetics of polymerization. However, this also favored the occurrence of side reactions to the extent that at a temperature as high as 220°C, gelation occurred within less than 4 hours.

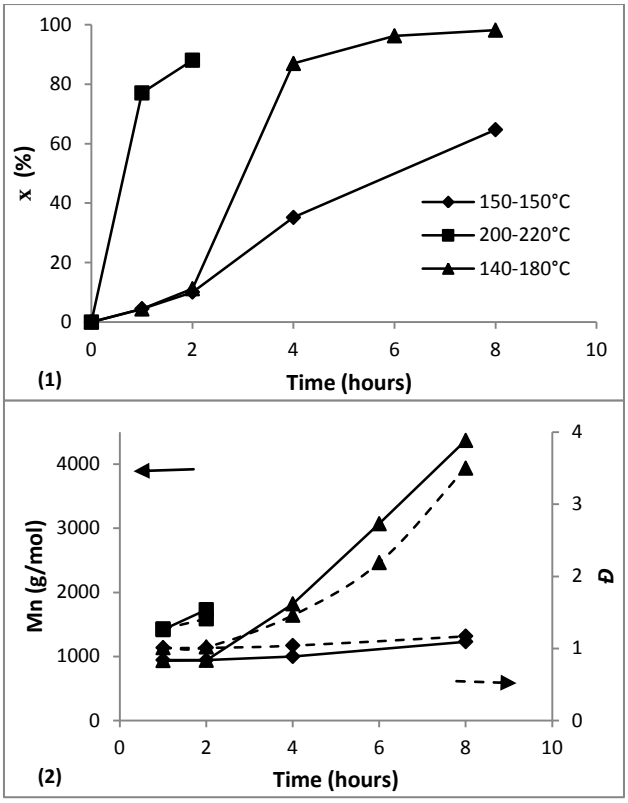

Figure III-5. Time dependence of (1) conversion, (2) molar mass and dispersity for zinc acetate-catalyzed polycondensation of M3HS performed at different temperatures

Hence, due to their cross-linking ability, soluble HBPEs of high molar masses can only be successfully synthesized under very specific conditions (time-temperature-loading in catalyst). Otherwise, only oligomers of low molar masses or gels are produced. This experimental window was found to be specific to each individual monomer.

MALDI-TOF MS analyses were carried out on M3HS-derived soluble HBPEs. This technique is a powerful tool giving information about different structural formations and repeating units in even complex polymeric systems.[12] A typical MALDI-TOF mass spectrum obtained is presented in Figure III-6.

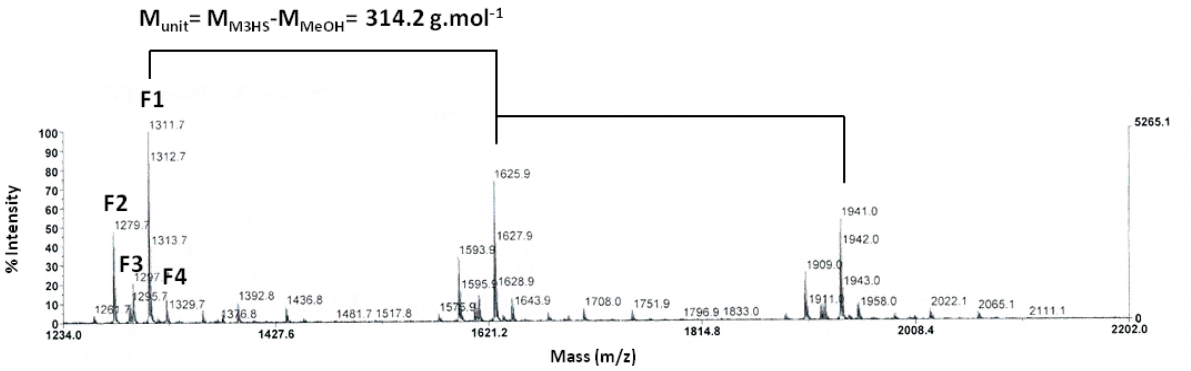

Figure III-6. MALDI-TOF MS analysis of M3HS-based HBPE (Matrix trans-3-idoleacrylic acid)

Four distinct families of peaks were identified by analyzing the different signals. F1 refers to the HBPE population actually obtained by the statistical polycondensation of M3HS (n x (M_{unit}) + M_{MeOH} + M_{Na} where M_{unit} = M_{M3HS}-M_{MeOH} = 314.2 g.mol^{-1}). A mass difference of 32 g.mol^{-1}, compared to the regular hyperbranched polyester structure, was interpreted as being the result of the formation of lactones (n x (M_{unit}) + M_{Na}). These subunits are generated by intramolecular esterification reaction of the carbonyl group in the focal point with an hydroxyl function of the same hyperbranched molecule (**F2**, Scheme III-5).

However, such cycle structures can also be obtained by intramolecular hydroxyl-ester interchange reactions. Molar masses remain unchanged when this reaction takes place between two groups of different branches (**F6**, Scheme III-6). In this case, the interchange just leads to a rearrangement of the HBPE architecture. By contrast, the intramolecular hydroxyl-ester interchange reaction that occurs between groups of the same branch, results in the formation of two species of lower molar masses, one of them containing a cyclic branch (**F5**, Scheme III-6). Analysis by MALDI-TOF MS cannot distinguish one cyclic structure from the others (**F2** and **F5**) since both types of reaction lead to the same molar mass decrease, *i.e.* 32 g.mol^{-1}. A combination with spectroscopic and even chromatographic methods would be required to get valuable information about the distribution of ring formation within HBPEs as demonstrated by Fradet and coworkers,[12,13] and Frey and coworkers[14] on poly(bis-MPA) HBPEs (see Chapter I, section 2.1.3.3).

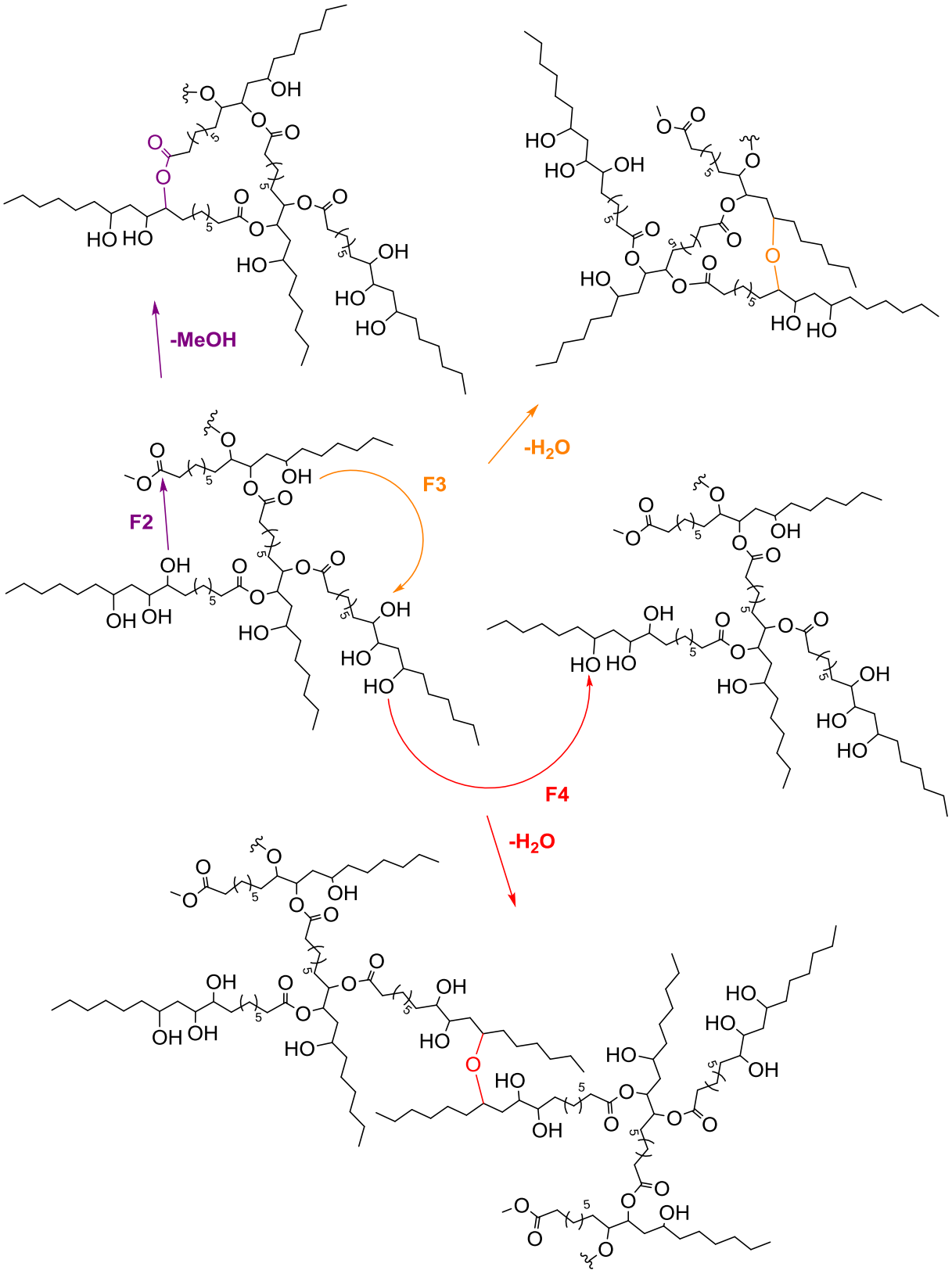

Scheme III-5. Possible side reactions and related families: (F2) intramolecular esterification, (F3) intra- and (F4) intermolecular etherification accounting for the gel formation during the synthesis of HBPEs

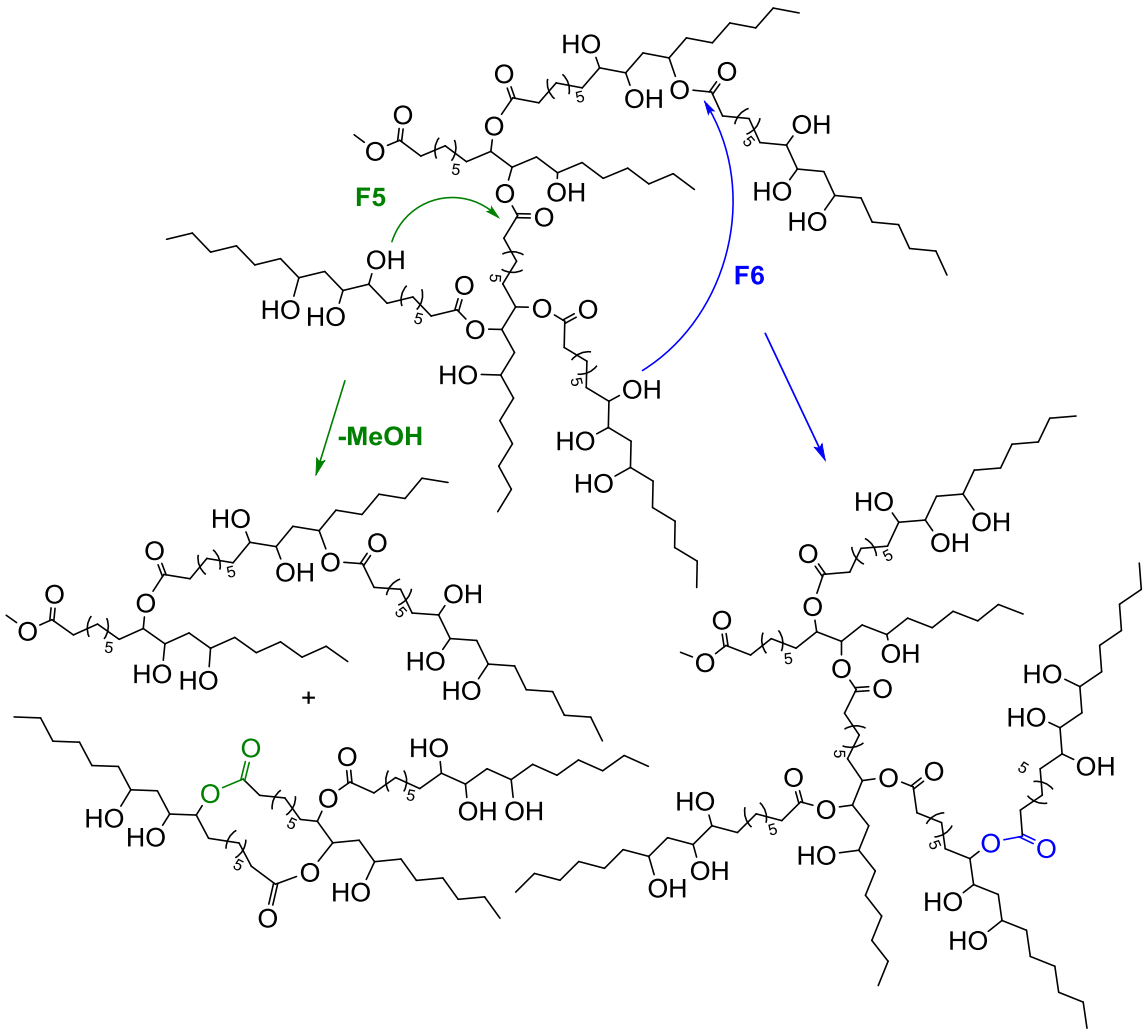

Scheme III-6. Possible side reactions and related families of polymers obtained: intramolecular hydroxyl-ester interchange between groups of (F5) the same branch or (F6) different branches

The family **F3** was detected at *m/z* - 18 g.mol^{-1} (Scheme III-5). The elimination of one molecule of water reflected the occurrence of intramolecular etherification between two hydroxyl groups (n x (M_{unit}) + M_{MeOH} + M_{Na} – M_{H2O}). This side reaction results in the formation of hyperbranched macromolecules with a cyclic branch as well. Intramolecular cyclizations through ester or ether bonds may reduce achievable molar masses of HBPEs but do not yield cross-linked materials. As highlighted in Chapter I, gelation is due to etherification side reaction that takes place intermolecularly leading to more than one focal group per molecule (n x (M_{unit}) + 2 x M_{MeOH} + M_{Na} – M_{H2O}). Accordingly, a series of peaks was observed at *m/z* + 14 g.mol^{-1} (= M_{MeOH}-M_{H2O}) and assigned to the formation of ether bridges between polymeric chains (**F4**, Scheme III-5).

These side reactions (intramolecular esterification, intra- and/or intermolecular etherification) were not quantified, but appeared to occur whatever the catalyst employed (TBD and zinc acetate) and compete with the transesterification reaction during the whole polymerization, *i.e.* not only at high conversion rates. Similar observations were made upon polymerizing M2HS and M2HB.

As a complement to these MALDI-TOF MS analyses, high-resolution magic-angle spinning (HR-MAS) NMR spectroscopy was applied as a mean to investigate the structure of the cross-linked polymers obtained.[13,15] This technique enables to characterize materials that are not strictly solids, such as swellable gels under high-resolution conditions. Figure III-7 presents the ^{13}C HR-MAS spectra of both (1) soluble and (2) gel-like HBPEs prepared by polycondensation of M3HS, in $CDCl_3$. The signal at 44.36 ppm was easily assigned to the methoxy carbon (-O**C**H_3). It is interesting to note that these two samples differ in their content of unreacted A groups: 3.6% for (1) *vs.* 0.8% for (2) showing that gelation occurred at very high conversion rates.

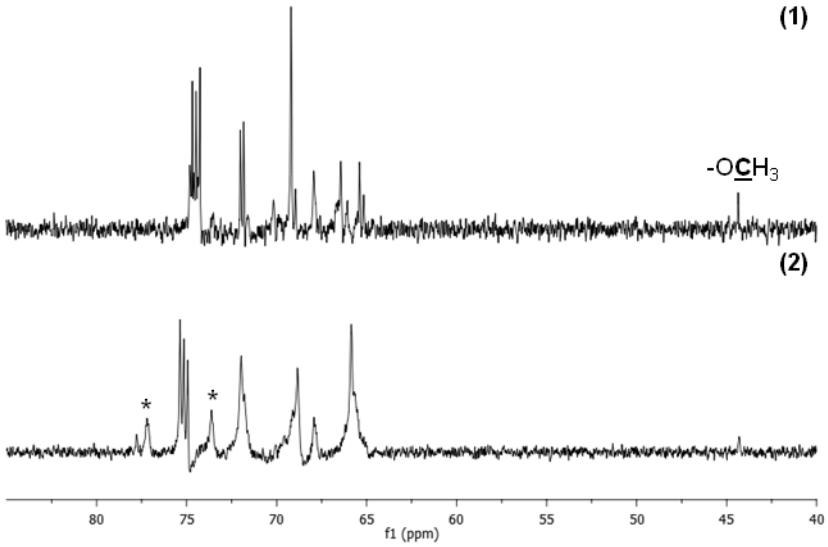

Figure III-7. Stacked ^{13}C HR-MAS spectra of (1) soluble and (2) gel-like M3HS-based HBPEs in $CDCl_3$ (focus on the region from 40 to 85ppm) (*) additional peaks

In the region of the quaternary carbons (60-80 ppm), the spectrum of the cross-linked polymer (2) shows at least two additional signals at 77.21 and 73.61 ppm (indicated by *). 2D NMR techniques could not be conducted to properly assign all these peaks. However, both chemical shifts correspond well with ether structures. For instance, Komber and coworkers extensively studied the structure of poly(bis-MPA) HBPEs and detected the presence such of ether bonds (-O**C**H_2-) at 73.2 ppm.[15]

In summary, MALDI-TOF MS and NMR analyses revealed that several side reactions occur during the expected transesterification polymerization of AB_n-type monomers including intramolecular esterification, and intra- and/or intermolecular etherification. The formation of ether bonds between polymeric chains yields macromolecules with two or more focal points that can act as cross-linking agents at high conversions. Long reaction times, high temperatures and increased loadings in catalyst were found to favor the formation of cross-linked polymers. The fact that these aliphatic HBPEs are prone to side reactions under

thermal treatment, supports the approach adopted in this PhD work, namely the use of Fatty Acid Methyl Esters (FAMEs) as synthetic precursors of HBPEs, instead of Fatty Acid (FA) derivatives. Indeed, for comparison purpose, the polycondensation of the acid form of M2HS, *i.e.* 9,10-dihydroxystearic acid (2HSA), was attempted. However, the higher reaction temperatures required to achieve its polymerization in the melt, were shown to favor the occurrence of side reactions. Therefore, only oligomers of low molar masses or gels were formed. These side attempts are described in more detail in supporting information.

2.3 Polycondensation of M2HU and MA

Optimization of the reaction conditions, considering the higher reactivity of M2HU and MA provided by the presence of primary alcohols, was required to synthesize soluble polyesters of hyperbranched architecture. For that purpose, parameters including the reaction time, temperature and when necessary the loading in catalyst were adjusted.

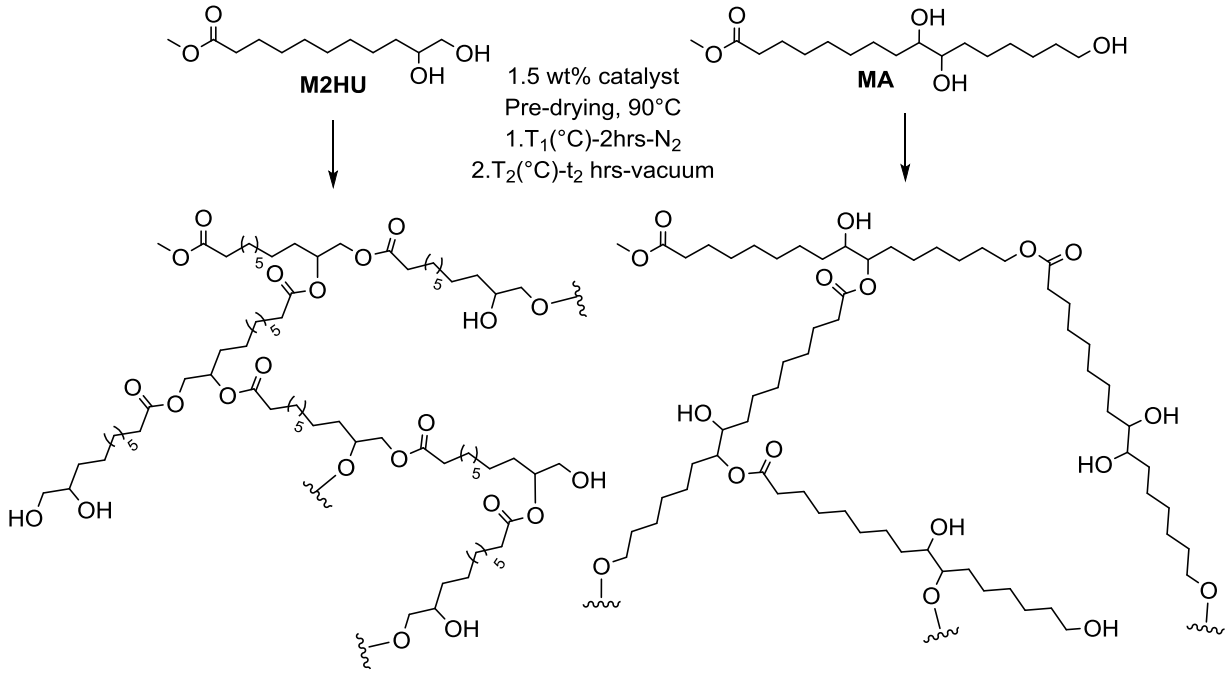

Scheme III-7. HBPE synthesis from M2HU and MA

Polycondensations of M2HU and MA were carried out in the melt following a similar two-step-one-pot procedure (Scheme III-7), including a two-hour oligomerization stage at T_1(°C) under nitrogen blowing, followed by a polymerization stage at T_2(°C) under dynamic vacuum during t_2 hours. All polymerizations were stopped as soon as the viscosity of the reaction mixture increased. A pre-drying of the monomer alone at 90°C under dynamic vacuum was consistently performed before the addition of the catalyst with a loading of 1.5 wt%, except otherwise mentioned. SEC data are summarized in Table III-4.

Table III-4. Molar masses and dispersity of HBPEs obtained by self-condensation of M2HU and MA

Entry	Ref.	Cat.	T_1(°C)[1]	T_2(°C)[2]	t_2 (hours)[3]	x[4] (%)	$\bar{M}_n$[4] (g.mol^{-1})	$\bar{M}_w$[4] (g.mol^{-1})	$Đ$[4]
P13	M2HU	$Zn(OAc)_2$	120	140	8	99	2 400	5 600	2.33
P14		TBD	120	140	8	95	2 400	6 400	2.67
P15	MA	TBD	90	90	1	100	9 300	44 700	4.81
P16		NaOMe	90	90	2	98	4 800	13 900	2.90
P17		TBD	75	75	3	100	8 000	33 700	4.21
P18		TBD[5]	90	90	4	100	13 000	75 400	5.80

(1) Temprature of the oligomerization stage. (2) Temperature of the polymerization stage. (3) Time of the last stage of polymerization. (4) determined by SEC in THF – calibration PS standards. (5) Loading in TBD: 1 wt%.

As for HBPEs issued from M2HU, gelation was avoided by simply decreasing the temperature of the polymerization stage to 140°C. On the other hand, further decrease in T_2 to 120°C slowed down the kinetics of polymerization and yielded oligomers only ($\bar{M}_n$ < 900 g.mol^{-1}). Within 8 hours at 140°C, conversions over 95% were achieved with both zinc acetate and TBD. P13 and P14 displayed molar masses of 2 500 g.mol^{-1}, which corresponds to $\overline{DP}_n$ equal to 10.These results are consistent with previous literature. Indeed, Meier and coworkers reported the synthesis of an AB_2-type monomer of similar structure to M2HU, *via* the thiol-ene addition of 1-thioglycerol on methyl undecenoate, and its subsequent polycondensation using TBD as catalyst with a loading of 5 mol% *i.e.* which accounts for 3 wt% (Scheme III-8).[16] The corresponding thiolated HBPEs were reported to display molar masses in the same range, from 3 500 to 4 500 g.mol^{-1}. In contrast, Li and coworkers achieved higher molar masses than P13, in between 19 200-29 500 g.mol^{-1} with this same thiolated AB_2-type monomer using equivalent concentration of $Zn(OAc)_2$.[17] This was correlated to the presence of a sulfur atom in β-position of the terminal diol, which certainly impacts the etherification side reactions.

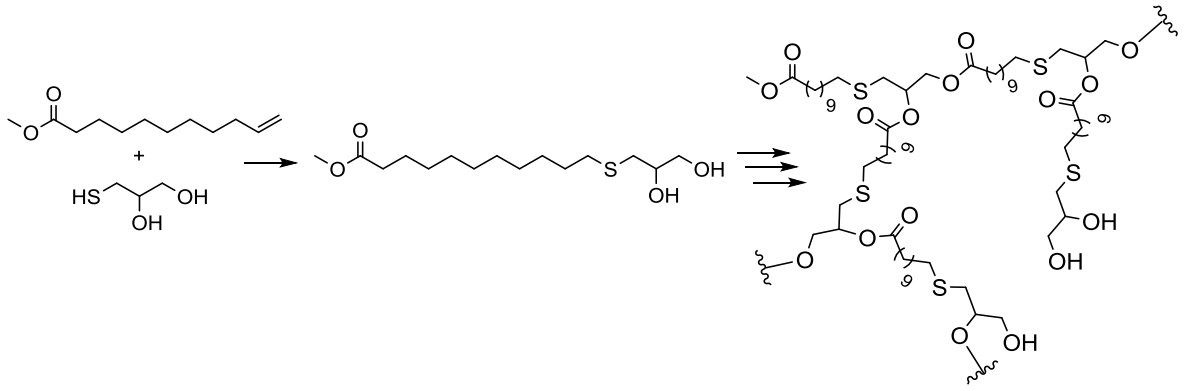

Scheme III-8. Thiol-ene addition of 1-thioglycerol on methyl 10-undecenoate and related HBPEs

In contrast to M2HU, MA displays a non-sterically hindered primary alcohol, which is expected to increase the reactivity of this AB_3-type monomer in polycondensation. Soluble HBPEs were first obtained by decreasing both temperatures of oligomerization (T_1) and

polymerization (T_2) to 90°C. Zinc acetate generally shows a poor activity at such low range of temperatures. Catalysis using TBD or NaOMe was thus preferred. Molar masses in between 5 000 to 8 000 g.mol^{-1} were achieved at full conversions (P15, P16, Table III-4). Polycondensation of MA was attempted at $T_1 = T_2 = 75$°C as well (P17). In these conditions, however, the viscosity of the reaction mixture quickly increased preventing the efficient stirring of the system, thereby limiting the molar masses achievable. Decreasing the loading in TBD proved to slow down the kinetics of polymerization (P18, Table III-4), but enabled to reach higher molar masses, up to 13 000 g.mol^{-1}. Irrespective of the reaction conditions, dispersities were found in the range 2.90-5.80.

To the best of our knowledge, the present work states the first intentional synthesis of HBPEs from MA. Veld and coworkers reported the selective polymerization of the primary hydroxyl groups of isopropyl aleuritate using Novozym 435, an enzyme which consists of *Candida antartica* Lipase B immobilized on a polyacrylic resin (Scheme III-9). Linear polyesters of moderate molar masses, *i.e.* 2 000-5 900 g.mol^{-1}, were obtained in low yields (< 43%).[18] In order to mimic non-toxic and fully biodegradable biopolymers like plant cutin, Benítez and coworkers investigated the polycondensation of aleuritic acid at 90°C in toluene using 4-dodecylbenzenesulfonic acid as catalyst and obtained rubber-like materials within three hours.[19] More recently, the same team reported the synthesis of polyhydroxyester films with a 300 µm thickness by the melt non-catalyzed polymerization of aleuritic acid directly in air at 150°C.[20]

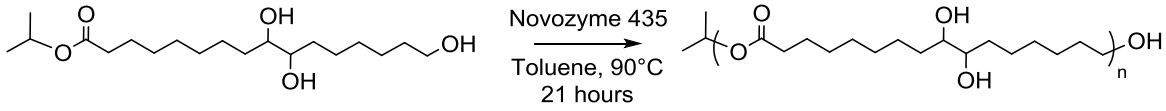

Scheme III-9. Novozym 435-catalyzed selective polymerization of isopropyl aleuritate

To conclude, in this work, a set of novel renewable HBPEs whose molar masses ranged from 3 000 to 13 000 g.mol^{-1} was synthesized by polycondensation of different oily-derived AB_n-type monomers. The presence of primary alcohols significantly increased the reactivity of M2HU and MA in polycondensation, so much that cross-linked materials were formed. This phenomenon of gelation was ascribed to the occurrence of intermolecular etherification side reactions, as evidenced by MALDI-TOF MS analyses. Optimization of the polymerization conditions was thus required to achieve soluble HBPEs. These novel oily-derived polyesters were then characterized in terms of molecular structure, thermal stability and thermo-mechanical properties.

3. Influence of monomer structure on HBPE properties

The chemical structure of the HBPEs was first confirmed by FT-IR analyses. Figure III-8 summarizes the different spectra obtained with polyesters derived from M2HB (1), M2HU (2), M3HS (3) and MA (4). Absorption bands characteristic of the hydroxyl and ester functions were observed at 3 400 and 1 734 cm^{-1}, respectively. Investigations into the fine structure of the HBPEs were then performed by NMR spectroscopy wherever possible.

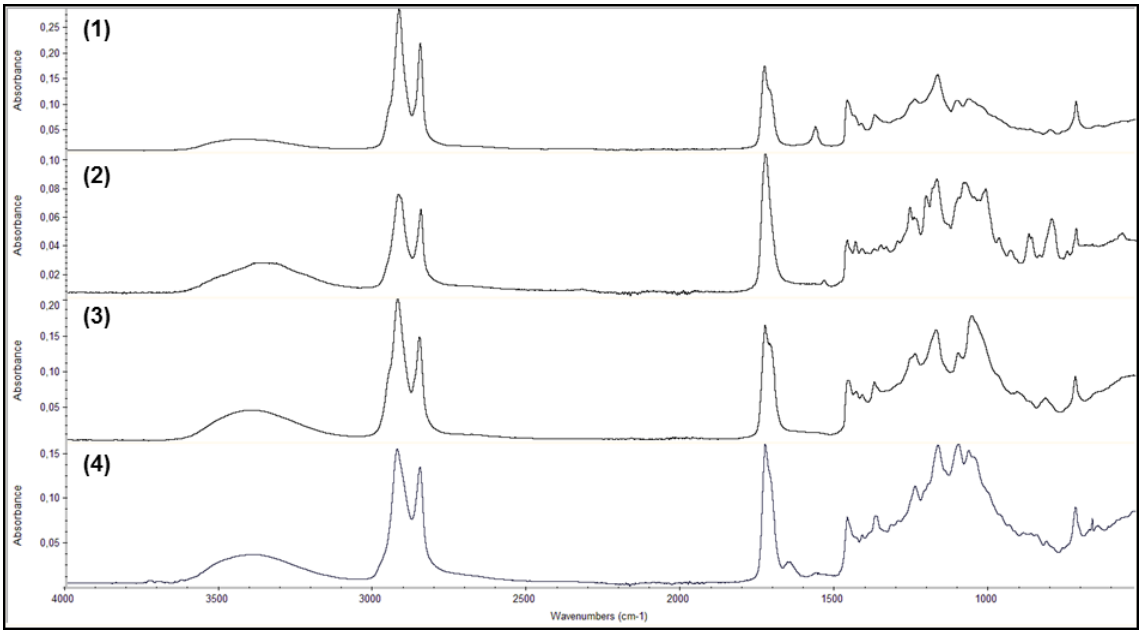

Figure III-8. Stacked FT-IR spectra of HBPEs obtained by polycondensation of (1) M2HB, (2) M2HU, (3) M3HS and (4) MA

3.1. Structural characterization

Since M2HB and M2HS (Chapter II) display very similar structures, HBPEs derived from the former monomer were easily characterized by ^{1}H NMR spectroscopy (see the detailed assignment in Figure III-9). This also allowed determining the degree of branching, as summarized in Table III-5.

Table III-5. Catalyst dependence of DB values for M2HB-based HBPEs

Entry	Catalyst	$\bar{M}_n$ [1] ($g.mol^{-1}$)	$Đ$ [1]	$DB_{Fréchet}$ [2]	DB_{Frey} [2]
P5	$Zn(OAc)_2$	3 000	1.93	0.29	0.09
P6	$Zn(OAc)_2$	5 600	>11	0.26	0.18
P7	TBD	5 600	3.05	0.39	0.33
P8	NaOMe	9 200	3.27	0.30	0.30

(1) determined by SEC in THF – calibration PS standards. (2) determined by ^{1}H NMR

As already discussed in the previous chapter, DBs were calculated based on either Fréchet equation[21] or with the Frey formula.[22] Higher values were systematically obtained for $DB_{Fréchet}$ (Table III-5). This was explained by the presence of unreacted monomers, since both definitions led to similar results at high conversion rates (P8). The branching density of HBPEs derived from M2HB was also found to depend on the catalyst of polymerization employed. Indeed, zinc acetate once again appeared to favor the formation of rather linear structures with DB values lower than 0.18, whereas TBD and NaOMe resulted in more branched polyesters with DBs in the range 0.30-0.33.

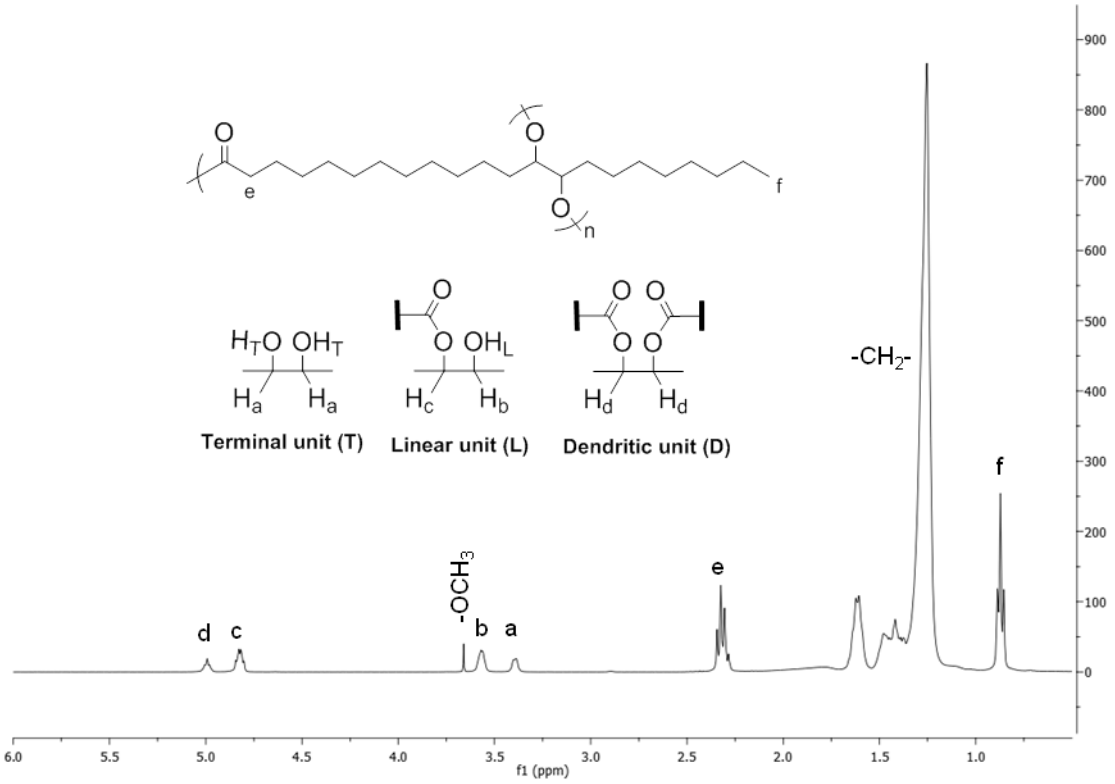

Figure III-9. ^{1}H NMR spectrum of P8 obtained by polycondensation of M2HB in $CDCl_3$

Considering the unequal reactivity of the primary and secondary alcohols of M2HU, HBPEs derived from this AB_2-type monomer are not described on the basis of three, but four different subunits (Scheme III-10). These polyesters were preferably characterized in DMSO-d_6, due to a strong overlapping of the signals in $CDCl_3$. With the help of 2D NMR techniques (see supporting information, Figure SI III-5), ^{1}H NMR spectrum of P14 was partly elucidated as can be seen in Figure III-10 (1).

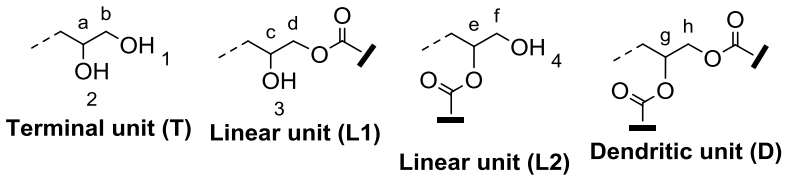

Scheme III-10. Different subunits of M2HU-derived HBPEs

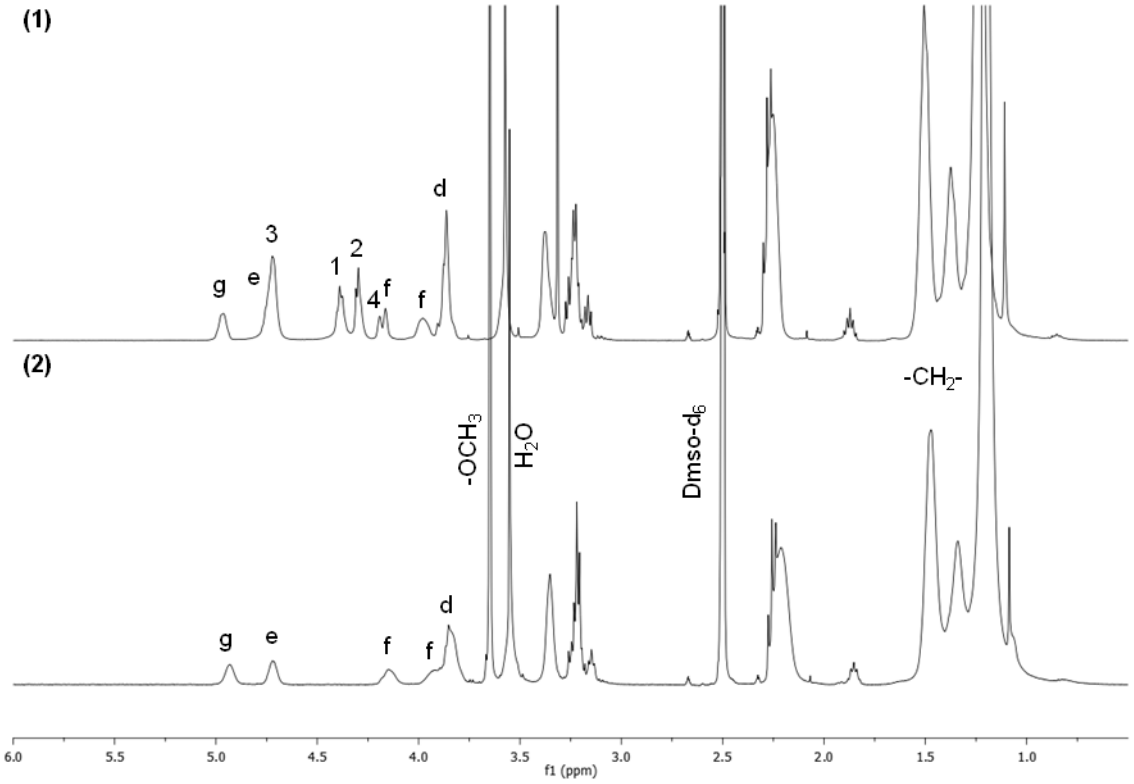

Figure III-10. Stacked ^{1}H NMR spectra of P14 in (1) DMSO-d_6 and (2) DMSO-d_6 & a few drops of water

Protons H_d, H_e and H_g characteristic of the subunits L1, L2 and D, respectively, were identified at 3.85, 4.72 and 4.93 ppm. For the purpose of subsequently assessing the molar ratio in linear unit L2, a few drops of water were added in the NMR tube in order to 'switch off ' the signals assigned to the hydroxyl functions. And accordingly, as can be seen in Figure III-10 (2), all peaks attributed to $-OH_1$, $-OH_2$, $-OH_3$ and $-OH_4$ were no longer observed. Therefore, based on the respective integration of protons H_d (L1), H_e (L2) and H_g (D), the degree of branching of P14 was found to be equal to 0.25. This result tended to indicate the formation a rather linear structure, in agreement with the higher reactivity of primary alcohols upon secondary ones. However, as discussed in the previous chapter, this value may have been underestimated since the degree of branching was measured in DMSO-d_6.

^{1}H-NMR spectroscopy is a powerful tool for unraveling the chemical structure of polymeric materials. However, this technique shows limitations for systems of high complexity, as it is the case for the HBPEs derived from AB_3-type monomers. Taking M3HS as example, there are not three but four different possibilities to incorporate the AB_3 monomer in the hyperbranched architecture: terminal (T), linear (L), semi-dendritic (*s*D) and perfectly dendritic (D) units. Since the three hydroxyl groups of M3HS are not chemically equivalent, the number of accessible configurations is increased to 8, leading to a strong overlapping of the proton signals, as shown in Figure III-11.

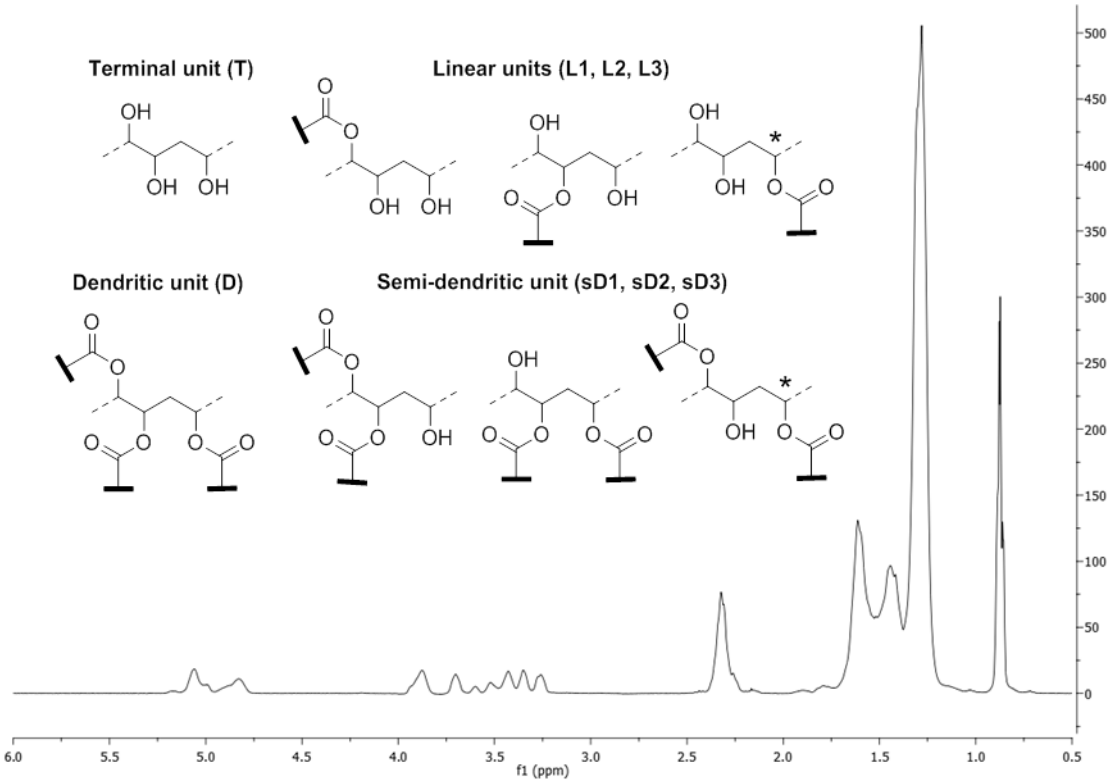

Figure III-11. ^{1}H NMR spectrum of a HBPE derived from M3HS in $CDCl_3$ and schematic representation of terminal, linear, semi-dendritic and dendritic units

According to previous literature,[22] the DB of HBPs obtained by the statistical polycondensation of AB_3-type monomers is defined as a function of the molar ratios of L, *s*D and D units as follow:

$$DB = \frac{2D+sD}{\frac{2}{3}(3D+2sD+L)} \quad \textbf{(III-1)}$$

Attempts to assign all peaks of this ^{1}H NMR spectrum, however, revealed that the three hydroxyl functions are sufficiently distant so that the protons characteristic of linear and semi-dendritic units (indicated by *) show equivalent chemical shifts. Hence, this technique was not relevant for the characterization of the branching density of M3HS-based HBPEs.

Quantitative ^{13}C NMR investigations were thus carried out, but were not conclusive either (see the complex ^{13}C NMR spectrum obtained in Figure SI III-4). In such case, attention should be drawn to the development of indirect methods of measurements of the DB, *e.g.* the determination of the HBPE functionality by titration of the hydroxyl end-groups for example. It is noteworthy that as pointed out by Frey and coworkers, the DB of HBPs prepared by polycondensation of AB_3-type monomers reaches a limit value of 0.44 (instead of 0.5 with AB_2-type monomers) after completion.

The structure of MA is not suitable to a determination of the DB of its related HBPEs by NMR spectroscopy, since its three hydroxyl functions are too far from each other. This technique was only used to assess the reactivity ratio of primary and secondary alcohols. The protons H_b, H_c and H_d characteristic of the formation of 'linear' and 'dendritic' units from the vicinal diol were easily identified at 3.58, 4.82 and 4.98 ppm, respecttively. After substitution, the methylene carbons in α-position of the primary alcohols (H_f) are deshielded to 4.06 ppm. The reactivity ratio between primary and secondary alcohols was thus determined based on the relative integrations of H_f, H_c and H_d.

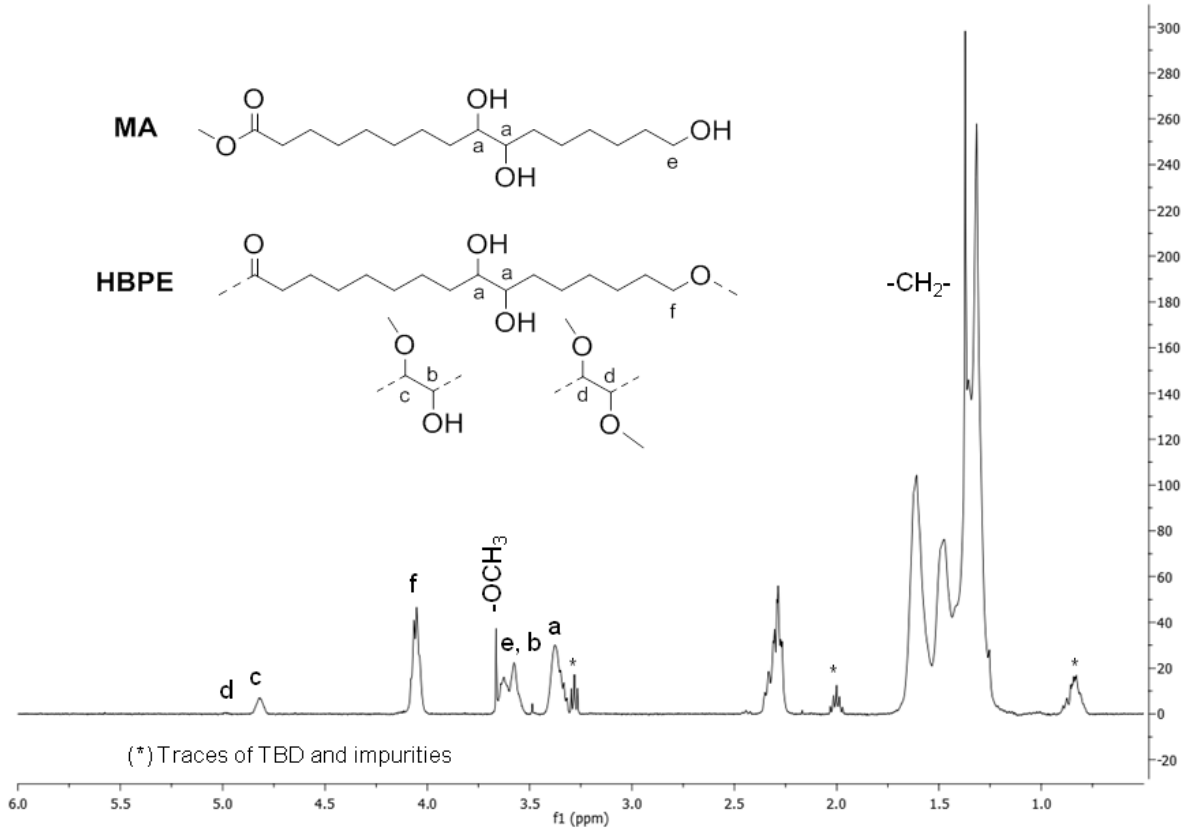

Figure III-12. ^{1}H NMR of P15 obtained by polycondensation of MA in $CDCl_3$

Values achieved in the range 2.98 to 3.21 were independent of the catalyst employed (TBD or NaOMe). An increase to 3.38 was besides noticed when the polymerization was performed at 75°C (instead of 90°C). Due to the higher reactivity of the primary alcohols compared to the secondary ones, HBPEs derived from MA displayed as expected, a more linear structure than the previous materials synthesized.

3.2. Thermal properties

Thermal stability of our HBPEs was investigated by TGA under a nitrogen stream at a heating rate of 10°C.min^{-1} (Table III-6). In this study, thermal stabilities in between 254 and 332°C, were achieved except with HBPEs derived from M2HU. P13 and P14 indeed show the lowest 5% weight loss degradation temperatures in this series of experiments, of 204 and 230°C, in agreement with the low molar masses display by these two samples ($\overline{M}_n \leq 2\ 500$ g.mol^{-1}). As was the case for materials derived from M2HS (Chapter II), HBPEs prepared using zinc acetate (P6, P9 and P13) appeared less stable than their homologues obtained with TBD or NaOMe. Their thermal degradation was accelerated at high temperatures by residual traces of $Zn(OAc)_2$ catalyzing their depolymerization. Overall, HBPEs synthesized with zinc acetate displayed $T_d^{5\%}$ in between 254 and 272°C, whereas with the other catalysts, values were reported in the range 296 to 332°C.

Table III-6. Thermal properties of HBPEs derived from M2HB, M3HS, M2HU and MA

Entry	Monomer	DSC			TGA
		T_g (°C)	T_m (°C)	T_c (°C)	$T_d^{5\%}$ (°C)
P6[1]	M2HB	-	20	14	260
P7		-	22	12	298
P8		-	23	12	332
P9[1]	M3HS	-3	-	-	254
P10		-1	-	-	305
P12		3	-	-	299
P13[1]	M2HU	-	61	44	204
P14		-	54	36	230
P15	MA	-15	43	13[2]	326
P16		-17	36	14[2]	nd.
P17		-14	40	19[2]	296
P18		-14	38	25[2]	326

(1) HBPE prepared using $Zn(OAc)_2$ as catalyst. (2) crystallization temperature upon heating. nd. = not determined

Thermal properties of our HBPEs were investigated by DSC. Results are given in Table III-6 as well. Glass transition and melting temperatures were determined from the second heating scan at 10°C.min^{-1} and crystallization temperatures from the first cooling scan, except otherwise mentioned. As expected, HBPEs derived from M3HS displayed amorphous properties. However, higher glass transition temperatures were achieved compared to M2HS-based HBPEs, in the range -10 to 9°C (for M2HS, $-32.5 \leq T_g \leq -20$°C). This is easily explained by the higher functionality of the AB_3 monomer.

Indeed, as discussed in the previous chapter, the glass transition of HBPs is unlike linear polymers, greatly affected by the nature and content of end-group moieties. The number of polar hydroxyl end-groups increasing with the monomer functionality, stronger interactions, *i.e.* hydrogen bonding, likely take place within M3HS-based HBPEs at equivalent molar masses. As for MA which is also an AB_3-type monomer, the corresponding HBPEs only showed slightly higher T_g values, *i.e.* in between -17 and -14°C, due to their more linear structure.

More interestingly, HBPEs prepared from M2HB, M2HU and MA were semi-crystalline. DSC thermograms obtained greatly varied from one monomer to the other. Concerning M2HB, the higher chain length between two branching points compared to M2HS (11 carbon atoms *vs.* 7) appeared to enhance the flexibility of polymeric chains, and thus allow crystallinity as clearly stated in Figure III-13 (1). The relatively high melting enthalpy measured (ΔH_m = 30.3 $J.g^{-1}$) indicates a high degree of crystallinity, which explains why the glass transition is barely visible.

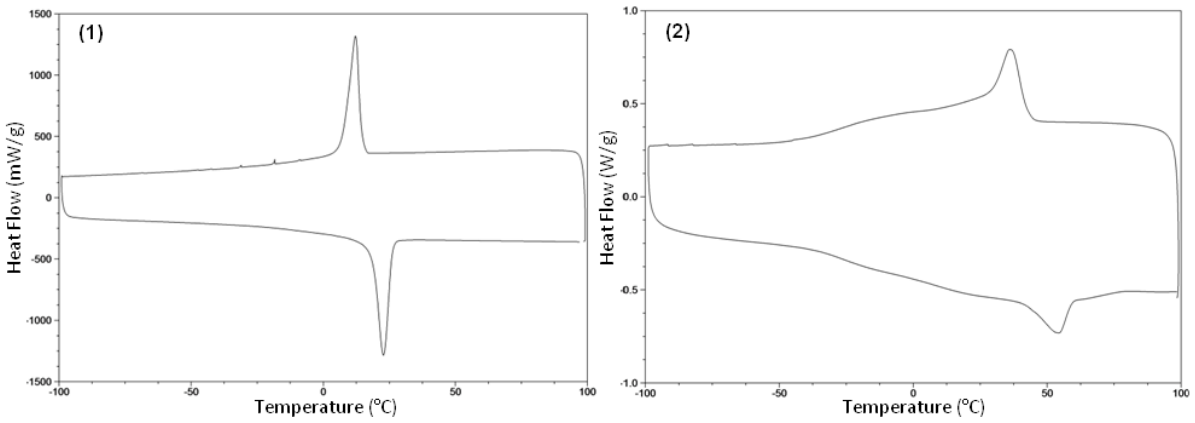

Figure III-13. DSC thermograms at 10°C.min^{-1} for HBPEs derived from (1) M2HB and (2) M2HU

The semi-crystalline character of M2HB-based HBPEs was further investigated by wide-angle X rays diffraction measurements (WAXS), carried out as a function of the temperature at 5, 25 and 80°C. Figure III-14 depicts the different WAXS patterns obtained. Results clearly confirm the semi-crystalline properties of the HBPEs. Apart from the apparent large amorphous halo, two diffraction peaks can be distinguished. Their position as well as their intensity depend on the temperature of analysis. At 80°C, *i.e.* well above the melting point, these two diffraction peaks disappeared leading to a broad amorphous halo, due to the lost of crystallinity at that temperature.

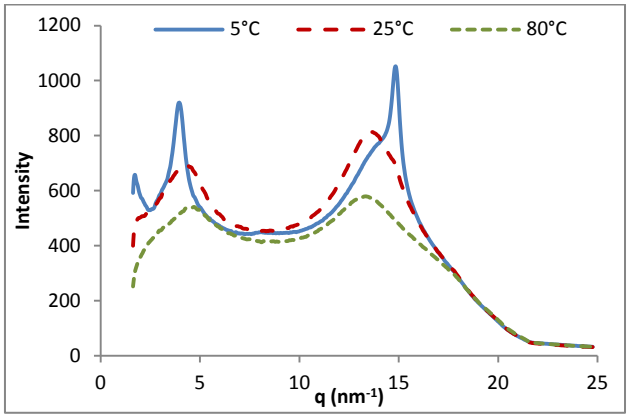

Figure III-14. WAXS patterns at 5, 25 and 80°C of a HBPE prepared from M2HB

The absence of pendant alkyl chains which act as plasticizers also appeared to endow the HBPEs derived from M2HU with semi-crystalline properties, as can be seen in Figure III-13 (2). Complex melting and crystallization patterns were however observed, probably due to the unsymmetrical nature of the diol affecting the chain mobility and preventing the formation of stable crystals.

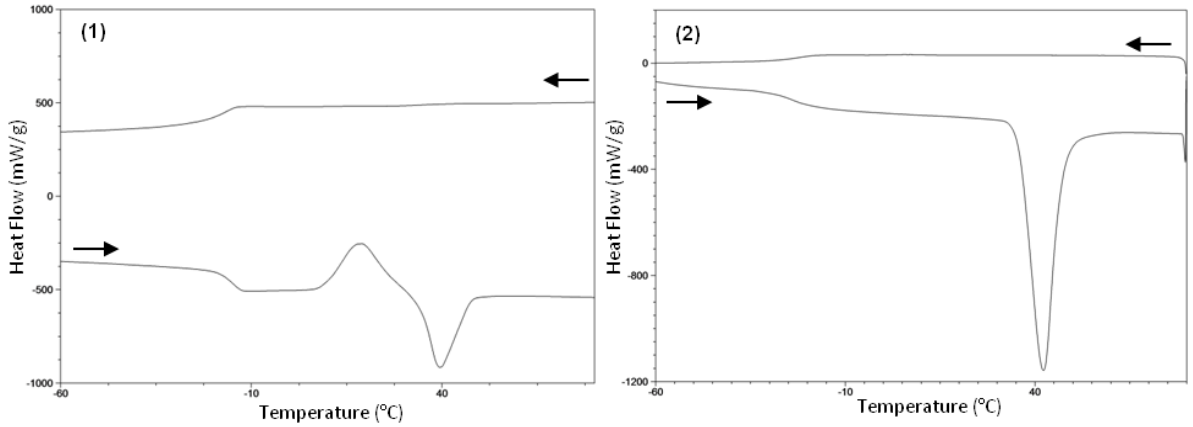

Figure III-15. DSC thermograms at 10°C.min^{-1} for a MA-HBPE analyzed at (1) t_0 and (2) t_0 + 15 days

Lastly, the more linear structure displayed by MA-based HBPEs was shown to induce crystallinity as well. DSC thermograms obtained showed unique behavior. One HBPE derived from MA was first characterized by DSC at a given time t_0 (Figure III-15 (1)). Upon heating, the polymer exhibited a glass transition, and an exothermic peak directly followed by a melting endotherm (ΔH_m = 19.8 J.g^{-1}). However, no crystallization was observed upon cooling. Two weeks later, as the sample turned to a white color, the HBPE was analyzed again by DSC (Figure III-15 (2)). This time, the thermogram displayed one glass transition and an important melting endotherm (ΔH_m = 41.9 J.g^{-1}) upon heating.

The exothermic peak observed on the first trace is characteristic of a cold crystallization. Polymeric chains gain in mobility right after the glass transition temperature allowing crystallization. No exothermic peak was observed upon cooling since the rate of $10°C.min^{-1}$ applied is too fast compared with the kinetics of crystallization. The chain mobility of MA-based HBPEs is in fact limited by the branching points provided by the secondary alcohols, resulting in a slow crystallization.

Conclusion

The platform of oily-derived AB_n-type monomers was extended to four novel synthons of different structures where the length between two branching points, presence of pendant alkyl chains and primary or secondary alcohols, could be varied. Three of these monomers were prepared by acid hydrolysis of epoxidized vegetable oils, the fourth synthon being a naturally occurring AB_3 fatty acid that was simply esterified for the need of this study. These AB_2/AB_3-type monomers were successfully employed as building blocks for the synthesis of hyperbranched polyesters.

Correlations between monomer structure and tailor-made HBPE properties were studied in comparison with the results previously obtained with M2HS (Chapter II). An increase in the monomer functionality (n = 3) did not impact its reactivity in polycondensation. Similar molar masses were indeed achieved with M3HS, in the range 5 000-10 000 $g.mol^{-1}$. However, the as-formed HBPEs displayed more complex architecture that could not be clearly elucidated by NMR spectroscopy. The presence of primary alcohols enhanced the reactivity of M2HU and MA, and enabled to tune the branching density of the related HBPEs. The formation of rather linear structures was shown to induce crystallinity. A higher chain length between two branching points or the absence of pendant alkyl chains that act as plasticizers, endowed as well the HBPEs with semi-crystalline properties as demonstrated with M2HB and M2HU. Glass transition and melting temperatures were found in the range -17 to 3°C, and 20 to 61°C, respectively.

The gelation phenomenon by which cross-linked materials were formed, was investigated by MALDI-TOF MS analyses. The occurrence of different side reactions was evidenced, including cyclization through ester or ether bonds and intermolecular etherification. This latter reaction results in HBPEs with two or more focal points acting as cross-linkers at high conversion rates. Tailoring reaction conditions (time, temperature, loading in catalyst) to the monomer reactivity allowed us to prevent gelation and thus to synthesize soluble polyesters of hyperbranched architecture.

The synthesis of AB_n monomers of higher functionality was considered. AB_4 or even AB_6 synthons may be prepared by acid hydrolysis of epoxidized methyl esters of linoleic (C18:2) or linolenic acid (C18:3). However, only oligomers of low molar masses would be achieved due to steric hindrance. Thereafter, another route has been investigated for the functionalization of FAMEs with the idea of producing AB_2-type monomers of higher reactivity. Results obtained through thiol-ene addition are discussed in the next chapter.

References

(1) Testud, B.; Grau, E.; Pintori, D.; Taton, D.; Cramail, H. New branched polymers, their preparation process and thereof. EU 14306642 A1, 2014.
(2) Scanlan, J. T.; Swern, D. *J. Am. Chem. Soc.* **1940**, *62*, 2309.
(3) Subra Rao, R.; Achaya, K. T. *J. Sci. Ind. Res. (India).* **1960**, *19B*, 482–484.
(4) McKay, A. F.; Bader, A. R. *J. Org. Chem.* **1948**, *13* (1), 75–85.
(5) Khuddus, M. A.; Usui, Y.; Swern, D. *J. Am. Oil Chem. Soc.* **1973**, *50*, 524–528.
(6) Warwel, S.; Klaas, M. R.; Sojka, M. Process for the preparation of vicinal diols and/or expoxides. US 5 344 946, 1994.
(7) Boyer, A.; Cloutet, E.; Tassaing, T.; Gadenne, B.; Alfos, C.; Cramail, H. *Green Chem.* **2010**, *12* (12), 2205–2213.
(8) Vogel, A. I.; Tatchell, A. R.; Furnis, B. S.; Hannaford, A. J.; Smith, P. W. G. *Vogel's Textbook of Pratical Organic Chemistry fifth edition*, Pearson Ed.; Dorling Kindersley, 1989.
(9) White, J. E.; Earls, J. D.; Sherman, J. W.; López, L. C.; Dettloff, M. L. *Polymer* **2007**, *48* (14), 3990–3998.
(10) Cravotto, G.; Calcio Gaudino, E.; Barge, A.; Binello, A.; Albertino, A.; Aghemo, C. *Nat. Prod. Res.* **2010**, *24* (5), 428–439.
(11) Flory, P. J. *J. Am. Chem. Soc.* **1952**, *74* (1932), 2718–2723.
(12) Voit, B. I.; Lederer, A. *Chem. Rev.* **2009**, *109* (11), 5924–5973.
(13) Chikh, L.; Tessier, M.; Fradet, A. *Polymer* **2007**, *48* (7), 1884–1892.
(14) Burgath, A.; Sunder, A.; Frey, H. *Macromol. Chem. Phys.* **2000**, *201* (7), 782–791.
(15) Komber, H.; Ziemer, A.; Voit, B. I. *Macromolecules* **2002**, *35* (9), 3514–3519.
(16) Türünç, O.; Meier, M. A. R. *Macromol. Rapid Commun.* **2010**, *31* (20), 1822–1826.
(17) Bao, Y.; He, J.; Li, Y. *Polym. Int.* **2013**, *62*, 1457–1464.
(18) Veld, M. A. J.; Palmans, A. R. A.; Meijer, E. W. *J. Polym. Sci. Part A Polym. Chem.* **2007**, *45* (3), 5968–5978.
(19) Heredia-Guerrero, J. A.; Heredia, A.; García-Segura, R.; Benítez, J. J. *Polymer* **2009**, *50* (24), 5633–5637.
(20) Benítez, J. J.; Heredia-Guerrero, J. A.; Guzmán-Puyol, S.; Domínguez, E.; Heredia, A. *J. Appl. Polym. Sci.* **2015**, *131* (4), 41328–41335.
(21) Hawker, C.; Lee, R.; Fréchet, J. M. J. *J. Am. Chem. Soc.* **1991**, *4588* (113), 4583–4588.
(22) Hölter, D.; Burgath, A.; Frey, H. *Acta Polym.* **1997**, *48* (1-2), 30–35.

Experimental methods

Methyl 9,10,12-trihydroxystearate (M3HS)

Epoxidation step: Methyl esters of castor oil and formic acid (0.3 eq.) were added in a reactor equipped with a mechanical stirrer, a dropping funnel and a condenser. The resulting mixture was heated at 40°C for 1 hour under stirring condition. At 40°C, hydrogen peroxide (50%, 2 eq.) was added dropwise to the reactor using a dropping funnel while maintaining the temperature in the reactor close to 70–75°C. As the reaction is exothermic, a cooling system was used to cool down the reactor. The reaction was monitored by gas chromatography and oxiran titration. The reaction mixture was then cooled down to room temperature and the aqueous phase was discarded. The organic layer was washed with an aqueous solution of sodium hydroxide (0.1N) until the pH became neutral. The organic phase was then dried under vacuum at 60°C to afford a clear and slightly yellow liquid with a precipitate. The precipitate isolated by filtration was identified as the methyl 9,10,12-trihydroxystearate, the yellow liquid corresponded to the epoxidized methyl esters of castor oil.

Hydroxylation step: Epoxydized methyl esters of castor oil (10 kg) was placed along with an aqueous solution of phosphoric acid (12 % w/w, 5 kg) and *tert*-butanol (3 kg) as solvent in a reactor equipped with a condenser and a mechanical stirrer. The resulting mixture was heated at 90°C under vigorous stirring. The reaction was monitored by gas chromatography. When the reaction was completed, the aqueous phase was discarded at 50°C. t*ert*-Butanol was eliminated under vacuum distillation. The organic phase was then washed with hot water until the pH reached 6-7 and dried under vacuum.

Isolation: Methyl 9,10,12-trihydroxystearate was recrystallized in cyclohexane (3 times, 20-40 $g.L^{-1}$) an dried under vacuum. The product was then dissolved in a minimum of dichloromethane (DCM) and injected in a Flash chromatography apparatus from Grace. The constituents were separated on a silica column, using a dichloromethane-methanol gradient and an Evaporating Light Scattering Detector (ELSD). Two fractions were collected corresponding to M3HS and its acid form. M3HS was obtained as a white solid powder (purity: 98.1%). Yield: 25%.

Methyl 13,14-dihydroxybehenate (M2HB)

Refined erucic acid rapeseed oil (800 kg) was heated under stirring condition at 65°C in the presence of methanol (190 kg) and sodium methanolate (19 kg) for 2 hours. The thus-obtained methyl esters were decanted and the glycerol phase discarded. Methyl esters of erucic acid rapeseed oil were then washed with water, dried under vacuum and distilled on a falling film reactor (200 $L.hour^{-1}$) in order to concentrate the erucic acid methyl ester up to 95%. The procedure followed to prepare M2HB starting from distilled methyl erucate was then identical to the one described previously to obtain M2HS (Chapter II). The epoxidized intermediate was obtained as a whitish solid in high yield (95%). After dihydroxylation, the crude mixture was purified by means of neutralization with potassium hydroxide and recrystallization in cyclohexane, to afford M2HB as a white powder (purity: 94%). Yield of the overall synthesis: 80%.

Methyl 10,11-dihydroxyundecanoate (M2HU)

Epoxidation step: Methyl undecenoate (15 g, 0.076 mol) and *m*-cpba (39.2 g, 0.227 mol) were stirred at room temperature in DCM (20 $mL.g^{-1}$ of product) overnight. 3-chlorobenzoic formed as side product precipitated in DCM. The reaction mixture was thus first filtered to get rid of 3-chlorobenzoic, washed with aqueous sodium sulfite Na_2SO_3 (3 x 50 mL), aqueous sodium bicarbonate $NaHCO_3$ (4 x 50 mL) and brine (2 x 50 mL) until the pH became neutral. The organic phase was then dried over anhydrous magnesium sulfate, filtered and DCM was removed on a rotary evaporator to afford methyl 10-epoxyundecenoate. Yield: 92%.

Hydroxylation step: Methyl 10-epoxyundecenoate (2.5 g) was charged in a round-bottom flask equipped with a mechanical stirrer, an oil bath and a condenser. The epoxidized intermediate was dissolved in 50 mL of a 1:1 (v/v) mixture of water and *tert*-butanol under stirring. After the addition of phosphoric acid (85% w/w, 3 wt%), the reaction flask was heated under reflux at 90°C. 4 hours later, the aqueous phase was discarded at 50°C and *tert*-butanol was removed under vacuum distillation. After the addition of 50 mL DCM, the organic phase was washed twice with water (2 x 50 mL) and brine (1 x 50 mL), dried over anhydrous magnesium sulfate, filtered and solvent was removed on a rotary evaporator. M2HU was obtained as a white powder (purity: 99%). Yield: 57%.

Methyl aleuritate (MA)

Methyl aleuritate was prepared by esterification of aleuritic acid in methanol. A round-bottomed flask was charged with aleuritic acid (5 g), 50 mL of methanol and Amberlyst 15 resin (1 g, 20 wt%). The mixture was heated at 70°C under reflux for 24 hours. After reaching room temperature, the resin was filtered on celite, the methanol removed under vacuum and 100 ml of DCM was added. The organic phase was washed twice with water, dried on anhydrous magnesium sufalte and DCM was removed under vacuum. Methyl aleuritate was obtained as a white solid powder (purity: 97.3%). Yield: 75%.

General procedure for polyester synthesis

All transesterification reactions were performed in bulk, in a Schlenk flask equipped with a magnetic stirrer, a nitrogen inlet tube and an oil-bath heating system. The experimental two-step-one-pot procedure applied was similar to the preparation of HBPEs derived from M2HS (and described in Chapter II). After one hour of pre-drying at 90°C under dynamic vacuum, one catalyst was added with a loading of 1.5% relative to monomer weight, except otherwise mentioned. A reduced concentration in TBD (1 wt%) was indeed tested in an attempt to control the polycondensation of MA. After 2 hours of oligomerization at T_1(°C) under nitrogen blowing, the temperature was raised to T_2(°C) and dynamic vacuum was applied until the viscosity of the reaction mixture suddenly increased. Reaction conditions were optimized as followed. M3HS and M2HB were preferably polymerized at T_1 = 120°C and T_2 = 160°C, M2HU at T_1 = 120°C and T_2 = 140°C and MA at T_1 = T_2 = 75 to 90°C. HBPEs prepared from M3HS were obtained as colorless and highly viscous materials, while polycondensation of M2HB, M2HU and MA afforded whitish waxes. The observed change in texture was the first sign of the semi-crystalline character of these HBPEs.

Polymerization of 9,10-dihydroxystearic acid (2HSA)

For comparison purpose, the polymerization behavior of the acid form of M2HS, namely, 9,10-dihydroxystearic acid (2HSA) has been examined. 2HSA bears as reactive functions one carboxylic acid (A) and two secondary alcohols (B). Its polycondensation thus proceeds *via* esterification reaction *vs.* transesterification mechanism with M2HS, and involves the formation of water as co-product instead of methanol (Scheme SI III-1).

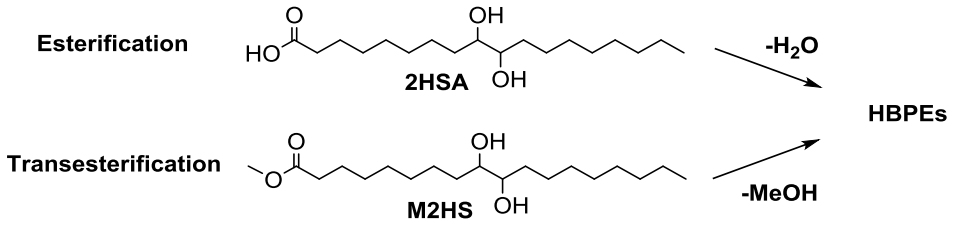

Scheme SI III-1. Synthetic pathways to HBPEs starting from 2HSA and M2HS

2HSA was provided by the *ITERG* technical center with a chemical purity over 98%, as determined by GC analysis. This AB_2-type monomer was successfully characterized by ^{1}H NMR spectroscopy in DMSO-d_6 as shown in (Figure SI III-1 (1)). According to DSC experiments, 2HSA displayed a significantly higher melting point than its methyl ester form, *i.e.* 139°C for 2HSA *vs.* 70°C for M2HS. Higher reaction temperatures, *i.e.* $T \geq 160$°C, were thus considered to be able to perform its polymerization in the melt-phase. Besides, dynamic vacuum was applied during the whole polycondensation in order to adequately remove water thereby shifting the equilibrium towards the formation of HBPEs.

Only two assays were performed. Polycondensation of 2HSA was first attempted at 160°C in the presence of catalytic amounts of anhydrous zinc acetate, *i.e.* 1.5 wt%. Obviously, TBD was not tested, the acidity of the reagent deactivating the organic base. The reaction was stopped after 24 hours since no increase in viscosity was observed. A white solid, very similar in general appearance to 2HSA, was obtained indicating that a low conversion was achieved. The formation of oligomers was evidenced in ^{1}H NMR spectroscopy (Figure SI III-1 (2)) by the appearance of signals characteristics of the linear (H_b and H_c protons) and dendritic units (H_d protons), at 3.57, 4.83 and 4.97 ppm, respectively. Molar ratios of linear (L) and dendritic units (D) however remained very low, *i.e.* L = 0.06 and D = 0.08 (P19, Table SI III-1). In addition, the as-formed oligomers were similarly to 2HSA, insoluble in THF which prevented the characterization of their molar masses by SEC.

Table SI III-1. Preliminary investigations of the step-growth polymerization of 2HSA: values for T, L and D as determined by ^{1}H NMR

Entry	T	L	D	T + L + D
2HSA	0.95	0	0	0.95
P19	0.76	0.06	0.08	0.90
P20	0.16	0.24	0.10	0.50

T, L and D molar ratios determined based on the respective integration of $H_a/2$, H_b and $H_d/2$

In contrast, an increase in the reaction temperature to 200°C yielded after 24 hours, a white wax (P20, Table SI III-1). ^{1}H NMR analysis of the as-formed material (Figure SI III-1 (3)) evidenced an increase in the L and D molar ratios up to 0.24 and 0.10, respectively, revealing the formation of a noticeable branched structure in higher yield than P19. The presence of ester linkages was stated by the slight upfield shift of the methylene protons (H_g), adjacent to the carbonyl functions to 2.32 ppm. However, the sum of the molar ratios T, L and D was noted to be no longer equal to 1, *i.e.* T + L + D = 0.50 for P20 *vs*. 0.95 for 2HSA (Table SI III-1). This suggested the occurrence of undesired side reactions involving the hydroxyl moieties and the formation of an insoluble fraction to which the missing protons would belong. In other words, P20 was a gelled product and Figure SI III-1 (3) only characterized its $CDCl_3$ soluble fraction.

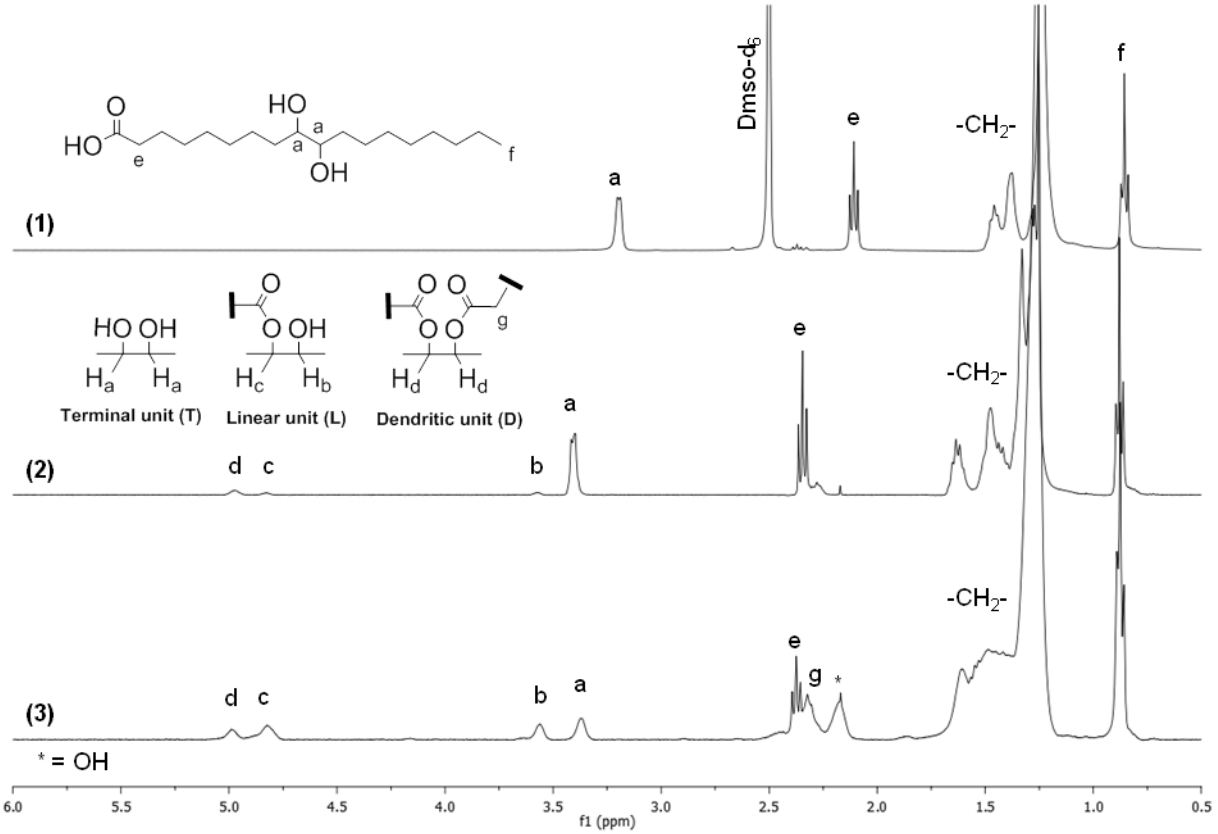

Figure SI III-1. Stacked ^{1}H NMR spectra of (1) 2HSA in DMSO-d^6, and related branched polyesters (2) P19 and (3) P20 in $CDCl_3$

In brief, the higher reaction temperatures, *i.e.* $T \geq 160°C$ compared to M2HS, required to achieve the polymerization of 2HSA in the melt-phase, therefore favored the occurrence of etherification side reactions over the formation of HBPEs. One can even presume that the acidity of the reagent itself catalyzed these dehydration reactions. These side assays justify the approach adopted in the course of this thesis, namely the use of Fatty Acid Methyl Esters (FAMEs) as synthetic precursors of HBPEs, instead of Fatty Acid (FA) derivatives.

To efficiently polymerize 2HSA, some options can however be considered. The addition of monofunctional end-capping reagents, *i.e.* A-type monomers, is primordial to carry out its polycondensation in the melt-phase. Solution polymerizations can also be applied. The milder reaction conditions required, as well as dilution of the monomer may indeed be effective in avoiding gelation caused by intermolecular interactions.

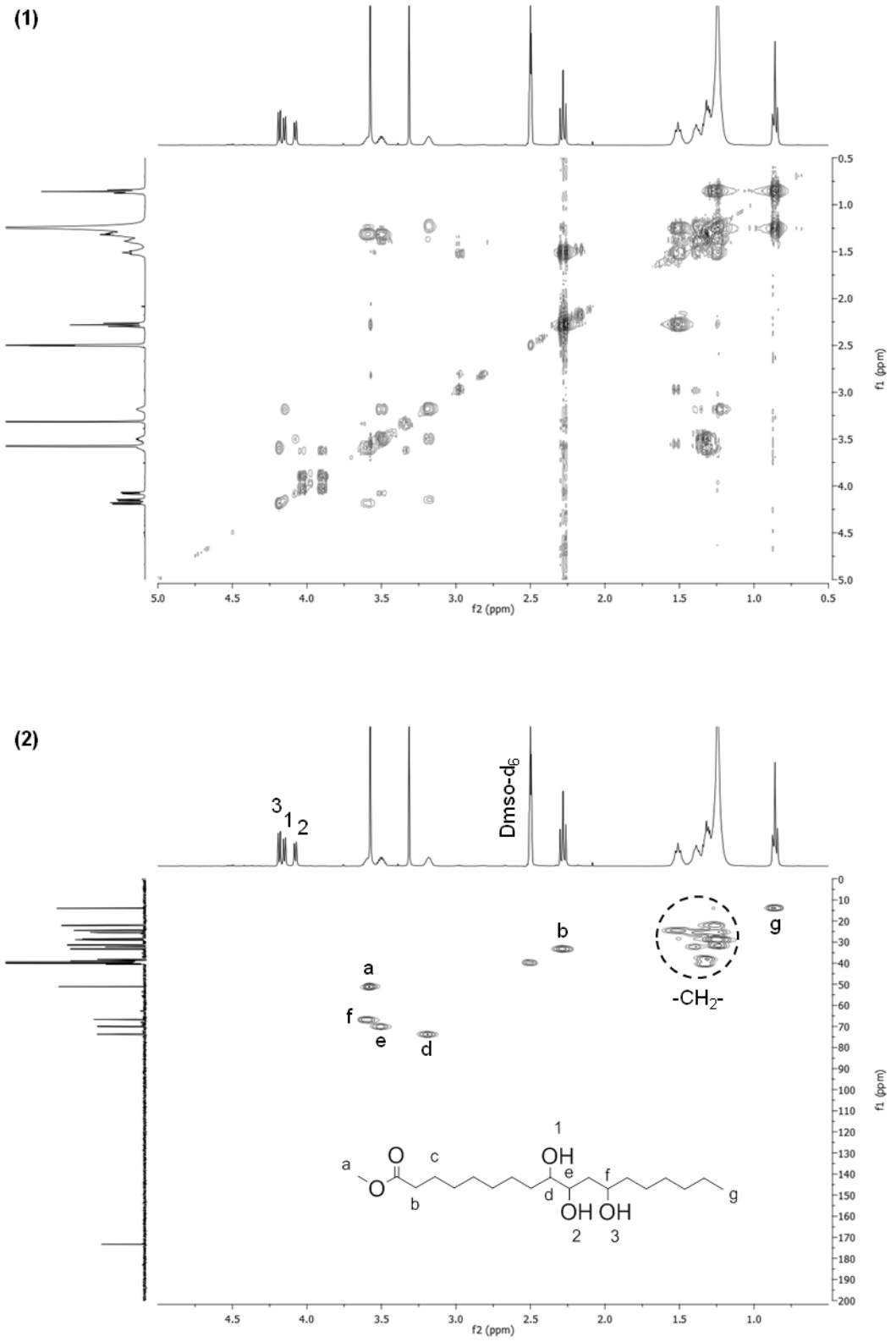

Figure SI III-2. (1) ^{1}H-^{1}H COSY and (2) ^{1}H-^{13}C HSQC of M3HS in DMSO-d$_6$

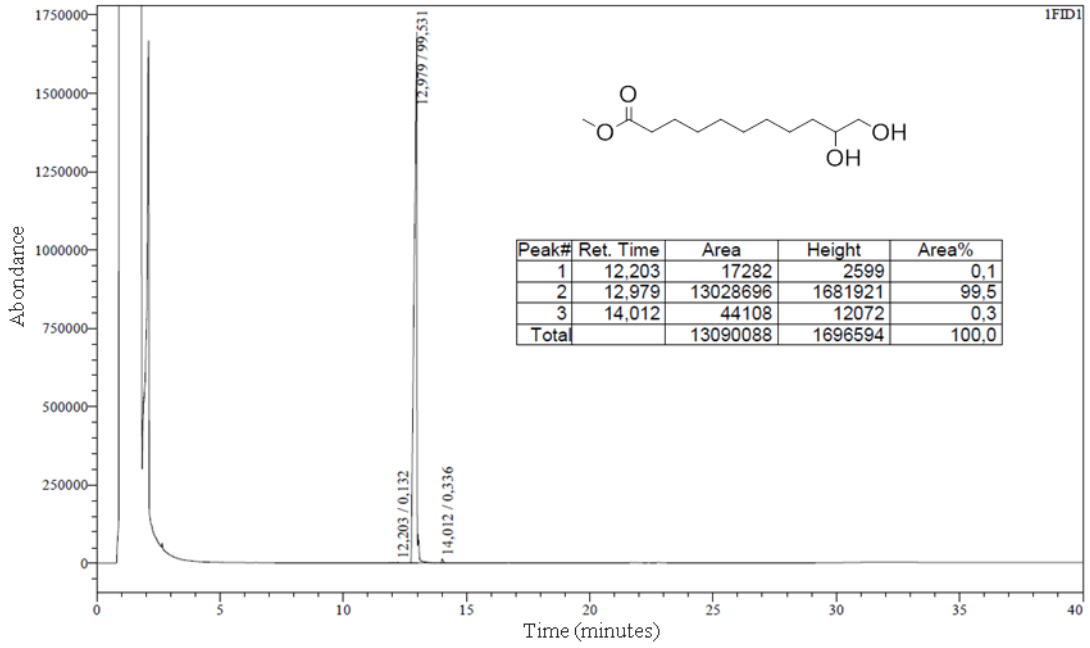

Peak#	Ret. Time	Area	Height	Area%
1	12,203	17282	2599	0,1
2	12,979	13028696	1681921	99,5
3	14,012	44108	12072	0,3
Total		13090088	1696594	100,0

Figure SI III-3. Gas Chromatogram of M2HU

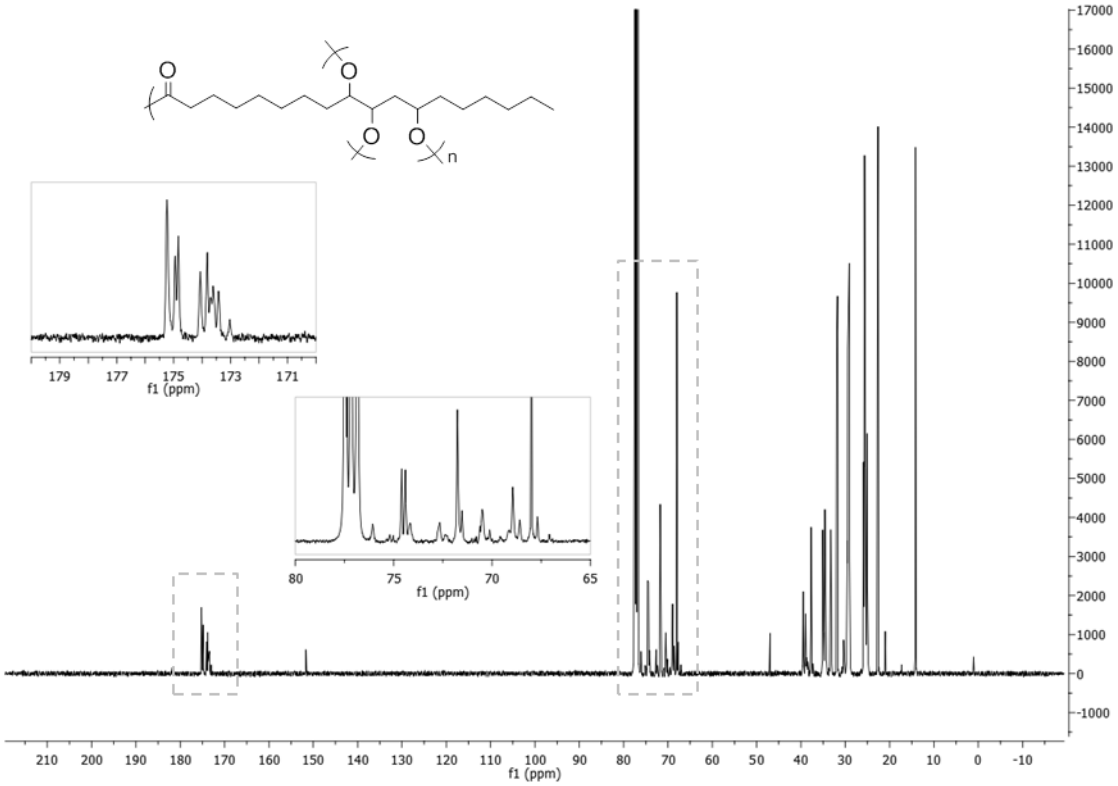

Figure SI III-4. ^{13}C NMR spectrum of a M3HS-based HBPE in $CDCl_3$

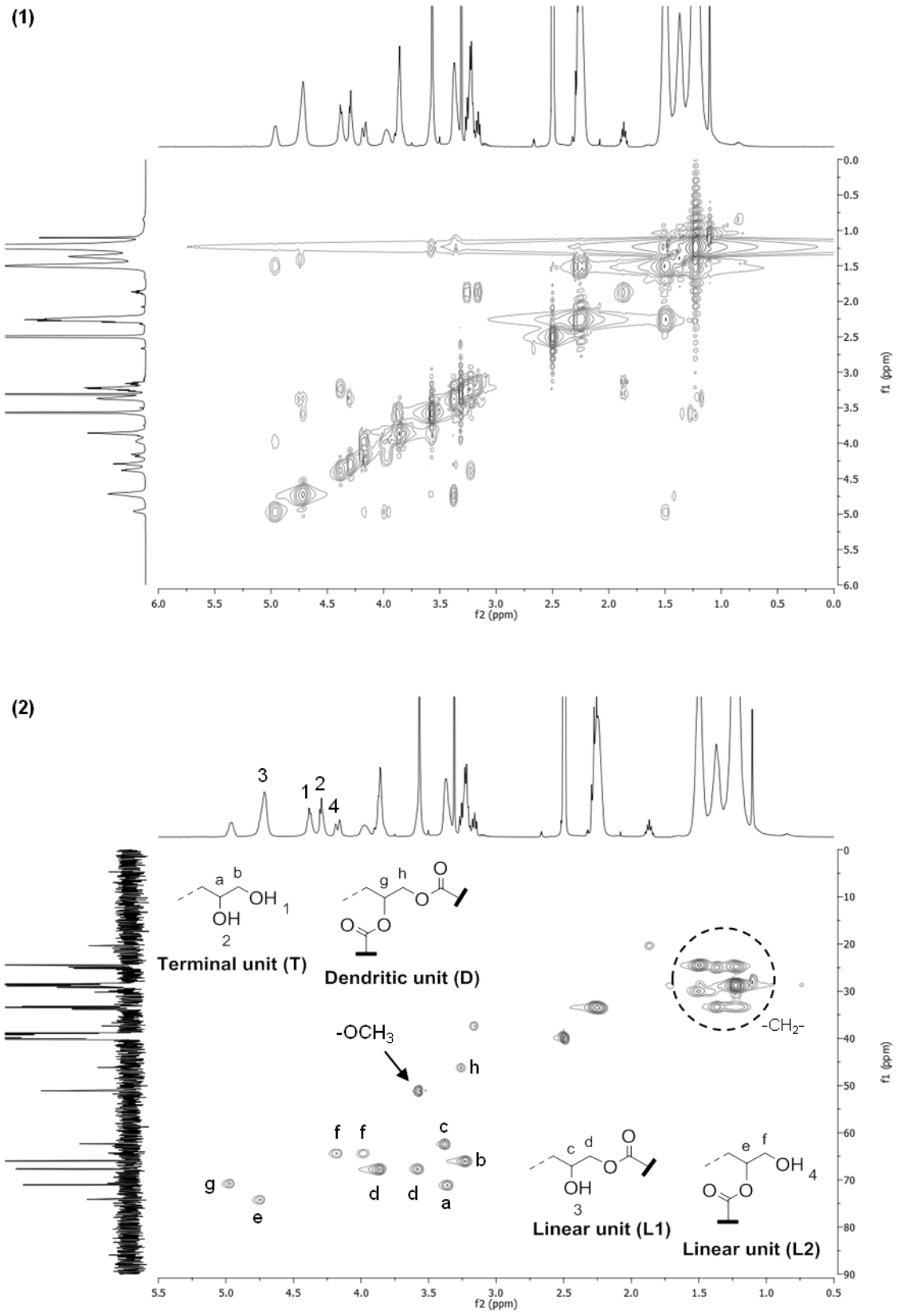

Figure SI III-5. (1) ^{1}H-^{1}H COSY and (2) ^{1}H-^{13}C HSQC of a M2HU-derived HBPE in DMSO-d$_6$

Chapitre IV. Design of new fatty acid-derived precursors of AB_2-type *via* thiol-ene additions for the synthesis of HBPEs

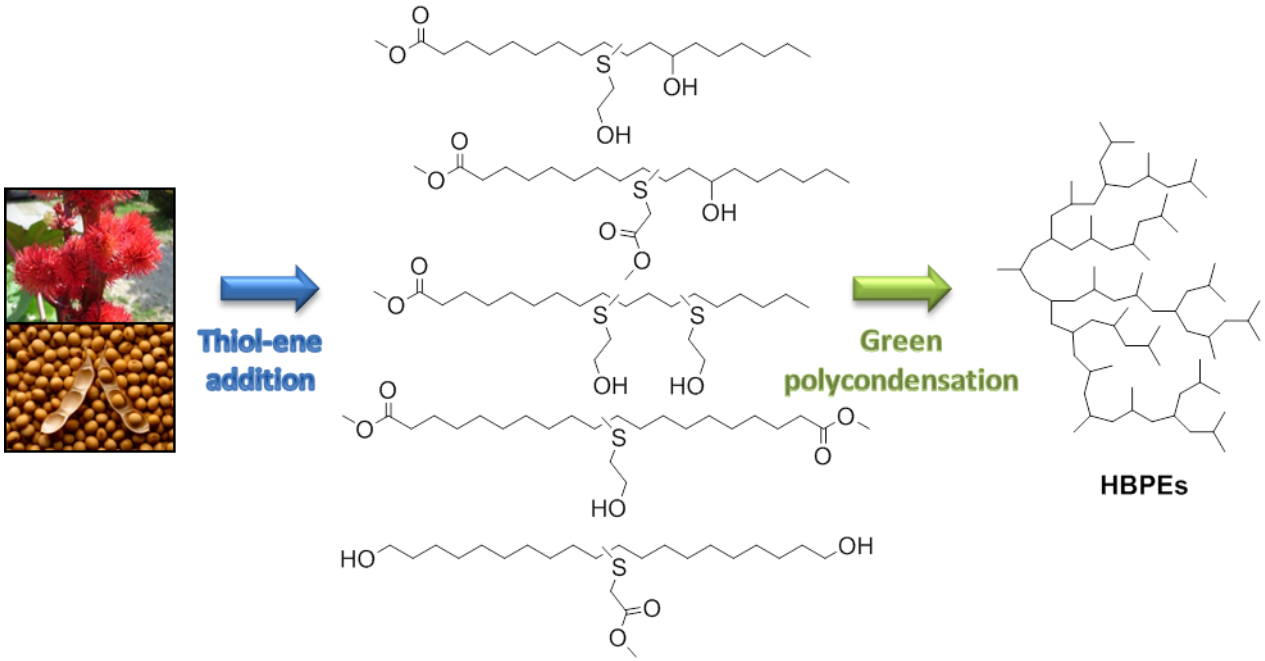

Part of this Chapter has been warranted as a patent.

Table of Contents

Introduction

The previous chapters described the development of a versatile platform of AB_2 and AB_3-type monomers by acid hydrolysis of epoxidized vegetable oils. Dihydroxylation of internal olefins was the key step enabling the formation of secondary alcohols in vicinal position. The reactivity of these multifunctional precursors was further studied in polycondensation. The 1,2-diol structure was shown to limit somehow both the molar masses and DB values achievable, due to steric hindrance. This negative substitution effect was supported by kinetic experiments performed with M2HS, using either zinc acetate or TBD as catalyst (Chapter II).

The present work is dedicated to the design of more reactive fatty acid-based AB_2-type monomers. For that purpose, the so-called "thiol-ene click" coupling reaction was preferred over other strategies. This route allowed the incorporation of both ester functions and primary alcohols, *i.e.* more reactive than secondary ones, as discussed in Chapter III. In addition, the metathesis reaction was applied so as to dimerize the FAMEs and thus drive apart the reactive functions, thereby preventing steric hindrance. The synthesis of five novel HBPE precursors of AB_2 and A_2B-type was thus investigated, starting from methyl esters of ricinoleic, linoleic and undecenoic acid. The so-formed monomers were characterized by means of GC, FT-IR and NMR spectroscopies. The higher reactivity of these precursors was confirmed in polycondensation. To prevent gelation and thus synthesize soluble polyesters of hyperbranched architecture, special efforts were made to optimize the reaction conditions by varying parameters like the reaction time, the temperature, the loading in catalyst, and even investigating other types of catalysts such as enzymes. Insights into the structure of the corresponding sulfur-containing HBPEs were provided by SEC and NMR spectroscopy. Their thermal stability and thermo-mechanical properties were also evaluated by TGA and DSC analyses.

1. Thiol-ene addition for the synthesis of vegetable oil-based AB_2-type precursors

In order to prepare more reactive fatty acid-based precursors of HBPEs, the synthesis of five new hydroxyester monomers was investigated by means of thiol-ene and metathesis reactions (Scheme 0-1). Classified as a click chemistry reaction, the thiol-ene addition has

emerged as an outstanding tool in polymer synthesis in general,[1,2] and in particular in the functionalization of FAMEs. [3–6] Interestingly, thiol-ene reaction can be achieved in a single step instead of two *via* the acid hydrolysis of epoxidized vegetable oils, simple to execute and generally gives high yields. The reaction proceeds by addition of a functional thiol onto a double bond, most often *via* a free radical mechanism that can be thermally or photo-initiated. The thiol-ene coupling is a versatile technique that can introduce both ester and primary alcohols. Thiol-ene click reaction has already been widely studied for the synthesis of oily-derived thermoplastics and thermosets.[3–9] Only Meier and Li's groups reported its use for the preparation of HBPE precursors of AB_2-type, as highlighted in Chapter I.[10,11]

In this study, three monomers of AB_2 and A_2B-type were prepared by the direct thiol-ene addition of both 2-mercaptoethanol and methyl thioglycolate onto methyl esters of ricinoleic (M2H-Ric and DMH-Ric) and linoleic acid (M2H-Lin). The methyl 10-undecenoate and 10-undecen-1-ol were selected for the preparation of DMH-Und (A_2B) and M2H-Und (AB_2) in two steps, due to the presence of terminal double bonds that were expected to undergo efficient metathesis dimerization (A_2 and B_2) and subsequent introduction of the antagonist function (B and A) through thiol-ene coupling. The chemical structure of the so-formed precursors was assessed by GC, FT-IR and NMR spectroscopies.

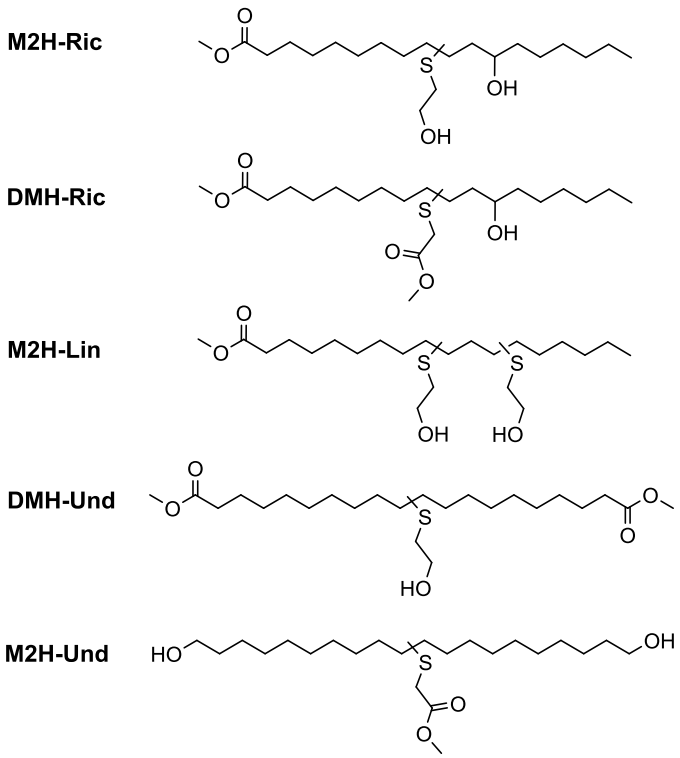

Scheme 0-1. Platform of AB_2 and A_2B monomers prepared by thiol-ene/metathesis coupling reactions

1.1. Direct functionalization of fatty acid derivatives via thiol-ene addition

Castor oil represents a very interesting substrate. Indeed, due to the presence of one toxic protein in its structure, *i.e.* the ricin, it is the only non-edible oil studied in the course of this thesis. Therefore, the use of castor oil as renewable resource for the production of bio-based polymeric materials does not directly compete with the food and feed industry. Moreover, castor oil contains up to 90% of ricinoleic acid, one mono-unsaturated FA with 18 carbon atoms and one hydroxyl group.[12] This naturally occurring AB-type synthon was converted, in this work, into either an AB_2 or an A_2B-type monomer *via* the thiol-ene addition of 2-mercaptoethanol and methyl thioglycolate, respectively (Scheme 0-2).

Thiol-ene additions were carried out in absence of any solvent, all reagents being liquid at room temperature, using an excess of thiols (3 equivalents/double bonds) according to previous literature.[13] Reactions were performed by photo-chemical initiation based on two different devices. Small scale experiments were run with a simple UV lamp (6 W). As illustrated in Figure 0-1, the addition of 2-mercaptoethanol proceeded very slowly in the absence of photo-initiator. Prolonged reaction time, over 24 hours, was required to achieve complete conversion, even operating at a short wavelength of 254 nm, *i.e.* high irradiance.

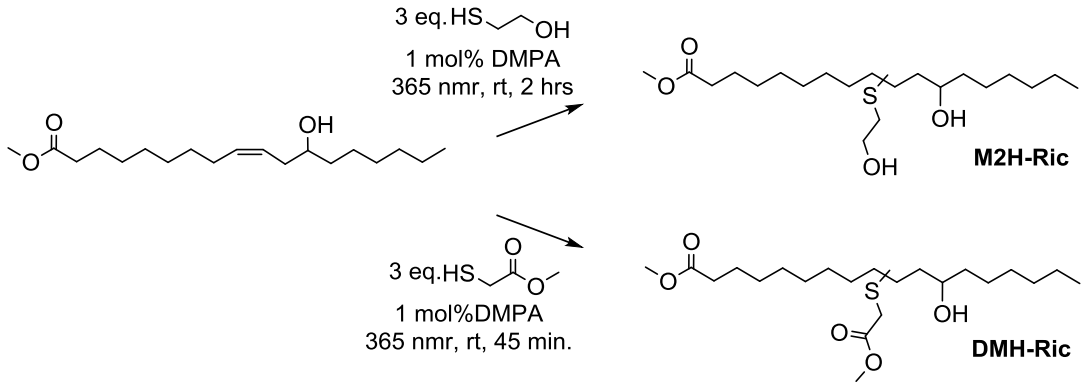

Scheme 0-2. Synthetic pathways to M2H-Ric and DMH-Ric *via* the thiol-ene addition of 2-mercaptoethanol and methyl thioglycolate onto methyl ricinoleate

The use of 2,2-dimethoxy-2-phenylacetophenone (DMPA) as photo-initiator, at a wavelength of 365 nm, was found to be very efficient in terms of reaction duration. Full conversions were indeed reached in less than 2 hours, with concentrations as low as 1 mol%. The thiol-ene addition of methyl thioglycolate was even faster. Under the same conditions, 45 minute reaction time was enough to obtain quantitative conversion.

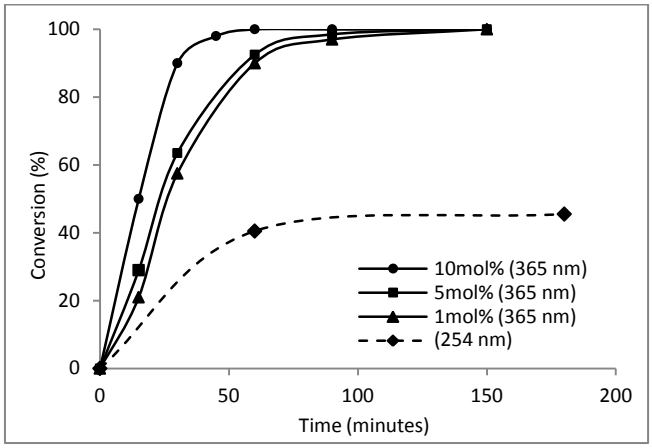

Figure 0-1. Kinetics of the addition of 2-mercaptoethanol onto methyl ricinoleate on 0.5 g scale: influence of the loading in DMPA used as photo-initiator

Large scale reactions were then run in a different set up to maximize the radiation exposure of the reaction mixture, using a high power (450 W) UV reactor equipped with a source mediated 225-365 nm. While prolonged reaction times were needed, up to 3 and 6 hours, with methyl thioglycolate and 2-mercaptoethanol, respectively, to achieve full conversions under the UV lamp (6 W), 15 minutes were enough to obtain M2H-Ric and DMH-Ric in quantitative yields on a 10 g scale in the UV reactor. Attention should however be paid to the residence time of the reaction mixture within this device. Prolonged exposures (over 24 hours) indeed appeared to favor the occurrence of side reactions, as evidenced by the appearance of numerous additional signals in ^{1}H NMR spectroscopy. Though, these undesired reactions were not identified up to date.

Another AB_2-type monomer bearing two primary alcohols as reactive functions was prepared, similarly to M2H-Ric starting from methyl ester of linoleic acid (Scheme 0-3). This polyunsaturated FAME features a 18-carbon atom chain with two *cis* double bonds (18:2). The synthesis of M2H-Lin was directly performed in the UV reactor, using 6 equivalents of 2-mercaptoethanol (3 equivalents/double bonds). In the absence of photo-initiator and solvent, complete conversion was achieved within 20 hours.

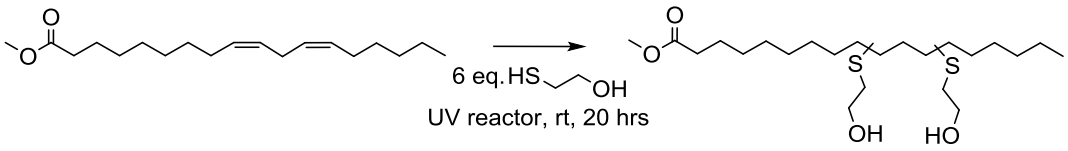

Scheme 0-3. Synthetic pathway to M2H-Lin *via* the thiol-ene addition of 2-mercaptoethanol onto methyl linoleate

In any cases, the reactions were monitored by ^{1}H NMR spectroscopy until complete disappearance of the signals characteristic of the double bond protons. Unreacted 2-mercaptoethanol was removed by washing the reaction mixtures with water, while the excess of methyl thioglycolate was vacuum distilled. A flash chromatography based on a mixture of cyclohexane/ethyl acetate enabled to get rid of the DMPA when required.

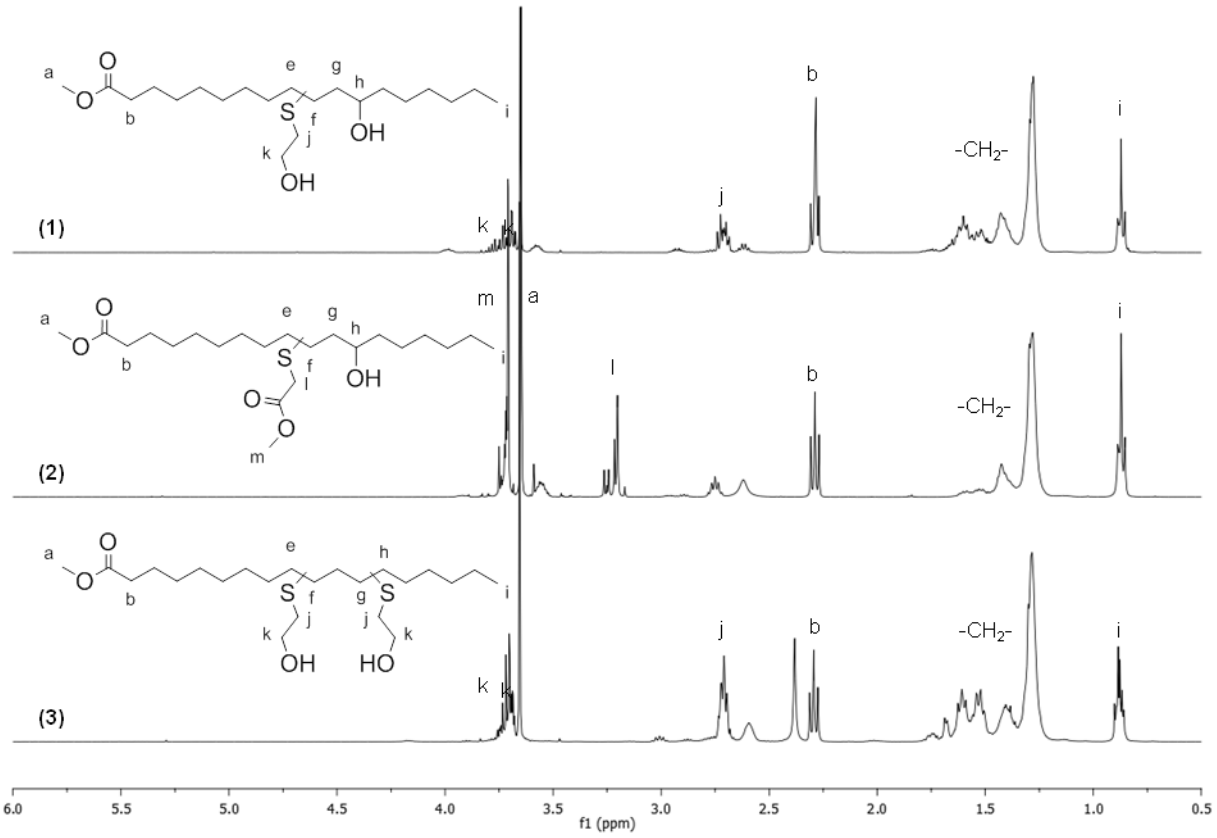

Figure 0-2. Stacked ^{1}H NMR spectra of (1) M2H-Ric, (2) DMH-Ric and (3) M2H-Lin in $CDCl_3$

Stacked ^{1}H NMR spectra of M2H-Ric, DMH-Ric and M2H-Lin are given in Figure 0-2. The presence of protons H_j, H_k and H_l, H_m confirms the incorporation of 2-mercaptoethanol and methyl thioglycolate, respectively. Due to the non regioselectivity of the thiol-ene addition onto internal double bonds, complex product mixtures were obtained. 2D NMR techniques were thus required to fully assign all peaks of ^{1}H NMR spectra as shown in Figure 0-3 for M2H-Ric. In this particular case, the presence of chiral centers in the starting material, involves the formation of 4 different diastereoisomers that do not necessarily display equivalent chemical shifts. This explains why signals f_2 and h_2 appeared duplicated. Detail assignments of DMH-Ric and M2H-Lin are depicted in Figure 0-4 and Figure 0-5, respectively. As for M2H-Lin, the three possible regioisomers, *i.e.* (1) addition in f and g, (2) f and h, or (3) e and h positions of the conjugated double bonds, were distinguished.

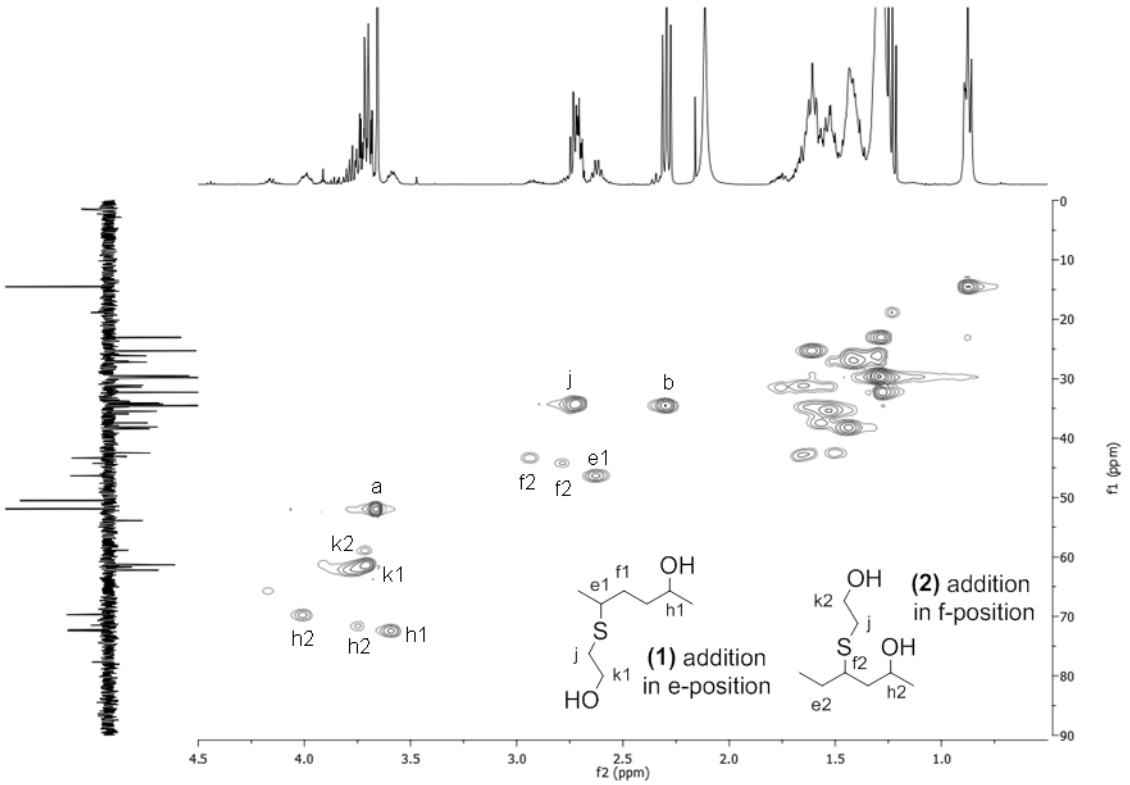

Figure 0-3. ^{1}H-^{13}C HSQC spectrum of M2H-Ric in $CDCl_3$

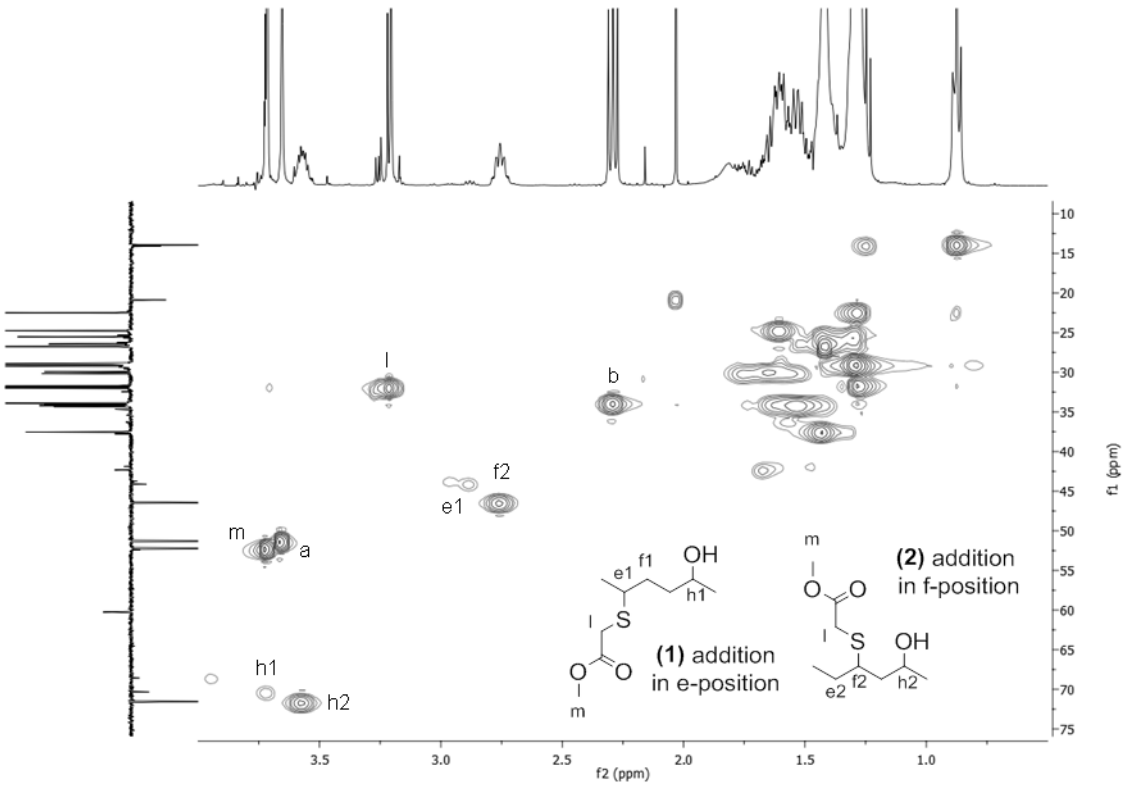

Figure 0-4. ^{1}H-^{13}C HSQC spectrum of DMH-Ric in $CDCl_3$

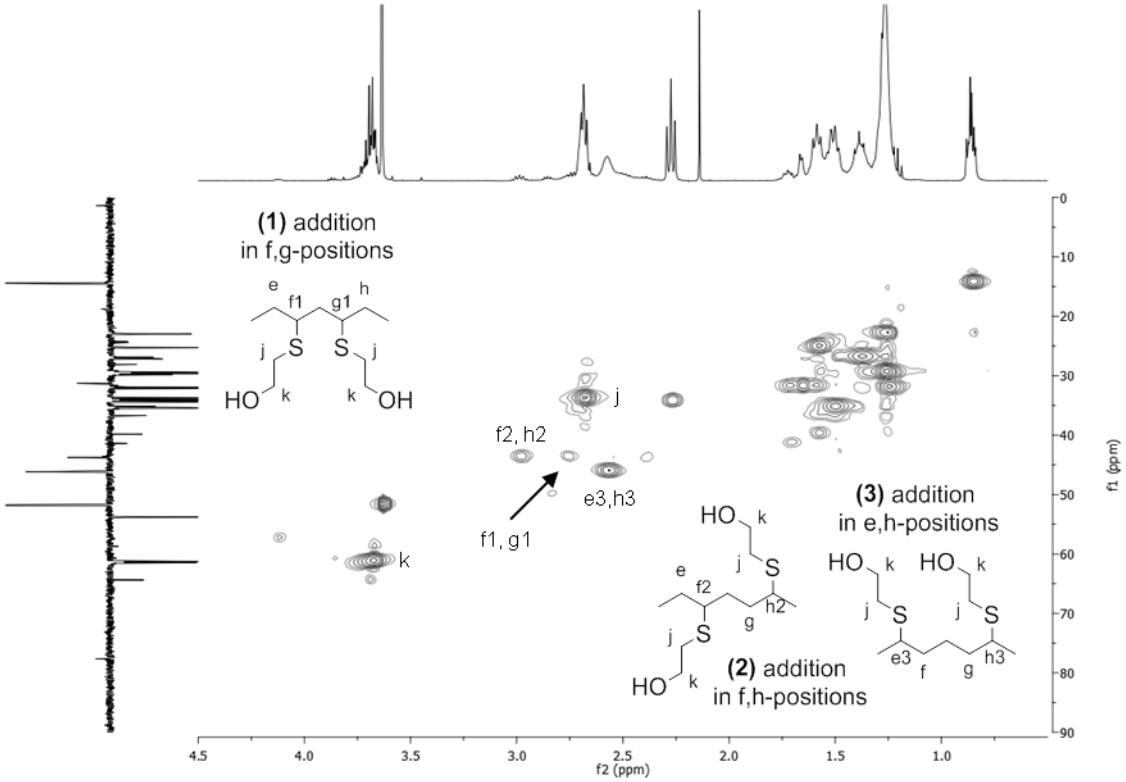

Figure 0-5. ^{1}H-^{13}C HSQC spectrum of M2H-Lin in $CDCl_3$

FT-IR spectra of both AB_2 and A_2B-type monomers were in accordance with their chemical structure as shown in Figure 0-6. Characteristic absorption bands of the hydroxyl and ester functions, were observed at 3 400 and 1 740 cm^{-1}, respectively, along with another band at 724 cm^{-1} specific of C-S stretching bonds.

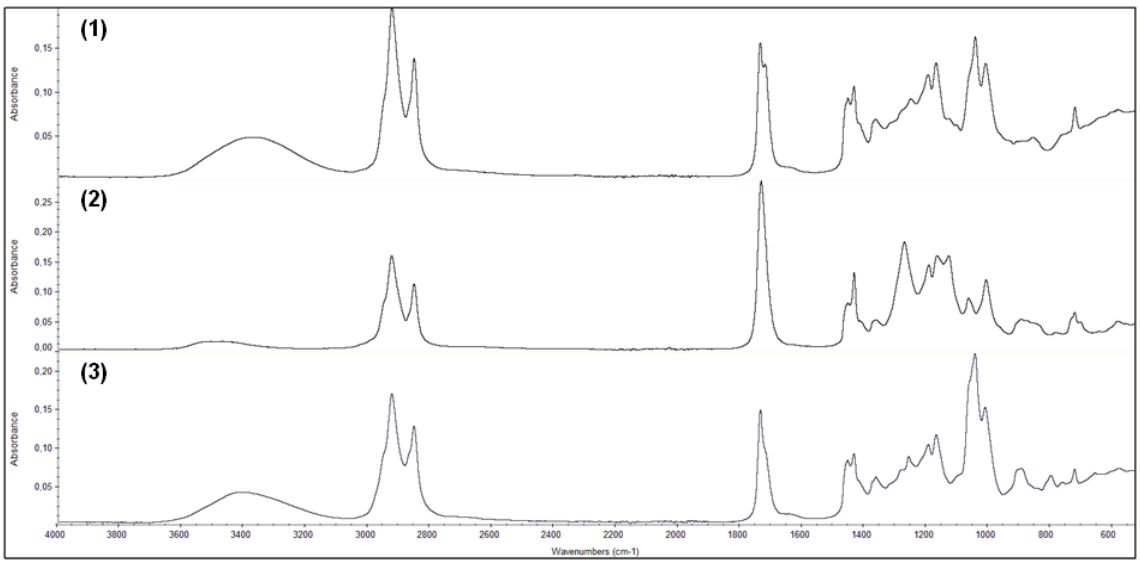

Figure 0-6. Stacked FT-IR spectra of (1) M2H-Ric, (2) DMH-Ric and (3) M2H-Lin

M2H-Ric, DMH-Ric and M2H-Lin were obtained as colorless viscous liquids in high yields (90%). Their chemical grade was confirmed by GC analyses over 96%, except for M2H-Lin whose purity was questioned. Several non-identified species were indeed detected in the corresponding chromatogram (Figure 0-7).

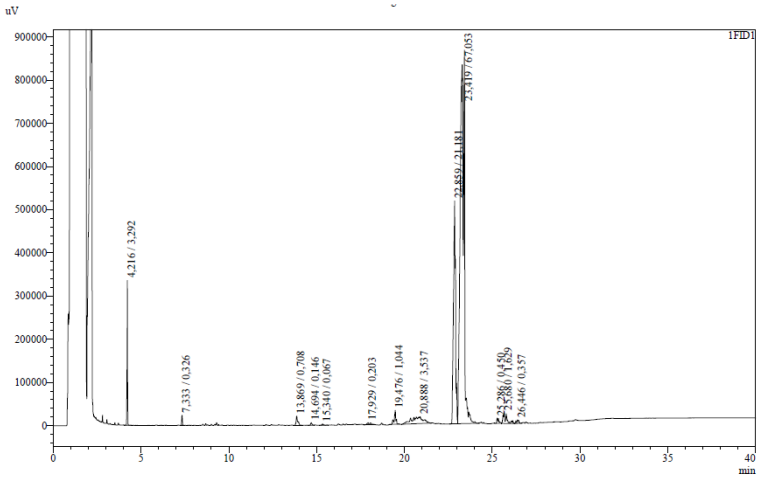

Figure 0-7. Gas chromatogram of M2H-Lin

The multimodal distribution centered at a retention time of 23 minutes, accounting for 88.2%, was assigned to the different regioisomers of M2H-Lin (addition in e and f, or e and g, or e and h positions of the conjugated double bonds). The heavier species which appeared at higher retention times (2.44%) could be attributed to potential Diels-Alder coupling reactions. UV irradiations might indeed catalyze isomerization of methyl linoleate double bonds resulting in conjugated systems. Some of the lower molar masses were suspected to be due to oxidation reactions since thiol-ene additions were not performed under inert atmosphere. The so-formed ketones might undergo photochemical cleavage, *i.e.* Norrish reactions. Even if the purity grade of this synthon was questionable, M2H-Lin was still subjected to polycondensation reaction. Results obtained were interpreted with caution in the light of all these elements.

1.2. Thiol-ene reaction on metathesis product

Since its first development in 1950s, olefin metathesis has shown a constant development especially thanks to the discovery of the reaction mechanism by Chauvin and coworkers in 1971, and the emergence of efficient and tolerant metathesis catalysts by the group of Schrock and Grubbs in the 1990s.[14–18] Since then, a multitude of chemical transformations were developed including self-metathesis, cross-metathesis, ring-closing and ring-opening metathesis, giving access to a variety of novel monomers.[19–21] Metathesis was even applied to polymerization methods such as ring-opening polymerization metathesis and acyclic diene metathesis polymerization.[22,23]

In this work, self-metathesis was used as a means to prepare two multifunctional precursors of A_2B and AB_2-type with even less sterically hindered reactive functions. Were used as raw materials, methyl 10-undecenoate and 10-undecen-1-ol, some castor oil derivatives possessing 11 carbon atoms and one terminal unsaturation. As indicated in Scheme 0-4, the synthetic pathway involved two steps. First, a diester (or diol) was produced by self-metathesis of the FA derivatives. The antagonist alcohol function (or ester) was then introduced by thiol-ene addition of 2-mercaptoethanol (or methyl thioglycolate) onto the internal unsaturations of the dimerized intermediates.

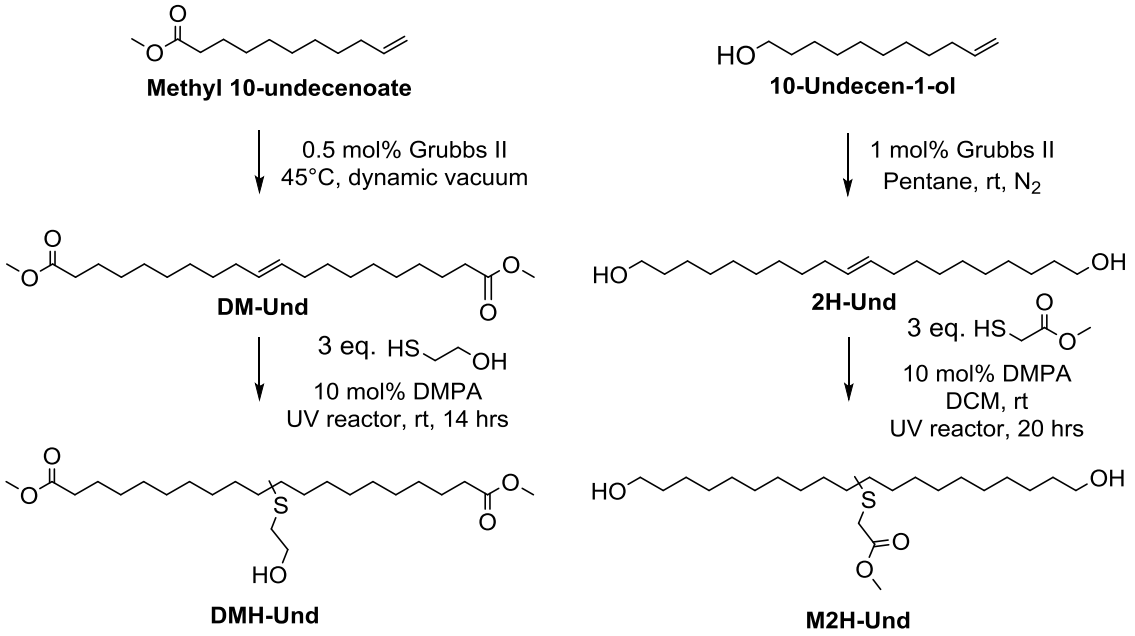

Scheme 0-4. Synthetic pathways to DMH-Und and M2H-Und starting from methyl 10-undecenoate and 10-undecen-1-ol

1.2.1. Metathesis reaction

The limiting step of this synthetic pathway is unquestionably the metathesis reaction. Although long-chain α,ω-dicarboxylic acids were successfully synthesized using ruthenium-based catalysts,[20] conversions reported were generally low mainly because these reactions are subjected to a thermodynamic equilibrium. Besides, the removal of the Grubbs second generation catalyst resulted in significant product losses.

The yield of the 10-undecen-1-ol self-metathesis is particularly low, only 44%. This reaction was performed using the Grubbs II metathesis catalyst, with a loading of 1 mol% in dried pentane at room temperature during 48 hours. As the reaction proceeded, the diol got precipitated out of the solution, which shifted the reaction equilibrium towards the formation of the A_2 intermediate. After 48 hours under nitrogen atmosphere, the conversion reached 96%. The obtained diol (2H-Und) was recovered by filtration and purified twice by recrystallization in cold pentane. This last step would need to be further optimized.

The self-metathesis of methyl 10-undecenoate resulted in higher yield of diesters (66%). This reaction was carried out in bulk using 0.5 mol% of Grubbs II metathesis catalyst according to previous literature.[24] Dynamic vacuum was applied to remove ethylene by-product thereby shifting the equilibrium towards the formation of the B_2 intermediate (DM-Und). Complete conversion was achieved within 40 hours. DM-Und was then purified by column chromatography using a mixture of cyclohexane and ethyl acetate as eluent.

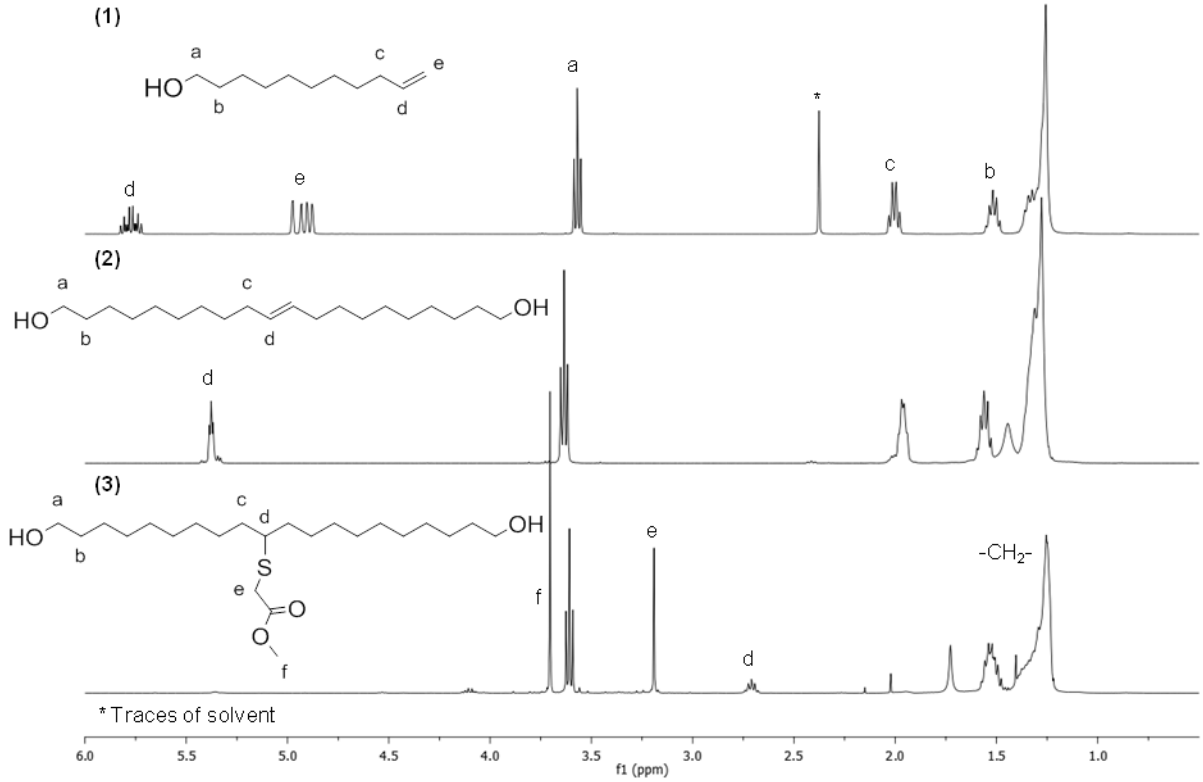

Figure 0-8. Stacked ^{1}H NMR spectra of (1) 10-undecen-1-ol, (2) 2H-Und and (3) M2H-Und

The formation of the diesters and diols was monitored in ^{1}H NMR spectroscopy by the disappearance of the signals characteristics of the terminal double bonds at 5.81-5.74 and 5.00-4.90 ppm, along with the appearance of a multiplet at 5.38 ppm due to the symmetrical character of the central double bonds (Figure 0-8 and Figure 0-10). Both dimerized products were obtained as white powders and characterized by GC analyses.

Despite the quite low reaction temperature (rt to 45°C), isomerization side reactions were detected, as illustrated in Figure 0-9 with 2H-Und intermediate. Products actually obtained resulted from the cross-metathesis reactions of various positional isomers of the double bonds. Preventing isomerization side reactions was not particularly wanted. Nevertheless, it was important to know at that stage, that we were not dealing with intermediates of well-defined structure, but rather with a mixture of unsaturated diesters and diols of various chain lengths.

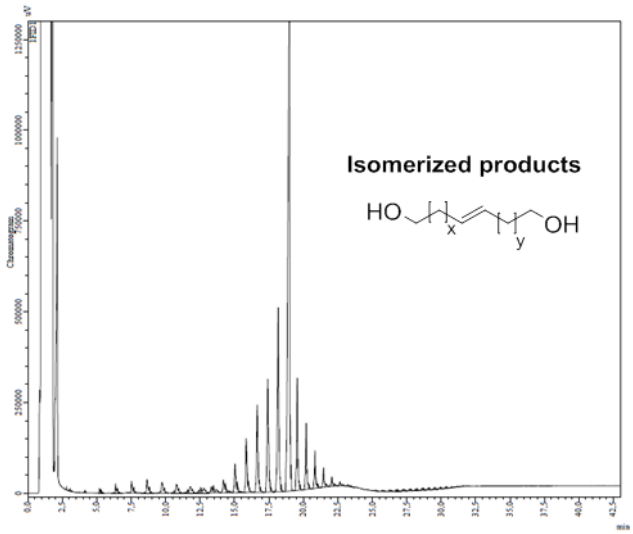

Figure 0-9. Gas chromatogram of 2H-Und, product of 10-undecen-1-ol self-metathesis

Isomerization side reactions were extensively studied in the literature. This phenomenon creates irregularity in the polymer structure, altering in some cases its physical properties. Various methods were thus investigated to prevent these undesired side reactions. Different parameters such as the reaction time and temperature, as well as the nature of the metathesis catalyst (1st or 2nd generation), were shown to limit double bond isomerization. The addition of tetrachloro-1,4-benzoquinone was even found to suppress this side reaction.[25–27]

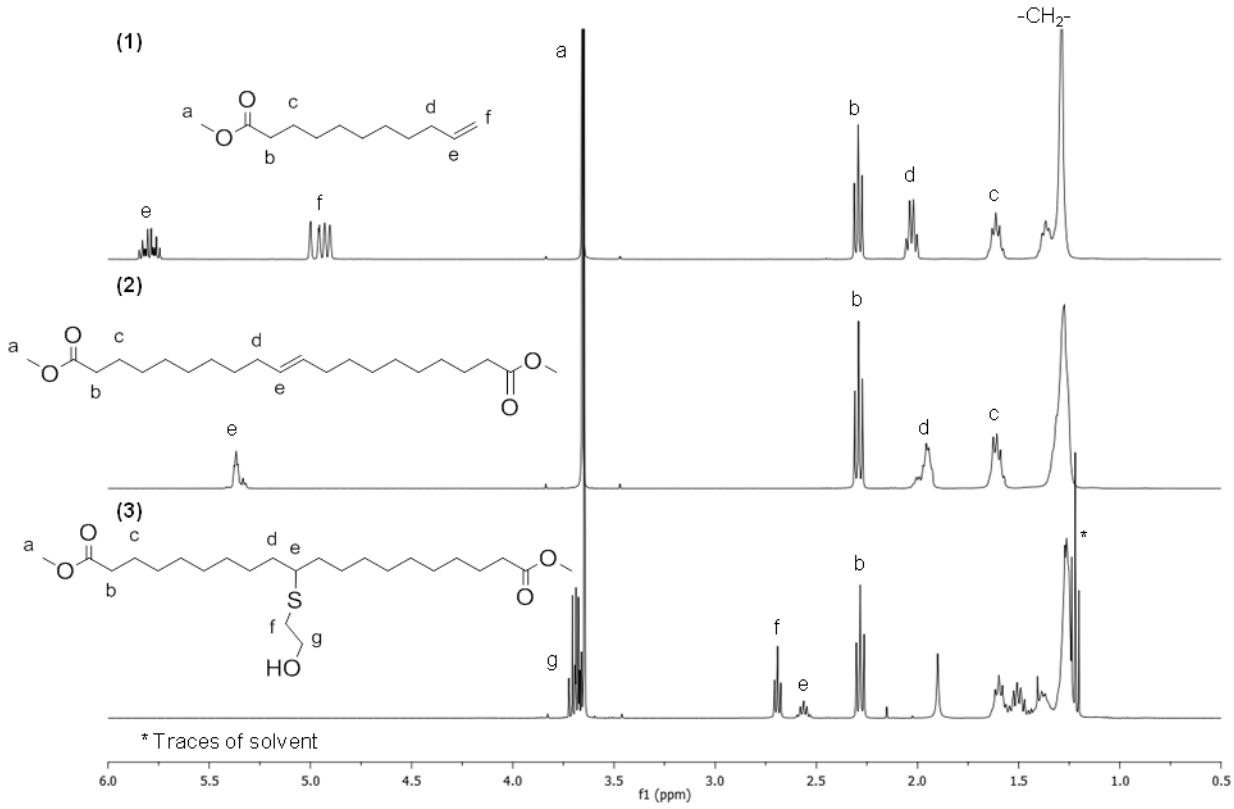

Figure 0-10. Stacked ^{1}H NMR spectra of (1) methyl 10-undecenoate, (2) DM-Und and (3) DMH-Und

3.2.4. Thiol-ene addition

Multifunctional precursors DMH-Und and M2H-Und were formed by thiol-ene reactions with 2-mercaptoethanol and methyl thioglycolate, respectively. These additions were carried out in solution of DCM, both intermediates being solid at room temperature, with an excess of thiols (3equivalents/double bonds). The thiol-ene reactions were performed within the UV reactor (lamp mediated 225-365 nm) using DMPA as photo-initiator with a relatively high loading of 10 mol% to limit the residence time of the reaction mixtures within the reactor. After work-up (see Experimental and Supporting Information), both A_2B and AB_2-type monomers were obtained in high yields (90-95%), as viscous materials, more or less colored (yellow to brown shades depending on the residual traces of Grubbs II catalyst).

Due to their 'symmetric' structure, M2H-Und and DMH-Und were successfully characterized by ^{1}H NMR spectroscopy (Figure 0-8 and Figure 0-10). Both reactions were monitored by the disappearance of the internal double bond signals at 5.38 ppm. After addition of methyl thioglycolate, protons H_d of the FA backbone displayed lower field signals, at 2.71 ppm. The same phenomenon was observed with 2-mercaptoethanol, protons H_e being identified at 2.56 ppm. The introduction of methyl thioglycolate was confirmed by the appearance of two singlets at 3.70 and 3.19 ppm, respectively, attributed to the methoxy group and the methylene protons in between the ester and the sulfur atom. Signals assigned to 2-mercaptoethanol were observed at 3.70-3.65 ppm (m, CH_2) and 2.69 ppm (t, CH_2).

These two monomers were also characterized by GC analyses (see Figure SI 0-1 for DMH-Und). However, this technique did not allow us to determine their purity grade due to the occurrence of isomerization side reactions.

In summary, five new multifunctional precursors of HBPEs were successfully synthesized starting from methyl esters of ricinoleic, linoleic and undecenoic acid. For that purpose, thiol-ene addition was applied in order to introduce both reactive primary alcohols and ester groups. Interestingly, in this latter case, polycondensation of the so-formed A_2B-type monomers will result in the formation of methyl ester-terminated HBPEs, as opposed to the hydroxyl-ended polymers developed up to date. In addition, metathesis coupling reactions were carried out with the idea of driving apart the reactive functions, thereby minimizing steric hindrance during polymerization reactions. In the next section, the influence of the precursor structure on its reactivity in polycondensation, and the properties of the related HBPEs is discussed.

2. Synthesis of sulfur-containing Hyperbranched Polyesters

The five well-defined A_2B and AB_2-type monomers were used as building blocks for the synthesis of novel HBPEs. In the first instance, M2H-Ric was used as a sulfur-containing monomer model and its polymerization behavior was examined in detail. A close study of the influence of the reaction conditions was performed as a means to tune the branching density and macromolecular characteristics of the related HBPEs. Therefore, the reactivity of the four other monomers of the platform was studied in polycondensation. Insights into the macromolecular characteristics and structural composition of the related HBPEs were obtained by SEC and NMR spectroscopy. Optimizations of the reaction conditions were performed on a case-by-case basis.

2.1. Study of M2H-Ric polycondensation

2.1.1. Preliminary results and chemical structure

Polymerization tests of M2H-Ric were first performed following the procedure optimized in Chapter II regarding the transesterification reaction of M2HS (Scheme 0-5). All syntheses were carried out in bulk using catalysts with a loading of 1.5% relative to monomer weight. After a pre-drying of the monomer alone at 90°C to remove any traces of solvent and especially water, the temperature was raised to 120°C and a catalyst was added. The mixture was therefore allowed to react during two hours under nitrogen blowing. In a final stage, the temperature was further increased to 160°C and dynamic vacuum was applied. The reactions were quenched as soon as the viscosity suddenly increased.

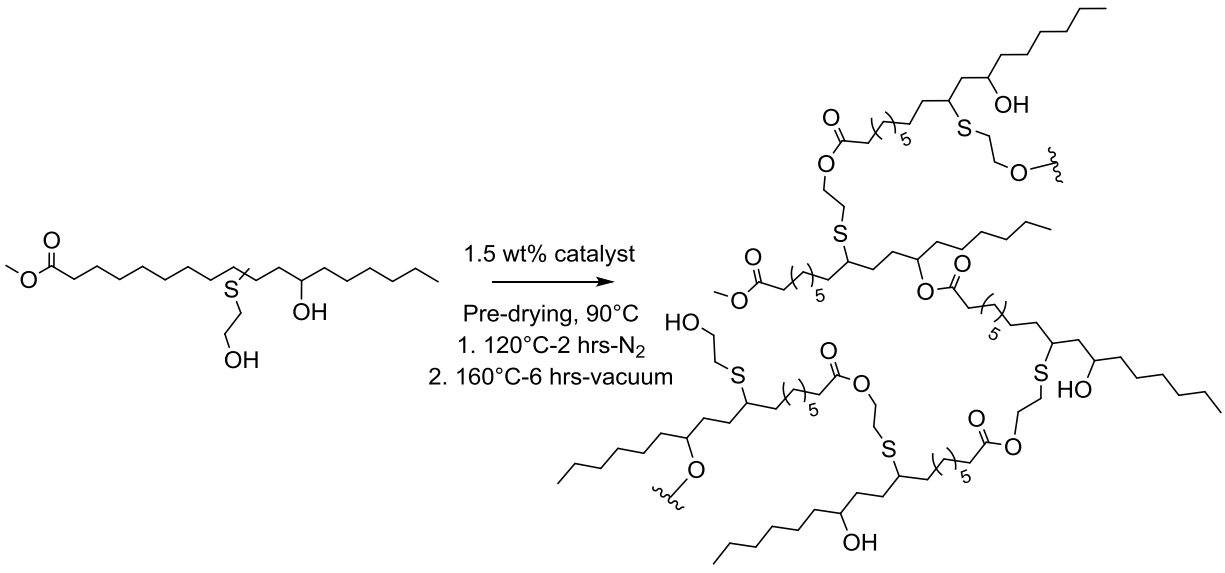

Scheme 0-5. HBPE synthesis from M2H-Ric

A quick comparison of the results obtained with M2HS and M2H-Ric was sufficient to demonstrate the higher reactivity brought by a single primary alcohol (Table 0-I). Full conversions were indeed achieved within 8 hours (instead of 15 hours with M2HS), and HBPEs with molar masses twice higher, from 7 000 to 10 000 $g.mol^{-1}$, were formed whatever the catalyst of polymerization employed. Broader dispersities were observed ($Đ$ = 4.06-4.22).

Table 0-I. Macromolecular characteristics of HBPEs obtained by polycondensation of M2H-Ric: comparison with M2HS

Entry	Monomer	Catalyst	Time (hours)	x^1 (%)	$\bar{M}_n{}^1$ ($g.mol^{-1}$)	$\bar{M}_w{}^1$ ($g.mol^{-1}$)	$Đ^1$
P1	M2HS	$Zn(OAc)_2$	15	98	3 500	9 500	2.71
P2		TBD	15	100	4 100	10 100	2.46
P3		NaOMe	15	100	6 100	18 800	3.08
P4	M2H-Ric	$Zn(OAc)_2$	8	99	10 000	41 900	4.19
P5		TBD	8	100	9 300	37 800	4.06
P6		NaOMe	8	100	7 100	30 000	4.22

(1) determined by SEC in THF – calibration PS standards.

The progress of the polymerization was monitored in ^1H NMR spectroscopy by the disappearance of the methoxy group at 3.66 ppm. In comparison with the ^1H NMR spectrum of M2H-Ric, and based on additional 2D NMR analyses (see Figure SI 0-3), the chemical structure of these HBPEs was elucidated. ^1H NMR spectrum of P5 is illustrated as an example in Figure 0-11. After the formation of ester linkages, methylene protons k_p and h_p adjacent to the primary and secondary alcohols, displayed downfield signals at 4.18 and 4.86 ppm, respectively.

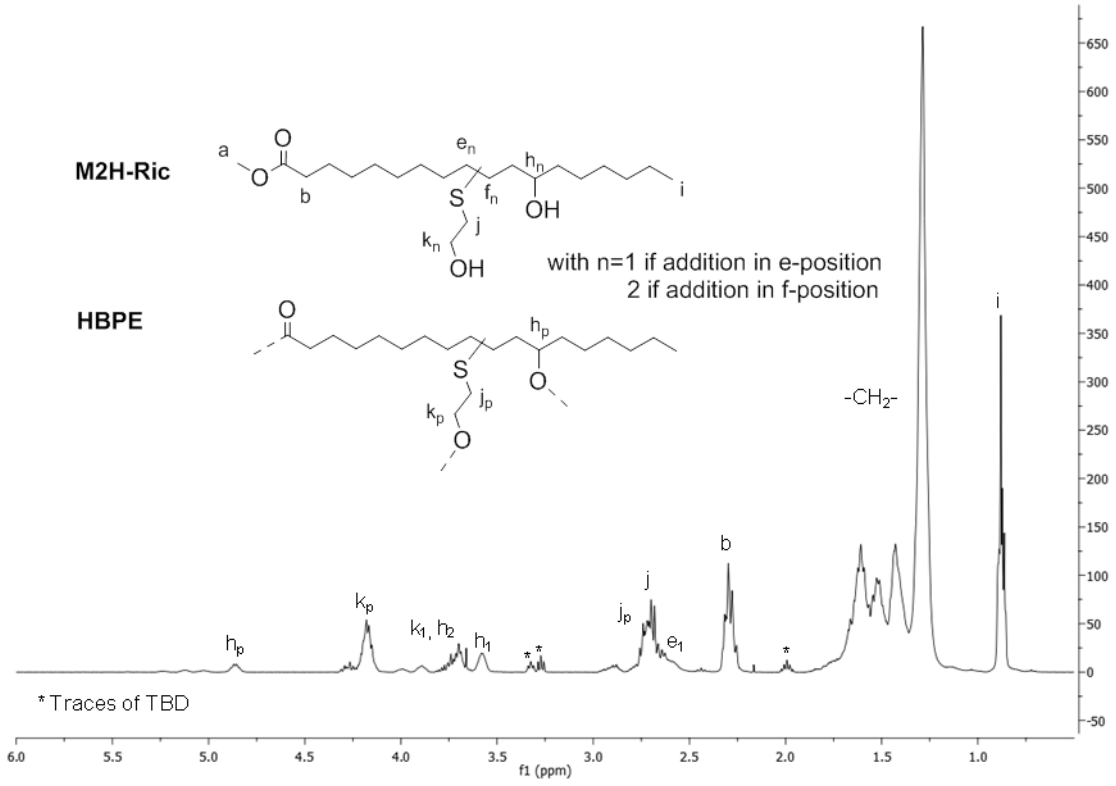

Figure 0-11. ^1H NMR spectrum of P5 obtained by polycondensation of M2H-Ric in $CDCl_3$

Similarly to MA (Chapter III), the structure of M2H-Ric does not allow the determination of the DB of its related HBPEs by NMR spectroscopy, its two hydroxyl functions being too far from each other. This technique was however used to assess the reactivity ratio between primary and secondary alcohols (*r*) based on the relative integrations of protons k_p and h_p. Values obtained, *i.e.* 7.13 for P4, 1.25 for P5 and 5.18 for P6, varied depending on the catalyst of polymerization employed. Once again TBD was found to favor the formation of the most branched architecture (P5), while $Zn(OAc)_2$ and NaOMe yielded HBPEs with a rather linear structure.

M2H-Ric-derived HBPEs were also characterized by FT-IR analyses (see Figure SI 0-2). Typical ester carbonyl and hydroxyl stretching vibrations were clearly detected at 1 732 and 3 428 cm^{-1}, respectively, and one absorption band characteristic of thio-ether linkages (C-S) could still be observed at 724 cm^{-1}.

2.1.2. Experimental condition screening

Further investigations of the reaction conditions were performed in order to 'test the limits' of this system. The influence of key parameters including the polymerization temperature, the nature and loading in catalyst, was studied onto the reactivity ratio of primary and secondary alcohols (*r*). Results of this screening are summarized in Table 0-II.

Table 0-II. Polycondensation of M2H-Ric: experimental condition screening and macromolecular characteristics of the related HBPEs

Entry	T_2(°C)[1]	Catalyst	Time (hours)	x^2 (%)	$\bar{M}_n$ [2] (g.mol^{-1})	$\bar{M}_w$ [2] (g.mol^{-1})	$Đ^2$	r^3
P7	140	TBD	45	100	6 050	18 300	3.03	5.25
P8	150	TBD	22	100	10 400	52 700	5.07	1.79
P5	160	TBD	8	100	9 300	37 800	4.06	1.25
P9[4]	160	TBD	8	100	10 000	50 900	5.09	2.67
P10[5]	160	TBD	15	100	7 900	30 800	3.90	3.45
P11	160	*m*-TBD	8	46	1 250	1 300	1.04	nd.
P12	160	Sb_2O_3	8	34	1 200	1 300	1.08	17
P13	160	DBTO	8	97	5 300	16 600	3.13	1.37
P14	160	$Sn(Oct)_2$	8	99	5 900	23 100	3.92	9.69
P15	160	$Ti(OiPr)_4$	8	74	1 600	1 900	1.19	11.8
P16	160	$Ti(OBu)_4$	Gelation					
P17[5]	140	$Ti(OBu)_4$	4	100	9 900	113 550	>11.5	8.78
P18[5]	120	$Ti(OBu)_4$	4	98.7	5 900	22 000	3.73	9.88

(1) Temperature of the 2nd stage of polymerization. (2) determined by SEC in THF – calibration PS standards. (3) determined by ^{1}H NMR spectroscopy based on the ratio $\frac{k_p}{2\,h_p}$. (4) 5 g scale, instead of 0.5 g. (5) Loading in catalyst of 1 wt%.

Polycondensations of M2H-Ric were attempted at lower temperatures (T_2) of 140 (P7) and 150°C (P8), while maintaining the temperature of oligomerization (T_1) at 120°C. This series of experiments was conducted using TBD as catalyst. As expected, decreasing the temperature T_2 was found to slow down the kinetics of polymerization. Almost one day (22 hours) was required to reach full conversion at 150°C, while 45 hours were needed at 140°C. P8 gave higher molar masses, above 10 000 $g.mol^{-1}$, and broader dispersity than P7, while retaining a hyperbranched architecture (r = 1.79). Further decrease in the reaction temperature, however, favored the formation of a more linear structure (r = 5.25). Scaling-up the polycondensation reaction (5 g, P9), as well as decreasing the loading in TBD (1 wt%, P10), also enabled to tune the branching density of these HBPEs as stated by the raised reactivity ratios of 2.67 and 3.45, respectively (Table 0-IV).

The activity of other catalysts including *m*-TBD, antimony trioxide (Sb_2O_3), dibutyltin(IV) oxide (DBTO), stannous octoate ($Sn(Oct)_2$), titanium(IV) butoxide ($Ti(OBu)_4$) and isopropoxide ($Ti(OiPr)_4$), was examined. Within 8 hours at 160°C, only tin-based catalysts gave interesting results. P13 and P14 indeed exhibited molar masses in between 5 000 and 7 000 $g.mol^{-1}$ and almost full conversions ($x \geq 97\%$). Interestingly, one should notice that while DBTO actually yielded HBPEs (r = 1.37), $Sn(Oct)_2$ favored the formation of rather linear polyesters (r = 5.18-9.69).

In these screening conditions, $Ti(OBu)_4$ showed such efficiency to catalyze M2H-Ric polycondensation that gel-like materials were obtained within 2 hours (P16). Decreasing the reaction time, temperature and loading in catalyst was thus required to achieve soluble fractions of HBPEs (P17, P18) of molar masses in the range 6 000-10 000 $g.mol^{-1}$. However, in these conditions, $Ti(OBu)_4$ was found to generate polymers with a rather linear structure (r = 8.78-9.88).

To sum up, apart from its higher reactivity in comparison to M2HS, M2H-Ric proved to be a versatile precursor with its two hydroxyl functions of unequal reactivity, making it an ABB' monomer. The branching density of the corresponding HBPEs could thus be simply tuned by adjusting the reaction conditions, *e.g.* T_2(°C), t (hours), loading in catalyst. The choice of the catalyst was also shown to be crucial. While TBD or DBTO yielded polyesters of branched architecture ($r \leq 2$), $Zn(OAc)_2$, $Sn(Oct)_2$, $Ti(OBu)_4$ and NaOMe tended to form polymers exhibiting more linear structures (r = 5-10).

2.2. Structure-reactivity of sulfur-containing monomers

The polycondensation behavior of the four other A_2B and AB_2-type monomers was then investigated in detail. For that purpose, DMH-Ric, M2H-Lin, DMH-Und and M2H-Und were first polymerized under the same conditions than those used for M2H-Ric (Scheme 0-5). This series of experiments gave rise to two distinct scenarii. With its single secondary alcohol, DMH-Ric displayed a poor reactivity. As shown in Table 0-III, only oligomers of low molar masses from 1 500 to 2 500 g.mol^{-1}, were achieved irrespective of the catalyst employed (P19 and P20). Even after prolonging the reaction time up to 39 hours, conversions did not exceed 90%.

Table 0-III. Macromolecular characteristics of HBPEs obtained by polycondensation of DMH-Ric and M2H-Lin: comparison with M2H-Ric

Entry	Monomer	Catalyst	Time (hours)	x^1 (%)	$\bar{M}_n{}^1$ (g.mol^{-1})	$\bar{M}_w{}^1$ (g.mol^{-1})	$Đ^1$
P4	M2H-Ric	$Zn(OAc)_2$	8	99	10 000	41 900	4.19
P5		TBD	8	100	9 300	37 800	4.06
P19	DMH-Ric	$Zn(OAc)_2$	39	87	2 550	4 350	1.71
P20		TBD	39	91	1 550	1 900	1.23
P21[2]	M2H-Lin	$Zn(OAc)_2$	4	92	3 200	7 700	2.41
P22[2]		TBD	6	95	4 100	16 200	3.95

(1) Determined by SEC in THF – calibration PS standards. (2) Gelation within 8 hours.

In contrast, the presence of two primary alcohols provided M2H-Lin with a higher reactivity than M2H-Ric, so much that gel-like materials were achieved within 8 hours. Soluble fractions obtained before gelation, after 4 hours of polymerization with zinc acetate (P21) and 6 hours with TBD (P22), respectively, gave encouraging molar masses in between 3 000 and 4 000 g.mol^{-1}.

Lastly, DMH-Und and M2H-Und appeared as the most reactive precursors in this series, their polycondensation yielding cross-linked materials within the first two hours of oligomerization at 120°C. These results confirmed our strategy of attaching great importance to the nature and steric hindrance of the functional groups in order to design monomers of higher reactivity. The aim was therefore to ‘control’ their polymerization. Optimizations of the reaction conditions were performed on a case-by-case basis.

2.2.1. Polycondensation of DMH-Ric

The lower reactivity of DMH-Ric was eventually not surprising since this synthon bears only one secondary alcohol as reactive function. In order to actually form HBPEs of interesting molar masses, and not just oligomers, polycondensation of this A_2B-type monomer was attempted on a higher range of temperatures.

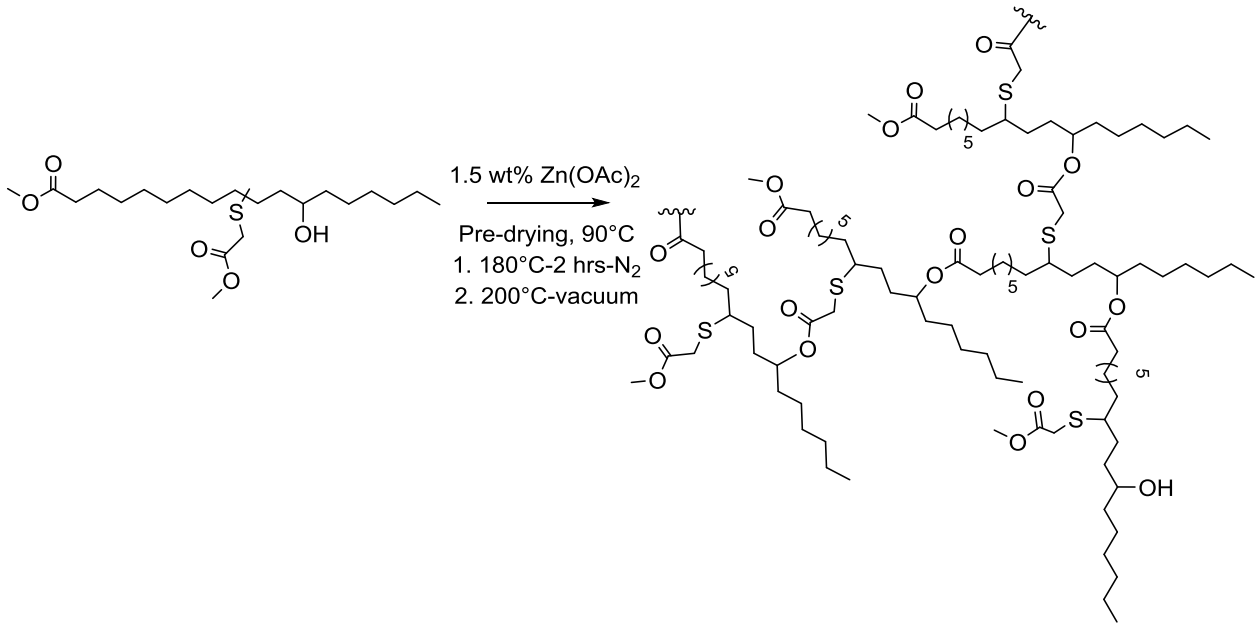

Scheme 0-6. HBPE synthesis from DMH-Und

As can be seen in Scheme 0-6, both temperatures of oligomerization (T_1) and polymerization (T_2) were raised to 180 and 200°C, respectively. TBD can sublime at such temperature, thereby reducing its catalytic activity. One metallic catalysis based on zinc acetate was thus preferred. The polymerization reaction was monitored by SEC (THF, PS calibration). Aliquots were directly taken out from the mixture and analyzed without further purification. The kinetics depicted in Figure 0-12 revealed that even if conversion reached 80% within 8 hours, molar masses did not exceed 2 000 $g.mol^{-1}$. Further increase in the reaction time did not show any improvement. To the contrary, a significant decrease in molar masses was noted after 25 hours suggesting the occurrence of undesired side reactions.

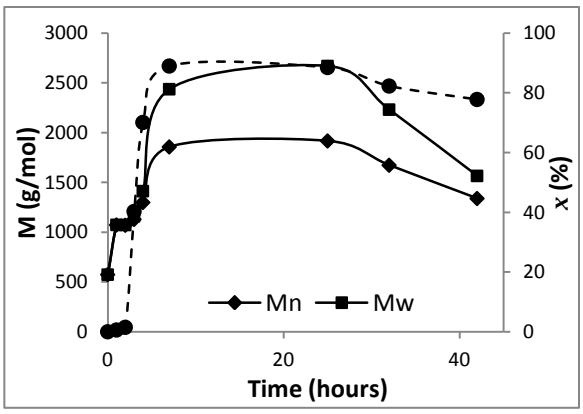

Figure 0-12. Kinetics of zinc acetate-catalyzed polycondensation of DMH-Ric (solid lines: $\bar{M}_n$, $\bar{M}_w$ and dashed line: conversion rate)

The FT-IR spectrum of a sample collected after 40 hours of reaction is presented in Figure 0-13. The broad absorption band characteristic of the O-H stretching could no longer be observed over 3 000 cm^{-1}, indicating that the side reactions in question, involved the focal point.

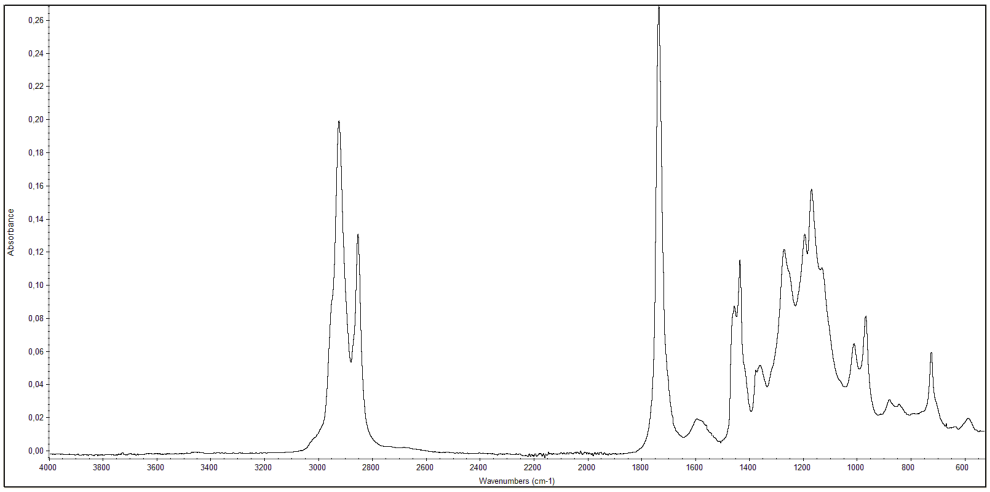

Figure 0-13. FT-IR spectrum of DMH-Ric derived HBPE after 40 hours of polymerization at 180/200°C

The reaction progress was monitored as well by ^{1}H NMR spectroscopy (Figure 0-14). After 8 hours (1), the formation of HBPEs was supported by the downfield signal of the proton h_p in α-position of the hydroxyl function. Similarly to ^{1}H NMR of DMH-Ric, two peaks were distinguished at 5.06 (h_2) and 4.86 (h_1) ppm, due to the non regioselectivity of the thiol-ene addition onto internal double bonds, *i.e.* substitution in e- or f-position.

In contrast, after 40 hours of reaction (2), the intensity of these signals significantly decreased and the appearance of several multiplets was noted at 5.45-5.31, 2.21-2.08 and 2.06-1.94 ppm. 2D NMR techniques were required to assign these peaks (see supporting information, Figure SI 0-4). ^{1}H-^{13}C HSQC analysis revealed that the multiplet (protons g_s and h_s) identified at 5.45-5.31 ppm was directly attached to carbon atoms with chemical shift of 131-129 ppm, attributable to carbon-carbon double bonds. Based on ^{1}H-^{1}H COSY experiment, the two other signals at 2.21-2.08 and 2.06-1.94 ppm were assigned to the methylene protons f_s and j_s adjacent to the unsaturations.

This result is in agreement with the previous investigations described in Chapter III by MALDI-TOF MS to better understand the gelation phenomenon. Dehydration also occurs as side reaction during the polycondensation of DMH-Ric, but due to the lower concentration in hydroxyl functions, it results in the major formation of alkenes instead of ether bridges. The trans-isomer is presented in Figure 0-14, since this conformation is the more thermodynamically stable.

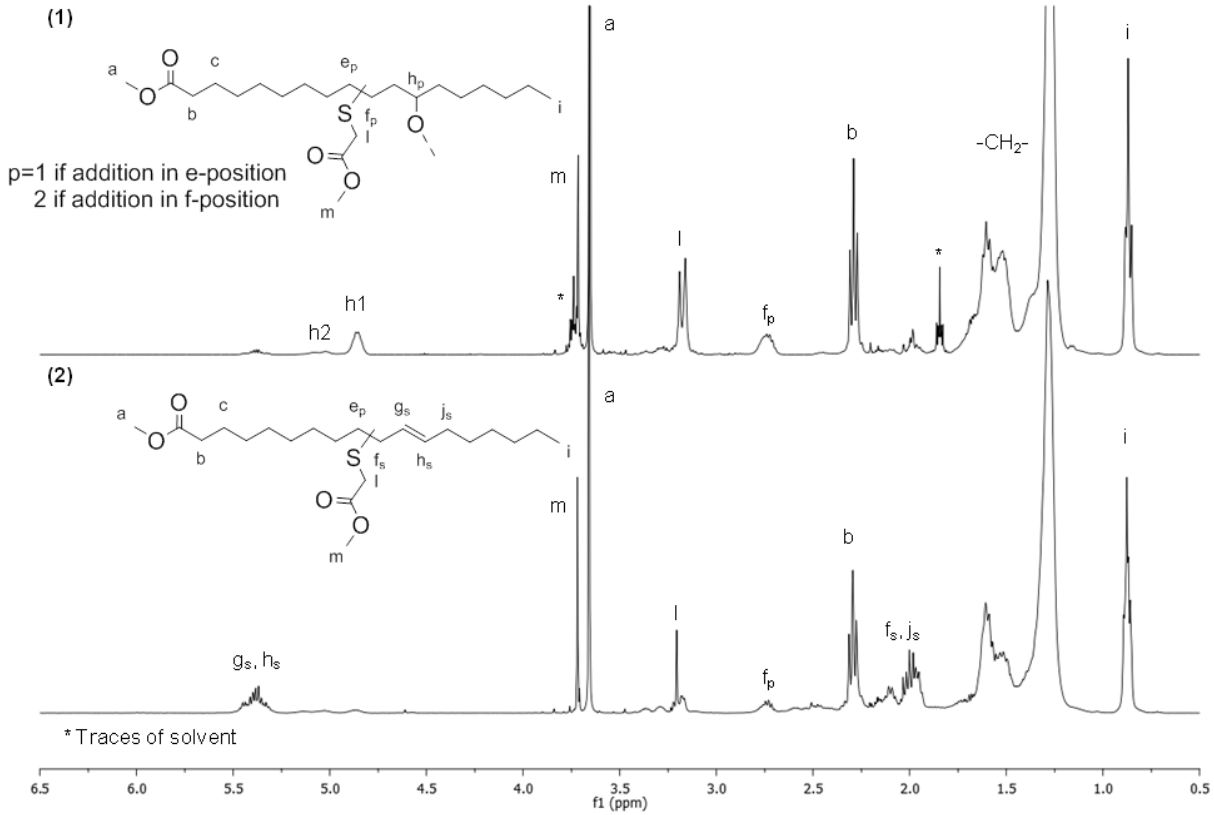

Figure 0-14. Stacked ^{1}H NMR spectra of HBPE prepared by polycondensation of DMH-Ric at 180/200°C after (1) 8 hours and (2) 40 hours of reaction in $CDCl_3$

The dehydration side reaction became dominant at high temperatures and long reaction times, but actually competed with the transesterification during the whole polymerization. The characteristic signals of double bond protons were indeed already present after 8 hours of reaction, even if barely visible. Therefore, the low reactivity of this A_2B-type monomer could not be simply offset by an increase in the polymerization temperature due to these limitations.

2.2.2. Polycondensation of M2H-Lin

The polycondensation of M2H-Lin turned out to be more difficult to accomplish, despite the numerous attemtps (Table 0-IV). A first screening of catalysts performed in the standard conditions of this study, *i.e.* T_1 = 120°C, T_2 = 160°C (Scheme 0-7) demonstrated that the presence of two primary alcohols significantly increases the reactivity of this AB_2-type monomer, compared to previous synthons. Whatever the catalyst employed, *e.g.* $Zn(OAc)_2$, TBD, $Ti(OBu)_4$ and DBTO, polycondensations ended up with insoluble gel-like materials within 3 to 8 hours (P23, P24, P25 and P26). Decreasing the loading in catalyst from 1.5 to 1 wt% did not allow a better control over the polymerization reactions (attempts carried out with $Zn(OAc)_2$ and TBD, P27 and P28). To the contrary, gelation was found to occur sooner. Besides, molar masses achieved before gelation, from 1 400 to 4 100 $g.mol^{-1}$, appeared limited in comparison with the results previously obtained with M2H-Ric.

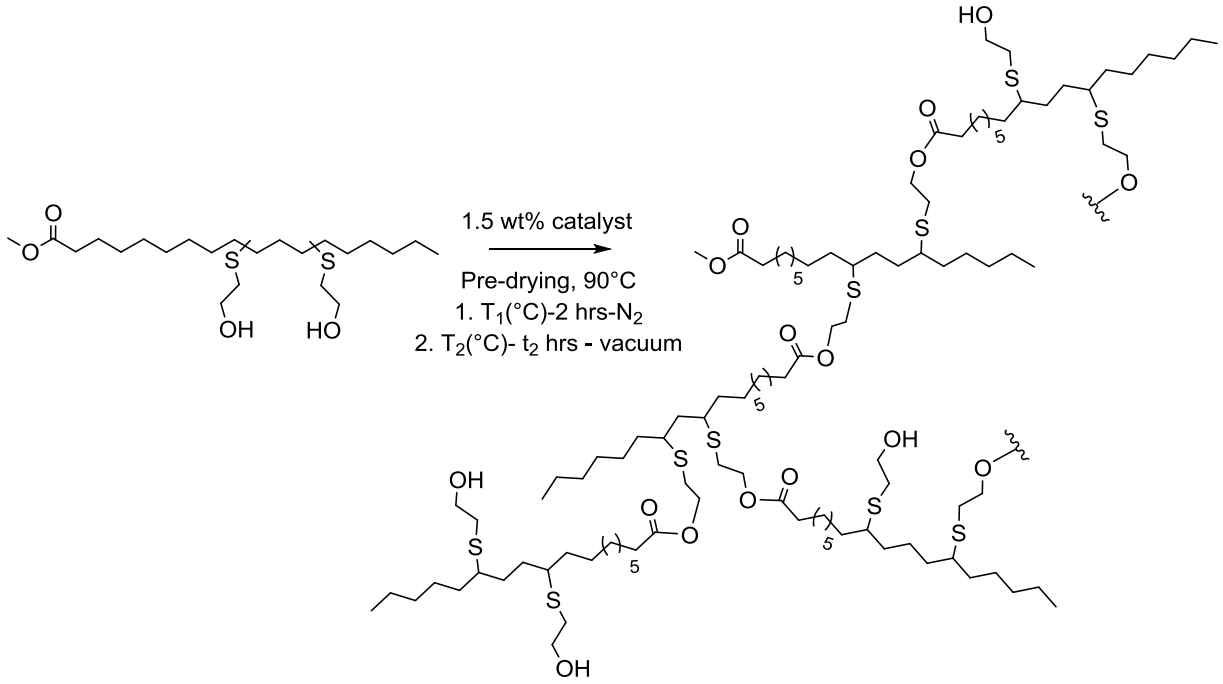

Scheme 0-7. HBPE synthesis from M2H-Lin

Convinced that better results could be expected, efforts were thus made to revisit our procedure, and in particular the time-temperature window. This series of experiments was performed using TBD as catalyst with a loading of 1.5 wt%. The reaction progress was monitored by SEC (THF, PS calibration).

Table 0-IV. Polycondensation of M2H-Lin: experimental condition screening and macromolecular characteristics of related HBPEs

Entry	Cat.	T_1(°C)	T_2(°C)	t_2 (hours)	x^1 (%)	$\bar{M}_n{}^1$ (g.mol^{-1})	$\bar{M}_w{}^1$ (g.mol^{-1})	$Đ^1$	Gelation
P23	$Zn(OAc)_2$	120	160	4	92	3 200	7 700	2.41	8 hours
P24	TBD	120	160	6	95	4 100	16 200	3.95	8 hours
P25	$Ti(OBu)_4$	120	160	2	88	2 800	6 400	2.29	3 hours
P26	DBTO	120	160	2	47	1 400	1 550	1.11	3 hours
P27[2]	$Zn(OAc)_2$	120	160	4	86	2 500	4 800	1.92	6 hours
P28[2]	TBD	120	160	4	93	3 800	11 900	3.13	6 hours
P29[3]	TBD	120	160	9	93	3 600	10 500	5.60	/
P30	TBD	90	90	14	81	2 150	3 200	1.49	/
P31	TBD	120	120	6	93	4 300	18 700	4.35	/
P32	TBD	120	140	6	95	4 700	32 000	6.81	10 hours
P33	NaOMe	120	140	6	96	4 700	22 000	4.68	/

(1) SEC in THF – calibration PS standards. (2) Loading in catalyst: 1 wt%. (3) Batch from Nu-Chek Prep.

At $T_1 = T_2 = 90$°C (P30), the kinetics led to poor conversion even after 16 hours of reaction (81%), and only oligomers were formed ($\bar{M}_n$ < 2 200 g.mol^{-1}). Decreasing the reaction temperature, however, allowed delaying the formation of cross-linked materials (P30, P31 *vs.* P24, P32). HBPEs of slightly higher molar masses and broader dispersity than P23 ($\bar{M}_n$ = 4 700 g.mol^{-1}, $Đ$ = 4.35) were achieved in this way at $T_1 = T_2 = 120$°C without the risk of gelation. P31 was therefore characterized by ^{1}H NMR spectroscopy (Figure 0-15).

The polymerization reaction was confirmed by the decrease in the integration of the methoxy proton peak at 3.66 ppm (-OCH_a) along with the downfield shift of the methylene protons (k_p) in α-position of the hydroxyl functions, after the formation of the ester linkages. Even using NaOMe as catalyst at T_1 = 120°C and T_2 = 140°C (P33), molar masses did not exceed 4 700 g.mol^{-1}.

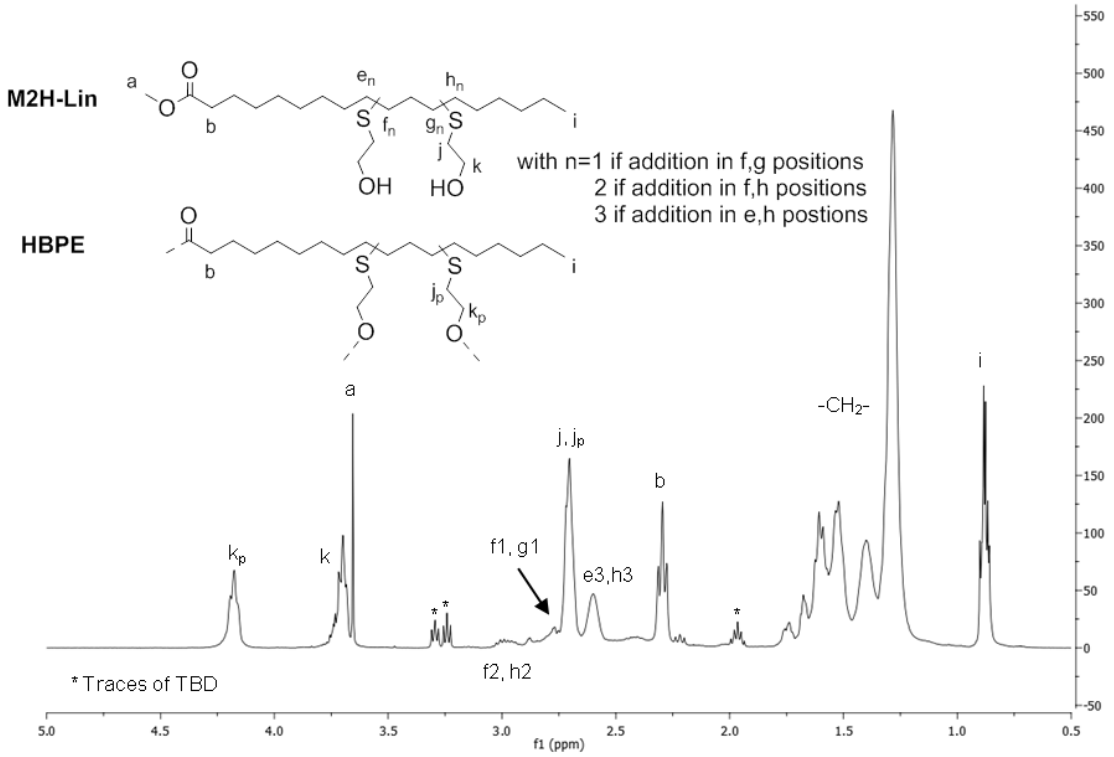

Figure 0-15. ^{1}H NMR spectrum of P31 obtained by polycondensation of M2H-Lin in $CDCl_3$

Given that the purity of M2H-Lin was questioned (see section 1.1 of this chapter), a second batch was prepared starting from one methyl ester of linoleic acid with a purity grade of 99% supplied by NuCheck Prep (instead of the 95% pure methyl linoleate purchased from TCI Europe previously used). One polycondensation was attempted using TBD as catalyst (P29, Table 0-IV). P29 displayed fulfilling molar masses of 3 600 g.mol^{-1}, but still lower than the results obtained with the previous batch (P24). These two tests show that the range of impurities is of great importance in polycondensation and a single undesired species can turn everything upside down.

These comments should not be misunderstood. All the results obtained with M2H-Lin are interesting. Molar masses achieved are just not as high as expected in view of the results obtained with M2H-Ric. The observed gelation trend indicates a preponderance of the etherification side reactions that in this case, could not be simply limited by reducing the reaction temperature or loading in catalyst.

In these circumstances, another catalytic system was considered, namely an enzymatic polymerization. This sustainable approach has gained a growing interest in recent years.[28] Even if biocatalysis is not yet seen as economically competitive, due to the high cost of enzymes and the rather long reaction times associated, enzymatic pathways offer many advantages for polyester synthesis. They allow to trigger highly selective reactions under mild and neutral conditions, at low temperatures and often in quantitative conversions.[29] Lipases have nowadays reached an important place in the library of proposed catalysts of polycondensation.[30,31] The commercially available *Candida antartica* lipase B (CalB) is definitely the most common enzyme used in polymer synthesis, both in bulk and in organic media. The literature of the past 10 years is full of examples with regards to the synthesis of linear as well as branched polyesters, catalyzed by CalB and sometimes even starting from lipidic substrates. To only name one, Gross and coworkers successfully prepared HBPEs by the CalB-catalyzed polycondensation of oleic diacid and glycerol as detailed in Chapter I.[32]

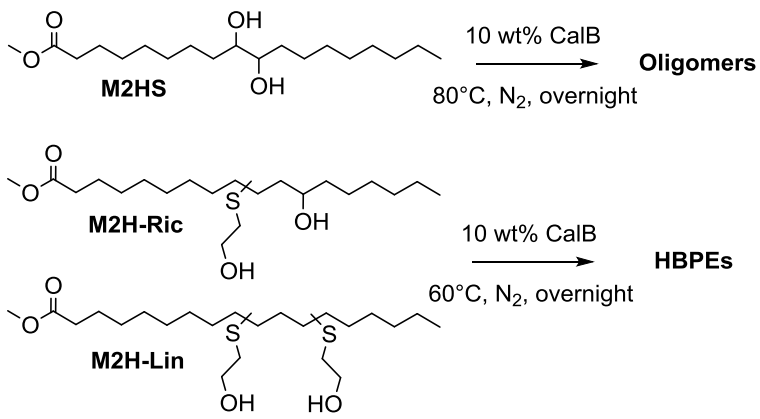

Scheme 0-8. Enzymatic polymerization of M2HS, M2H-Ric and M2H-Lin

In this study, the catalytic activity of CalB was examined with three different substrates: M2HS, M2H-Ric and M2H-Lin, bearing primary and/or secondary alcohols as reactive functions (Scheme 0-8). M2H-Ric and M2H-Lin were better suited to undergo enzymatic polymerization, compared to M2HS, since these monomers are liquids at room temperature. Enzymes are known to be temperature-sensitive, and generally the lipase CalB is not used above 80°C, otherwise the catalyst would be denatured. However, in our strategy to set up a green process, all polymerization tests were performed in bulk. Polycondensation of M2HS was thus conducted overnight at 80°C, just above the melting point of the monomer (T_m = 71°C), while the other AB_2-type synthons were reacted at 60°C. All polymerizations were carried out under nitrogen blowing in an open system (schlenk directly connected to a mineral oil bubbler) in order to remove the methanol formed and shift the equilibrium towards the formation of HBPEs.

The lipase employed, supplied by Chiral Vision (Immozyme) was supported on acrylic beads ensuring an efficient recovery of the catalyst by simple filtration. CalB was added right after the pre-drying step with a loading of 10% relative to monomer weight, according to previous literature.[32]

Table 0-V. Enzymatic polycondensation of M2HS, M2H-Ric and M2H-Lin

Entry	Monomer	x^1 (%)	$\bar{M}_n{}^1$ (g.mol^{-1})	$\bar{M}_w{}^1$ (g.mol^{-1})	$Đ^1$
P34[2]	M2HS	56	1 000	1 100	1.10
P35	M2H-Ric	97	3 100	5 000	1.61
P36	M2H-Lin	95	3 200	9 000	2.81

(1) SEC in THF – calibration PS standards. (2) T_2 = 80°C.

Results obtained with M2HS and M2H-Ric highlighted one distinctive feature of CalB, its selectivity towards primary alcohols (Table 0-V). Polycondensation of M2HS through secondary alcohols proceeded indeed more slowly and, only dimers and trimers were formed after one night with poor conversion (x < 60%). In contrast, P35 and P36 yielded molar masses up to 3 000 g.mol^{-1} and high conversions ($x \geq$ 95%). However, P35 exhibited a fully linear structure (DB = 0) according to ^{1}H NMR characterization (see supporting information, Figure SI 0-5).

Experimental conditions have not yet been optimized (loading in CalB, T(°C), time, catalyst recycling, etc.). However, the results obtained with M2H-Lin look really promising. This isolated test demonstrates that CalB catalysis can be an adequate solution to the high reactivity of the AB_2-type monomer.

2.2.3. Polycondensation of DMH-Und and M2H-Und

The higher reactivity of DMH-Und and M2H-Und was confirmed since the preliminary tests performed in polymerization and summarized in Table 0-VI. The first soluble HBPE samples were formed by decreasing both temperatures of oligomerization (T_1) and polymerization (T_2) to 90°C. Though, P42 formed a partly cross-linked material after only one hour of reaction under nitrogen blowing. The organic catalyst TBD was preferred in this range of temperatures (Scheme 0-9).

M2H-Und being liquid at room temperature, its polymerization was performed at 30°C to afford HBPEs without any risk of gelation (P40). In these conditions, however, the viscosity of the reaction mixture dramatically increased preventing the stirring system from working, thereby limiting the molar masses ($\bar{M}_n$ = 4 000 g.mol^{-1}) and conversion achievable (x = 91%). Consequently, the polymerization of M2H-Und was attempted in solution of toluene (P41). For that purpose, the whole reaction was carried out under nitrogen at 60°C.

Table 0-VI. Polycondensation of DMH-Und and M2H-Und: experimental condition screening and macromolecular characteristics of related HBPEs

Entry	Monomer	T(°C)[1]	t[2] (hours)	x[3] (%)	$\bar{M}_n$[3] (g.mol^{-1})	$\bar{M}_w$[3] (g.mol^{-1})	$Đ$[3]	Gelation
P37	DMH-Und	30	16	96	5 850	16 300	2.79	/
P38		60	4	98	6 900	40 700	5.90	/
P39		90	3	99	10 000	49 800	4.98	Complete in 4 hours
P40	M2H-Und	30	4	91	4 000	44 400	>11	/
P41[4]		60	49	77	2 700	6 050	2.24	/
P42		90	1	96	3 800	20 900	5.50	partial
P43[5]		90	43	99	1 800	2 200	1.22	/

(1) $T_1 = T_2 = T(°C)$. (2) t = duration of the whole polymerization. (3) Determined by SEC in THF – calibration PS standards. (4) Solution of toluene. (5) Loading in TBD: 0.75 wt%.

In dilute medium, the kinetics of polymerization significantly slowed down and molar masses reached a plateau at 2 700 g.mol^{-1} over 50 hours. Similarly, only oligomers were obtained by halving the loading in TBD (P43).

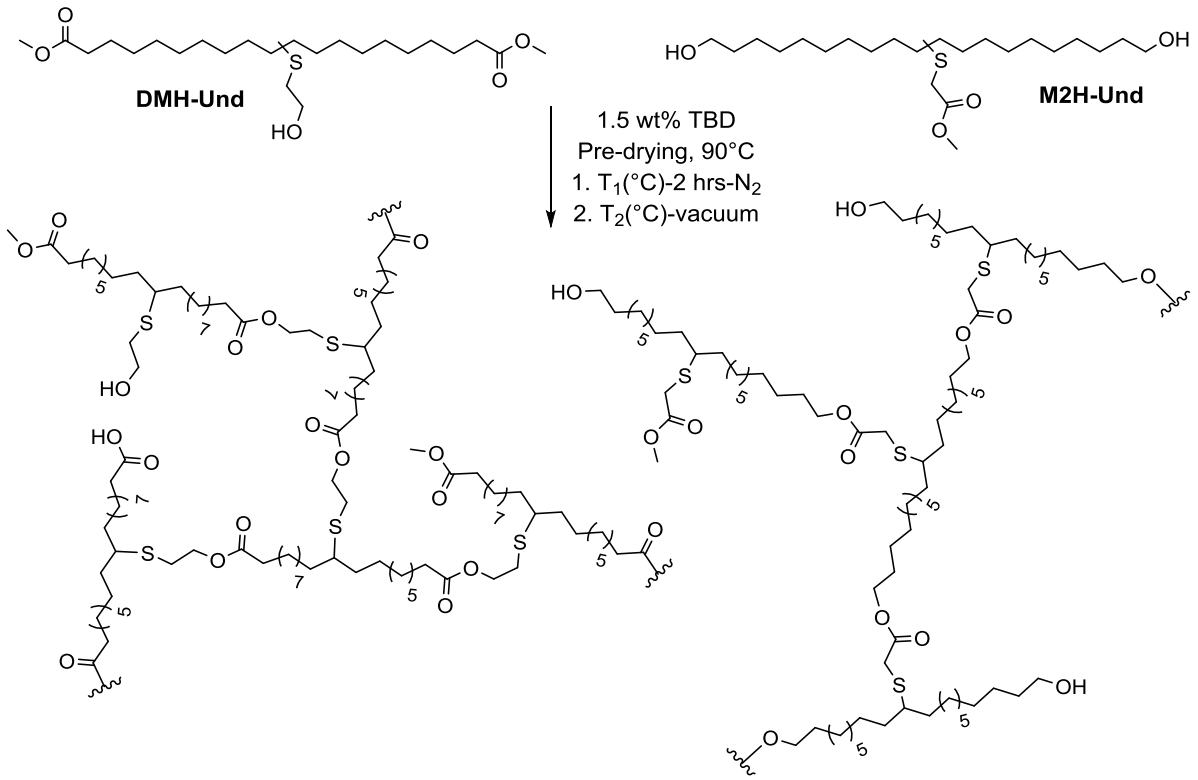

Scheme 0-9. HBPE synthesis from DMH-Und and M2H-Und

Results obtained with DMH-Und, A_2B analogue of M2H-Und, were significantly different. All polycondensations (P37, P38 and P39) yielded HBPEs with molar masses in the range 6 000 and 10 000 g.mol^{-1} and quantitative conversions (x > 96%), whatever the reaction temperature tested (30, 60 and 90°C). This observation could not be explained by different growth patterns since both polymerizations involve the condensation of an ester group (A) with an alcohol (B).

The differences in reactivity noted between the AB_2 and A_2B-type monomers were rather correlated to the etherification side reactions that, unlike the transesterification, proceed between two hydroxyl functions. Polycondensation of M2H-Und afforded polyesters bearing polyol chain-ends while polymerization of DMH-Und gave ester-terminated HBPEs. The higher concentration in hydroxyl-ended moieties might promote the etherification side reactions during the polycondensation of M2H-Und, leading to cross-linked materials instead of soluble HBPEs.

Taking spectra of P39 and P40 (Figure 0-16) as examples, the formation of HBPEs was confirmed by ^{1}H NMR spectroscopy. Polymerizations of DMH-Und and M2H-Und were followed by the downfield shift of the signals H_g and H_a, that are characteristic of the methylene protons in α-position of the primary alcohols, to 4.18 and 4.10 ppm, respectively, after the formation of the ester linkage. Regarding M2H-Und based HBPEs, the reaction progress was also evaluated through the decrease in the integral of the methoxy protons (H_f) at 3.66 ppm.

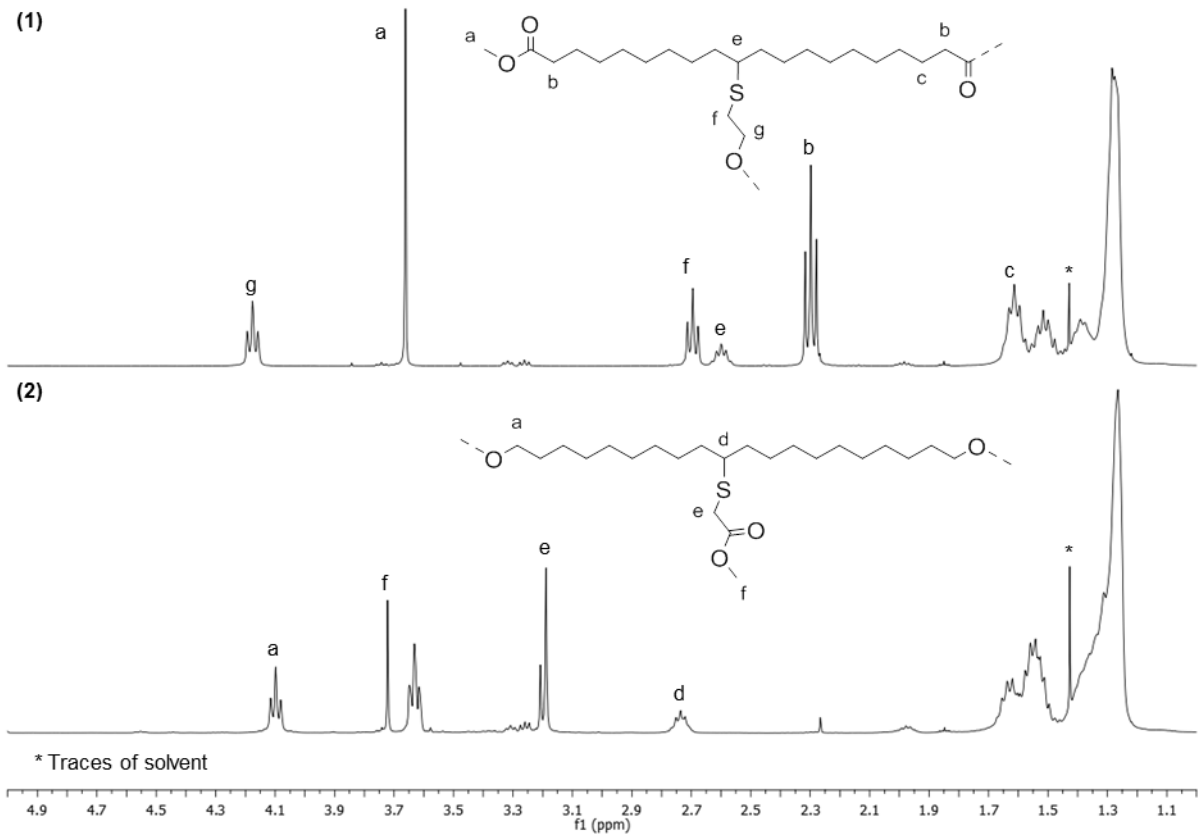

Figure 0-16. Stacked ^{1}H NMR spectra of (1) P39 and (2) P40 in $CDCl_3$

In brief, the approach discussed in this chapter, *i.e.* the introduction of primary alcohols combined with the separation of the reactive functions, has been proved right. M2H-Ric, M2H-Lin, DMH-Und and M2H-Und did show a higher reactivity in polycondensation than monomers of the acid hydrolysis of epoxidized vegetable oil platform, described in previous chapters of this manuscript. As a consequence, polyesters of similar molar masses, in the range 3 000 to 10 000 $g.mol^{-1}$, were achieved in shorter reaction times, and/or by applying lower temperatures of polymerization. These preliminary results, apart from M2H-Ric that was studied in great detail, are highly promising. The higher reactivity of these thiolated monomers was also suspected to influence the branching density of the related HBPEs. Nevertheless, one drawback associated with this approach is the impossibility of determining the DB by direct methods, *e.g.* NMR spectroscopy.

Regarding the most reactive monomers, the process of polymerization must be reconsidered. To deal with the rapid increase in viscosity related to polymerization temperatures in between 30 and 70°C, other routes could be envisaged. For instance, the use of a mechanical stirring system would be required for the scale-up production of both monomers and polymers. Implementation of the polymerization in dilute or dispersed media, *i.e.* organic solvents, ionic liquids or supercritical CO_2, also represents interesting options. Taking M2H-Und as an example, in some cases, it is no longer enough to reduce the reaction temperature to limit the etherification side reactions leading to gelation. The addition of chain stoppers, *i.e.* A-type monomers, is for instance a possibility to be considered to control the polycondensation of AB_n-type monomers. Enzymatic polymerization proved to be an interesting option as well. The lipase CalB indeed showed good activity to catalyze the polycondensation of M2H-Lin.

3. Thermal properties

With the exception of the oligomers achieved with DMH-Ric, thermal properties of the thiolated HBPEs were investigated by DSC experiments. The reported data are from soluble samples of hyperbranched architecture; in other words, the cross-linked materials were not characterized. Glass transition and melting temperatures were determined from the second heating scan at $10°C.min^{-1}$ and crystallization temperatures from the first cooling scan. Results obtained are summarized in Table 0-VII.

Table 0-VII. Thermal properties of HBPEs derived from M2H-Ric, M2H-Lin, DMH-Und and M2H-Und

Entry	Monomer	DSC			TGA
		T_g (°C)	T_m (°C)	T_c (°C)	$T_d^{5\%}$ (°C)
P4	M2H-Ric	-37	/	/	304
P5		-36	/	/	300
P6		-35	/	/	307
P7		-37	/	/	314
P8		-35	/	/	309
P9		-36	/	/	313
P10		-36	/	/	299
P13		-40	/	/	293
P14		-42	/	/	308
P17		-36	/	/	298
P18		-38	/	/	299
P31	M2H-Lin	-47	/	/	266
P35		-46	/	/	284
P36		-50	/	/	269
P37	DMH-Und	-56	-29	-44	298
P38		-51	-26	-42	284
P40	M2H-Und	-40	-20	-35	266

HBPEs derived from M2H-Ric and M2H-Lin were found to be amorphous (Figure 0-17 (1)) with glass transition temperatures in the range -42 to -35°C, and -50 to -47°C, respectively. The lower T_g values achieved with M2H-Lin-based HBPEs could be partly explained by their lower molar masses. In addition, the branching density of the HBPEs derived from M2H-Ric, as evaluated by the reactivity ratio between primary and secondary alcohols (*r*), did not show any influence on T_g values.

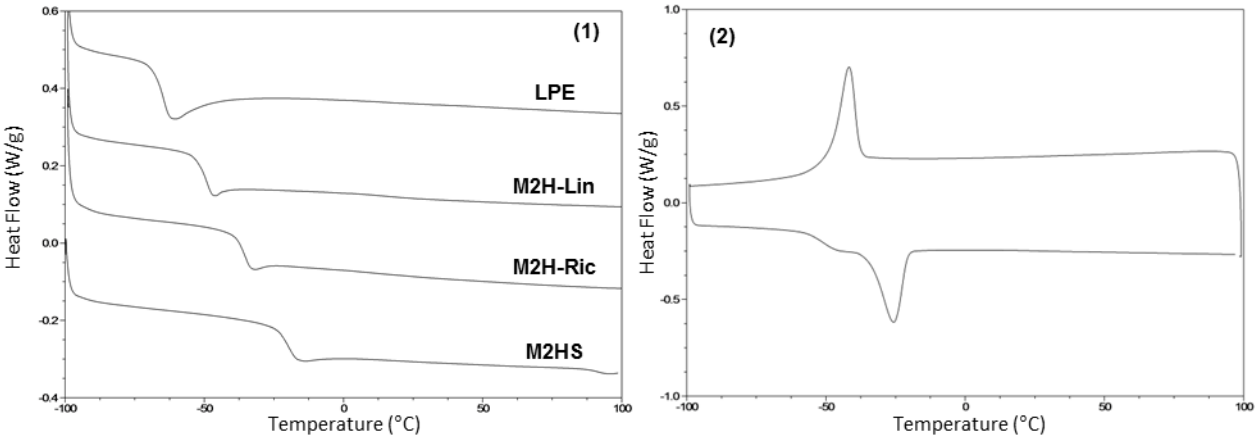

Figure 0-17. DSC thermograms of (1) HBPEs derived from M2H-Ric, M2H-Lin, M2HS and linear reference (LPE) and (2) HBPE derived from DMH-Und (P37)

A linear reference was synthesized starting from methyl oleate for comparison purpose (Scheme 0-10). To this end, the thiol-ene addition of an excess of 2-mercaptoethanol was carried out under UV irradiations using 1 mol% DMPA as photoinitiator. Full conversion was reached within 15 minutes. The so-formed AB monomer was then polymerized in the conditions optimized for M2H-Ric using $Zn(OAc)_2$ as catalyst. A linear polyester (LPE) with molar masses of $\bar{M}_n$ = 9 700 g.mol^{-1} and quite broad dispersity ($Đ$ = 3.65) was achieved. Characterizations by ^{1}H NMR spectroscopy of both monomer and polymer, are provided in supporting information (see Figure SI 0-6). LPE was also found to display an amorphous behavior (Figure 0-17 (1)) but gave lower glass transition temperature than that of its hyperbranched analogues, *i.e.* T_g = -65°C.

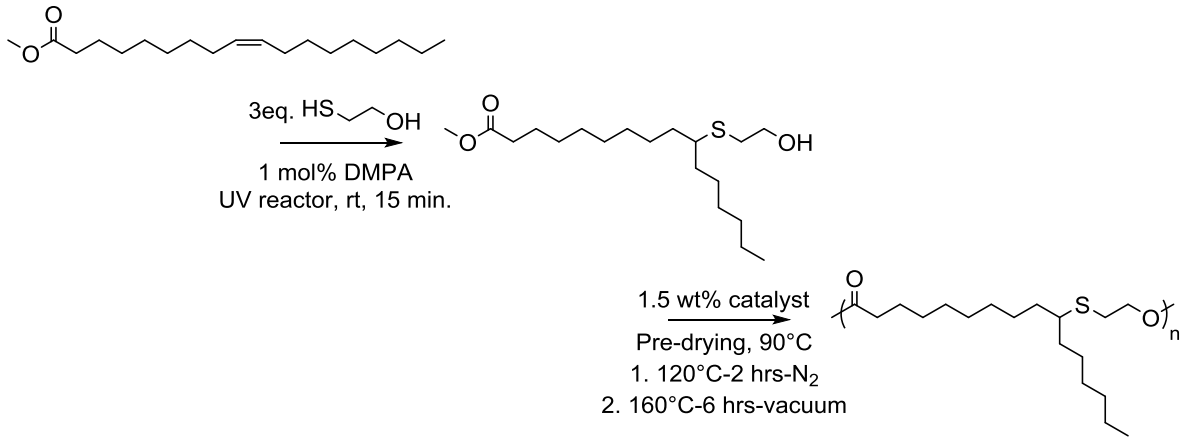

Scheme 0-10. Synthetic route to a thioether-containing linear polyester analogue (LPE)

As illustrated in Figure 0-17 (2) with P37, HBPEs derived from DMH-Und and M2H-Und were shown to be semi-crystalline in agreement with the results previously obtained in Chapter III. The absence of pendant alkyl chains acting as plasticizers, again seemed to induce crystallization. In addition, ester-terminated HBPEs achieved with DMH-Und gave lower T_g values, in between -56 and -51°C, than that of the hyperbranched polyesters polyols derived from M2H-Und (T_g = -40°C) . This result was expected since the end-group effect on the glass transition temperature is very strong in HBP systems.

The chemical character of the polymer backbone yet plays an important role on T_g values as illustrated hereafter. Thermal properties of these thiolated HBPEs were compared to those of the HBPEs synthesized *via* the acid hydrolysis of epoxidized vegetable oil route. Overall, the thioether-containing HBPEs displayed lower T_g values, in the range -56 to -35°C (*vs*. -35 to 3°C, Chapters II and III).

These results could be explained by the presence of sulfur atoms, which are known to impart flexibility to the polymeric chains, *i.e.* single C-S bonds are indeed longer than C-C bonds.[33] The increase in mobility endowed by the thioether linkages also accounted for the lower T_g values of M2H-Lin derived HBPEs in comparison with M2H-Ric based HBPEs, and the amorphous character of LPE while the linear reference synthesized in Chapter II by polycondensation of methyl 12-hydroxystearate was semi-crystalline (Table 0-VII).

In this study, 5% weight loss degradation temperatures up to 313°C were achieved. HBPEs derived from M2H-Ric exhibited the higher heat resistance in this series, with $T_d^{5\%}$ values in the range 299 to 313°C. The other thioether-containing HBPEs appeared less stable with $T_d^{5\%}$ values in between 266 and 298°C, likely due to their lower molar masses. Overall, the thiolated HBPEs gave lower $T_d^{5\%}$ values than that observed for the HBPEs prepared by the acid hydrolysis of epoxidized vegetable oil platform as illustrated with M2HS in Figure 0-18. This was correlated to the lower thermal degradation of thioether linkages.

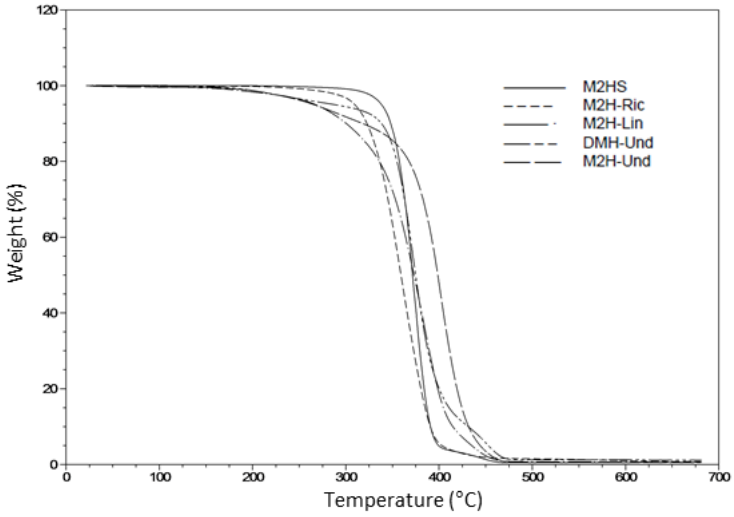

Figure 0-18. Weight loss as a function of temperature for HBPEs derived from M2HS, M2H-Ric, M2H-Lin, DMH-Und and M2H-Und from TGA experiments at 10°C.minutes^{-1} under nitrogen atmosphere

Conclusion

In conclusion, five new HBPE precursors of A_2B and AB_2-type were successfully prepared by means of thiol-ene addition and metathesis. The approach developed in this chapter, *i.e.* introduction of primary alcohols and separation of reactive functions, has been proved right. Apart from DMH-Ric whose polycondensation yielded only oligomers, the higher reactivity of the other monomers was confirmed in polymerization. HBPEs of molar masses in the range 3 000 to 10 000 $g.mol^{-1}$ were achieved in shorter reaction times and/or by applying lower polymerization temperatures than previous cases discussed in Chapters II and III. However, it was found difficult to accurately characterize the branching density of the related HBPEs owing to the separation of the reactive functions. Another issue with this family of monomers was the occurrence of gelation at earlier stages of the polymerization. Hence, the process itself has to be revisited somehow. Several routes have been explored, one of the most promising being the enzymatic catalysis.

This second platform of AB_n-type monomers yet broadens the range of oily-derived HBPEs to thiolated materials. Introducing hetero-atoms into the very core of HBPs is nowadays a major challenge since these hetero-functional groups provide materials with unique performances.[34] Here, the presence of sulfur atoms was shown to influence the thermal properties of related HBPEs. Thioether linkages indeed impart flexibility to the polymeric chains resulting in lower T_g values, but weaken their thermal stability with reduced $T_d^{5\%}$ in between 266 to 313°C. Lastly, the presence of thioether linkages allows the post-modification of the HBPE backbone by oxidation or quaternization of the sulfur atoms with the idea of tuning the properties of these materials. The post-functionalization of the core, as well as of the periphery of these HBPEs is presented in the next chapter.

References

(1) Hoyle, C. E.; Bowman, C. N. *Angew. Chemie Int. Ed.* **2010**, *49* (9), 1540–1573.
(2) Lowe, A. B. *Polym. Chem.* **2010**, *1* (1), 17–36.
(3) Samuelsson, J.; Jonsson, M.; Brinck, T.; Johansson, M. *J. Polym. Sci. Part A Polym. Chem.* **2004**, *42* (24), 6346–6352.
(4) Türünç, O.; Meier, M. A. R. *Eur. J. Lipid Sci. Technol.* **2013**, *115* (1), 41–54.
(5) Desroches, M.; Caillol, S.; Lapinte, V.; Boutevin, B. *Macromolecules* **2011**, *44*, 2489–2500.
(6) Jaillet, F.; Desroches, M.; Auvergne, R.; Boutevin, B.; Caillol, S. *Eur. J. Lipid Sci. Technol.* **2013**, *115*, 698–708.
(7) Lligadas, G.; Ronda, J. C.; Galià, M.; Cádiz, V. *J. Polym. Sci. Part A Polym. Chem.* **2013**, *51* (10), 2111–2124.
(8) Nohra, B.; Candy, L.; Blanco, J.-F.; Guerin, C.; Raoul, Y.; Mouloungui, Z. *Macromolecules* **2013**, *46* (10), 3771–3792.
(9) Pham, P. D.; Lapinte, V.; Raoul, Y.; Robin, J.-J. *J. Polym. Sci. Part A Polym. Chem.* **2014**, *52*, 1597–1606.
(10) Türünç, O.; Meier, M. A. R. *Macromol. Rapid Commun.* **2010**, *31* (20), 1822–1826.
(11) Bao, Y.; He, J.; Li, Y. *Polym. Int.* **2013**, *62*, 1457–1464.
(12) Mutlu, H.; Meier, M. A. R. *Eur. J. Lipid Sci. Technol.* **2010**, *112* (1), 10–30.
(13) More, A. S.; Gadenne, B.; Alfos, C.; Cramail, H. *Polym. Chem.* **2012**, *3* (6), 1594.
(14) Hérisson, J.-L.; Chauvin, Y. *Die Makromol. Chemie* **1970**, *141* (3487), 161–176.
(15) Schaverien, C. J.; Dewan, J. C.; Schrock, R. R. *J. Am. Chem. Soc.* **1986**, *108* (10), 2771–2773.
(16) Schrock, R. R.; DePue, R. T.; Feldman, J.; Schaverien, C. J.; Dewan, J. C.; Liu, A. H. *J. Am. Chem. Soc.* **1988**, *110* (5), 1423–1435.
(17) Schrock, R. R.; Murdzek, J. S.; Bazan, G. C.; Robbins, J.; DiMare, M.; O'Regan, M. *J. Am. Chem. Soc.* **1990**, *112* (10), 3875–3886.
(18) Nguyen, S. T.; Johnson, L. K.; Grubbs, R. H.; Ziller, J. W. *J. Am. Chem. Soc.* **1992**, *114* (10), 3974–3975.
(19) Rybak, A.; Meier, M. A. R. *Green Chem.* **2007**, *9* (12), 1356.
(20) Meier, M. A. R. *Macromol. Chem. Phys.* **2009**, *210* (13-14), 1073–1079.
(21) Winkler, M.; Meier, M. A. R. *Green Chem.* **2014**, *16*, 3335–3340.
(22) Bielawski, C. W.; Grubbs, R. H. *Prog. Polym. Sci.* **2007**, *32* (1), 1–29.
(23) Mutlu, H.; De Espinosa, L. M.; Meier, M. A. R. *Chem. Soc. Rev.* **2011**, *40* (3), 1404–1445.
(24) Ngo, H.; Jones, K.; Foglia, T. *J. Am. Oil Chem. Soc.* **2006**, *83* (7), 629–634.
(25) Hong, S. H.; Sanders, D. P.; Lee, C. W.; Grubbs, R. H. *J. Am. Chem. Soc.* **2005**, *127* (49), 17160–17161.
(26) Djigoué, G. B.; Meier, M. A. R. *Appl. Catal. A Gen.* **2009**, *368* (1-2), 158–162.
(27) Fokou, P. A.; Meier, M. A. R. *Macromol. Rapid Commun.* **2010**, *31* (4), 368–373.
(28) Miletic, N.; Loos, K.; Gross, R. A. *Enzymatic polymerization of polyester*; Wiley-VCH Verlag & Co. KGaA: Weinheim, Germany, 2010.
(29) Vilela, C.; Sousa, A. F.; Fonseca, A. C.; Serra, A. C.; Coelho, J. F. J.; Freire, C. S. R.; Silvestre, A. J. D. *Polym. Chem.* **2014**, *5*, 3119–3141.
(30) Gross, R. A.; Kumar, A.; Kalra, B. *Chem. Rev.* **2001**, *101* (7), 2097–2124.
(31) Kobayashi, S. *Macromol. Rapid Commun.* **2009**, *30* (4-5), 237–266.
(32) Zhang, Y.; Yang, Y.; Cai, J.; Lv, W.; Xie, W.; Wang, Y.; Gross, R. A. In *Biobased Monomers, Polymers, and Materials*; Smith, P. B., Gross, R. A., Eds.; ACS Symposium series: Washington, 2012; p 111.
(33) Maisonneuve, L.; Wirotius, A.; Alfos, C.; Grau, E.; Cramail, H. *Polym. Chem.* **2014**, *5*, 6142–6147.
(34) Yan, D.; Gao, C.; Frey, H. *Hyperbranched polymers: Synthesis, Properties, and Applications*; John Wiley & Sons, Inc., 2011.

Experimental methods

General procedure of direct thiol-ene addition

Thiol-ene addition of 2-mercaptoethanol (M2H-Ric, M2H-Lin): fatty acid methyl esters and 2-mercaptoethanol (3 equivalents/double bond) were stirred at room temperature under UV irradiations. Two different devices were tested. Preliminary experiments were performed with a simple UV lamp (254 or 365 nm, 6 W) while production scaling-up was carried out within a UV reactor (source mediated 225-365 nm, 450 W) where the exposure was maximized. DMPA was added as photo-initiator during the preparation of M2H-Ric with a loading of 1 mol%. After the disappearance of double bond protons monitored by ^{1}H NMR spectroscopy, the reaction mixture was dissolved in DCM and thoroughly washed with water (x 2) and brine (x 1). The organic phase was then dried over anhydrous magnesium sulfate, filtered and DCM was distilled off on a rotary evaporator. DMPA was removed when necessary by Flash chromatography (apparatus from Grace). The constituents were separated on silica column using a cyclohexane/ethyl acetate gradient (85/15: v/v).

M2H-Ric: methyl ricinoleate (10 g, 32 mmol) and 2-mercaptoethanol (7.5 g, 96 mmol). M2H-Ric was obtained as a colorless viscous liquid in high yield (92%). Its purity grade was determined by GC (96.8%).

M2H-Lin: methyl linoleate (5 g, 17 mmol) and 2-mercaptoethanol (8 g, 102 mmol). M2H-Lin was obtained as a colorless viscous liquid in high yield (96%).

Thiol-ene addition of methyl thioglycolate: the experimental procedure for the synthesis of DMH-Ric was similar to the preparation of M2H-Ric. Only the functional thiol changed.

DMH-Ric: Methyl ricinoleate (5 g, 16 mmol) and methyl thioglycolate (5 g, 47 mmol). Once the reaction was complete, the excess of methyl thioglycolate was removed under vacuum distillation. DMH-Ric was then purified by Flash chromatography (apparatus from Grace) using a cyclohexane/ethyl acetate gradient (90/10: v/v) to get rid of DMPA. DMH-Ric was obtained as a viscous liquid in high yield (90%). Its purity grade was determined by GC (94%).

General procedure of thiol-ene addition onto metathesis products

Self-metathesis of methyl-undecenoate: methyl undecenoate (15 g, 76 mmol) and 2nd generation Grubbs catalyst (0.3 g, 0.38 mmol) were charged into a 100mL round-bottom flask equipped with a vacuum line. The reaction mixture was vigorously stirred at 45°C under dynamic vacuum for 40 hours, after what the flask was cooled down to room temperature and 2 mL of ethylvinyl ether was added to deactivate the Grubbs catalyst. Dynamic vacuum was applied again to remove the excess of ethylvinyl ether. Dimethyl 1,20-eicos-10-enediote (DM-Und) was then purified by column chromatography using a mixture of cyclohexane and ethyl acetate as eluent (95/5: v/v). DM-Und was obtained as a white to brownish solid. Yield: 66%.

Self-metathesis of 10-undecen-1-ol: 10-undecen-1-ol (10 g, 59 mmol) and 2nd generation Grubbs catalyst (0.49 g, 0.57 mmol) were dissolved in 50 mL of pentane. The solvent was dried prior to reaction on CaH_2 at room temperature. The flask equipped with a nitrogen inlet and a mineral oil bubbler, was vigorously stirred under inert atmosphere at room temperature during 48 hours. As the reaction was going on, the intermediate diol (2H-Und) got precipitated shifting the equilibrium towards the formation of products. Then, ethylvinyl ether was added to deactivate the Grubbs catalyst. 2H-Und was recovered by filtration and purified by recrystallization in cold pentane (x 2). 2H-Und was obtained as a white powder. Yield: 44%.

Both dimerized products, DM-Und and 2H-Und, were characterized by GC analyses. In each case, several isomers were detected due to undesired isomerization side reactions.

Thiol-ene additions

DMH-Und: DM-Und (5 g, 14 mmol) and 2-mercaptoethanol (3.2 g, 41 mmol) were dissolved in DCM and stirred at room temperature under UV irradiations (source mediated 225-365 nm, 450 W). DMPA was added as photo-initiator with a loading of 10 mol%. After the disappearance of double bond protons monitored by ^1H NMR spectroscopy, the reaction mixture was washed with water (x 2) and brine (x 1). The organic phase was then dried over anhydrous magnesium sulfate, filtered and DCM was distilled off on a rotary evaporator. DMPA was removed by Flash chromatography (apparatus from Grace). The constituents were separated on silica column using a cyclohexane/ethyl acetate gradient (90/10: v/v). DMH-Und was obtained as a viscous liquid. Yield: 95%.

M2H-Und: 2H-Und (4 g, 13 mmol) and methyl thioglycolate (4.1 g, 39 mmol) were dissolved in DCM and stirred at room temperature under UV irradiations (source mediated 225-365 nm, 450 W). DMPA was added as photo-initiator with a loading of 10 mol%. After the disappearance of double bond protons monitored by ^{1}H NMR spectroscopy, the excess of methyl thioglycolate was removed by distillation under vacuum and DMPA by Flash chromatography (apparatus from Grace). The constituents were separated on silica column using a cyclohexane/ethyl acetate gradient (85/15: v/v). M2H-Und was obtained as a viscous liquid. Yield: 91%.

General procedure of polymerization

All transesterification reactions were performed in bulk, in a Schlenk flask equipped with a magnetic stirrer, a nitrogen inlet tube and an oil-bath heating system. The experimental two-step-one-pot procedure applied was similar to the preparation of HBPEs derived from M2HS (and described in Chapter II). After one hour of pre-drying at 90°C under dynamic vacuum, one catalyst was added with a loading of 1.5% relative to monomer weight except otherwise mentioned. Reduced concentrations in TBD (0.75-1 wt%) were indeed tested in an attempt to control the polycondensation of M2H-Und. After 2 hours of oligomerization at T_1(°C) under nitrogen blowing, the temperature was raised to T_2(°C) and dynamic vacuum was applied until the viscosity of the reaction mixture suddenly increased. Reaction conditions were optimized as followed. M2H-Ric and M2H-Lin were respectively polymerized at T_1 = 120°C and T_2 = 160°C, and T_1 = 120°C and T_2 = 140°C. Regarding DMH-Ric, higher reaction temperatures were applied to compensate its low reactivity, *i.e.* T_1 = 180°C and T_2 = 200°C. However, in these conditions, dehydration side reactions were favored. Due to their higher reactivity, DMH-Und and M2H-Und were preferably polymerized on lower range of temperatures, namely $T_1 = T_2$ = 30 to 90°C. HBPEs were obtained as highly viscous materials to waxes, generally colored with yellow to brown shades.

When polycondensations were attempted in solution, the experimental procedure slightly differed. After one pre-drying step at 90°C, M2H-Und (0.5 g) and TBD (7.5 mg, 1.5 wt%) were dissolved in toluene. The Schlenk flask equipped with a nitrogen inlet and a mineral oil bubbler was then maintained at 60°C under magnetic stirring and nitrogen atmosphere during 2 days.

Enzymatic polymerizations were performed in bulk at T = 80°C for M2HS, and T = 60°C for M2H-Ric and M2H-Lin. Monomer (0.5 g) was charged in a Schlenk flask equipped with a nitrogen inlet, a mechanical stirrer and a mineral oil bubbler. After one pre-drying at 90°C,

the *Candida Antartica* lipase B (CalB) was added with a loading of 10 wt% relative to monomer weight. The reaction mixture was stirred overnight at T(°C) under nitrogen blowing. Once the Schlenk flask was cooled down to room temperature, THF was added to the reaction mixture. The enzyme catalyst was recovered by simple filtration. After removal of the solvent on a rotary evaporator, HBPEs were obtained as colorless viscous materials.

Supporting Information

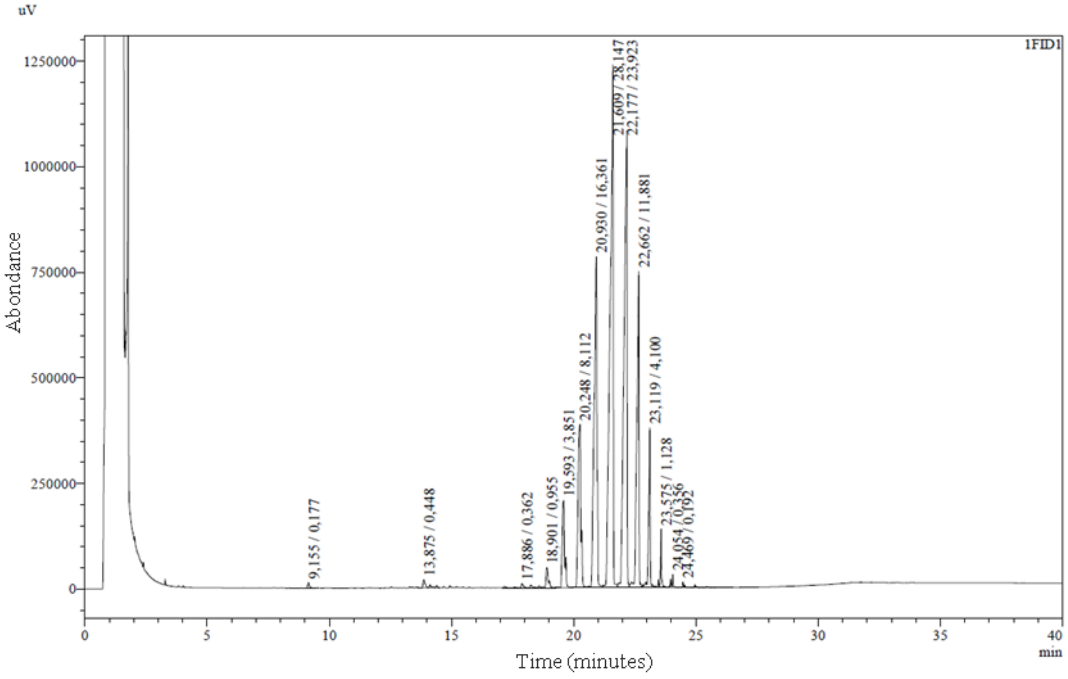

Figure SI 0-1. Gas chromatogram of DMH-Und

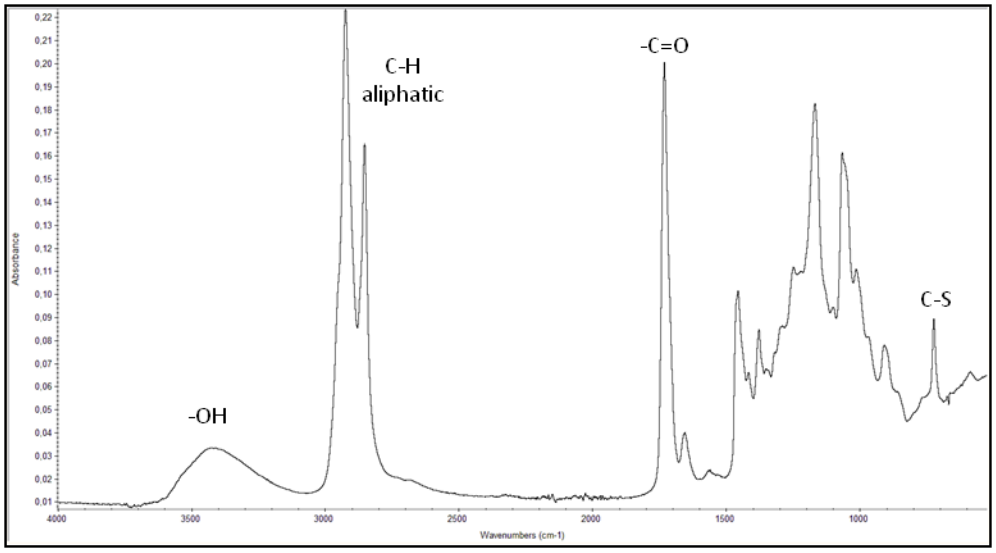

Figure SI 0-2. FT-IR spectrum of a HBPE obtained by polycondensation of M2H-Ric

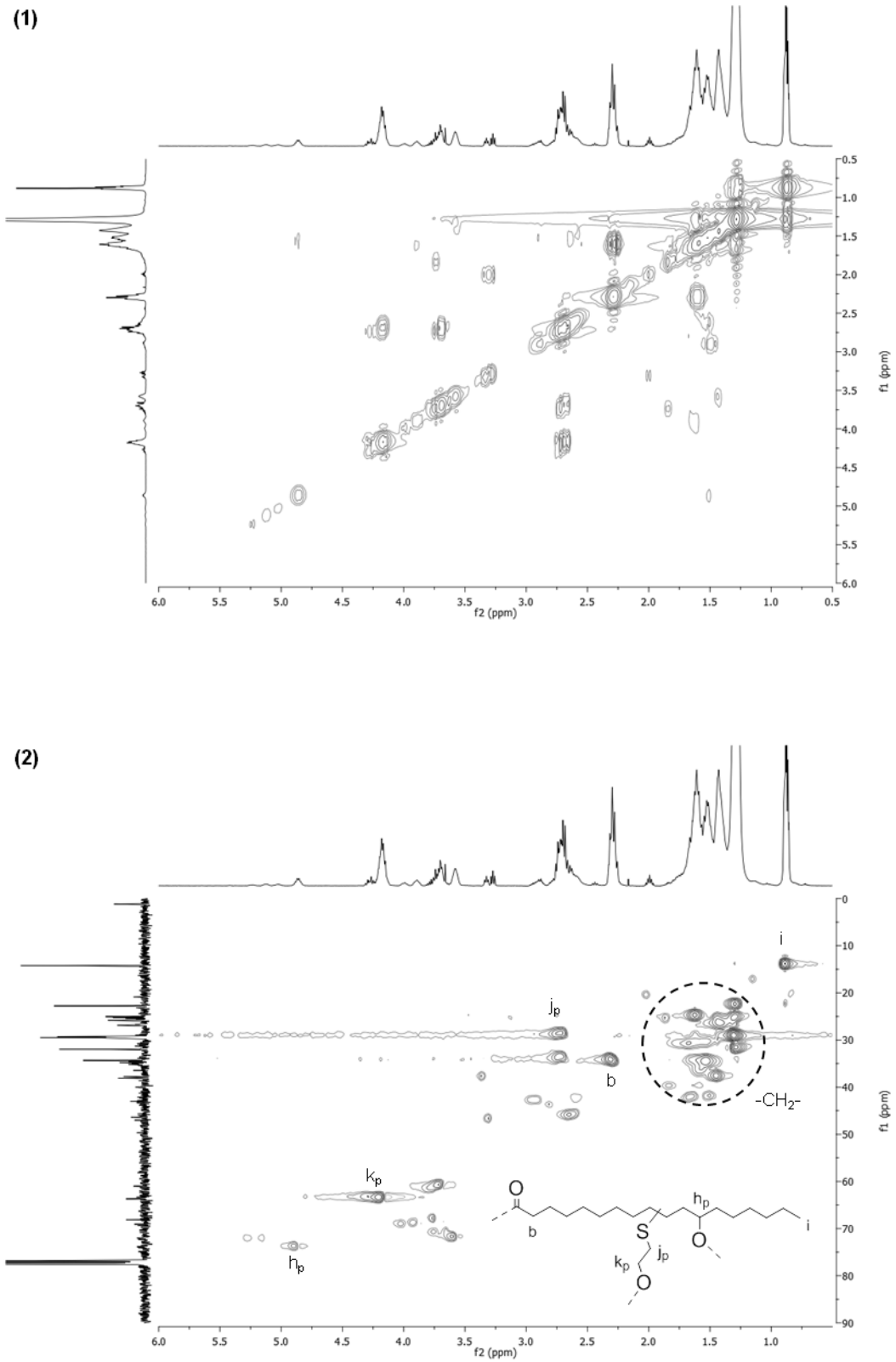

Figure SI 0-3. (1) ^{1}H-^{1}H COSY and (2) ^{1}H- ^{13}C HSQC of P5 in $CDCl_3$

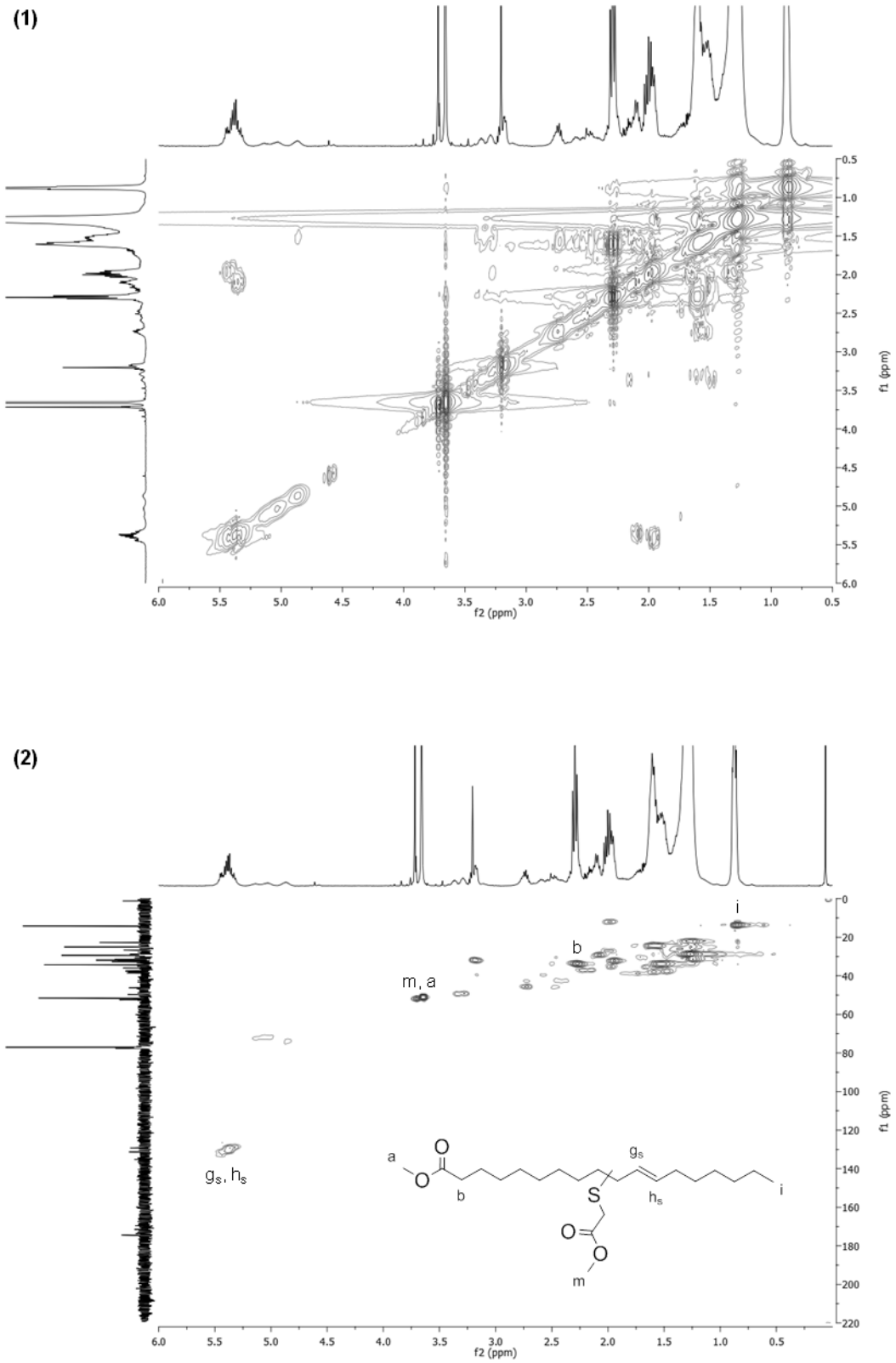

Figure SI 0-4. (1) ^{1}H-^{1}H COSY and (2) ^{1}H-^{13}C HSQC of a HBPE prepared by polycondensation of DMH-Ric (conditions: 40 hours at 180/200°C) in $CDCl_3$

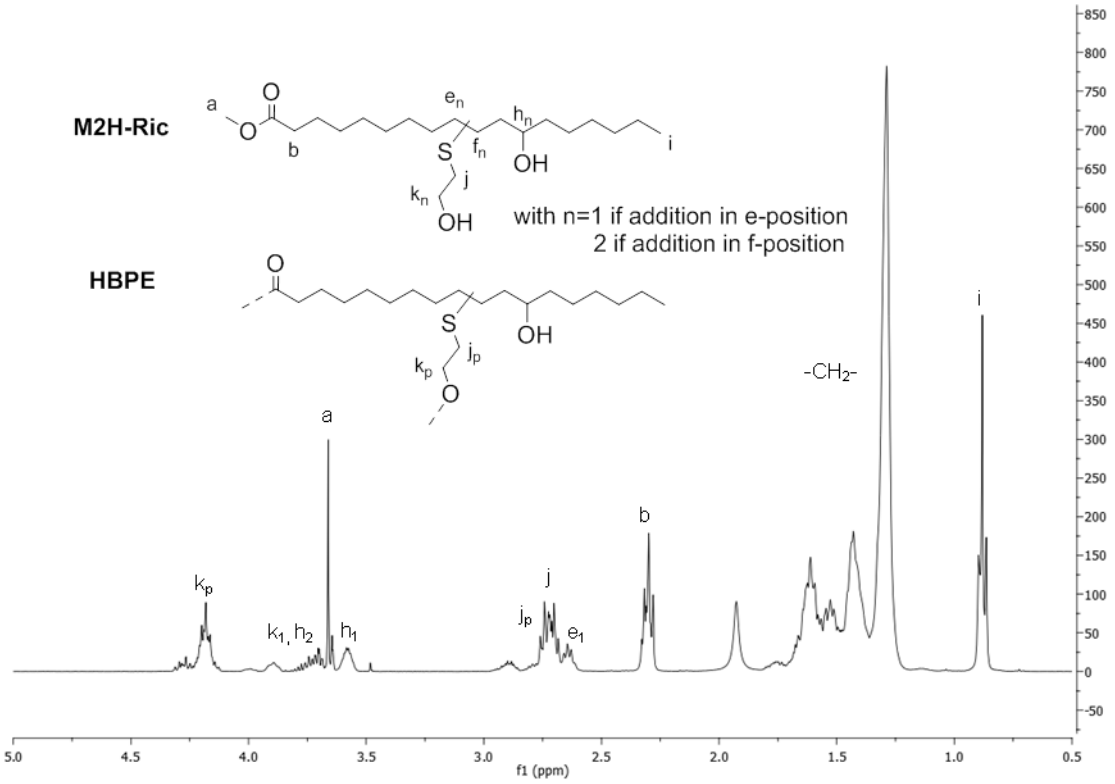

Figure SI 0-5. ^{1}H NMR spectrum of P35 obtained by CalB-catalyzed polycondensation of M2H-Ric in $CDCl_3$

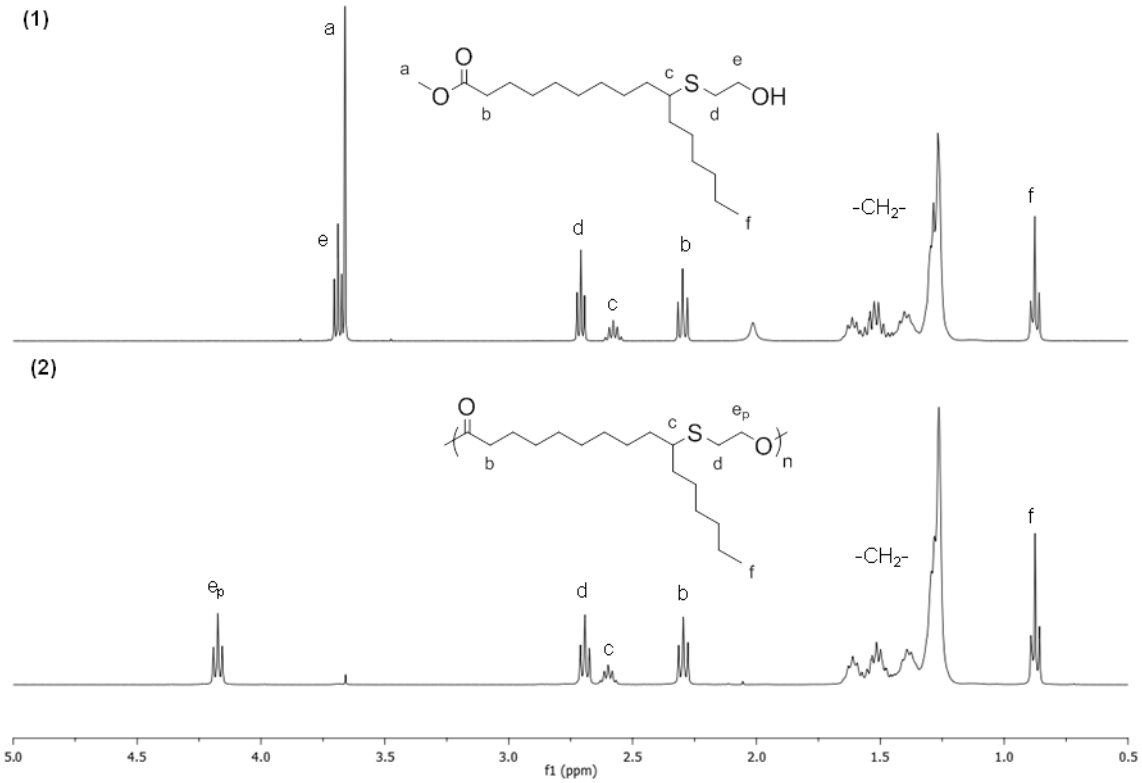

Figure SI 0-6. Stacked ^{1}H NMR spectra of (1) AB monomer and (2) its related LPE in $CDCl_3$

Chapitre IV. Towards the functionalization of Hyperbranched Polyesters

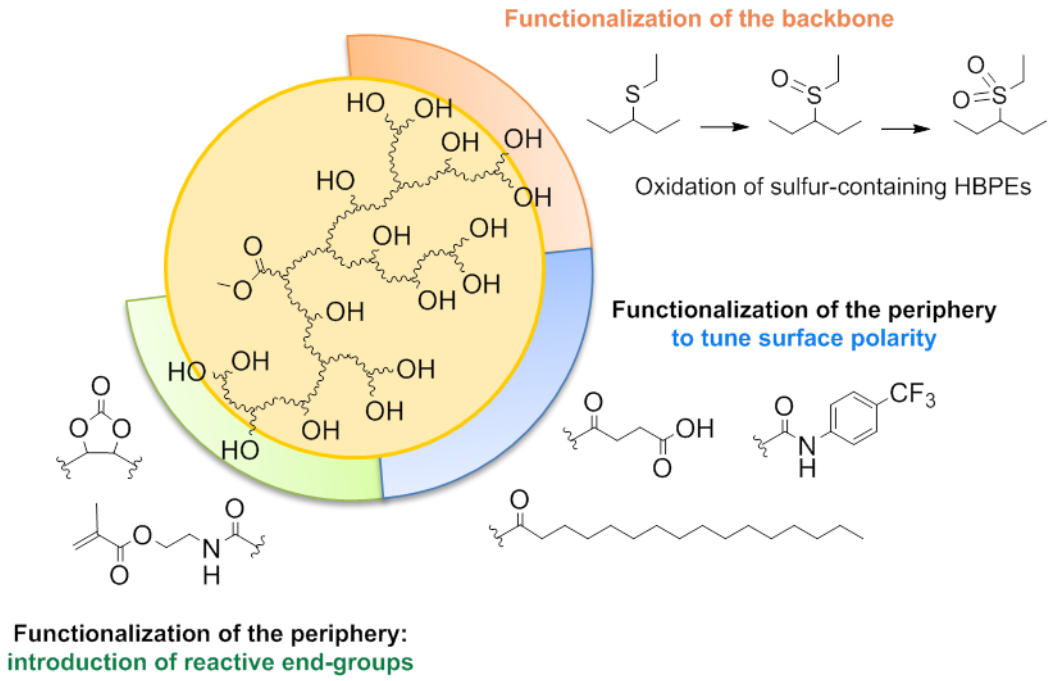

Table of Contents

Introduction

Over the past decade, great progress has been made in the functionalization of hyperbranched polymers (HBPs) from their periphery to their core.[1–3,4] The densely branched framework of these systems was described to confine the external reactive molecules from access thereby making the functionalization of the backbone more difficult than the periphery, though not impossible. Such chemical modifications were mainly reported on petroleum-based HBPs and involved a variety of simple and straightforward reactions. In particular, the use of click chemistries was extensively studied in recent years.[5,6] Modification of the core as well as the periphery of HBPs has been recognized to influence numerous of the physical and chemical properties of the as-derivatized HBPs, *i.e.* solubility, compatibility, thermal stability, crystallinity, as well as chemical recognition, adhesion to surfaces, self-assembly, etc. Functionalization of HBPs thus provides a powerful tool for tailoring structures and properties of these materials.

The present work constitutes a preliminary investigation into the functionalization of either the core or the periphery of some of the hyperbranched polyesters (HBPEs) synthesized in the previous chapters, with the idea of tuning their properties and thus broadening the scope of their applications. For that purpose, simple and as far as possible "green" processes, using mild organo-catalyzed reactions and bio-based reactants, were developed. First, functionalization of the backbone of sulfur-containing HBPEs developed in Chapter IV was examined by successive oxidations of the thioether linkages to sulfoxide and sulfone groups. Chemical modifications of the surface properties of HBPEs described in Chapter II were then conducted by introducing a variety of functional groups at the periphery, including some carboxylic acids, alkyl chains, fluoro-containing moieties, methacrylate and cyclic carbonate end-groups. Derivatizations of these hydroxyl-ended HBPEs mainly used traditional methods of ester and urethane syntheses. The structure of the functionalized HBPEs was determined by means of NMR and FT-IR spectroscopies. The impact of these chemical modifications was mostly studied on their solubility, thermal stability and thermo-mechanical properties.

1. Functionalization of the backbone

The presence of sulfur atoms in the main chain of our HBPEs, which were introduced by means of thiol-ene and transesterification reactions (Chapter IV), allowed us to post-functionalize their backbone by oxidation of the thioether groups to sulfoxides or sulfones (Scheme 0-1). Such modifications have already been described on linear oily-derived polymers, but have never been attempted on systems of hyperbranched architecture. The oxidation process was reported to impact the solubility of the resulting materials as well as their thermal stability and crystallinity. For instance, Du Prez and coworkers described the preparation of polyethylene-like polythioethers by thermal thiol-ene polyaddition of an α-olefinic ω-thiol monomer derived from 10-undecenoic acid and their subsequent oxidation with hydrogen peroxide.[7] While the polysulfoxide derivatives remained soluble in polar solvents such as DMF or DMSO, the polysulfone homologues could no longer be dissolved in any solvent tested. Cádiz and coworkers reported the synthesis of fully bio-based ABA triblock copolyesters bearing thioether linkages from PLA and castor oil derivatives.[8] The corresponding polysulfones showed improved thermal stability and decrease of crystallinity.

The following study was performed on HBPEs ($\overline{M}_n$ = 9 700 g.mol^{-1}, $Đ$ = 7.34, P1) prepared by polycondensation of M2H-Ric according to the procedure described in Chapter IV. These polyesters were modified to their polysulfoxide and polysulfone analogues by selective oxidation of thioether functionality. Insights into the fine structure of the oxidized products were investigated by means of NMR and FT-IR spectroscopies. Their thermal stability and thermo-mechanical properties were also analyzed by DSC and TGA.

1.1. Selective oxidation to polysulfoxides and polysulfones

According to previous literature, hydrogen peroxide alone is able to selectively oxidize thioethers to sulfoxide or sulfone groups, depending on the reaction temperature.[9] Indeed, with the same oxidizing agent, Meier and coworkers prepared the sulfoxide intermediate product of a FAME derivative, by carrying out the oxidation at room temperature; while the sulfone analogue was obtained by heating at 70°C. Partial hydrolysis of the ester group was however described to accompany the high temperatures; and further attempts to decrease the reaction temperature thereby minimizing this side reaction, resulted in incomplete conversions.

In the present work, oxidation of the sulfur-containing HBPEs to their polysulfoxide analogues (P2) was actually performed in the presence of 2 equivalents of hydrogen peroxide (30 wt% in H_2O) per sulfur atoms. The reaction was conducted in chloroform at room temperature for 24 hours. To avoid polymer degradation, alternative routes were considered for the formation of the sulfone derivatives (P3). The oxidation process was performed using *m*-chloroperbenzoic acid (*m*-cpba) in a thioether:*m*-cpba molar ratio of 1:2, in DCM as solvent at room temperature (Scheme 0-1).

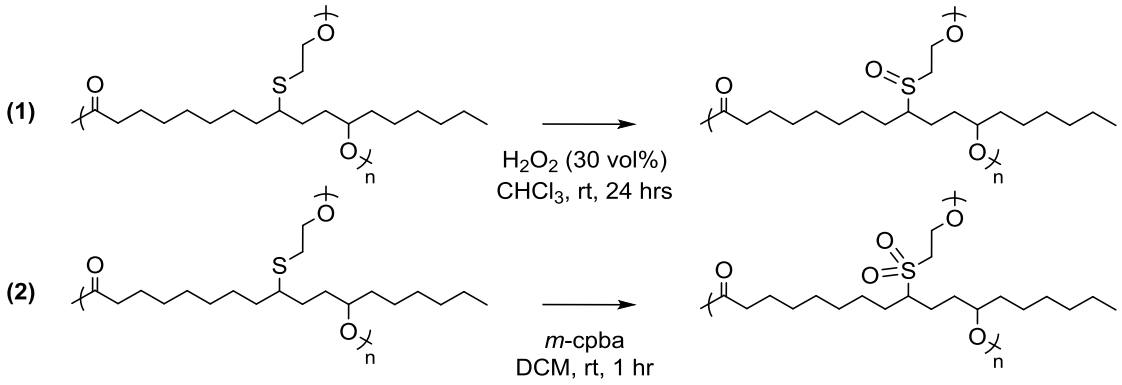

Scheme 0-1. Oxidation of sulfur-containing HBPEs to (1) polysulfoxide and (2) polysulfone derivatives

After work-up (see Experimental and Supporting Information), the chemical structure of the oxidized products was confirmed by FT-IR analyses (Figure 0-1). The formation of sulfoxide groups was stated by the appearance of a strong band at 1 018 cm^{-1} characteristic of the -S=O bond stretching. Its subsequent oxidation to polysulfones was assessed by the presence of two absorption bands at 1 118 and 1 282 cm^{-1}. Oxidations appeared in both cases selective since no absorption band characteristic of sulfone moieties was observed in the spectrum of the polysulfoxide analogue, and vice versa.

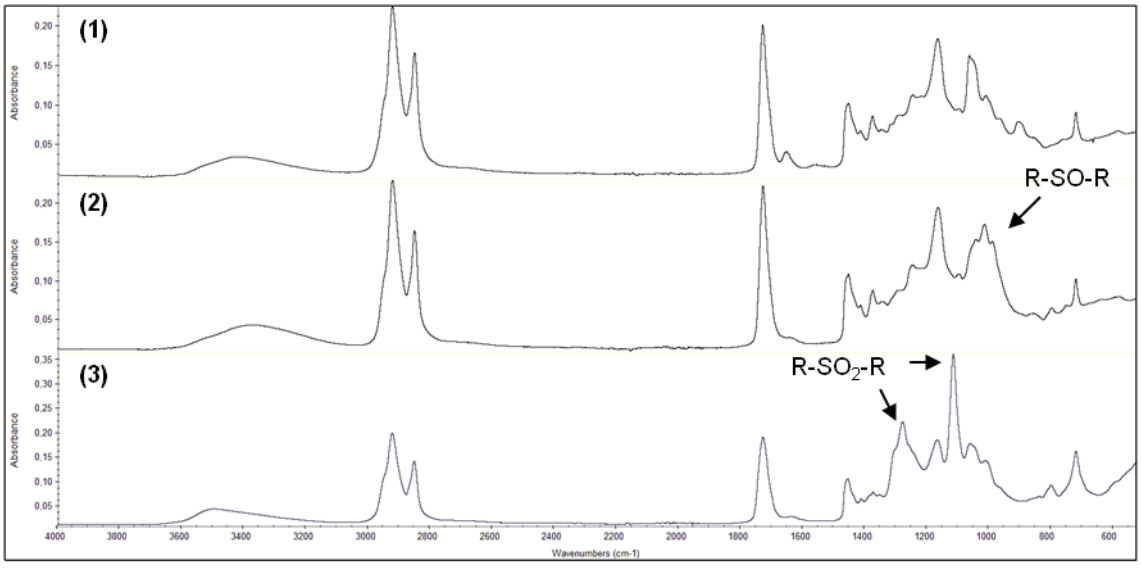

Figure 0-1. Stacked FT-IR spectra of (1) M2H-Ric based HBPEs, and its related (2) polysulfoxide and (3) polysulfone analogues

Oxidized polymers were characterized as well by ^{1}H NMR spectroscopy as both samples remained soluble in chloroform (Figure 0-2). No significant change was noticed after the oxidation to sulfoxides, which does not however mean that the reaction was not complete. The formation of sulfone moieties was confirmed by the downfield signals of the protons adjacent to the sulfur atoms including e_s, f_s and j_s to 3.40-2.80 ppm, and the methylene ones k_s in α-position of the primary alcohols to 4.50ppm. ^{1}H NMR spectrum of the hyperbranched polysulfones remains complex and further 2D NMR analyses would be required to assign all peaks.

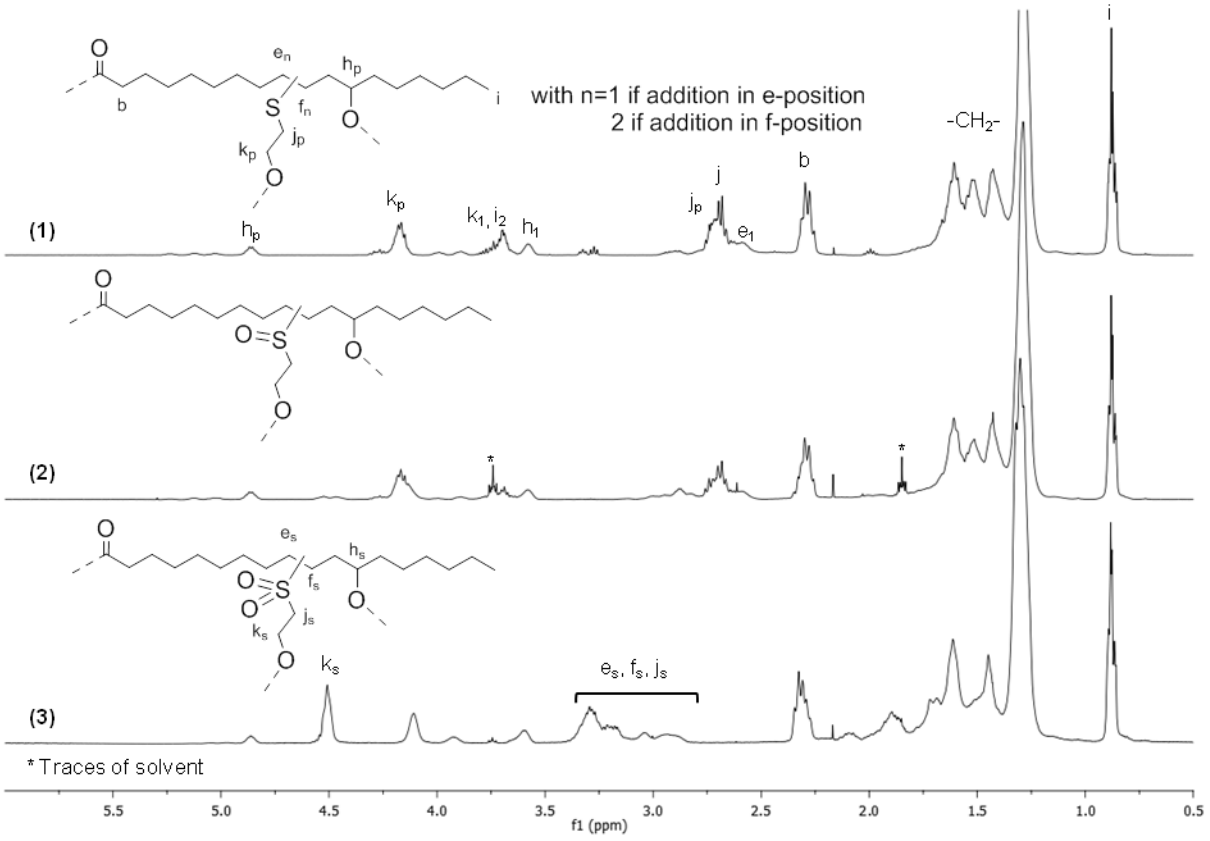

Figure 0-2. Stacked ^{1}H NMR spectra of (1) M2H-Ric based HBPEs and its related (2) polysulfoxide and (3) polysulfone analogues in $CDCl_3$

Rather low yields were however achieved (< 73%), suggesting the occurrence of degradation or cross-linking processes. This hypothesis was supported by SEC analyses. Table 0-I summarizes the macromolecular characteristics of hyperbranched polymers before and after oxidation. While the polysulfoxide analogue (P2) gave higher molar masses than P1, of 10 900 g.mol^{-1}, the polysulfone product (P3) displayed lower molar masses of 8 800 g.mol^{-1}. In both cases, the dispersity was noticed to decrease as well after oxidation.

Table 0-I. Macromolecular characteristics and thermal properties of M2H-Ric based HBPEs and its polysulfoxide and polysulfone analogues

Entry	Product	Yield (%)[1]	$\bar{M}_n$ [2] (g.mol^{-1})	$\bar{M}_w$ [2] (g.mol^{-1})	$Đ$[2]	T_g(°C)[3]	$T_d^{5\%}$(°C)[4]
P1	HBPE	/	9 700	71 200	7.34	-36	315
P2	HB polysulfoxides	73	10 900	55 900	5.13	-30	200
P3	HB polysulfones	64	8 800	35 600	4.04	-12	276

(1) Yield in wt% from starting material. (2) SEC in THF – calibration PS standards. (3) Determined by DSC from the second heating scan at 10°C.min^{-1}. (4) Determined by TGA.

It is noteworthy, that unlike previously described works on linear polymers, the oxidation process did not affect noticeably the solubility of the polysulfoxide and polysulfone derivatives. P2 and P3 indeed remained soluble in $CHCl_3$ and THF, allowing their full characterization. One can see here the influence of the hyperbranched architecture.

1.2. Thermal properties

Thermal properties of HBPEs were investigated by DSC experiments. Consecutive heating and cooling runs were performed at 10°C.min^{-1}. Glass transition temperatures were determined from the second heating scan. Results obtained are summarized in Table 0-I. Similarly to the starting raw material (P1), the oxidized forms (P2, P3) were amorphous (Figure 0-3). Higher glass transition temperatures of -30°C for the polysulfoxide analogue and -12°C for the polysulfone derivative were however achieved. This was easily explained by the increasing polarity of the sulfoxide and sulfone groups.

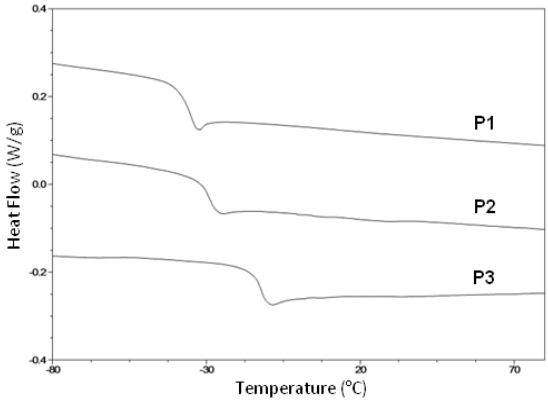

Figure 0-3. DSC thermograms at 10°C.min^{-1} of P1, P2 and P3

The thermal behavior of sulfur-containing HBPEs and their oxidized forms was comparatively studied by TGA under a nitrogen stream, at a heating rate of 10°C.min^{-1}. All polymers gave negligible weight residues, *i.e.* less than 2%. Data obtained are summarized in Table 0-I. The oxidation process was shown to decrease the thermal stability of the HBPEs as illustrated in Figure 0-4.

A common two-step pattern of decomposition was followed by all polymers, except for the hyperbranched polysulfoxide (P2). Its TGA derivative of weight loss as a function of the temperature indeed showed an additional degradation in between 150 and 200°C assigned to the thermolysis of the sulfoxide group.[10] This results in the formation an olefin and a sulfenic acid thereby decreasing the 5% degradation temperature of P2 to 200°C. This phenomenon was however not supported by DSC experiments, since the heating and cooling runs were performed from -100 to 100°C. In contrast to what had been previously reported in the literature regarding linear oily-derived polymers,[7,8] the hyperbranched polysulfone derivative also displayed a lower thermal stability than the starting HBPE with a $T_d^{5\%}$ of 275°C.

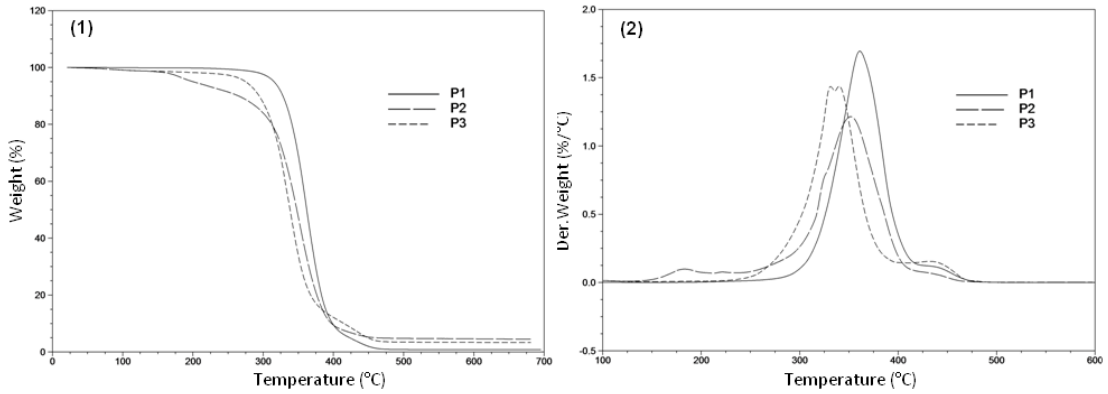

Figure 0-4. (1) Weight loss as a function of temperature (2) Derivative of weight loss with temperature for P1, P2 and P3 from TGA experiments at 10°C.min^{-1} under nitrogen atmosphere

To summarize, sulfur-containing HBPEs were oxidized to their polysulfoxide and polysulfone analogues, by reaction with two different oxidizing agents, *i.e.* H_2O_2 and *m*-cpba. FT-IR analyses evidenced the selectivity of such modifications. The synthesis of the oxidized products involved straightforward and inexpensive reactions easy to scale-up. The oxidation process did not affect the solubility of the HBPE derivatives in common solvents, like $CHCl_3$ and THF, allowing their full characterization. Hyperbranched polysulfoxides and polysulfones showed higher glass transition temperatures, and against all expectations, reduced thermal stabilities.

2. Functionalization of the periphery

The properties of polymeric materials are also influenced by their end-groups. In comparison to linear polymers, this effect is even more pronounced with HBPs due to their larger number of terminal functions and their exposed placement. A large proportion of the end-groups is indeed located on the periphery of the globular-shaped HBPs. It therefore appeared very interesting to chemically modify the corona of some HBPEs designed in this PhD work with the aim at broadening their range of properties and targeting specific applications.

The next section highlights the advances in the post-functionalization of some of the hydroxyl-terminated HBPEs developed in Chapter II, by polycondensation of M2HS. These substrates were preferred over others (Chapters III and IV), because their structure was fully elucidated by ^{1}H NMR spectroscopy. A close look at the literature regarding the derivatization of commercially available HBPE Boltorn® indicated that possibilities are manifold. Diverse functional groups such as carboxylic and sulfonic acids,[11] alkyl tails,[12–14] PLA[15] or PEG[16] chains, to only name a few, were successfully introduced in the periphery with different perspectives. Likewise, a series of chemical modifications of our compounds was envisaged in order to develop a versatile platform of HBPEs with tunable properties by derivatization (Scheme 0-2). Hydroxyl-ended HBPEs were modified either with carboxylic acid groups or with hydrophobic moieties, *i.e.* alkyl tails and fluoro-containing compounds, in order to tune their miscibility in aqueous or oily phases. Other more specific functionalities were brought such as methacrylate and cyclic carbonate end-groups. The effect of these chemical modifications was mainly studied on the solubility, thermal stability and thermo-mechanical properties of the functionalized HBPEs.

2.1. Chemical modification and characterization

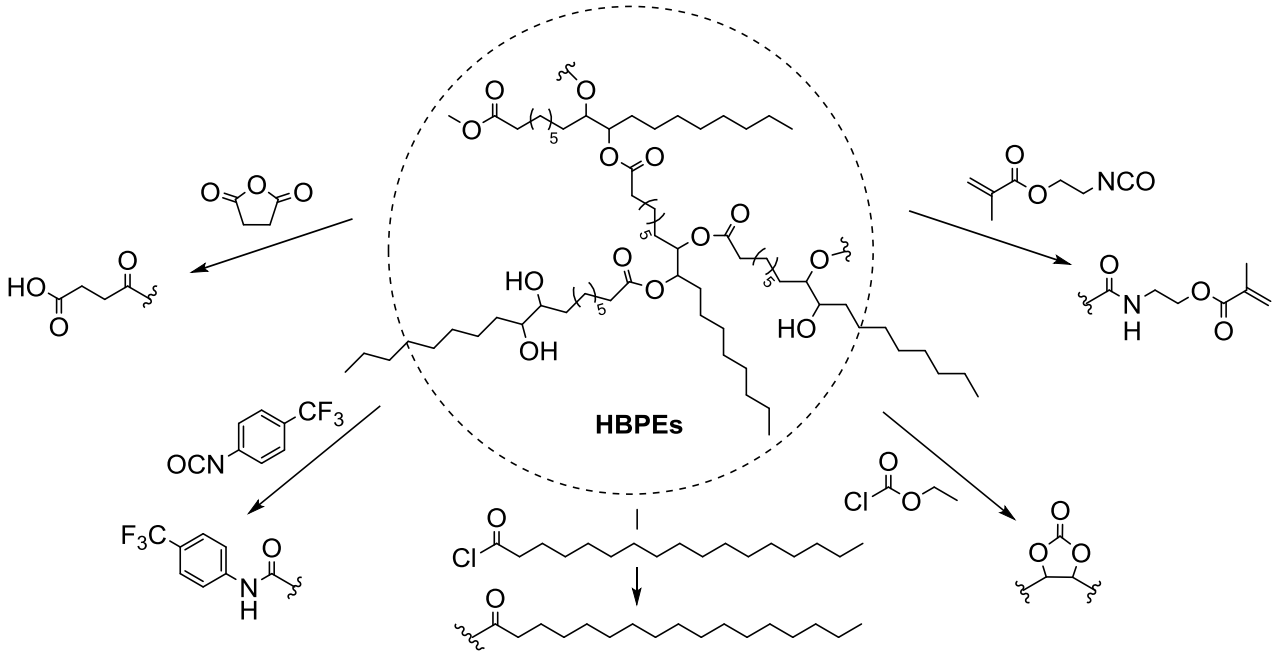

Scheme 0-2. Versatile platform of functionalized HBPEs developed by chemical derivatization

This study was performed with a HBPE sample ($\overline{M}_n$ = 2 800 g.mol^{-1}, $Đ$ = 1.97, DB = 0.14, P4) prepared at the ITERG center, on a 50 g scale, by polycondensation of M2HS using $Ti(OBu)_4$ as catalyst with a loading of 1 wt%. Its hydroxyl value determined according to the standard test method ASTMD 1957-86, reached 202.5 mg KOH/g.

Although a variety of chemical transformations can be employed for the functionalization of terminal hydroxyl groups, simple and efficient routes were preferred for this preliminary study. Derivatization of this hydroxyl-ended HBPE mostly involved traditional methods of ester and urethane syntheses. In addition, the 1,2-vicinal diols constituting the terminal units were selectively transformed into 5-membered cyclic carbonates. In all cases, the chemical structure of the modified HBPEs was assessed by means of NMR and FT-IR spectroscopies. Besides, since characterization of the macromolecular characteristics of HBPs remains a challenge, SEC analysis of the end-functionalized HBPEs is discussed in detail.

2.1.1. Esterification with carboxylic acids and derivatives

Hydroxyl-terminated HBPEs were first chemically modified with carboxylic acid moieties and alkyl tails. For that purpose, two different methods were employed. The introduction of carboxylic acid ended-moieties was performed by simply heating the HBPEs in presence of an excess of succinic anhydride (2 equivalents/OH groups), according to a procedure previously reported.[11] The esterification was carried out in solution. Various solvents of relatively low boiling point to facilitate the product purification were tested including THF, its methyl-analogue (*m*-THF) and toluene. In all cases, after 1 to 5 days depending on the reaction temperature, the unreacted succinic anhydride was removed by water washes (2 x 20 mL) and brine (1 x 20 mL). Esterified HBPEs were obtained as viscous liquids with more or less bright yellow shades.

Alkyl-terminated HBPEs were prepared by esterification with palmitoyle chloride in toluene as suggested in the literature.[13,14] Further addition of catalyst was however not required. The acyl chloride was introduced in 1.1 equivalents relatively to the OH groups, to prevent its partial hydrolysis by traces of water present within the reaction medium. The overall mixture was allowed to react at 80°C for 24 hours. After washing with water until neutral pH, one additional purification step was carried out in order to get rid of the residual traces of palmitic acid identified by NMR analyses, *i.e.* by addition of lithium hydroxide in THF as described in Chapter II. Alkyl terminated-HBPEs were afforded as colorless liquids, slightly less viscous than the starting material.

Figure 0-5 compares the ^{1}H NMR spectra of HBPEs before (1) and after modification with (2) succinic anhydride and (3) palmitoyl chloride. The partial esterification of the peripheral hydroxyl functions with carboxylic acid groups was stated by the decrease in the integral, or even the disappearance of the signals characteristics of the terminal units (H_a) at

3.39 ppm ,in favor of an increase in the molar ratio of the linear (H_b, H_c) or dendritic (H_d) ones. The methylene protons (H_s) of succinic anhydride were assigned to the multiplet centered at 2.68 ppm. The hydrogen of the carboxylic acid function was not always detected and its chemical shift varied from one analysis to the other. In contrast, its carbonyl carbon (-**C**OOH) could be distinguished from the ester ones (-**C**OOR) in ^{13}C NMR spectroscopy at 172 and 174 ppm, respectively (see supporting information, Figure SI 0-1).

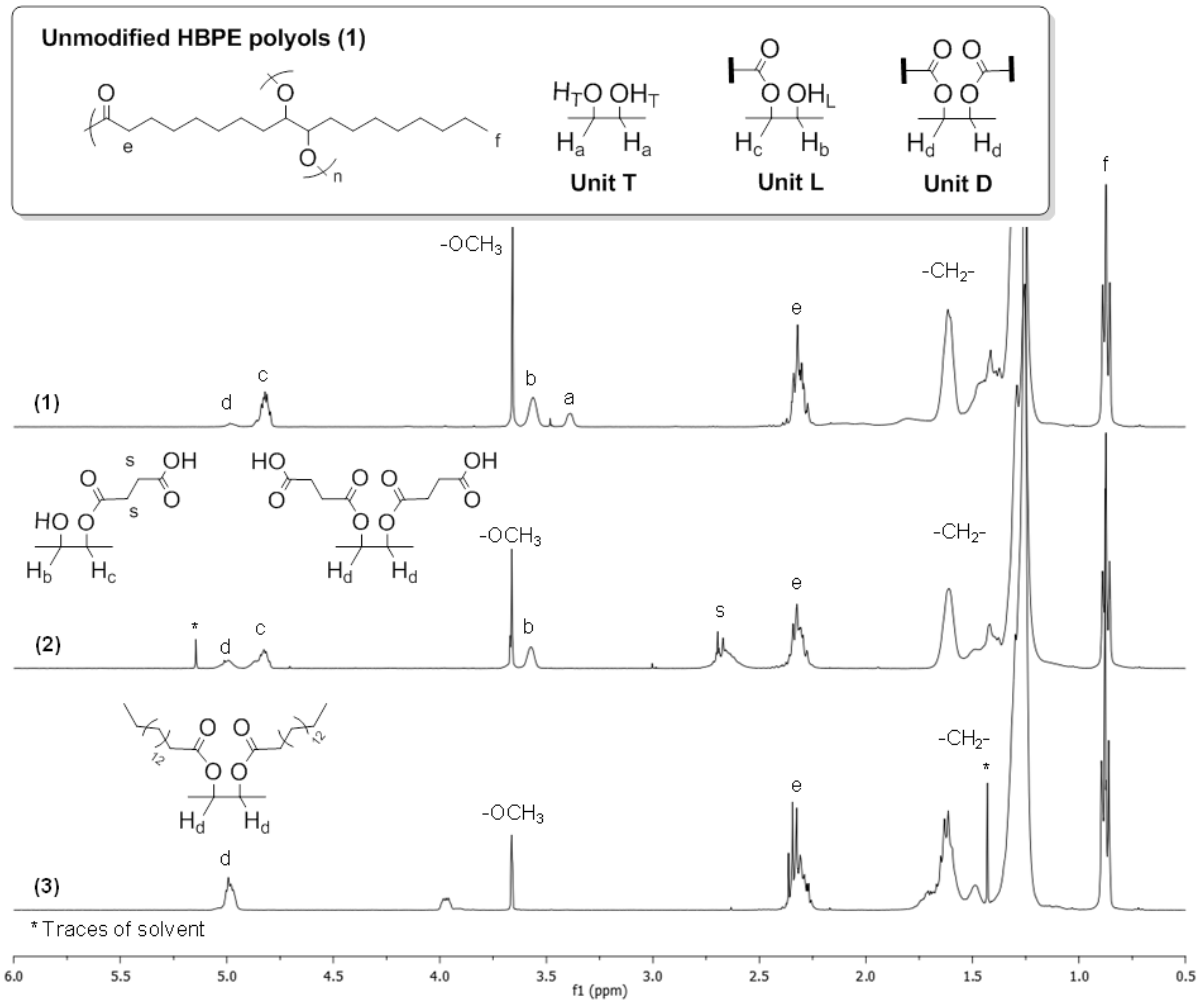

Figure 0-5. Stacked ^1H NMR spectra of HBPEs (1) before and after modification with (2) succinic anhydride and (3) palmitoyl chloride in $CDCl_3$

The chemical composition of the different carboxylic acid-terminated HBPEs thus prepared is summarized in Table 0-II. Values for T, L and D were determined by ^1H NMR spectroscopy, based on the respective integrations of the protons H_a, H_c and H_d. The degree of functionalization by esterification (*f*) was assessed using the signal intensities of the terminal and linear units. Whatever the conditions tested, the degree of functionalization *f* did not exceed 35% even after prolonged reaction times.

This was assigned to the low reactivity of the secondary alcohols bearing by M2HS-based HBPEs. Indeed, in similar conditions, Meng and coworkers managed to esterify in between 60 to 80% of the primary hydroxyl functions of the commercially available hyperbranched aliphatic polyester Boltorn® H20 (Perstorp Co.).[11] In addition, peripheral hydroxyl functions of M2HS-based HBPEs are more sterically hindered making their functionalization more difficult. Hence, the esterification process set up would need to be further optimized. For instance, higher reaction temperatures or further addition of a catalyst may be considered. In all cases, one particular attention would have to be paid to the reaction solvent whose influence should not be overlooked.

Table 0-II. Esterification of P4 with succinic anhydride: experimental condition screening

Entry	Solvent	T(°C)	Duration (days)	T^1	L^1	D^1	f^1 (%)
P4	/	/	/	0.13	0.71	0.04	/
P5	Toluene	90	1	0	0.67	0.22	31
P6	Toluene	90	3	0	0.64	0.23	35
P7	THF	60	3	0.02	0.82	0.05	12
P8	m-THF	70	5	0	0.85	0.06	13

(1) determined by ^{1}H NMR

In contrast, complete esterification of peripheral hydroxyl functions was achieved with palmitoyl chloride, as indicated by the disappearance of the signals assigned to both the terminal and linear units in ^{1}H NMR (Figure 0-5 (3)). FT-IR analyses confirmed a degree of functionalization of 100% since no absorption band characteristics of the hydroxyl functions was observed above 3 200 cm^{-1} (see supporting information, Figure SI 0-2). This indicated the accessibility of all OH groups of M2HS-based HBPEs for functionalization.

However, the integration of protons H_d did not reach the maximum value of 0.92, *i.e.* T+L+D = 0.92 for P4. In addition, the appearance of a multiplet was noted at 3.98-3.95 ppm. 2D NMR techniques were carried out to assign this signal (see supporting information, Figure SI 0-3). ^{1}H-^{13}C HSQC and DEPT-135 analyses revealed that these protons were directly attached to tertiary carbon atoms, with chemical shift of 64 ppm. This additional signal could arise from etherification side reactions (as discussed in Chapter III), to the extent of 31%, that were catalyzed by the hydrochloric acid formed as by-product of the esterification with an acyl chloride. Similarly to the close study detailed in Chapter III, MALDI-TOF MS should be conducted to validate or reject this hypothesis.

2.1.2. Carbonation of hydroxyl ended-moieties

Following the idea of tuning the surface properties of M2HS-based HBPEs, the 1,2-vicinal diols constituting their terminal units were selectively transformed into five-membered cyclic carbonates (5CC). Carbonation was performed using ethyl chloroformate and a stoichiometric amount of triethylamine (TEA) as deprotonating agent in THF, in dilute conditions according to previous literature (Scheme 0-3).[17] This route was preferred over non-phosgene method due to the higher conversion achieved. The reaction was indeed first attempted with dimethyl carbonate (DMC) under milder conditions using K_2CO_3 as catalyst but met with limited success.[18]

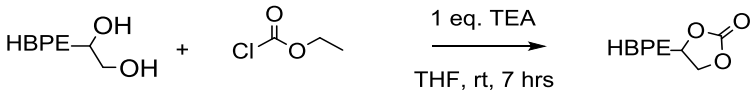

Scheme 0-3. Selective cyclization of 1,2-vicinal diols with ethyl chloroformate

Ethyl chloroformate was carefully added at 0°C and the reaction mixture was stirred at ambient temperature for 7 hours. After filtration of the precipitated TEA hydrochloride and water washes, the functionalized HBPE was obtained as a yellow viscous liquid, similarly to the starting material. The selective and complete carbonation of the 1,2-vicinal diols was confirmed in ^{1}H NMR, through the downfield shift of the protons in α-position of the terminal hydroxyl functions (H_{CC}) to 4.22 ppm after the formation of the 5CC moieties (Figure 0-6). Integrals of the linear units remained unchanged indicating that no linear carbonate was formed during the functionalization. The formation of 5CC was also stated in ^{13}C NMR spectroscopy, through the appearance of a signal at 155 ppm assigned to the carbonyl atom of carbonate groups.

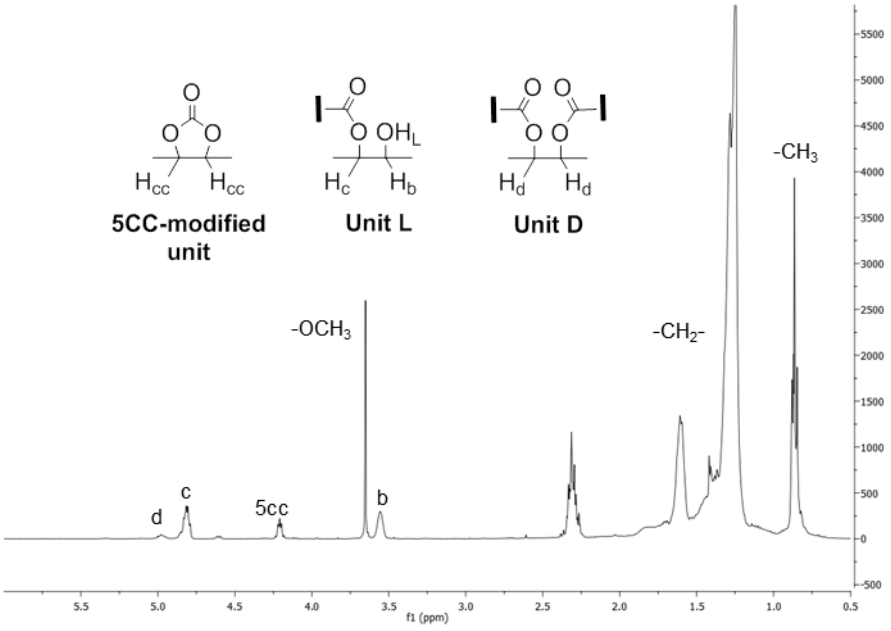

Figure 0-6. ^{1}H NMR spectrum of a HBPE modified with 5CC-ended moieties in $CDCl_3$

In FT-IR spectroscopy, after modification, an additional absorption band, characteristic of the cyclic carbonate moiety, was observed in the region of carbonyl groups, at 1 805 cm^{-1}. ^{13}C NMR and FT-IR spectra of the functionalized HBPE are given in supporting information (Figure SI 0-4 and Figure SI 0-5).

2.1.3. Addition of functional isocyanates

The second route investigated to modify the hydroxyl-ended HBPEs consisted in the addition of functional isocyanates *via* the formation of urethane linkages. The introduction of methacrylate and fluoro-containing moieties in periphery of P4 was thus carried out by reaction with 2-isocyanatoethyl methacrylate (IEMA) and 4-(trifluoromethyl)phenyl isocyanate (4TFPI).

Scheme 0-4. Modification of hydroxyl-terminated HBPEs by IEMA and 4TFPI

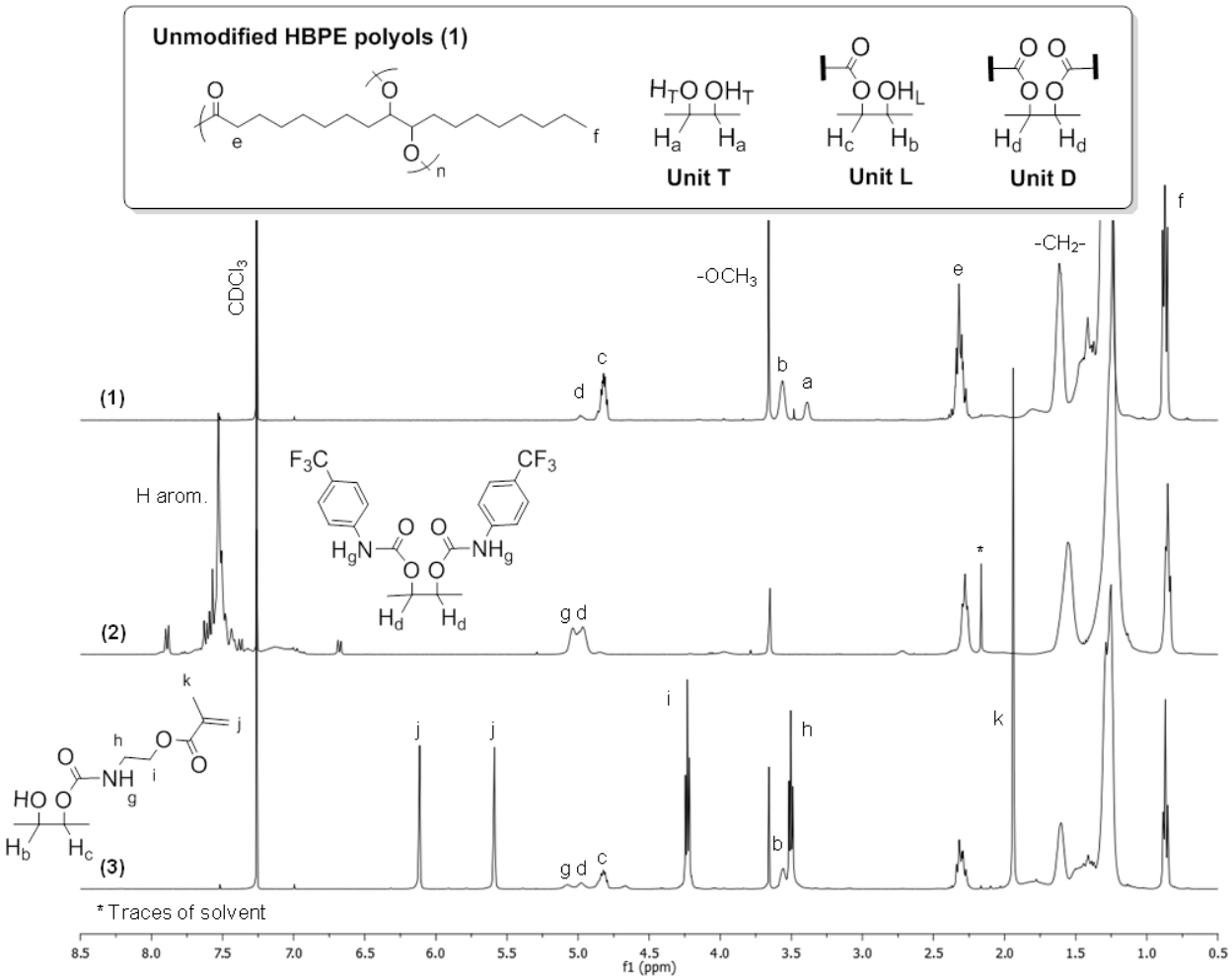

Figure 0-7. Stacked ^{1}H NMR spectra of HBPEs (1) before and after modification with (2) 4TFPI and (3) IEMA in $CDCl_3$

Additions were conducted in dichloromethane at room temperature according to previous literature (Scheme 0-4).[19] A slight excess of functional isocyanate (1.02 equivalents/OH groups) was used to drive the reaction to completion and triethylamine (TEA) was added as catalyst (10 mol%). Overall mixtures were allowed to react during 20 hours, after what unreacted IEMA and 4TFPI were respectively removed by precipitation in heptane and washes with DMF.

^{1}H NMR spectra of HBPEs before (1) and after modification with (2) 4TFPI and (3) IEMA are given in Figure 0-7. Aromatic protons observed above 7 ppm confirmed the incorporation of 4TFPI at the periphery of the HBPEs. The disappearance of the signals characteristics of both the terminal (H_a) and linear (H_b, H_c) units demonstrated the complete functionalization of the terminal hydroxyl functions. Evidence of the formation of urethane linkages was brought by the appearance of one signal at 5.04 ppm assigned to the urethane proton (-NH_g). The chemical structure of the functionalized HBPE was supported as well by FT-IR analyses (Figure 0-8). Characteristic absorption bands of urethane linkage appeared at 1 651 cm^{-1} (**O=C**-NH) and 1 540 cm^{-1} (**C-N**-H). Stretching bands detected at 1 601 and 1 411 cm^{-1} were assigned to the aromatic rings. As the functionalization was complete, the narrower band observed at 3 321 cm^{-1} was attributed to N-H stretching vibrations.

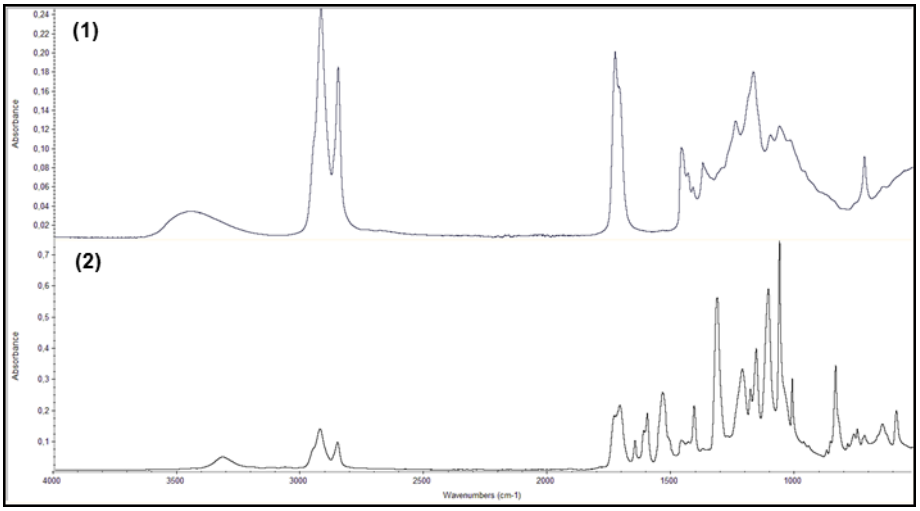

Figure 0-8. Stacked FT-IR spectra of HBPEs before (1) and after (2) modification with 4TFPI

Regarding the addition of IEMA, protons corresponding to the methacrylate moieties H_h, H_i, H_j and H_k were identified (Figure 0-7). Their high intensity was in fact due to the poor efficiency of the purification procedure set up. Signals characteristic of the linear units (H_b and H_c) were still visible, confirming the low degree of functionalization.

This result was assigned to the lower reactivity of aliphatic isocyanates compared to aromatic ones, the driving force of the addition being governed by the positive character of the carbon atom. Moreover, the nature of the aromatic substituent plays an important role. In this case, the presence of one electron-attracting group (-CF_3) in *para* position increased the relative reactivity of 4TFPI.

The addition of IEMA would require further optimization. Higher reaction temperatures should be considered to increase the degree of functionalization, thereby synthesizing HBPEs with polymerizable end groups.

2.1.4. Molar masses and molar mass distribution of modified HBPEs

Macromolecular characteristics of HBPEs before and after modification were investigated by means of SEC in THF, equipped with a differential RI detector (PS calibration). Only the sample functionalized with IEMA was not characterized due to its questionable purity. Table 0-III summarizes the results obtained. All chromatograms were shown to follow the same pattern indicating that no coupling reaction *via* esterification of the free carboxylic acid end-groups or ring-opening of the 5-membered cyclic carbonates occurred. In addition, the dispersity remained constant after modification, or even slightly decreased in some cases, probably due to fractionation during the purification steps. Interestingly, while P9, P10 and P11 reached higher molar masses than P4 as expected, *i.e.* in between 2 900 and 3 600 g.mol^{-1}, P5 displayed lower molar masses of 1 500 g.mol^{-1}.

Table 0-III. Macromolecular characteristics of derivatized HBPEs

Entry	Nature of the en-groups	$\bar{M}_n$ [1] (g.mol^{-1})	$\bar{M}_w$ [1] (g.mol^{-1})	$Đ$[1]
P4	-OH	2 800	5 600	2.00
P5	-COOH	1 500	2 150	1.43
P9	-$CO(CH_2)_{14}CH_3$	2 900	5 800	2.00
P10	5CC	3 300	6 000	2.00
P11	-$PhCF_3$	3 600	6 300	1.75

(1) determined by SEC in THF – calibration PS standards.

The observed decrease in the molar masses of the carboxylic acid-ended HBPEs was not assigned to the occurrence of degradation or cross-linking, since the esterification reaction was conducted in rather mild conditions. We hypothesized that the polarity of the end-groups grafted in periphery of M2HS-based HBPEs influence to some extent the material density. In this sense, the introduction of polar end-groups such as carboxylic acids could be the cause of an increased compacity of the polymer coils in solution; whereas the modification with more

or less hydrophobic moieties, *i.e.* alkyl tails, 5-membered cyclic carbonates, trifluorophenyl-moieties, could expand the HBPE macromolecules in solution. This scenario was considered with caution knowing that the reliability of molar mass characterization of HBPs by SEC using differential RI detector remains questionable as demonstrated in Chapter II. Further investigations by SEC coupled with MALLS detector would provide useful additional information, this technique giving access to the absolute molar masses of HBPEs as well as their radii of gyration.

In brief, numerous functional groups of diverse polarity including some carboxylic acids, alkyl tails, fluoro-containing compounds, methacrylate and cyclic carbonate moieties, were introduced at the periphery of M2HS-based HBPEs. Different synthetic approaches were implemented to this end. Complete conversions of the terminal hydroxyl functions were achieved by esterification with palmitoyl chloride and addition of 4TFPI. Preliminary tests performed by esterification with succinic anhydride and addition of IEMA established the proof-of-concept, but yielded only low degrees of functionalization. These routes would require further optimization. Lastly, the 1,2-vicinal diols were selectively transformed into 5-membered cyclic carbonates (5CC) by reaction with ethyl chloroformate. In the next section, the impact of such modifications was investigated on the thermal properties of the as-derivatized HBPEs, as well as their water-solubility.

2.2. Water-solubility

The introduction of carboxylic acid ended-moieties in periphery of M2HS-based HBPEs was indeed conducted with the aim at providing a higher water affinity to these lipophilic materials. The so-formed amphiphilic systems may find potential applications for encapsulation of hydrophobic actives, *e.g.* in cosmetics (creams, sprays, gels,), etc. The low degrees of functionalization achieved in the course of this study ($f \leq 35\%$) explained that the architectures tested at the LCPO, namely P5 and P6, failed to be water-soluble.

However, particular attention must be paid to the promising results recently obtained at the *ITERG* technical center. On site, the same batch of hydroxyl-terminated HBPE (P4) was esterified with succinic anhydride (2 equivalents/OH groups) in DMF at a higher temperature of 150°C as previously suggested. After water washes, extractions with ethyl acetate and subsequent drying under reduced pressure, a brown and viscous liquid was obtained. The success of the functionalization was assessed by a decrease in the hydroxyl value of the material from 202.5 to 94.3 mg KOH/g after modification and an increase in its acid value from 1.12 to 91.36 mg KOH/g.

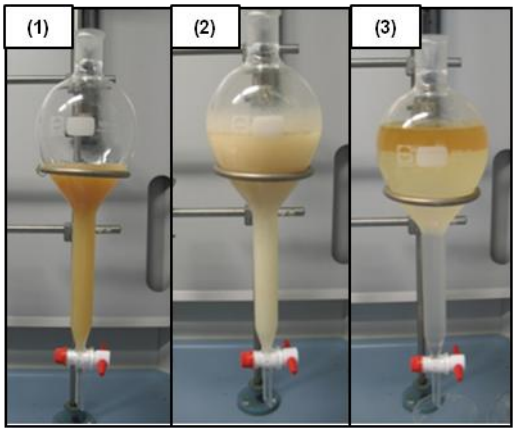

Figure 0-9. Tests of solubilization in water at different pH values: (1) dissolution in basic solution of 0.1 mol.L^{-1} K_2CO_3, (2) acidification with HCl solution of 0.1 mol.L^{-1} and (3) extraction with ethyl acetate

Solubility tests showed that the water solubility of the functionalized HBPE was pH-dependent. Indeed, the carboxylic acid-ended HBPE proved to be water-dispersible at basic pH (Figure 0-9 (1)). Acidification with a hydrochloric acid solution yielded a white emulsion as observed in Figure 0-9 (2). Subsequent extractions with ethyl acetate enabled to recover 93% in weight of the polymer initially introduced. In Figure 0-9 (3), the coloration of the organic phase is clearly observed during the extraction.

Although a lot is still to be done (optimization of the degree of functionalization, study of the micellar behavior of these amphiphilic polymers, etc.), preliminary results obtained are quite promising. The same strategy may be implemented to the design of other core-shell structures, by introducing some peripheral amino-acid or sugar moieties, and even PEG chains for their bio-compatible character.

2.3. Thermal properties

Excepted the sample modified with IEMA whose purity was not controlled, thermal properties of the diverse functionalized HBPEs were investigated by DSC experiments. Glass transition and melting temperatures were determined from the second heating run at 10°C.min^{-1}. Results obtained are given in Table 0-IV. As highlighted in previous chapters, the glass transition temperature of HBPEs with a large number of terminal hydroxyl functions is governed by their hydrogen bonding arrays. Partial or total substitution of the hydroxyl end-groups can thus have dramatic impact on T_g values.

Table 0-IV. Thermal properties of derivatized HBPEs

Entry	Nature of the end groups	DSC			TGA
		T_g (°C)	T_m (°C)	T_c (°C)	$T_d^{5\%}$ (°C)
P4	-OH	-30	/	/	248
P5	-COOH	-29	/	/	257
P7	-COOH	-34	/	/	252
P9	$-CO(CH_2)_{14}CH_3$	-53	-18.1	nd.	296
P10	-5CC	-40	/	/	231
P11	$-PhCF_3$	17	/	/	/

As can be seen in Table 0-IV, an overall decrease in the glass transition temperature was noted after modification, except for P11. The presence of fluorine atoms combined with the aromatic structure provided rigidity to the macromolecules, justifying the observed increase in the glass transition temperature up to 17°C. Besides, partial esterification of peripheral hydroxyl groups with succinic anhydride hardly affected the T_g values, since carboxylic acid moieties take part in the hydrogen bonding network.

In contrast, the lowest T_g value of -53°C (*vs.* -30°C for P4) was achieved with the alkyl-terminated HBPE (P9). In this particular case, a melting peak was also observed to accompany the decrease in the glass transition temperature (Figure 0-10). This phenomenon has already been reported in the literature for hyperbranched polyesters[12] and polyethers.[20] The attachment of alkyl chains was indeed shown to enhance the flexibility and induce crystallinity as well for chain lengths exceeded 12 to 14 carbon atoms. The crystallization was suggested to be an end-group phenomenon leaving the hyperbranched amorphous skeleton unaffected. In other words, the introduction of long alkyl chains could allow the formation of core-shell like structures with a crystalline surface and an amorphous core. A complex melting pattern was observed, likely due to the HBPE core disturbing considerably crystal formation. The crystallization being partly overlapped by the glass transition, T_c value was not determined.

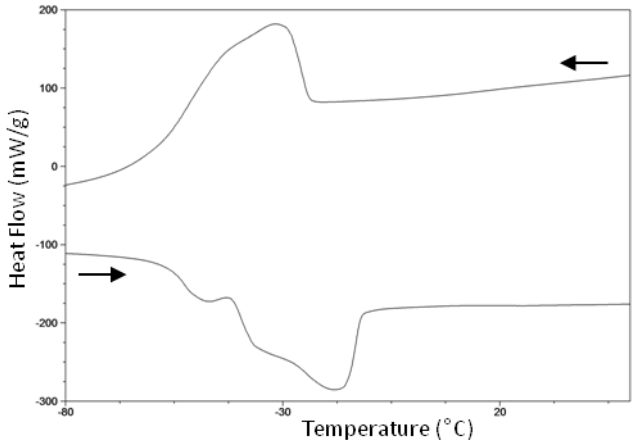

Figure 0-10. DSC thermogram of a HBPE modified with palmitoyl chloride

Thermal stability of derivatized HBPEs was investigated by TGA analyses under a nitrogen stream, at a heating rate of 10°C.min^{-1}. Data obtained are also summarized in Table 0-IV. The low 5% weight loss degradation temperature of the starting material (P4) was justified by the presence of residual traces of $Ti(OBu)_4$, which similarly to zinc acetate (see Chapter II), could catalyze the HBPE depolymerization. Overall, the functionalization of HBPEs led to an increase in the 5% weight loss degradation temperatures up to 296°C. P10 displayed the lowest $T_d^{5\%}$ value of 231°C probably due to the low thermal stability of 5-membered cyclic carbonates.

Conclusion

Examples of functionalization of both the core and the periphery of some of the HBPEs developed in this PhD work were presented, demonstrating the huge potential of these materials. Sulfur-containing HBPEs prepared by polycondensation of M2H-Ric were successively oxidized into their polysulfoxide and polysulfone analogues, while hydroxyl-ended HBPEs derived from M2HS were derivatized with different functional groups of various polarity including some carboxylic acids, alkyl tails, fluoro-containing compounds, methacrylate and 5-membered cyclic carbonate moieties. Such modifications were shown to affect the glass transition temprature of the related HBPEs, T_g values ranging from -53 to 17°C. In addition, side-chain crystallization was induced with long alkyl segments, *i.e.* number of methylene groups above 12. Derivatization with succinic anhydride imparted an amphiphilic character to the materials, allowing differentiation between a HBPE hydrophobic core and an hydrophilic shell created by the carboxylic acid groups. In addition, these carboxyl-terminated HBPEs were easily converted to their potassium salts enabling their dispersion in water.

This part of the work thus demonstrated the scope of tailoring HBPE structures and properties by means of derivatization. Simple and straightforward routes were established to tune the molecular architecture of HBPEs, thereby targeting specific applications. While carboxyl-ended HBPEs may find interesting uses in active delivery applications (host carriers of hydrophobic matter and drugs through water media), HBPEs modified with long alkyl tails could be employed as blend components in oily matrices, *e.g.* rheology modifiers, viscosity improvers. The introduction of reactive end-groups such as methacrylate or 5-membered cyclic carbonate moieties could finally be of great interest to compatibilize the HBPEs with PMMA or epoxy-matrices. Possibilities are manifold, all the more so these modifications were illustrated on substrates derived from M2HS and M2H-Ric but can be extended to the other HBPEs prepared during this thesis work.

References

(1) Inoue, K. *Prog. Polym. Sci.* **2000**, *25* (4), 453–571.
(2) Gao, C.; Yan, D. *Prog. Polym. Sci.* **2004**, *29* (3), 183–275.
(3) Voit, B. I.; Lederer, A. *Chem. Rev.* **2009**, *109* (11), 5924–5973.
(4) Yan, D.; Gao, C.; Frey, H. *Hyperbranched polymers Synthesis, Properties, and Applications*; John Wiley & Sons, Inc., 2011.
(5) Li, S.; Han, J.; Gao, C. *Polym. Chem.* **2013**, *4*, 1774–1787.
(6) Zheng, Y.; Li, S.; Weng, Z.; Gao, C. *Chem. Soc. Rev.* **2015**, *44*, 4091–4130.
(7) Van den Berg, O.; Dispinar, T.; Hommez, B.; Du Prez, F. E. *Eur. Polym. J.* **2013**, *49* (4), 804–812.
(8) Beyazkilic, Z.; Lligadas, G.; Ronda, J. C.; Galià, M.; Cádiz, V. *Polymer* **2015**, *68* (0), 101–110.
(9) Montero de Espinosa, L.; Gevers, A.; Woldt, B.; Grab, M.; Meier, M. A. R. *Green Chem.* **2014**, *16*, 1883–1896.
(10) Cubbage, J. W.; Guo, Y.; Mcculla, R. D.; Jenks, W. S. *J. Org. Chem.* **2001**, *66* (26), S4–S5.
(11) Meng, Q.; Chen, D.; Yue, L.; Fang, J.; Zhao, H.; Wang, L. *Macromol. Chem. Phys.* **2007**, *208* (5), 474–484.
(12) Malmström, E.; Johansson, M.; Hult, A. *Macromol. Chem. Phys.* **1996**, *197* (10), 3199–3207.
(13) Ornatska, M.; Peleshanko, S.; Genson, K. L.; Rybak, B.; Bergman, K. N.; Tsukruk, V. V. *J. Am. Chem. Soc.* **2004**, *126* (31), 9675–9684.
(14) Ornatska, M.; Bergman, K. N.; Goodman, M.; Peleshanko, S.; Shevchenko, V. V.; Tsukruk, V. V. *Polymer* **2006**, *47* (24), 8137–8146.
(15) Mesias, R.; Murillo, E. A. *J. Appl. Polym. Sci.* **2015**, *132* (10), 41589–41598.
(16) Tu, C.; Zhu, L.; Qiu, F.; Wang, D.; Su, Y.; Zhu, X.; Yan, D. *Polymer* **2013**, *54* (8), 2020–2027.
(17) Maisonneuve, L.; Wirotius, A.; Alfos, C.; Grau, E.; Cramail, H. *Polym. Chem.* **2014**, *5*, 6142–6147.
(18) Rokicki, G.; Rakoczy, P.; Parzuchowski, P.; Sobiecki, M. *Green Chem.* **2005**, *7* (7), 529–539.
(19) Ma, X.; Tang, J.; Shen, Y.; Fan, M.; Tang, H.; Radosz, M. *J. Am. Chem. Soc.* **2009**, *131* (41), 14795–14803.
(20) Sunder, A.; Bauer, T.; Mülhaupt, R.; Frey, H. *Macromolecules* **2000**, *33* (4), 1330–1337.

Experimental methods

Oxidation of M2H-Ric derived HBPEs: synthesis of hyperbranched polysulfoxides

M2H-Ric derived HBPE (0.45 g, 1.25 mmol) was dissolved in chloroform (40 mL/g of product) and subsequently a solution of hydrogen peroxide (30 wt%, 0.30 mL) was added to the reaction flask. The mixture was stirred at room temperature during 24 hours. The organic phase was then washed with aqueous solutions of sodium bicarbonate $NaHCO_3$ (2 x 20 mL) and brine (1 x 20mL), dried over anhydrous magnesium sulfate and filtered. After the removal of $CHCl_3$ under reduced pressure, the polysulfoxide product was obtained as a white wax. Yield: 73%.

Oxidation of M2H-Ric derived HBPEs: synthesis of hyperbranched polysulfones

M2H-Ric derived HBPE (0.48 g, 1.33 mmol) was dissolved in dichloromethane (20 mL/g of product) and subsequently, 3-chloroperbenzoic acid (0.66 g, 2.87 mmol) was added to the reaction flask. The mixture was stirred at room temperature during one hour. As the reaction was going on, 3-chlorobenzoic acid formed as co-product precipitated in DCM. The reaction mixture was then filtered, washed with aqueous sodium sulfite Na_2SO_3 (5 wt%, 2 x 20 mL), aqueous sodium bicarbonate $NaHCO_3$ (2 x 20 mL) and brine (1 x 20mL). The organic phase was dried over anhydrous magnesium sulfate, filtered and DCM was removed on a rotary evaporator to afford the polysulfone product as a white wax. Yield: 64%.

After work-up, hyperbranched polysulfoxides and polysulfones were obtained as sticky and cohesive waxes. Interestingly, hydrogen peroxide and *m*-cpba played a bleaching role eliminating most of the brownish color of the starting HBPEs, which is of high interest from an industrial point of view.

Esterification of M2HS-based HBPEs with succinic anhydride: synthesis of carboxyl-ended HBPEs

M2HS-based HBPEs (0.49 g) and succinic anhydride (0.37 g, 3.69 mmol) were dissolved in toluene (10 mL). The overall mixture was stirred at 90°C during 24 to 72 hours after which the unreacted succinic anhydride was removed by washes with water (2 x 20 mL) and brine (1 x 20 mL). The organic phase was then dried over anhydrous magnesium sulfate, filtered and toluene was removed on a rotary evaporator to afford the functionalized HBPE as a viscous liquid with more or less bright yellow shades.

Esterification of M2HS-based HBPEs with palmitoyl chloride: synthesis of alkyl-terminated HBPEs

M2HS-based HBPEs (0.47 g) and palmitoyl chloride (0.26 g, 2.20 mmol) were dissolved in toluene (10 mL). The overall mixture was stirred at 90°C during 24 hours after which the organic phase was washed with water until the pH became neutral. The excess of palmitoyl chloride present under its acidic form was removed by addition of lithium hydroxide in solution of THF according to the procedure described in Chapter II. Alkyl-terminated HBPE was obtained as a colorless viscous liquid.

Cyclization of the 1,2-vicinal diols: synthesis of HBPEs with cyclic carbonate end-groups

M2HS-based HBPEs (0.49 g) and triethylamine (0.18 g, 1.78 mmol) were dissolved in THF (20 mL). The subsequent addition of ethyl chloroformate (0.21 g, 1.94 mmol) was performed at 0°C. The reaction mixture was then stirred at room temperature during 7 hours, after which the precipitated triethylamine hydrochloride was filtered off and the filtrate was concentrated under vacuum. DCM was added to the crude product and the functionalized HBPE was then purified by washes with water (2 x 20 mL) and brine (1 x 20 mL). The organic phase was dried over anhydrous magnesium sulfate, filtered and DCM was removed on a rotary evaporator to afford HBPE-5CC as a yellow viscous liquid.

General procedure for the addition of functional isocyanates: synthesis of HBPEs with triflurophenyl- and methacrylate-ended moieties

M2HS-based HBPEs (0.49 g), the functional isocyanate (1.02 equivalents/OH groups) and triethylamine (18 mg, 0.018 mmol) were dissolved in DCM (10 mL). The overall mixture was allowed to react at ambient temperature during 20 hours, after which the organic phase was washed with water to get rid of the tertiary amine.

Addition of 4TFPI: 4-(trifluoromethyl)phenyl isocyanate (0.37g, 1.98 mmol). Excess of 4TFPI was removed by extraction with DMF affording trifluorophenyl-ended HBPE as white solid.

Addition of IEMA: 2-isocyanatoethyl methacrylate (0.28 g, 1.80 mmol). Unreacted IEMA was removed by precipitation in hexane (2-3 times). Methacrylate-ended HBPE was obtained as white gel-like material.

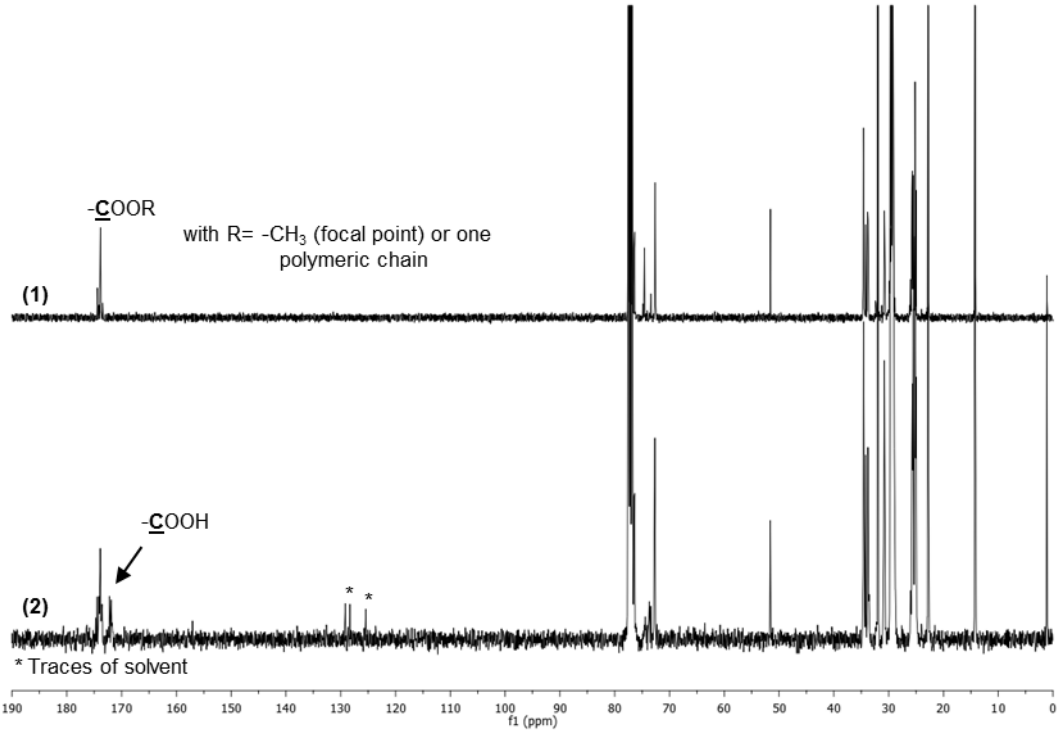

Figure SI 0-1. Stacked ^{13}C NMR spectra of HBPEs (1) before and (2) after modification with succinic anhydride in $CDCl_3$

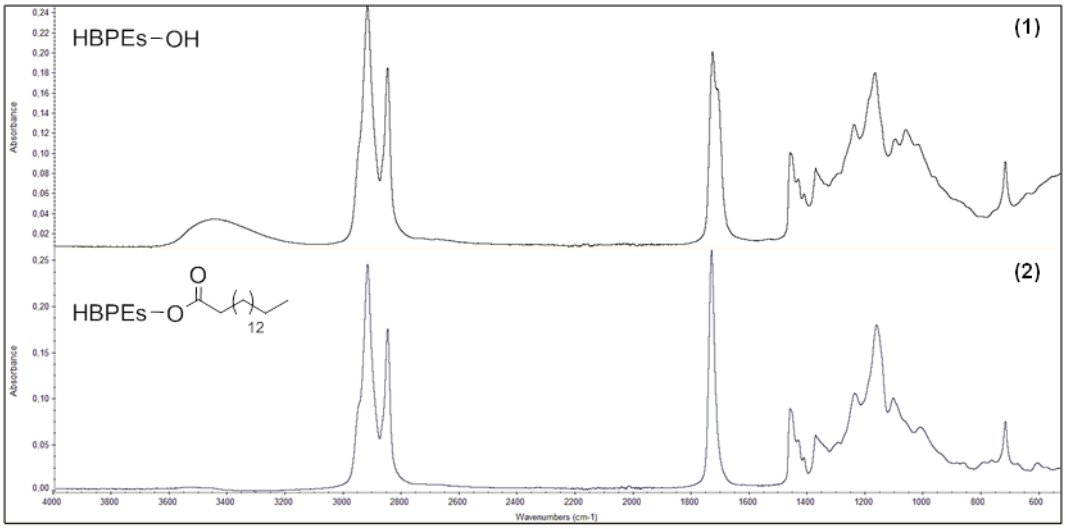

Figure SI 0-2. Stacked FT-IR spectra of HBPEs (1) before and (2) after modification with palmitoyl chloride

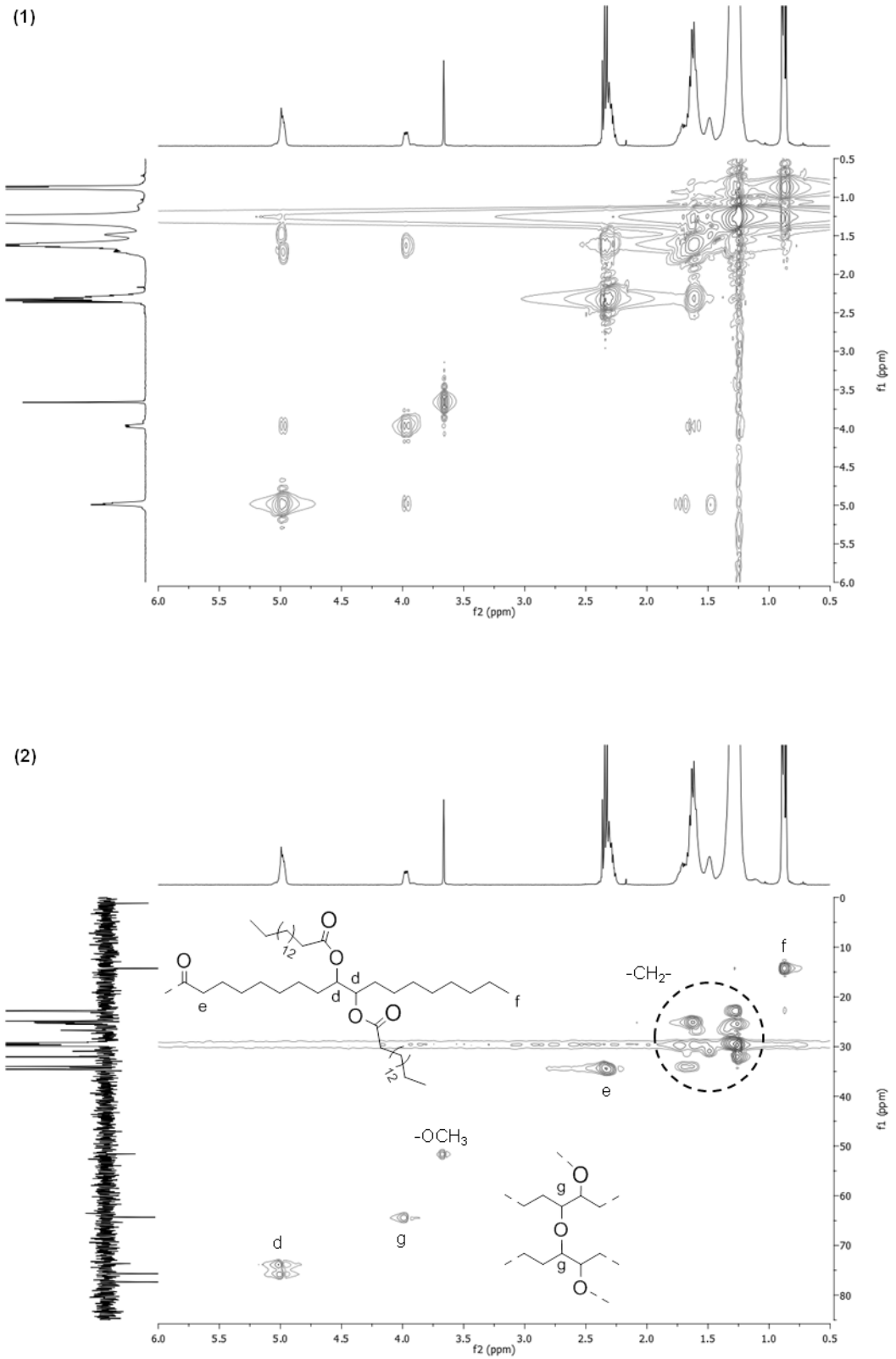

Figure SI 0-3. (1) ^{1}H-^{1}H COSY and (2) ^{1}H-^{13}C HSQC of a alkyl-terminated HBPE prepared by post-esterification with palmitoyl chloride in $CDCl_3$

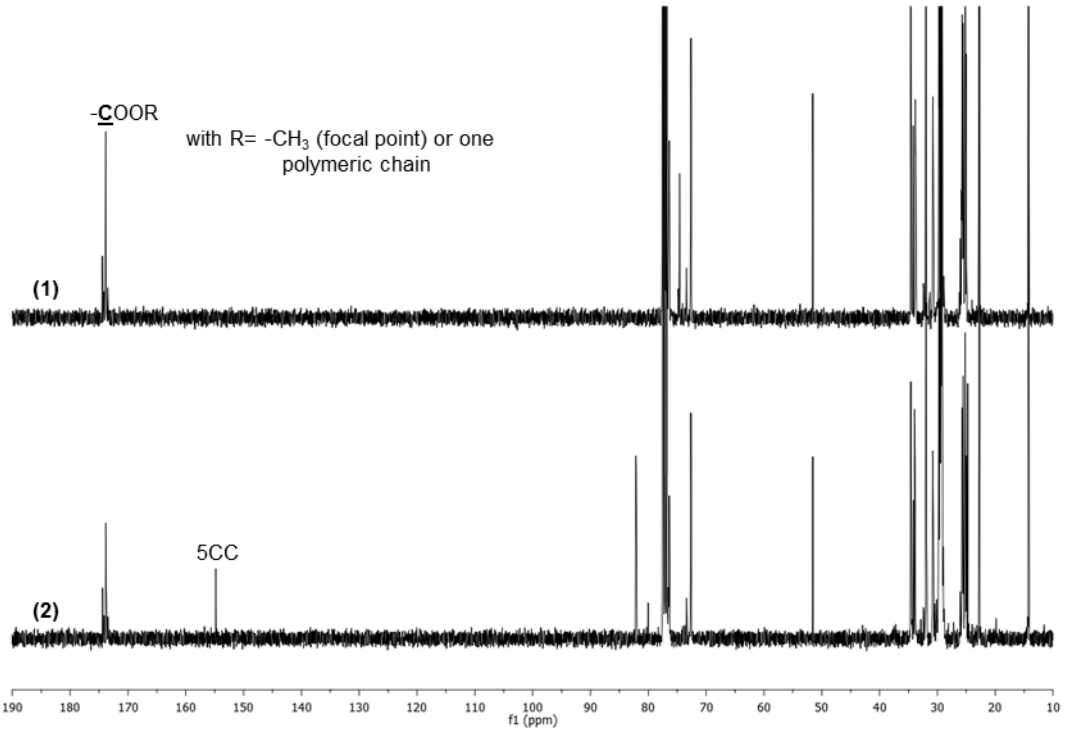

Figure SI 0-4. Stacked ^{13}C NMR spectra of HBPEs (1) before and (2) after modification with ethyl chloroformate in $CDCl_3$

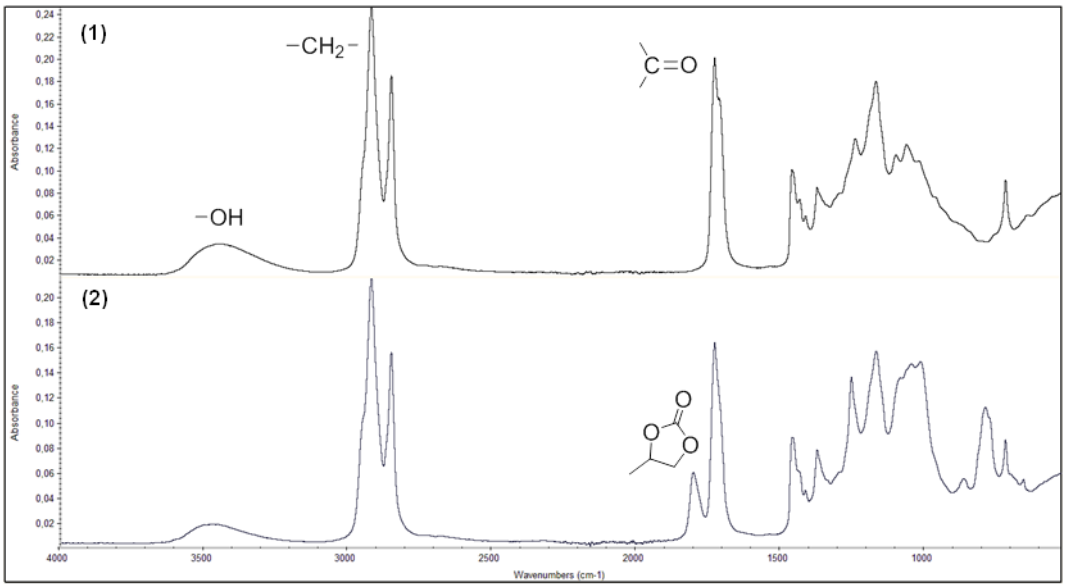

Figure SI 0-5. Stacked FT-IR spectra of HBPEs (1) before and (2) after modification with ethyl chloroformate

General conclusion and perspectives

The aim of this thesis was to use fatty acid methyl esters (FAMEs) as a platform for the design of more sustainable hyperbranched polyesters (HBPEs). As highlighted in the first part of this manuscript, this field is still in its infancy. Vegetable oils though represent a promising class of renewable feedstock for the polymer industry, owing to their abundant availability, relative low cost and inherent biodegradability. Their rich application possibilities make them industrially attractive, as daily demonstrated in oleo-chemistry. Vegetable oils are indeed already used for the manufacture of surfactants, lubricants, paintings and coatings. In this context, fatty acid methyl esters (FAMEs) obtained by transesterification of vegetable oils, represent interesting substrates for the design of novel polymer architectures. The inherent aliphatic structure of the FAMEs, coupled with the presence of ester groups and a large number of unsaturations enables the design of a variety of multifunctional building blocks, suitable to the preparation of aliphatic HBPEs.

A variety of novel renewable HBPEs with tunable properties was successfully synthesized during this PhD work. For that purpose, plant oils and/or FAMEs were chemically modified to access multifunctional precursors of AB_n-type, featuring ester (A) and alcohol moieties (B). Simple, safe and efficient chemical transformations were considered to provide industrial perspectives to this work in accordance with our partners' expectations (ITERG and SAS PIVERT). Two main platforms of AB_n-type monomers were therefore developed by acid hydrolysis of epoxidized vegetable oils (Chapters II and III) and thiol-ene/metathesis coupling reactions (Chapter IV). The subsequent polycondensation of these oily-derived monomers, performed in bulk in order to be in line with the principles of Green Chemistry that advocate the use of less hazardous and safer chemicals, gave access to novel renewable HBPEs.

A first platform of AB_2/AB_3-type monomers was prepared by acid hydrolysis of epoxidized vegetable oils. This reaction sequence enabled the introduction of diols in vicinal position. Dihydroxylation of the internal double bonds of methyl oleate resulted in the formation of methyl 9,10-dihydroxystearate (M2HS). This peculiar AB_2-type monomer was the subject of an intensive learning process regarding the synthesis and characterization of HBPEs. Its polymerization behavior was studied in detail, including the influence of the reaction time, temperature and loading in catalysts on the (macro)molecular characteristics of

the resulting materials. Among the variety of catalysts tested, zinc acetate, TBD and sodium methoxide, three systems with very different activation mechanisms, were found to be the most effective achieving molar masses in between 3 000-10 000 g.mol^{-1} and rather broad dispersities (from 2 to > 15). The degree of branching (DB) as determined by ^{1}H NMR spectroscopy, in between 0.07 and 0.45, confirmed the branching character of the as-devised polyesters. As expected, M2HS-derived HBPEs displayed amorphous properties with glass transition temperatures in the range -32.5 to -20°C and standard thermal stabilities for oily-derived polyesters with $T_d^{5\%}$ varying from 306 to 338°C.

In the light of the promising results obtained with M2HS, the platform of multifunctional precursors prepared by acid hydrolysis of epoxidized vegetable oils was extended to four novel AB_2/AB_3-type monomers of different structures. For that purpose, other substrates were considered including methyl esters of undecenoic (C11:1), erucic (C22:1), ricinoleic (C18:1) and aleuritic (C16:1) acids. Correlation between monomer structure and properties of tailor-made HBPEs were studied in comparison with the results previously obtained with M2HS. An increase in the monomer functionality (n = 3) resulted in HBPEs with higher glass transition temperatures, in between -10 to 9°C. A higher chain length between two branching points and the absence of pendant alkyl chains endowed polyesters with semi-crystalline properties. Melting temperatures were determined in the range 20 to 61°C.

Kinetics experiments performed with M2HS-derived HBPEs, however, revealed an intrinsic limitation to monomers of this first platform. The close vicinity of the two secondary alcohols generated by acid hydrolysis of epoxidized vegetable oils, was found to somehow restrict the molar masses and DB values achievable by the HBPEs. This prompted us to develop a second platform of AB_2-type monomers of higher reactivity by means of thiol-ene and metathesis coupling reactions. Thiol-ene addition is a versatile technique that allowed us to introduce both primary alcohols, more reactive than the secondary ones previously studied, and ester groups. In this latter case, polycondensation of the as-formed A_2B monomers resulted in the formation of methyl ester-terminated HBPEs, as opposed to the vast majority of hydroxyl-ended materials developed up to date. In addition, metathesis coupling reaction enabled to drive apart the reactive functions, thereby minimizing steric hindrance. The higher reactivity of the four newly prepared HBPEs was confirmed in polymerization: shorter reaction times and/or lower reaction temperatures were required to achieve HBPEs with similar molar masses in between 3 000-10 000 g.mol^{-1}. Interestingly, the presence of thio-ether linkages was found to impart flexibility to the related HBPEs, resulting in lower T_g values from -56 to -35°C, but also weakened their thermal stability with reduced $T_d^{5\%}$ in between 266 and 313°C.

Several challenges were addressed in this work. First, the control of monomers' purity was a critical issue in view of their subsequent melt polycondensation. Indeed, as exemplified with M2HS, the presence of acid fractions drastically limited the molar masses of polymers prepared. Besides, the approach by polycondensation of AB_n-type monomers was favored since according to Flory's theory, this route gives access to HBPs without risk of gelation. However, MALDI-TOF MS analyses showed that our oily-derived HBPEs could be prone, under thermal treatment, to numerous side-reaction reactions, *i.e.* cyclization, dehydration, etherification, etc., resulting in the formation of gelled products. Special efforts were thus made to optimize the reaction conditions in order to achieve soluble HBPEs with relatively high molar masses.

Lastly, complex structures of the as-devised HBPEs have presented a great challenge for full characterization. ^{1}H NMR spectroscopy was successfully applied to the determination of the DB of HBPEs derived from AB_2-type monomers bearing vicinal diols as reactive functions, *i.e.* M2HS, M2HB. Of particular interest was to compare differences in polymer structure resulting from polymerizations conducted using zinc acetate and TBD. Indeed, while zinc acetate was found to favor the formation of rather linear structures ($DB \leq 0.26$), TBD-catalyzed polycondensations yielded more branched architectures ($0.13 \leq DB \leq 0.45$). However, this spectroscopic technique shows limitations to characterize the branching density of HBPEs derived from monomers of higher functionality, *i.e.* M3HS, MA, and those belonging to the second platform developed, owing to the separation of the reactive functions.

To conclude, our initial goal of developing a range of novel oily-derived HBPEs with tunable properties was fulfilled. The so-formed polyesters exhibited apparent molar masses in between 3 000 and 13 000 g.mol^{-1}, *i.e.* knowing that these values are underestimated compared to their absolute molar masses, broad dispersities (Đ= 2 to >15) and tunable DBs from 0.07 to 0.45. In addition, HBPEs displayed amorphous to semi-crystalline properties depending on their constitutive monomer units, good thermal stability ($260 \leq T_d^{5\%} \leq 338$°C), high solubility and storage stability. In terms of applications, these oily-derived HBPEs could be first considered as additives, rheology modifiers, lubricants or components for coating resins. Besides, in the last part of this manuscript, an exploratory work was carried out regarding the post-functionalization of both the core and the periphery of these HBPEs with the aim at tuning their properties and thus opening the scope of their applications, from commodity plastics to advanced materials. One of the most promising modifications investigated is the introduction of carboxylic-ended moieties which was found to impart water-solubility to these oily-derived HBPEs.

The industrial perspectives of this project were highlighted by the registration of two patents. Optimization of the synthesis of M2HS-derived HBPEs at a pilot scale is currently undertaken at *ITERG* technical center, as well as a life cycle assessment. Research perspectives in this subject are also numerous. Progress in the characterization of the physico-chemical properties of these as-devised HBPEs, including their rheological behavior in dilute conditions and/or rather concentrated regimes, needs to be further carried out. The environmentally friendly additives developed in this thesis indeed represent promising candidates as lubricants or rheology modifiers (viscosity improver, reinforcing agent, etc.). Likewise, functionalization of both the core and the periphery of the HBPEs could be better exploited in the light of selected applications. Besides, a plethora of other hydroxyester AB_n-type monomers could be synthesized starting from fatty acid methyl esters. Interestingly, numerous examples have already been described in the literature without having been used as building blocks for the synthesis of HBPEs. In addition, by taking advantage of the important currently available library of diesters/diols and polyols already developed for the synthesis of oily-derived polyesters and polyurethanes, another option could be to explore the $A_2 + B_n$ approach. Lastly, the methodology developed in this PhD work could very well be extended to other polymer families, including some hyperbranched polyethers, polyamides or polyurethanes.

Materials and Methods

1. Materials

1,5,7-triazabicyclo[4.4.0]dec-5-ene (TBD, 98%), 2,2-dimethoxy-2-phenylacetophenone (DMPA, 99%), ethyl chloroformate (99%), Grubbs 2nd generation metathesis catalyst (Grubbs II), *meta*-chloroperbenzoic acid (*m*-cpba, <77%), 1,8-diazabicyclo[5.4.0]undec-7-ene (DBU, 98%), 7-methyl-1,5,7-triazabicyclo[4.4.0]dec-5-ene (m-TBD, 98%), anhydrous zinc acetate ($Zn(OAc)_2$, 99.99% trace metals basis), lithium hydroxide, 1,4-diazabicyclo[2.2.2]octane (DABCO, 98%), titanium(IV) butoxide (97%) and isopropoxide (99%), stannous octoate (95%), dibutyltin(IV) oxide (98%), sodium methoxide (powder, 95%), glycerol (99%), anhydrous *tert*-butanol (ACS reagent, ≥99.0%), 1,4-benzedimethanol (99%), 1,12-dodecanediol (99%), phosphoric acid (85%), hydrogen peroxide (30%) and 2-isocyanatoethyl methacrylate (IEMA, 98%) were obtained from Sigma Aldrich.

Methyl oleate (96%), 10-undecenoic acid (98%), 1,3-propanediol (99%), triethylamine (TEA, 99%), methyl thioglycolate (98%), 10-undecen-1-ol (99%), antimony(III) oxide (99.6%), succinic anhydride (99%), palmitoyl chloride (98%) were purchased from Alfa Aesar. Methyl 10-undecenoate (>96.0%), 2-mercaptoethanol (98%), aleuritic acid (>98%) and 4-(trifluoromethyl)phenyl isocyanate (4TFPI, 98%) were supplied from TCI Europe.

Fatty Acids and derivatives of high purity grade, *i.e.* methyl oleate (99%), methyl ricinoleate (99%), methyl linoleate (99%) were purchased from Nu-Chek Prep. *Candida Antartica* lipase B (CalB) supported on acrylic resin was supplied by Chiral Vision (Immozyme).

Methyl 9,10-dihydroxystearate (M2HS), methyl 9,10,12-trihydroxystearate (M3HS), methyl 13,14-dihydroxybehenate (M2HB) were kindly provided by ITERG (Pessac, France).

All products and solvents (reagent grade) were used as received except otherwise mentioned. The solvents were of reagent grade quality and were purified when necessary according to methods reported in the literature.

2. Methods

2.1. NMR spectroscopy

^{1}H and ^{13}C NMR experiments were conducted on Bruker Avance 400 spectrometer (400.20 MHz or 400.33 MHz and 100.63 MHz for ^{1}H and ^{13}C, respectively) at room temperature, in $CDCl_3$ as solvent except otherwise mentioned. Chemical shifts (δ) are reported in parts per million relative to the known solvent residual peak (δ = 7.26 ppm). DEPT- 135 (Distortion Enhanced Polarization Transfer) and two-dimensional analyses such as ^{1}H-^{1}H COSY (Homonuclear correlation spectroscopy), ^{1}H-^{13}C-HSQC (Heteronuclear single quantum coherence) and ^{1}H-^{13}C-HMBC (Heteronuclear multiple bond correlation) were also performed. Regarding the quantitative ^{13}C NMR analyses, an inverse gated decoupling sequence with a 30°C pulse angle was used. A pulse delay time of 20 seconds (D1) was employed.

^{1}H and ^{13}C high resolution magic angle spinning (HR-MAS) NMR experiments were performed by the *Centre d'Etude Structurale et d'Analyse des Molécules Organiques* (CESAMO, Bordeaux, France) on a Bruker Avance III 600 spectrometer. The instrument is equipped with a 4mm HR-MAS dual inverse $^{1}H/^{13}C$ probe with a magic angle gradient. All experiments were carried out at a magic angle (54.7°C) spinning rate of 3 kHz and a stabilized temperature of 313K.

2.2. Fourrier Transformed Infra-Red-Attenuated (FT-IR) spectroscopy

Infrared analyses were performed on a Thermoscientific Nicolet iS10 spectrometer using the attenuated total reflection mode. The spectra were recorded using 32 scans at a resolution of 4 wavenumbers.

2.3. Size Exclusion Chromatography

Size Exclusion Chromatography analyses (SEC) were performed in THF as the eluent (1 mL/min) at 40°C, on a PL-GPC 50 plus Integrated GPC from Polymer laboratories-Varian with a series of four columns from TOSOH (TSKgel TOSOH: HXL-L (guard column 6.0 mm ID x 4.0 cm L); G4000HXL (7.8 mm ID x 30.0 cm L); G3000HXL (7.8 mm ID x 30.0 cm L) and G2000HXL (7.8 mm ID x 30.0 cm L)). The elution times of the filtered samples were monitored using RI detectors with a calibration curve based on low dispersity polystyrene standards (PS). Trichlorobenzene was added as flow marker.

Absolute molar mass measurements were carried out with a multiangle LS detector (miniDAWN TREOS, Wyatt Technology) and a differential refractometer (Optilab rEX, Wyatt).Columns and detectors were thermostated at 40°C. Tetrahydrofuran (THF) was used as eluent at a flow rate of 1 mL/min, as it had a sufficient RI contrast and resulted in better separation than other solvents tested including chloroform and N,N'-dimethylformamide. Concentrations of the injected solutions varied from 15 to 9 mg/mL and were higher for lower molar mass samples. ASTRA V 5.3.4.20 software (Wyatt) was used for data processing.

2.4. Flash chromatography

Flash chromatography was performed on a Grace Reveleris apparatus equipped with ELSD and UV detectors (λ= 254 and 280 nm), by employing silica cartridges. Separations were carried out based on either dichloromethane/methanol (Chapters II and III) of cyclohexane/ethyl acetate (Chapter IV) gradient solvent.

2.5. Gas chromatography (GC-FID)

Gas chromatography analyses (GC) were performed by *Iterg* on a Shimadzu GC equipped with: Flame ionization detectors (FID, 380°C) and Zebron ZB-5HT (5% phenyl – 95% dimethylpolysiloxane) 15 m x 0.25 mm ID, 0.1 μm thickness capillary column. The carrier gas was hydrogen. The temperature program of the column was initially set at 60°C (volume injected: 1 μL), then increased to 370°C at a rate of 10°C.min^{-1} and held isothermally for 10 minutes.

2.6. Time-of-flight mass spectrometer with matrix-assisted laser desorption/ionization (MALDI-TOF MS)

MALDI-TOF MS analyses were performed by the *Centre d'Etude Structurale et d'Analyse des Molécules Organiques* (CESAMO, Bordeaux, France) on a Voyager mass spectrometer (Applied Biosystems). The instrument is equipped with a pulsed N2 laser (337 nm) and a time-delayed extracted ion source. Spectra were recorded in the positive-ion mode using the reflectron and with an accelerating voltage of 20 kV. Samples were dissolved in THF at 10 mg/ml. The IAA matrix (trans-3-indoleacrylic acid) was prepared by dissolving 10 mg in 1 ml of THF. A methanol solution of cationisation agent (NaI, 10 mg/ml) was also prepared. The solutions were combined in a 10:1:1 volume ratio of matrix to sample to cationisation agent. One to two microliters of the obtained solution was deposited onto the sample target and vacuum-dried.

2.7. Differential Scanning Calorimetry (DSC)

Differential Scanning Calorimetry (DSC) measurements were carried out on DSC Q100 apparatus from TA Instruments. For each sample, two cycles from -100 to 150°C (except otherwise mentioned) were performed at 10°C.min^{-1}. Glass transition and melting temperatures were calculated based on the second heating run.

2.8. Thermograimetric Analysis (TGA)

Thermogravimetric analyses (TGA) were performed on two different apparatus from TA Instruments depending on the availability: TGA Q50 and Q500 at heating rate of 10°C.min^{-1} under nitrogen atmosphere from room temperature to 700°C.

2.9. WAXS

X-ray measurements were obtained by Ahmed Bentaleb from the *Centre de Recherche Paul Pascal* (CRPP, Pessac, France) on a Rigaku Nanoviewer (XRF microsource generator, MicroMax 007HF), with a rotating anode coupled to a confocal Max-Flux® Osmic mirror (Applied Rigaku Technologies, Austin, USA) producing beam with a wavelength of 1,5418A° and an energy of 8KeV. Images were collected on a MAR345 image plate detector (MARResearch, Norderstedt, Germany). Samples were introduced into 1,5mm diameter glass capillaries (Glaskapillaren GLAS, Glas-Technik & Konstruktion, Schönwalde-Glien, Germany) and placed at a distance of 202mm from the detector (d = 345mm) providing access to 2θ angles in the range 1.5– 40°.

Les huiles végétales comme plateforme pour la conception de nouveaux polyesters hyper-ramifiés

Résumé : Ces travaux de thèse traitent de la valorisation des huiles végétales comme plateforme pour la synthèse de polyesters d'architecture hyper-ramifiée. Pour ce faire, l'approche par polycondensation de monomères de type AB_n ($n \geq 2$) a été privilégiée. Des précurseurs plurifonctionnels portant des fonctions ester (A) et alcool (B) ont ainsi été préparés par modification chimique d'huiles végétales et/ou d'esters méthyliques d'acide gras. Plusieurs méthodologies de synthèse simple, sûres et efficaces ont été mises en place afin de garantir une réalité industrielle à ce projet. Deux plateformes de monomères de type AB_n ont été obtenues par (1) hydrolyse acide d'huiles végétales époxydées et (2) en faisant appel à des réactions d'addition de thiol-ène et de métathèse. Le développement de procédés de polycondensation en masse, a alors permis l'accès à de nouveaux polyesters hyper-ramifiés. La densité de ramifications ainsi que les propriétés thermo-mécaniques de ces matériaux ont été modulées par le choix adapté de la structure chimique des précurseurs 'gras' utilisés. Enfin, un travail exploratoire a été conduit concernant la post-fonctionnalisation du cœur comme de la périphérie de ces polyesters hyper-ramifiés dans le but de moduler leurs propriétés et ainsi d'étendre la portée de leurs applications, des plastiques de commodité aux matériaux avancés.

Mots clés : *Polymères hyper-ramifiés, huiles végétales, ester méthyliques d'acide gras, polyesters, polycondensation, fonctionnalisation*

Vegetable oils as a platform for the design of novel Hyperbranched Polyesters

Abstract : The aim of this thesis was to use vegetable oils as a platform for the design of more sustainable polyesters of hyperbranched architecture. For that purpose, the approach by polycondensation of AB_n-type monomers ($n \geq 2$) was favored. Plant oils and/or fatty acid methyl esters were chemically modified to synthesize multifunctional precursors featuring ester (A) and alcohol moieties (B). Simple, safe and efficient chemical transformations were considered to provide industrial perspectives to this work. Two main platforms of AB_n-type monomers were developed by (1) acid hydrolysis of epoxidized vegetables oils and (2) thiol-ene/metathesis coupling reactions. The subsequent polycondensation of these oily-derived monomers, performed in bulk, gave access to novel renewable hyperbranched polyesters. The branching density as well as the thermo-mechanical properties of these materials were adjusted by designing and selecting the chemical structure of the fatty acid-based monomers. Finally, an exploratory work was carried out regarding the post-functionalization of both the core and the periphery of these hyperbranched polyesters with the aim at tuning their properties and thus opening the scope of their applications, from commodity plastics to advanced materials.

Keywords : *Hyperbranched polymers, vegetable oils, fatty acid methyl ester, polyesters, polycondensation, functionalization*

Laboratoire de Chimie des Polymères Organiques
16 avenue Pey-Berland
F-33607 PESSAC